Annex 24

Climate Change Analysis

For the GCF-FAO Project "Enhancing the resilience of Serbian forests to ensure energy security of the most vulnerable while contributing to their livelihoods and carbon sequestration (FOREST Invest) "

Table of Contents

List of Acronyms

Acronym	Definition
Wdef	Water deficit
WD	Wet days
VWD	Very wet days
VP	Vegetation productivity index
TX	Maximum temperature
TrN	Tropical nights
TN	Minimum temperature
TG	Average temperature
SnF	Snowfall
SnD	Snow depth
Serbia	Republic of Serbia
SD	Summer days
RRx	Mean precipitation intensity
RR	Accumulated precipitation
NDVI	Normalized Difference Vegetation Index
LAI	Leaf Area Index
ID	Ice days
HZ	Hardiness Zone
GS	Length of the growing season
GL	Length of the growing season
FD	Frost days
FAI	Forest Aridity Index
EQ	Ellenberg's Quotient
DS	Maximum length of dry spell
DD	Degree day
CH	Chill hours

GEOSPATIAL ANALYSIS

This section will an outline of the geographic context of Serbia

Summary

Topography - Serbia's topography can be divided into two regions based on its elevation and topography. The north of the Sava-Danube axis is characterized by the plains of the Vojvodina province, while the highlands are located in the south. The country's steeper slopes are generally located to the south of the Sava-Danube axis, with the strongest slopes in the northeast Balkan and Rhodope Mountain ranges. The country's elevation ranges from 17 meters above sea level in the plains of Vojvodina to 2164 m a.s.l. at the summit of Mount Midžor in the Balkan Mountain range.

Landcover - Nearly 40% of Serbia is covered by forests, primarily located south of the Sava-Danube axis and on highlands away from the three Morava valleys. Broad-leaved forests cover 28% of the country's area, while transitional woodland-shrub covers 6.5%. Mixed forest and coniferous forest make up only 3% of the country's area. The landscape to the north of the Sava-Danube axis is dominated by agriculture, except for the Fruška Gora Mountain range to the west and the Deliblato Sands to the east. The forest composition is mainly broad-leaved forest and transitional woodland-shrub in the southeast, and a mixture of broad-leaved forest, transitional woodland-shrub, coniferous forest, and mixed forest in the Dinarides mountains to the southwest.

Forest cover - Serbia experienced a notable decrease in total canopy cover between 2000 and 2015, with an approximate rate of -24 kha per decade, which continued during the 2015-2019 period. The Bor District in the east, near the border with Romania, saw the most significant forest loss. While the forest typology did not undergo significant changes in the past five years, the canopy cover area of deciduous broadleaf forests decreased, while that of evergreen needle leaf forests slightly increased.

Soil characteristics - Serbia has 8 main soil types: Cambisols, Phaeozems, Leptosols, Fluvisols, Vertisols, Gleysols, Luvisols, and Planosols, which cover more than 97% of the country's surface area. Cambisols and Phaeozems are the most common soils and are found almost exclusively south of the Sava-Danube axis. Fluvisols are present throughout the country, while Leptosols are found at high altitudes. Luvisols are concentrated in the Balkan Mountains and south of the Sava valley, Gleysols in the northeast, and Planosols mainly in the west. Vertisols are found around the three Morava valleys and close to the Timok and Nišava rivers. Sand, loam, and clay are almost equally distributed throughout most of the country, with some exceptions where sand content is higher. Water capacity is also evenly distributed throughout Serbia, with lower values found in the north and in valleys, and extremely high or low values found in specific areas.

Demography - The population of Serbia increased until 1994 and then slowly decreased to 6.9 million in 2019, with the rural population constantly decreasing from 4.7 million in 1960 to 3 million in 2019. The urban population increased until mid-2000 and then stabilized at around 4 million, reaching 3.9 million in 2019. As a result, the percentage of rural population decreased from 71% in 1960 to 44% in 2019. The main urban centers in Serbia are Belgrade, Novi Sad, Subotica, Kragujevac, Niš, and Leskovac, with most of the population located in these areas. The population outside urban centers is higher and more evenly distributed in the flatland North of the Sava-Danube axis than in the hilly regions of the South. The road network in Serbia is relatively well-serviced, with the larger part of the country less than 25 km away from an urban center. However, the Northern borders and Eastern Carpathian Mountain regions are less well-serviced, with smaller urban centers and lower population densities.

Surface water - The North of Serbia has a dense free-flowing surface water network with large discharge ratio, including the Danube, Tisa, and Sava rivers, and multiple canals of the Danube-Tisa-Danube network. In contrast, the South of Serbia has a more scattered network with smaller discharge

ratio, including the Morava, Ibar, Lim, and Timok rivers. There are also more large lakes and reservoirs in the South, such as the Iron Gate dam, Vlasina Lake, Perućac lake, and Gruža Lake. The North has easier access to surface water due to the flat topography and dense network, while the South may face difficulties and higher costs due to the hilly topography and scattered network.

Topography & Slope

This section will present the topography and slope distribution of the Republic of Serbia.

Topography

The distribution of elevation of the Republic of Serbia is presented in Figure 1.

Figure 1 – Distribution of elevation in the Republic of Serbia[1].
Elevation given above sea level (a.s.l.). ***Data source:*** *NASA / USGS / JPL-Caltech (Farr et al. 2007).*

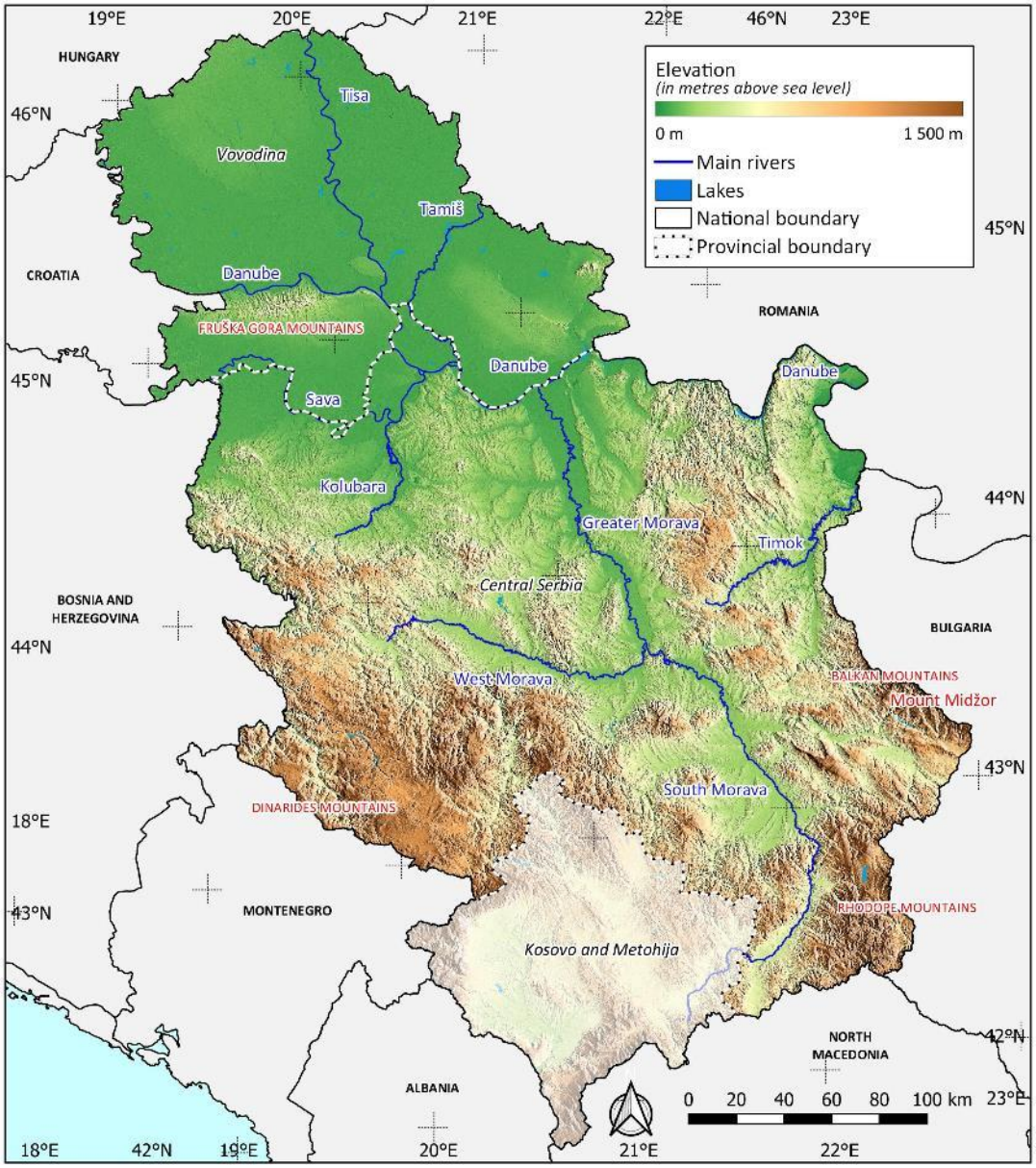

[1] The boundaries and names shown and the designations used on this map do not imply official endorsement or acceptance by the United Nations.

Serbia's topography features a wide range of elevations, ranging from 17 meters above sea level (a.s.l.) in the plains of Vojvodina to 2164 m a.s.l. at the summit of Mount Midžor on the country's southeastern border with Bulgaria in the Balkan Mountain range.

Geographically, Serbia can be divided into two distinct regions based on its topography. North of the Sava-Danube axis 'around the 44.7°N parallel) lies the flat and expanse of plains of the Vojvodina province. To the south of these rivers stand the highlands of the rest of the country. In the north, the level terrain is only interrupted by the Fruška Gora Mountain range, while the highlands in the south are defined by the three Morava valleys: the Greater Morava, the West Morava, and the South Morava.

Slope

The distribution of the topographic slopes of the Republic of Serbia is presented in Figure 2.

Figure 2 - Distribution of the topographic slope of the Republic of Serbia[2].
Data source: *NASA / USGS / JPL-Caltech (Farr et al. 2007).*

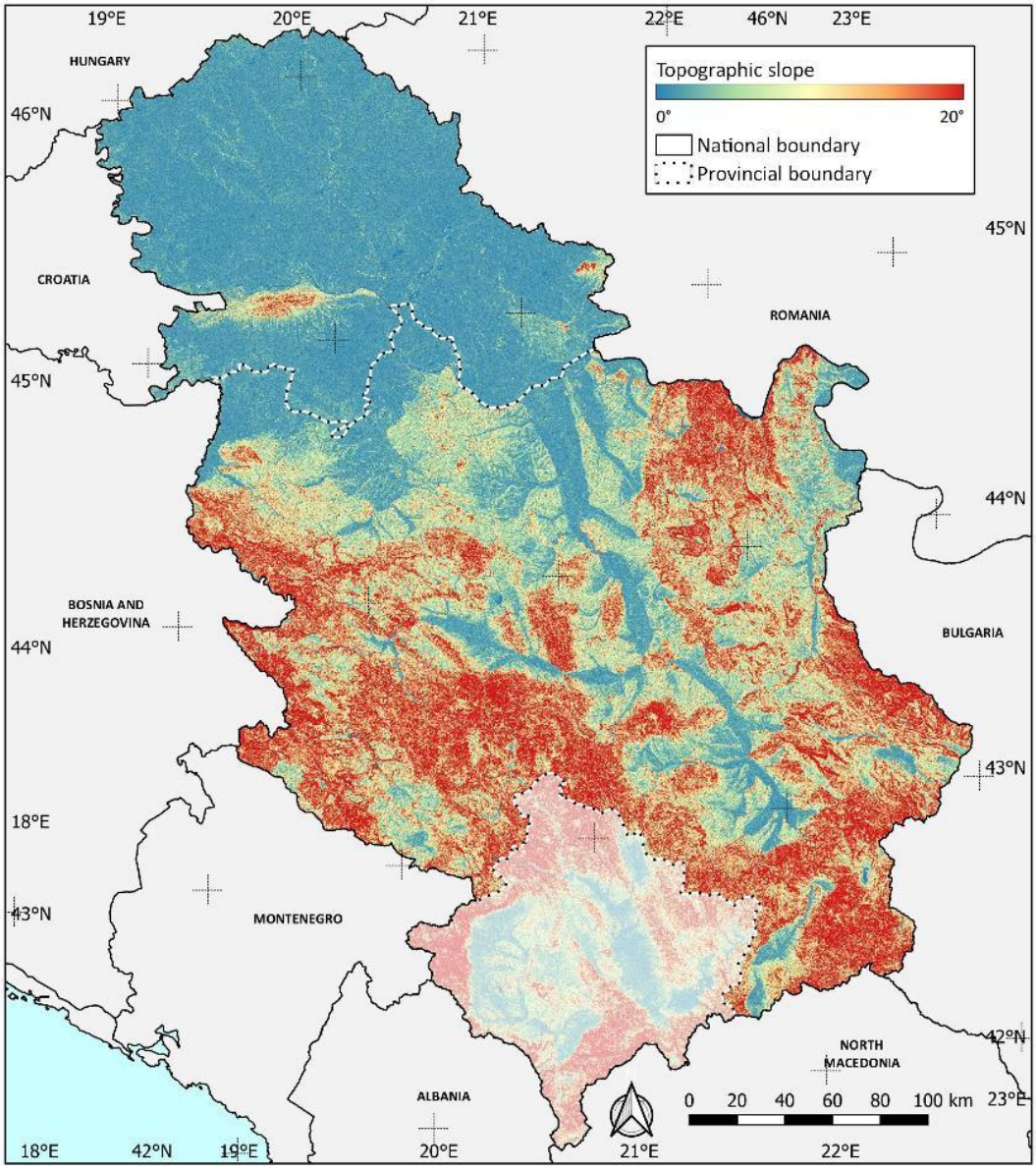

[2] The boundaries and names shown and the designations used on this map do not imply official endorsement or acceptance by the United Nations.

The distribution of the topographic slopes in the Republic of Serbia generally follows the same pattern as the distribution of elevations, with most of the steeper slopes located to the south of the Sava-Danube axis. In contrast, there are relatively few steep slopes to the north of this axis. The country's strongest slopes can be found in the northeast, specifically in the Balkan and Rhodope Mountain ranges.

Landcover

To describe the distribution of landcover in the Republic of Serbia, we rely on data from the CORINE Landcover (CLC) database (Figure 3 and Table 1).

CLC utilizes a 44-class nomenclature, with a minimum mapping unit of 25 hectares and a minimum mapping width of 100 meters. For the purposes of the following map, we have consolidated all classes belonging to the "Agricultural," "Artificial surface," and "Water bodies" groups into their respective categories to provide a more detailed focus on forested and natural vegetation classes. We Also merged “Artificial surface”, “Burnt Area”, “Bare Rocks”, “Beaches, dunes sands”, in one class renamed “Artificial surfaces and bare soil”.

Table 1 – Frequency distribution table for landcover classes in the Republic of Serbia.
Data source: *Copernicus CORINE Landcover 2018 (European Environmnet Agency (EEA) 2020)*

Class ID	***Class Description***	***Surface area*** *(in km^2)*	***Surface area*** *(in % of total)*
200	Agricultural areas	42716	55.10%
311	Broad-leaved forest	21776	28.09%
324	Transitional woodland-shrub	5012	6.47%
100	Artificial surfaces and bare soil	2694	3.48%
321	Natural grasslands	1880	2.43%
313	Mixed forest	1321	1.70%
312	Coniferous forest	892	1.15%
500	Water bodies	806	1.04%
411	Inland marshes	225	0.29%
333	Sparsely vegetated areas	188	0.24%
322	Moors and heathland	8	0.01%

Based on the CLC data, forested areas cover almost 40% of Serbia's surface area, mostly located south of the Sava-Danube axis. These forested areas are primarily located on the highlands away from the three Morava valleys. In contrast, the landscape to the north of the Sava-Danube axis, in the Vojvodina region, is dominated by agriculture, except for the Fruška Gora Mountain range to the west and the Deliblato Sands to the east.

The CLC reports that Broad-leaved forests cover 28% of the country's area, while Transitional woodland-shrub covers 6.5%. Mixed forest and coniferous forest together account for only 3% of the country's area. East of the Morava valley, the forest is mainly composed of broad-leaved forest and transitional woodland-shrub. In the Dinarides mountains to the west, the situation is more complex with a mixture of broad-leaved forest, transitional woodland-shrub, coniferous forest, and mixed forest.

Figure 3 – Distribution of the CORINE landcover classes in the Republic of Serbia[3]
Data source: *Copernicus CORINE Landcover 2018 (European Environmnet Agency (EEA) 2020).*

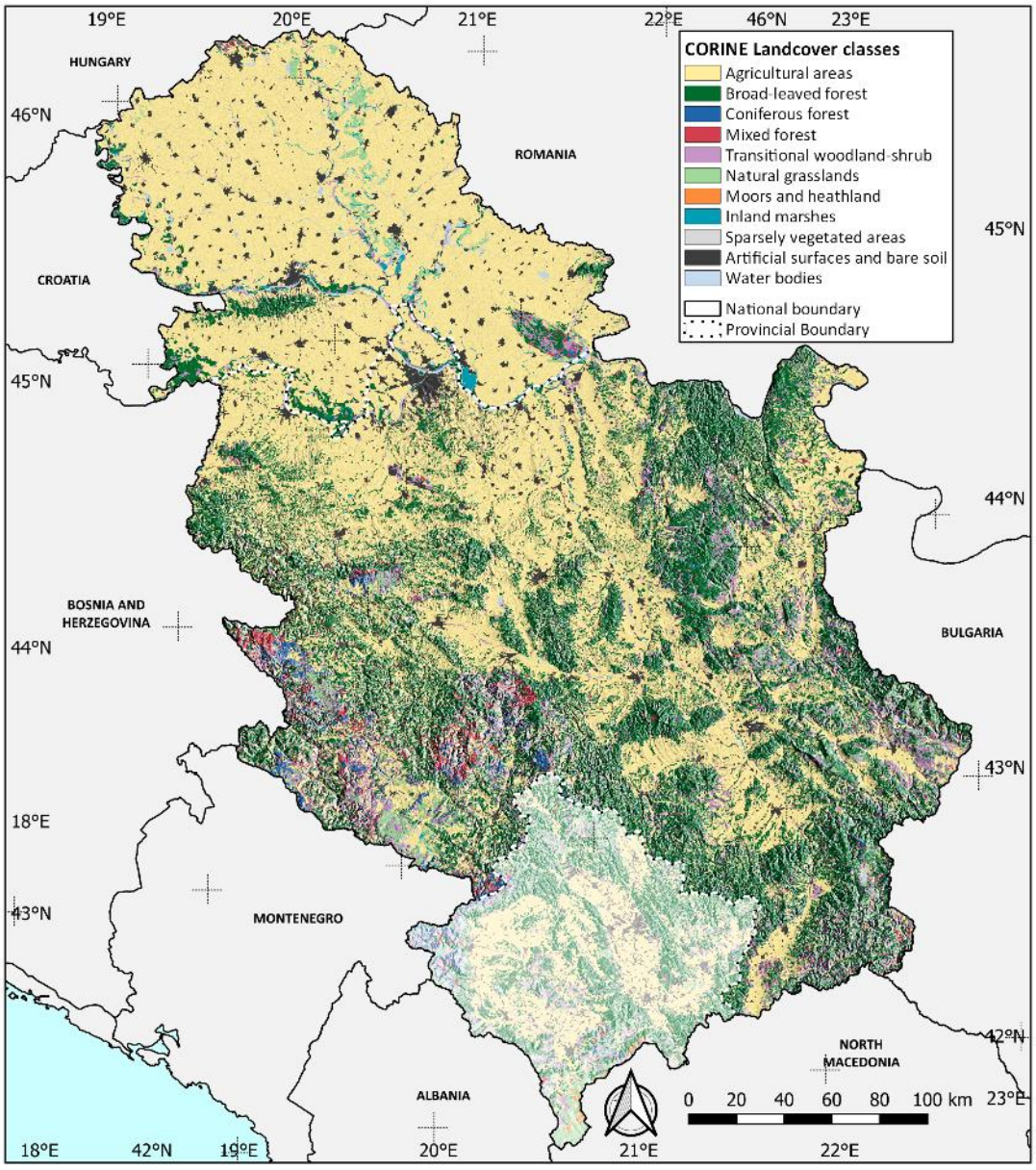

[3] The boundaries and names shown and the designations used on this map do not imply official endorsement or acceptance by the United Nations.

Forest cover

This section will present the canopy cover of the Republic of Serbia and its variation between 2000 and 2019. In this document, canopy cover is defined as the area covered by canopy closure for all vegetation taller than 5 m and given in kilo hectares.

Agricultural Census of 2012

Figure 4 displays the distribution of forests by municipality in the Republic of Serbia in 2012, based on census data. The census confirms that the majority of Serbia's forests are located south of the Tisa-Danube axis. In contrast, in the north of the country, most municipalities have very little forest coverage, with less than 10% of their area being covered by forests. In the south, however, many municipalities have at least 10% of their area covered by forests, with some municipalities having forest coverage above 40%, such as Vrnjačka Banja (142), Kruševac (10), and Despotovac (146).

Figure 4 - Distribution of forest cover by municipality in the Republic of Serbia in 2012[4].
Data source: Census of Agriculture 2012 (Statistical Office of the Republic of Serbia 2020)

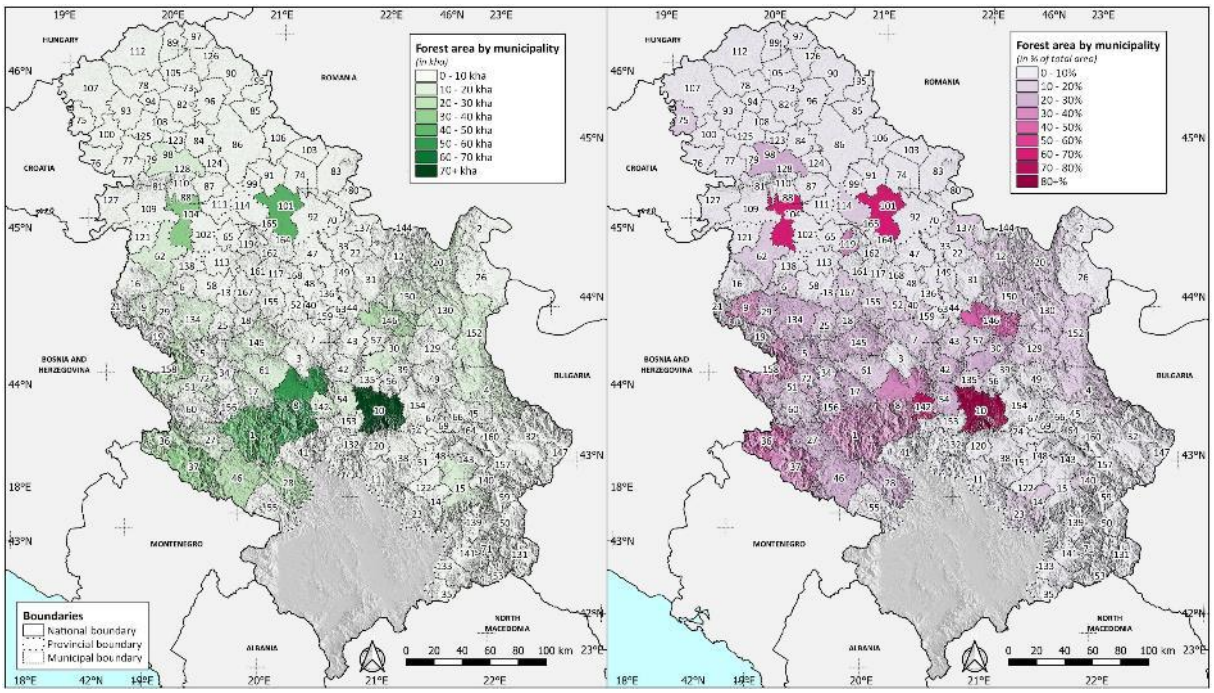

Notably, in the south of the country, the municipalities of Ivanjica (1) and Kraljevo (8) each have more than 40 kha of forest area, while the municipality of Kruševac (10) has more than 70 kha of forest area. Two exceptions can be found in the north of the country, along the Sava-Danube axis, with Ruma (104) and Pančevo (101) having more than 50% forest coverage in their respective areas.

[4] The boundaries and names shown and the designations used on this map do not imply official endorsement or acceptance by the United Nations.

Canopy cover between 2000 and 2015

The time series of the canopy cover area in the republic of Serbia can be observed in Figure 5.

Figure 5 – Total canopy cover area between 2000 and 2015
Data sources: Hansen Global Forest Change v1.8 (Hansen et al. 2013)

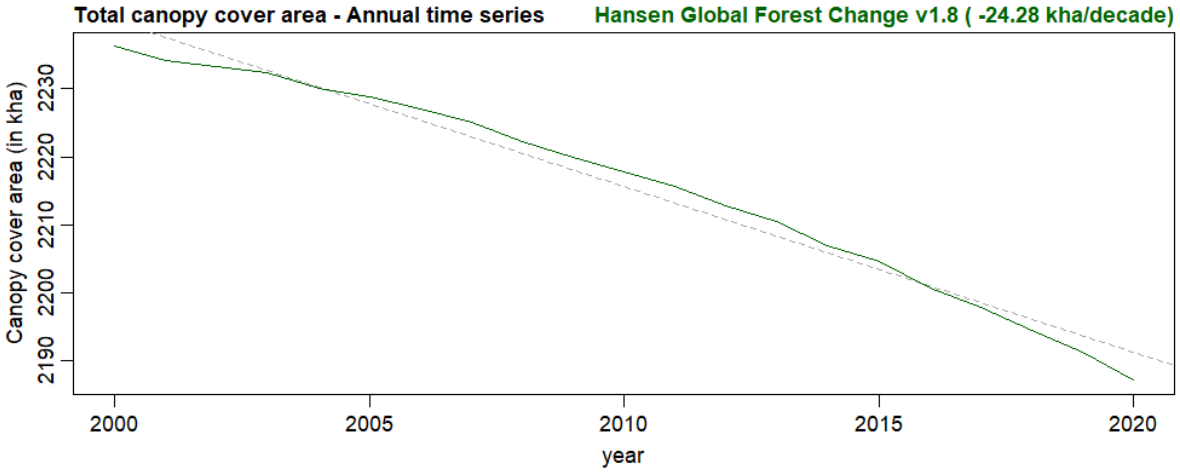

According to Hansen Global Forest Change v1.8, there was a decrease in total canopy cover in Serbia at a rate of approximately -24 kha per decade between 2000 and 2015.

Figure 6 displays the canopy cover maps for Serbia in 2000, 2005, 2010, and 2015.

The Hansen Global Forest Change v1.8 data confirmed the distribution of forest cover presented by the CLC data. Forest loss was observed throughout Serbia between 2000 and 2015, with the most significant losses occurring around water streams in the north and in the three Morava valleys in the south. Notably, the Fruška Gora Mountain range, a national park located in the north, did not experience significant forest loss. However, a hot spot of forest loss was observed in the Bor District in the east, near the border with Romania.

Figure 6 - Canopy cover in 2000, 2005, 2010 and 2015[5]

Data sources: Hansen Global Forest Change v1.8 (Hansen et al. 2013)

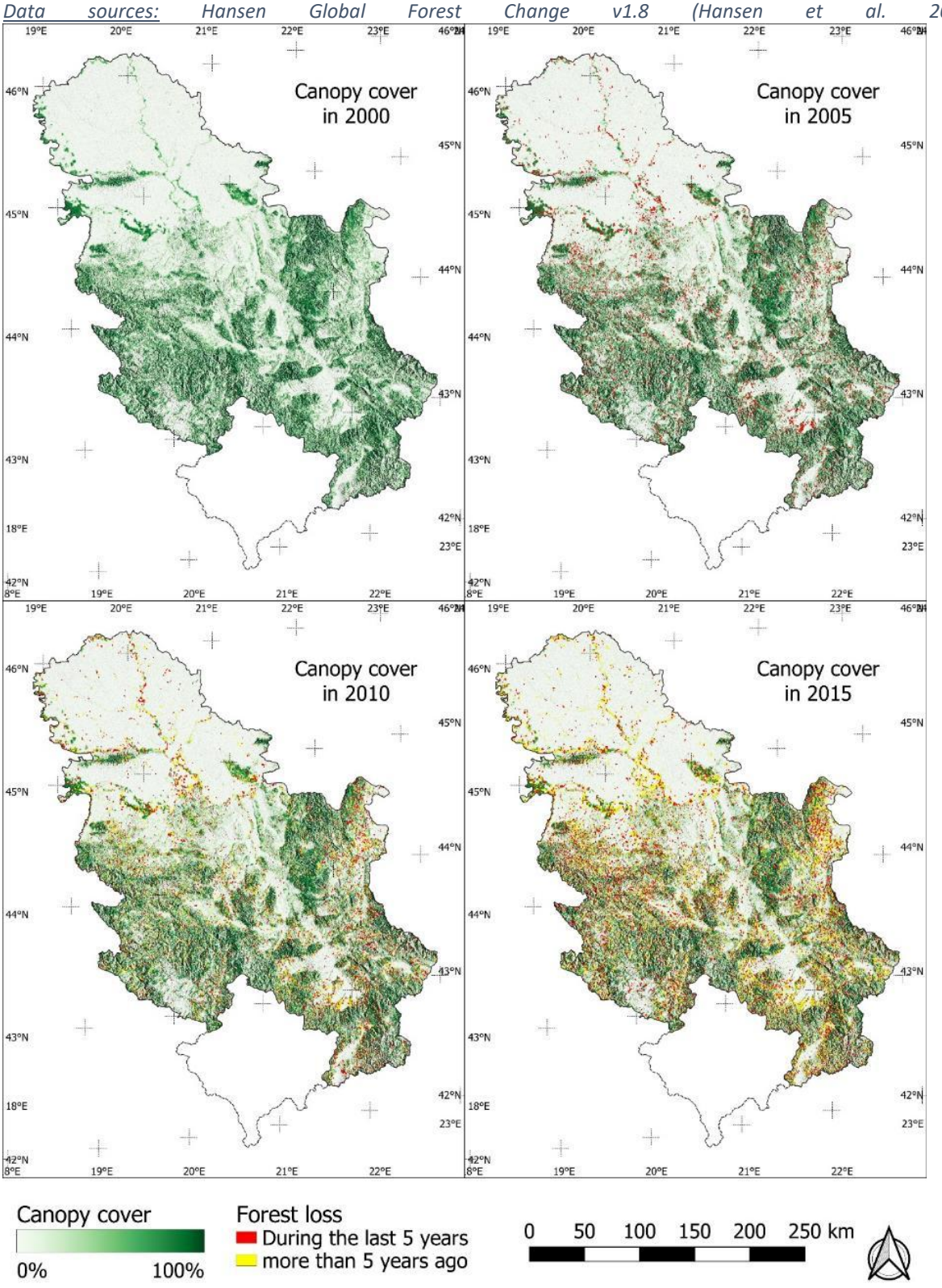

[5] The boundaries and names shown and the designations used on this map do not imply official endorsement or acceptance by the United Nations.

Canopy cover in Serbia since 2015

The time series of the canopy cover area between 2015 and 2019 in the republic of Serbia can be observed in Figure 7.

Figure 7 – Total canopy cover area between 2000 and 2015
Data sources: Copernicus Global Landcover Layers (Buchhorn et al. 2020).

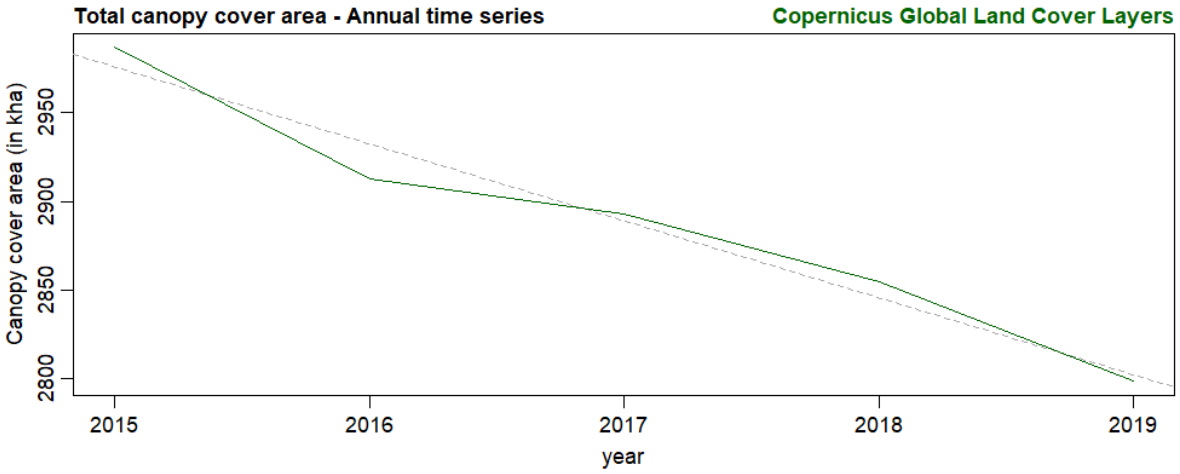

The more recent data provided by the Copernicus Global Landcover Layers confirms the decrease in total canopy cover area in Serbia. The rate of this decrease appears to be even higher than the one observed between 2000 and 2015 in the Hansen data. However, as only 5 years of data are available for this database, no statistically significant trend can be determined.

Figure 8 presents maps of the canopy cover in the Republic of Serbia in 2015 and 2019, as well as maps of the annual variations between those years.

The variation maps show ubiquitous loss of canopy cover, particularly between 2015 and 2016 and between 2018 and 2019. The Copernicus Global Landcover Layers indicate that the most significant loss in canopy cover between 2015 and 2019 occurred in the Bor District in the East of the country, near the border with Romania. This loss was already noticeable between 2000 and 2015, as indicated by the Hansen data.

Figure 8 - Canopy cover and canopy cover variation between 2015 and 2019[6]
Data sources: Copernicus Global Landcover Layers (Buchhorn et al. 2020).

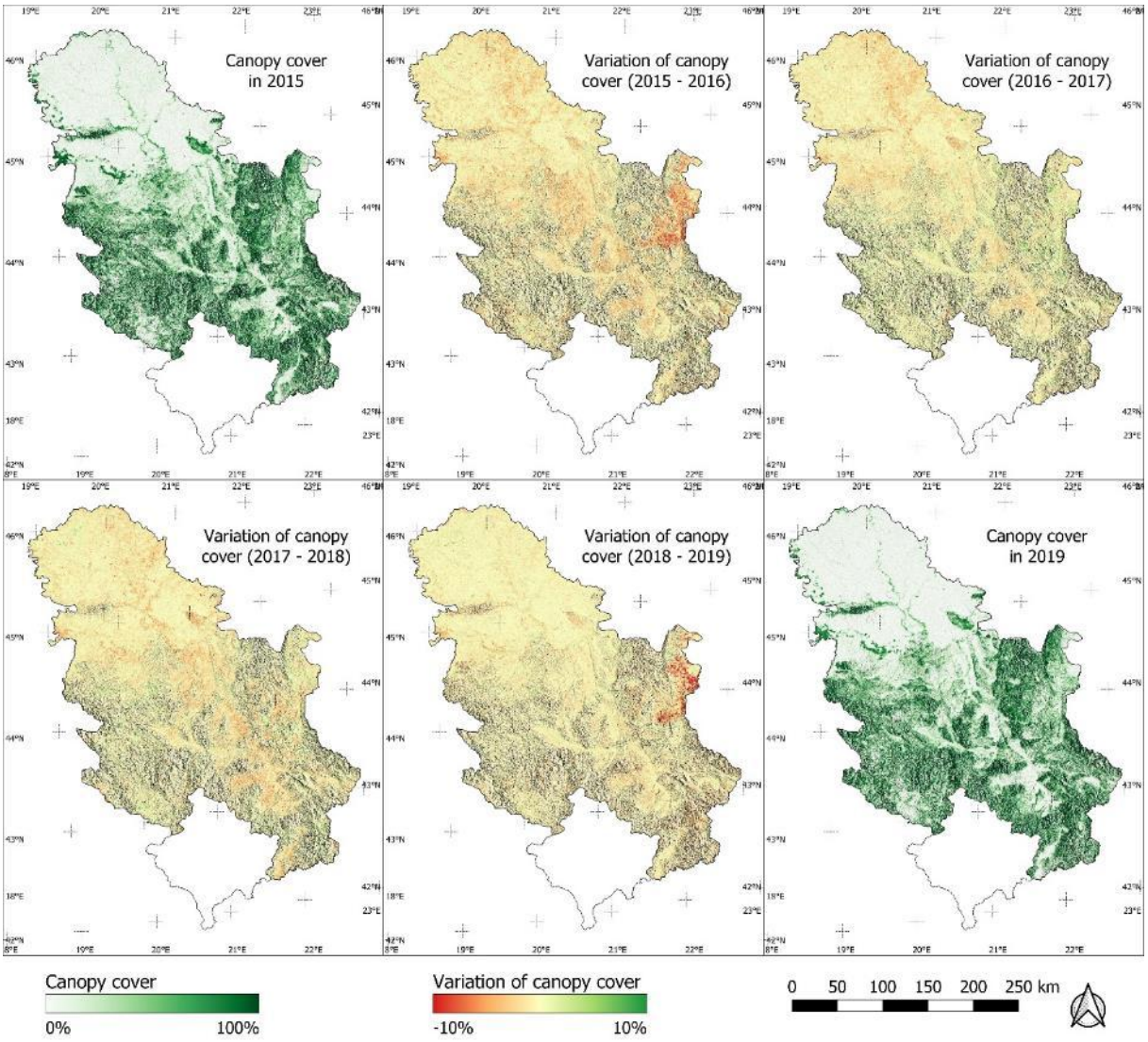

Figure 9 displays the forest typology maps in the Republic of Serbia for the period between 2015 and 2019.

The forest typology did not experience notable changes during the past five years. The Copernicus Global Landcover Layers corroborate the Corine Land Cover data, as deciduous broadleaf forests compose most of Serbia's forest, while evergreen needle leaf forests are mainly found mixed with deciduous broadleaf forest in the southwest of the country, in the Dinarides mountains.

[6] The boundaries and names shown and the designations used on this map do not imply official endorsement or acceptance by the United Nations.

Figure 9 – Forest typology between 2015 and 2019[7]
Data sources: Copernicus Global Landcover Layers (Buchhorn et al. 2020).

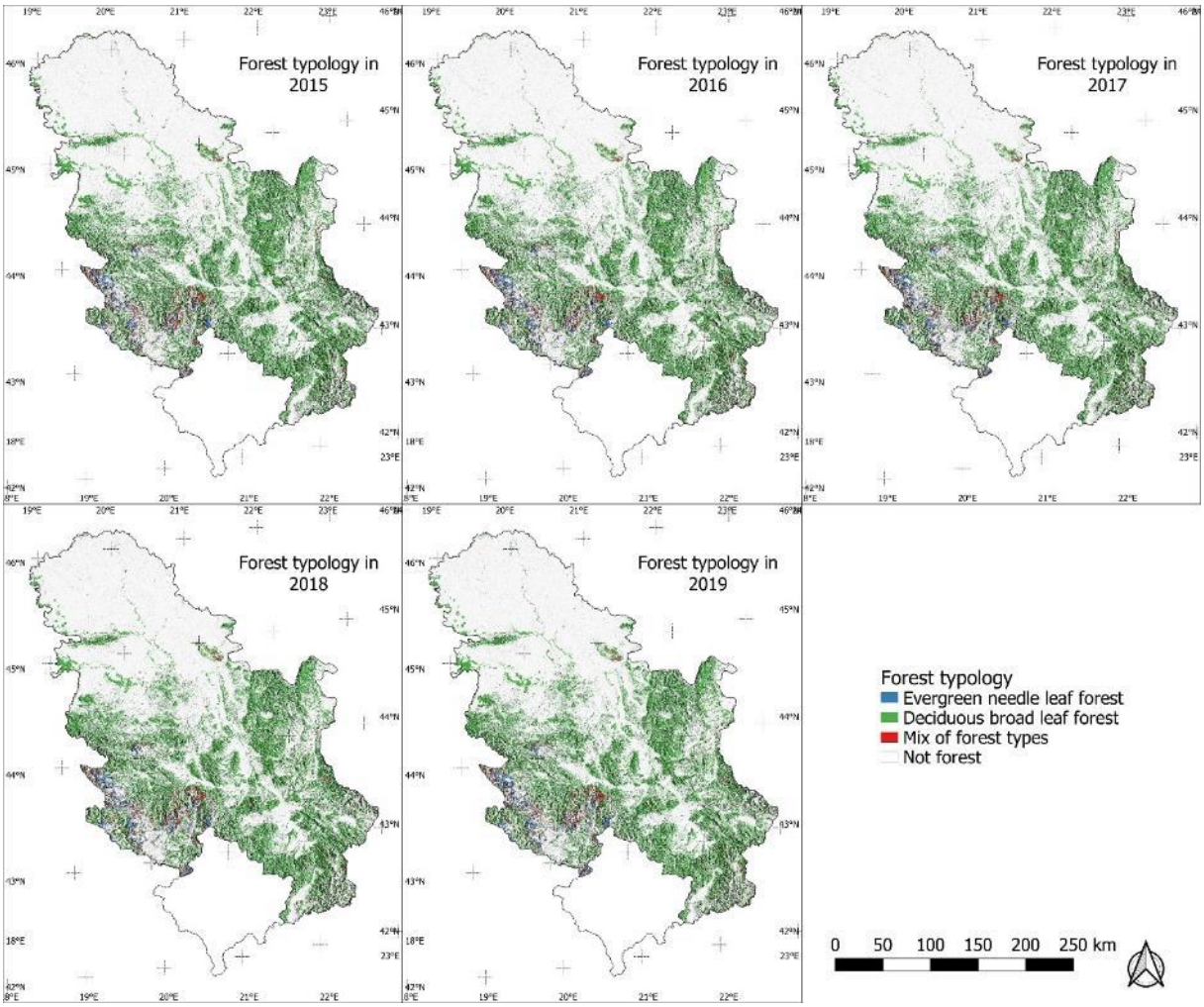

The time series of canopy cover area by forest type in Serbia between 2015 and 2019 is presented in Figure 10.

As the deciduous broadleaf forest is the most widespread forest type in Serbia, it suffered the largest loss of canopy cover area during the past five years, from 2,100 kha in 2015 to 1,950 kha in 2019. Interestingly, while the canopy cover area of deciduous broadleaf forests decreased, the evergreen needle leaf forest canopy cover area slightly increased, from 90 kha in 2015 to 100 kha in 2019. Finally, the mixed forest type remained relatively stable.

[7] The boundaries and names shown and the designations used on this map do not imply official endorsement or acceptance by the United Nations.

Figure 10 – Total canopy cover area by forest type between 2000 and 2015
Data sources: Copernicus Global Landcover Layers (Buchhorn et al. 2020).

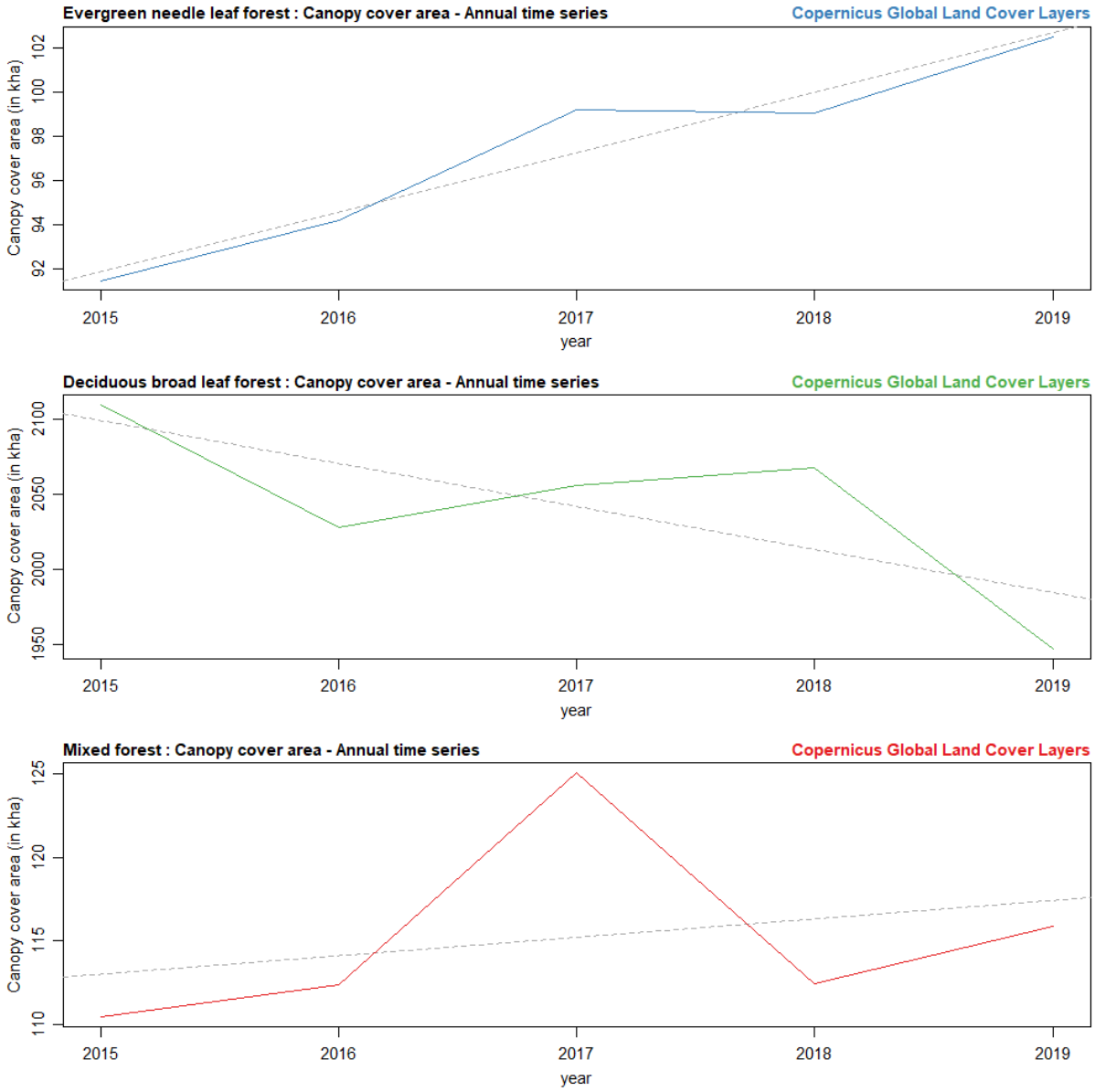

Soil characteristics

This section will present the soil compositions and taxonomy in the Republic of Serbia.

Soil classification

The distribution of soil types, following the Harmonized World Soil Database (HWSD) soil taxonomy, in the Republic of Serbia is presented in Figure 11 and Table 2.

The HWSD is the result of a collaboration between the FAO with IIASA, ISRIC-World Soil Information, Institute of Soil Science, Chinese Academy of Sciences (ISSCAS), and the Joint Research Centre of the European Commission (JRC). This data base combines existing regional and national updates of soil information worldwide with the information contained within the 1:5 000 000 scale FAO-UNESCO Soil Map of the World (Nachtergaele et al. 2010).

Figure 11 – Distribution of soil types in the Republic of Serbia following the HWSD taxonomy[8]
Data source: Harmonized World Soil Database (Nachtergaele et al. 2010)

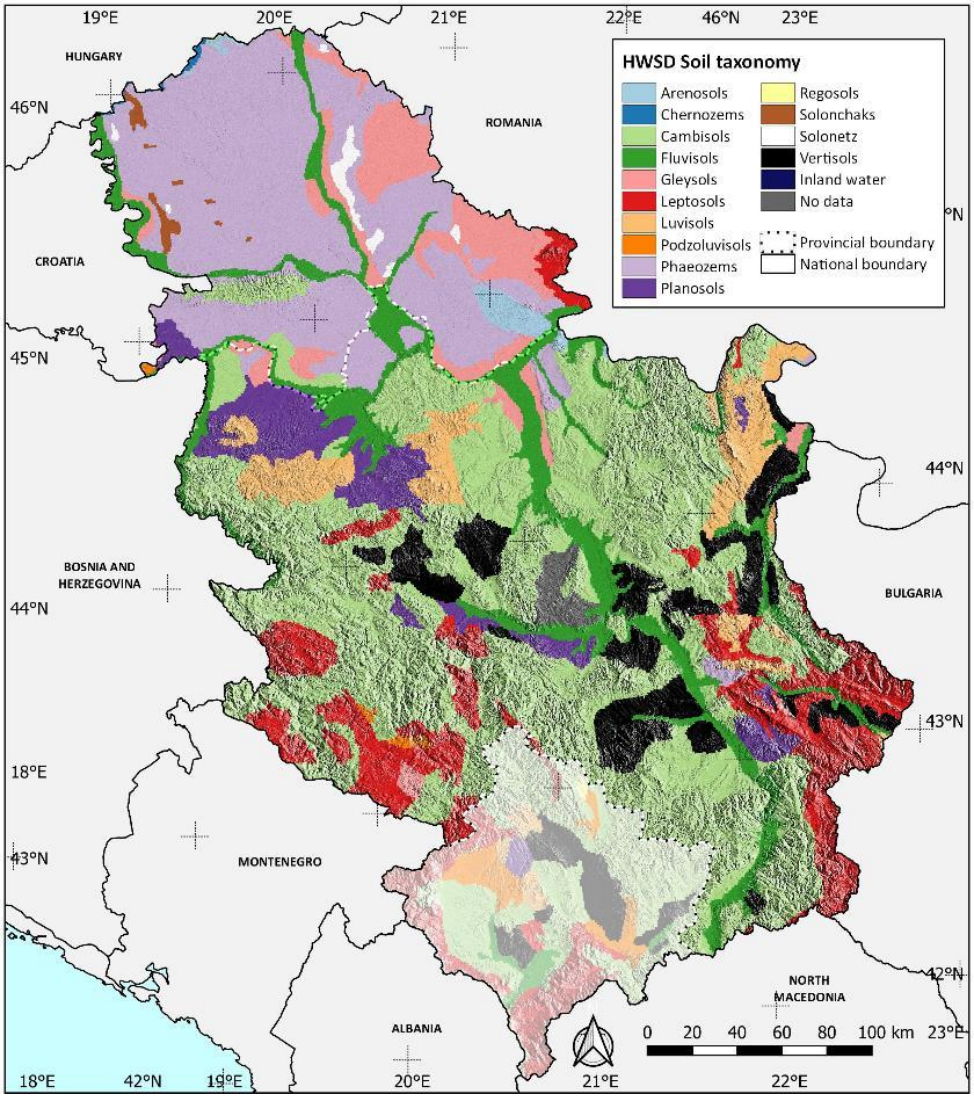

[8] The boundaries and names shown and the designations used on this map do not imply official endorsement or acceptance by the United Nations.

Serbia is characterized by a diverse range of soil types, with eight main soil types covering its territory. These soil types are distributed unevenly across the country and play a crucial role in shaping the local ecology, agriculture, and land use.

The most prevalent soil type in Serbia is Cambisols, covering 38% of the total area. It is primarily found to the south of the Sava-Danube Axis. Similarly, Phaeozems make up 19% of the total area and cover most of the Vojvodina region. Fluvisols, covering 9% of the area, are present throughout the country and are typically located along riverbanks, including the Danube, Sava, Tisa, and Morava rivers.

Leptosols are found at higher elevations, mainly in the Dinarides, Rhodopes, and Balkan Mountains. Luvisols are concentrated in the Balkan Mountains and southern Sava valley, while Gleysols are primarily located in the northeast of the country. Planosols, covering 5% of the area, are mainly found in the west, near the Sava valley. Finally, Vertisols are found around the three Morava valleys, the Timok river, and the Balkan Mountains near the Nišava river.

Overall, these seven soil types cover more than 97% of Serbia's total land area.

Table 2 - Frequency distribution table for soil types in the Republic of Serbia following the WRB taxonomy
Data source: (European Commission Joint Research Centre n.d.; Panagos et al. 2012)

Soil type	HWSD soil type ID	Surface area (in km^2)	Surface area (in % of total)
Cambisols	8	29 592	38,17%
Phaeozems	21	14 905	19,23%
Leptosols	16	7 601	9,80%
Fluvisols	9	7 328	9,45%
Vertisols	28	4 782	6,17%
Gleysols	11	4 124	5,32%
Luvisols	17	3 685	4,75%
Planosols	22	3 512	4,53%
No data	34	592	0,76%
Arenosols	4	568	0,73%
Solonetz	27	343	0,44%
Solonchaks	26	237	0,31%
Podzoluvisols	20	159	0,20%
Chernozems	6	88	0,11%
Inland water	31	3	0,00%
Regosols	25	1	0,00%

Soil sand, loam, and clay contents

The distribution of sand, loam, and clay in soils in the Republic of Serbia is presented in Figure 12.

Sand, loam, and soil content are close to balance (around 33% each, color close to white on the map) in most of the country area. There is slightly less sand and clay than loam in most of the country's soil. There are a few exceptions however, where sand content is higher.

Sand hot spots are ubiquitous throughout the country and can be found North and South of the Sava-Danube axis, at mid altitude, and following riverbanks. They are however more common in the

Southwest of the country. Throughout the country, the sand hotspots generally reach up to 40% in sand contents. Extreme concentration of sand can however be found at the Northern tip of the country, in the Southern part of the country (around Vladičin Han (139)), in the Southwest (around Kraljevo (8)) and around Krupanj (9) and Kragujevac (7). At these extreme spots, the sand content can reach more than 50%.

Figure 12 – Distribution of soil content of sand, loam, and clay, at 30 cm depth, in the Republic of Serbia[9]. ***Top left:*** *sand content.* ***Top right:*** *loam content.* ***Bottom:*** *clay content. Data source: (Hengl 2018).*

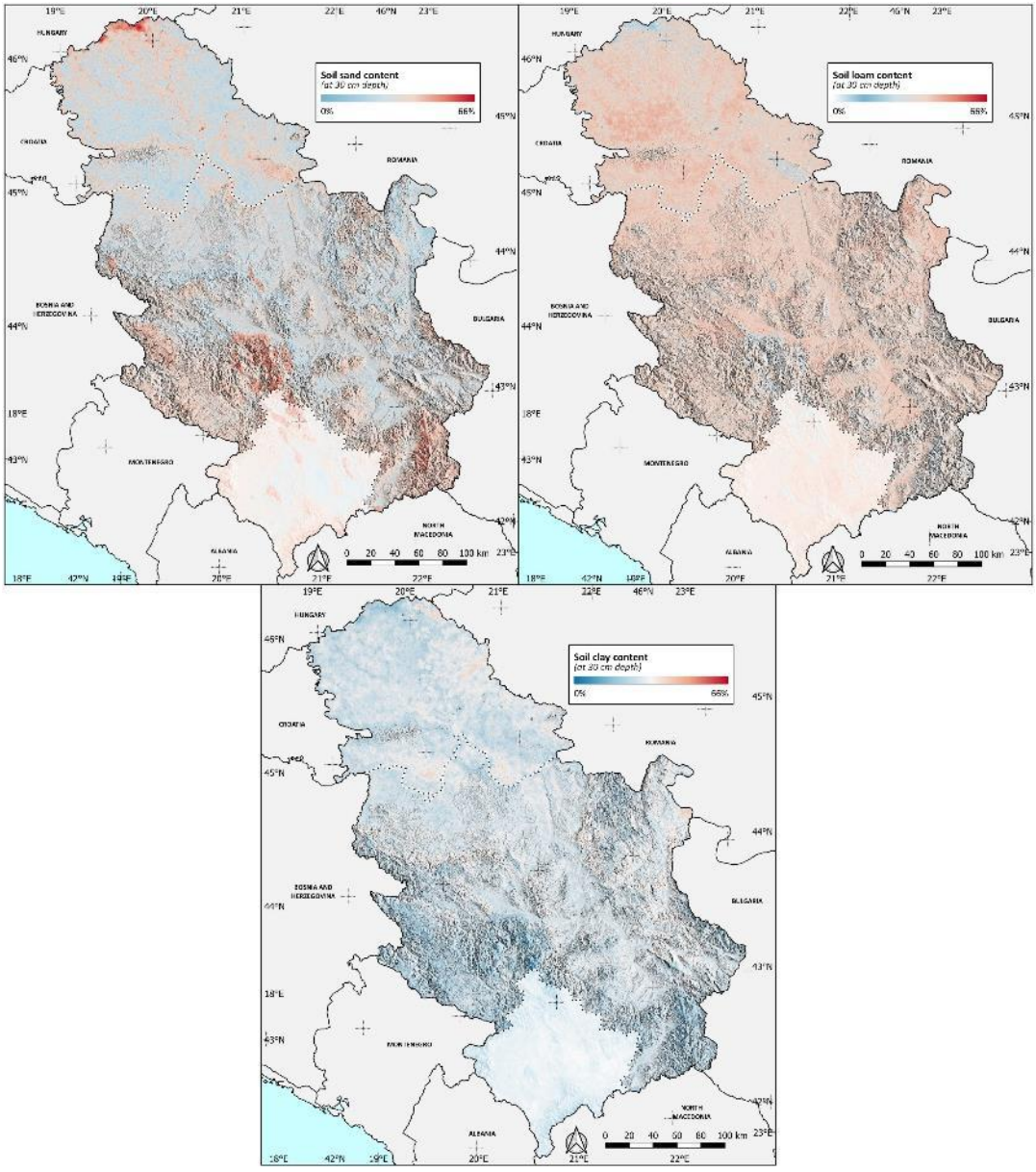

Soil water content

The distribution of water content of soils (field capacity) in the Republic of Serbia is presented in In Serbia, the distribution of soil water content is relatively even, with an average of around 30%.

[9] The boundaries and names shown and the designations used on this map do not imply official endorsement or acceptance by the United Nations.

However, there are some areas with lower values, such as the North of the country near the Fruška Gora Mountain range and the Northeast near Alibunar (74) municipality. In the South, lower values are concentrated in the valleys.

Along the Tisa River, high water content can be found, reaching 40% or more. Conversely, sand hotspots in areas such as Vladičin Han (139), Kraljevo (8), Krupanj (9), and Kragujevac (7) exhibit low water content, which can be lower than 20%.

Figure 13.

In Serbia, the distribution of soil water content is relatively even, with an average of around 30%. However, there are some areas with lower values, such as the North of the country near the Fruška Gora Mountain range and the Northeast near Alibunar (74) municipality. In the South, lower values are concentrated in the valleys.

Along the Tisa River, high water content can be found, reaching 40% or more. Conversely, sand hotspots in areas such as Vladičin Han (139), Kraljevo (8), Krupanj (9), and Kragujevac (7) exhibit low water content, which can be lower than 20%.

Figure 13 - Distribution of the soil water content at 30 cm depth in the Republic of Serbia[10].
Water content (i.e., field capacity) in volumetric percent for 33kPa and 1500kPa suctions. Data source: (Hengl and Gupta 2019)

[10] The boundaries and names shown and the designations used on this map do not imply official endorsement or acceptance by the United Nations.

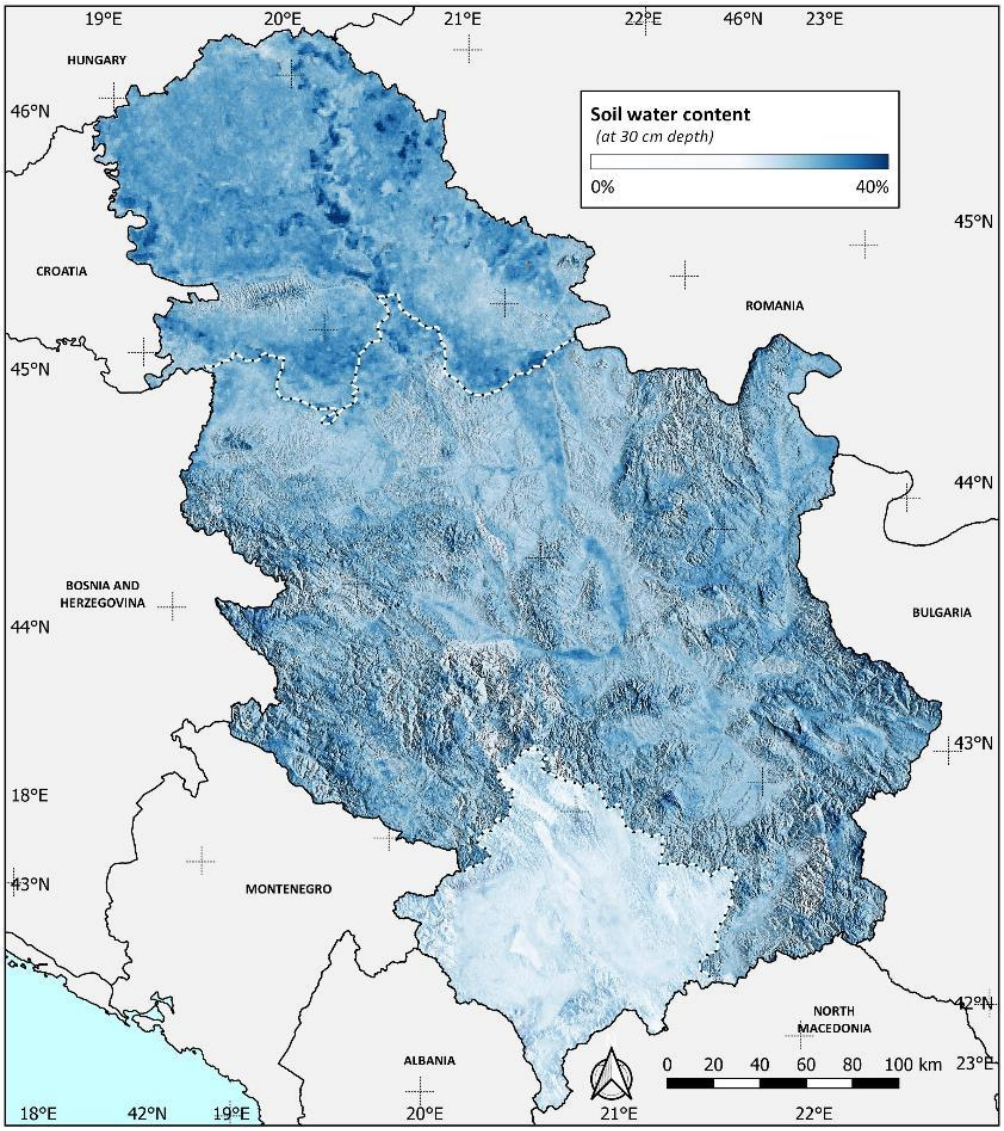

Demography

This section will present the distribution of population and urban centers in the Republic of Serbia.

Demographic trends

The demographic trends in the republic of Serbia are presented in Figure 14.

Figure 14 - Time series of the population in the Republic of Serbia
Time series over 1960-2020 period. ***In black:*** *total population.* ***In red:*** *urban population.* ***In green:*** *rural population.* ***In blue (dashed):*** *rural population (in % of total). Data source: World Bank (World Bank 2020)*

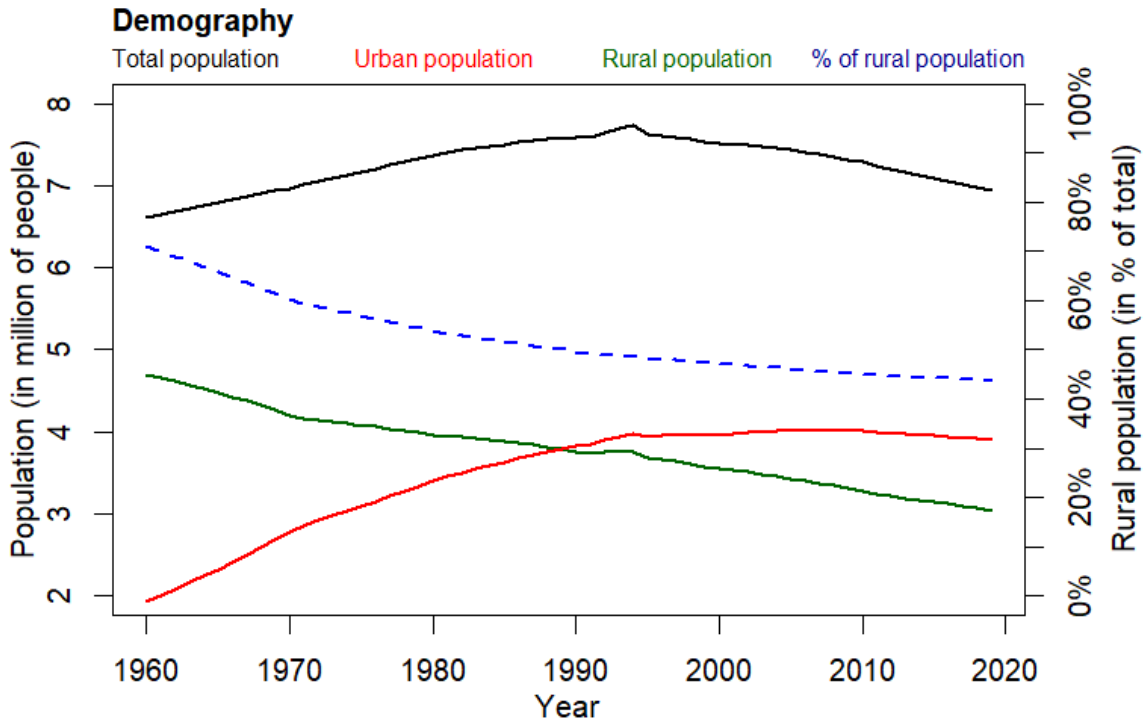

The Republic of Serbia experienced population growth until the mid-1990s, reaching a peak of 7.7 million in 1994. However, since 1995, the population has steadily declined, reaching 6.9 million in 2019.

Over the past six decades, Serbia has seen a consistent decline in its rural population, falling from 4.7 million in 1960 to 3 million in 2019. Conversely, the urban population increased until the mid-2000s, stabilizing at around 4 million in 2007 before declining to 3.9 million in 2019. These demographic shifts have led to a significant decrease in the percentage of rural population, from 71% in 1960 to 44% in 2019.

Current geographic distribution of population

The current geographic distribution of population in the Republic of Serbia is presented in Figure 15.

Figure 15 – Current geographic distribution of the population in the Republic of Serbia[11].
Data source: NASA SEDAC GPWv411: UN-Adjusted Population Density (Center for International Earth Science Information Network - CIESIN - Columbia University 2018)

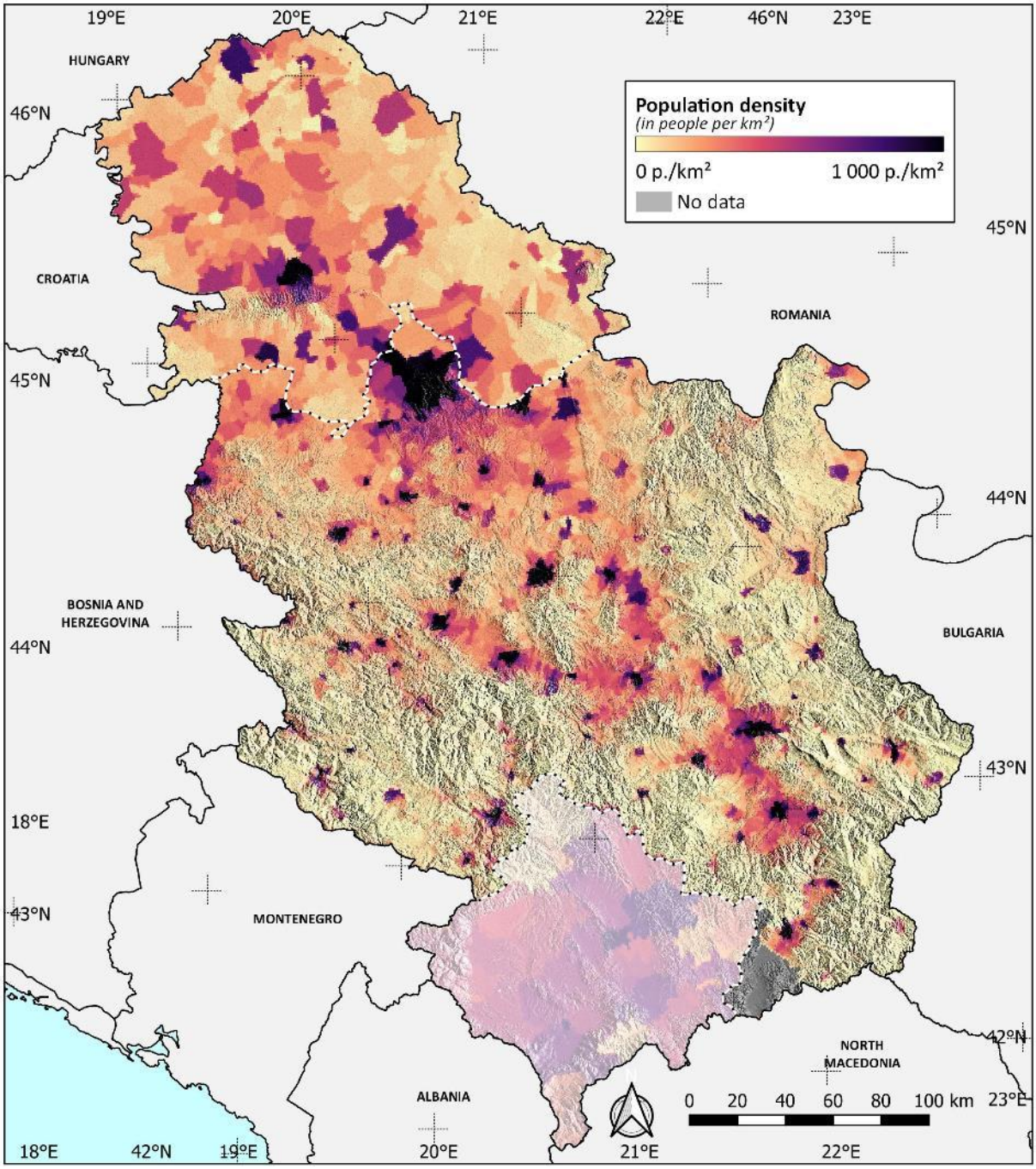

As expected from the demographic trends of the Republic of Serbia (see Figure 14), most of the Serbian population is located in the main urban center, the largest being Belgrade, Novi Sad, and Subotica in

[11] The boundaries and names shown and the designations used on this map do not imply official endorsement or acceptance by the United Nations.

the North, and Kragujevac, Niš and Leskovac in the South. The urban centers of the South of the country are for the most part located in valleys.

Outside the urban centers, the population is higher (50 to 100 people per km^2) and more evenly distributed in the flatland North of the Sava-Danube axis than in the hilly regions of the South. In the South of Serbia, most of the land outside urban center has less than 50 people per km^2.

Road distance to urban centres

To assess the quality of the road network of the Republic of Serbia, the road distance to main urban centers was calculated and presented in Figure 16.

Figure 16 - distribution of the roads distance to urban centers in the Republic of Serbia[12]
Main urban centers were defined as areas where the population density is above 1000 people per km^2. Distance off-road was modeled as 10 times longer than the same distance travelled on a road. Data source: NASA SEDAC GPWv411: UN-Adjusted Population Density (Center for International Earth Science Information Network - CIESIN - Columbia University 2018) and OpenStreetMap (OpenStreetMap Contributors 2020).

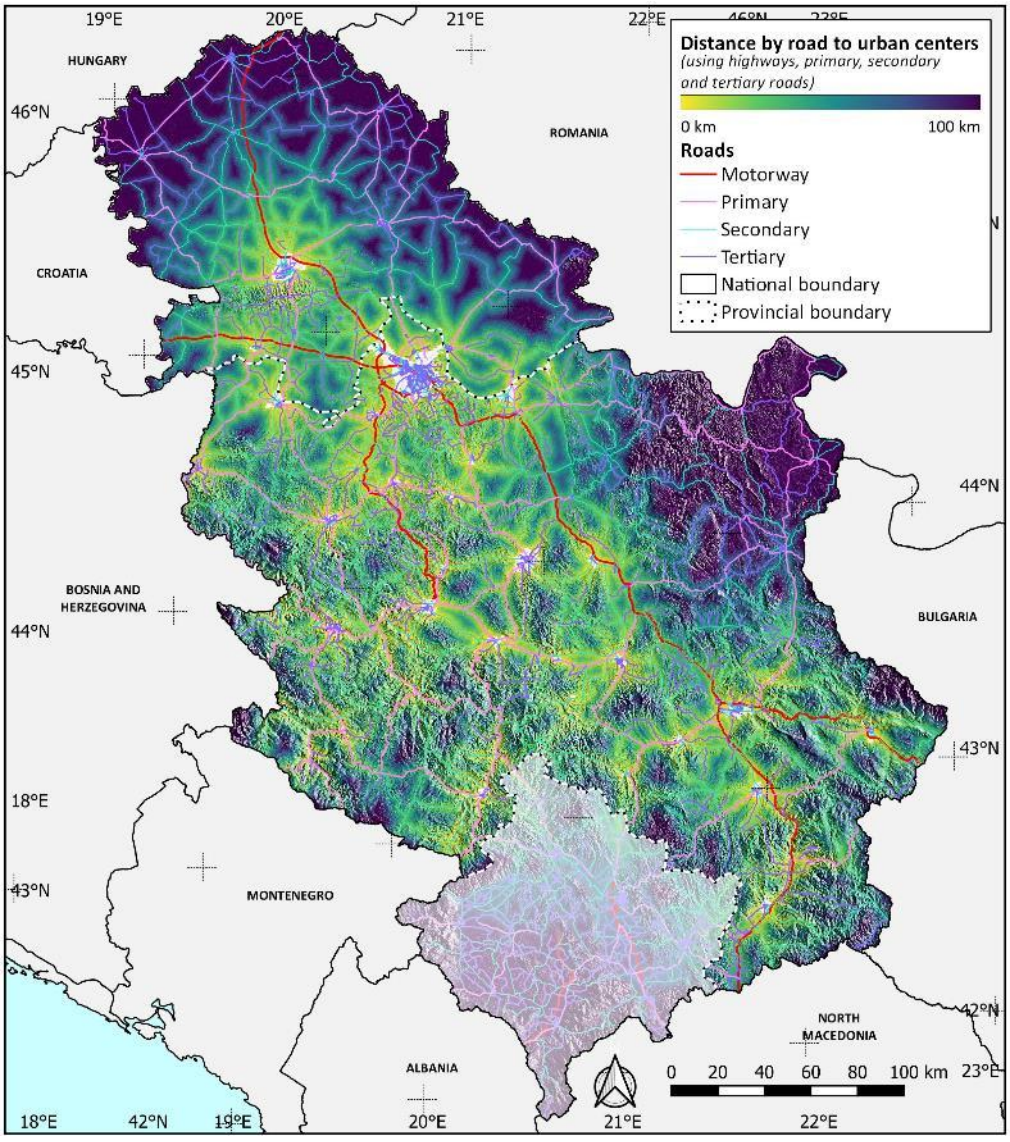

[12] The boundaries and names shown and the designations used on this map do not imply official endorsement or acceptance by the United Nations.

Serbia is relatively well serviced in term of road network. Indeed, the larger part of the country is less than 25 km away from an urban center.

However, there are two less well serviced areas. The first is the Northern borders of the country (borders with Croatia, Hungary, and Romania). Although the region is very well serviced in term of road network, there are not very large urban centers in the area, the larger urban center being Subotica (548 people per km^2). The second least well services area is in the Carpates mountains, at the Eastern border of the country. As for the Northern border region, the Eastern border region is pretty much well serviced in term of road, but lacks very large urban center, the larger urban center in the area being Negotin, with only 346 people per km^2.

Surface water

This section will present the distribution of surface and ground water resources in the Republic of Serbia.

Surface water distribution

The distribution of surface water resources for the Republic of Serbia is presented in Figure 17.

Figure 17 – Distribution of surface water in the Republic of Serbia[13].
In dark blue: *natural free flowing surface water.* ***In red:*** *man-made free flowing surface water.* ***In light blue:*** *still water. The width of the free-flowing surface water is proportional to the stream's water discharge. Map overlayed on a topographic map of the Republic of Serbia (data source: NASA / USGS / JPL-Caltech (Farr et al. 2007), see Figure 1). Data source: JRC Yearly Water Classification History (Pekel et al. 2016), and (Srbijavode 2020)*

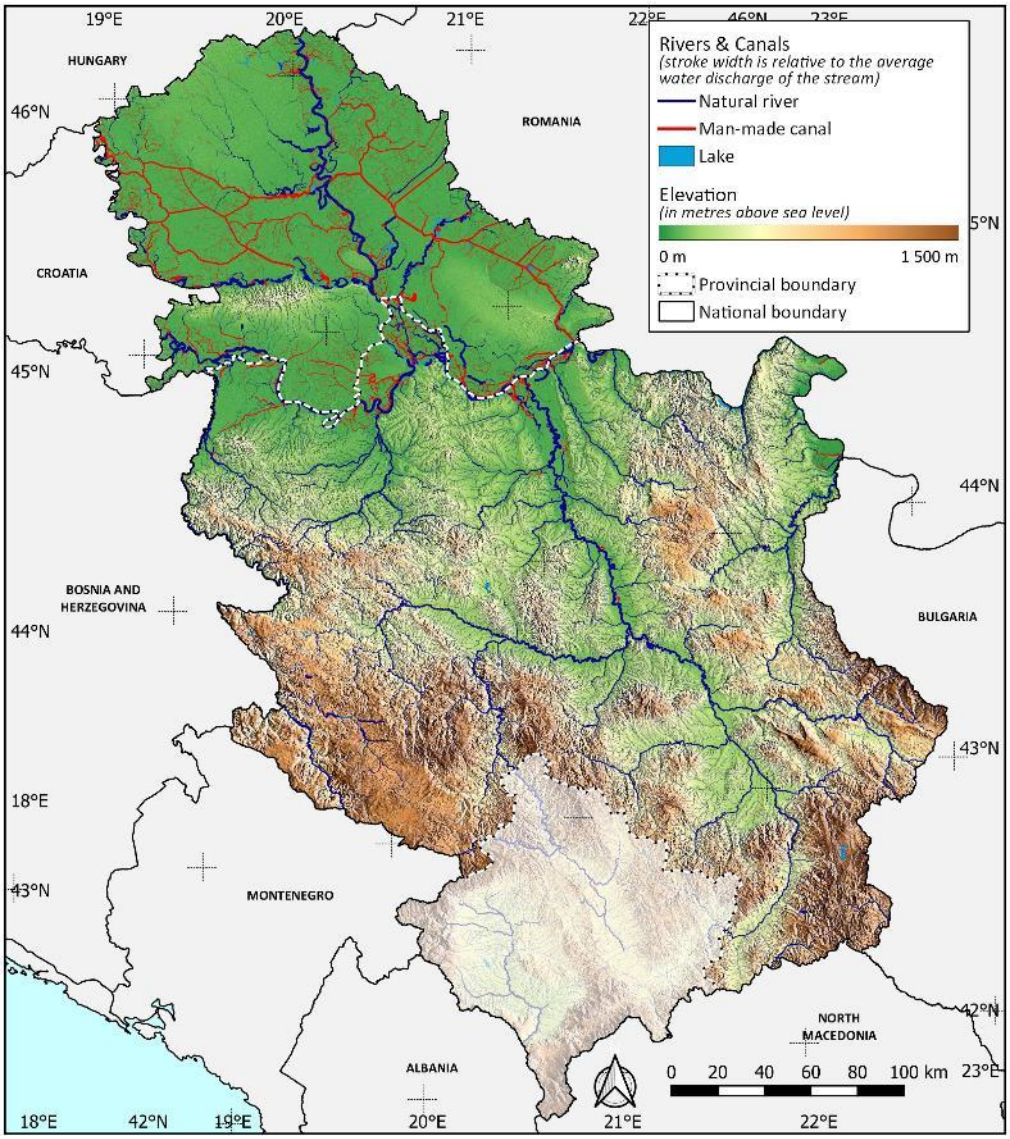

[13] The boundaries and names shown and the designations used on this map do not imply official endorsement or acceptance by the United Nations.

The surface water network in the Republic of Serbia is divided by the Sava-Danube axis into two distinct regions. To the North of the axis, the free-flowing surface water network is dense, with both natural and man-made streams. The region is home to large rivers such as the Danube, Tisa, and Sava, as well as multiple canals of the Danube-Tisa-Danube (DTD) network. Many of these rivers have high discharge ratios, making them significant water sources for the country.

In contrast, the free-flowing surface water network to the South of the Sava-Danube axis is more scattered, primarily consisting of the Morava and Ibar rivers and their tributaries. The Lim River is also present to the South-West, and the Timok River to the South-East. However, the discharge ratio of these rivers is generally lower than those of the Northern rivers, and no large-scale man-made water canals have been constructed in this region.

Regarding lakes and reservoirs, the South of the country is better equipped than the North. There are several significant bodies of water in the region, including the Iron Gate Dam on the Danube in the East, Vlasina Lake in the Southern tip of Serbia, Perućac Lake to the West (on the border with Croatia), and Gruža Lake in the center of the country near Knić municipality (53). In contrast, to the North of the Sava-Danube axis, no large lakes or reservoirs exist, with only a few bogs (such as Zasavica) and shallow fishponds (Ečka and Sakule) present.

Distance to surface water

To assess the potential for water transportation in the Republic of Serbia, we utilized a slope-distance analysis to estimate the cumulative degree-meter distance to the nearest surface water source, as shown in Figure 18. This approach accounts for both the distance and slope, providing a more comprehensive understanding of the topographical challenges facing transportation of water.

The results indicate a substantial difference between the North and South of Serbia in terms of distance to surface water sources. To the North of the Sava-Danube axis, the flat topography and dense surface water network means that a significant portion of the region is located within 2000°.m of a water source, making transportation of surface water relatively straightforward. However, in the South of the country, the more scattered surface water network and hilly topography means that there are very few areas within 2000°.m of a water source, with the exception of the Morava and Ibar valleys.

Figure 18 - Distribution of the distance from surface water in cumulative slope-distance in the Republic of Serbia[14].

Dark blue lines: *natural free flowing surface water stream.* ***Red lines:*** *man-made free flowing surface water stream.* ***In light blue:*** *still water. The width of the free-flowing surface water is proportional to the discharge of the stream.* ***Green line:*** *2 km flying distance from surface water. Data source: JRC Yearly Water Classification History (Pekel et al. 2016), (Srbijavode 2020) and NASA / USGS / JPL-Caltech (Farr et al. 2007)*

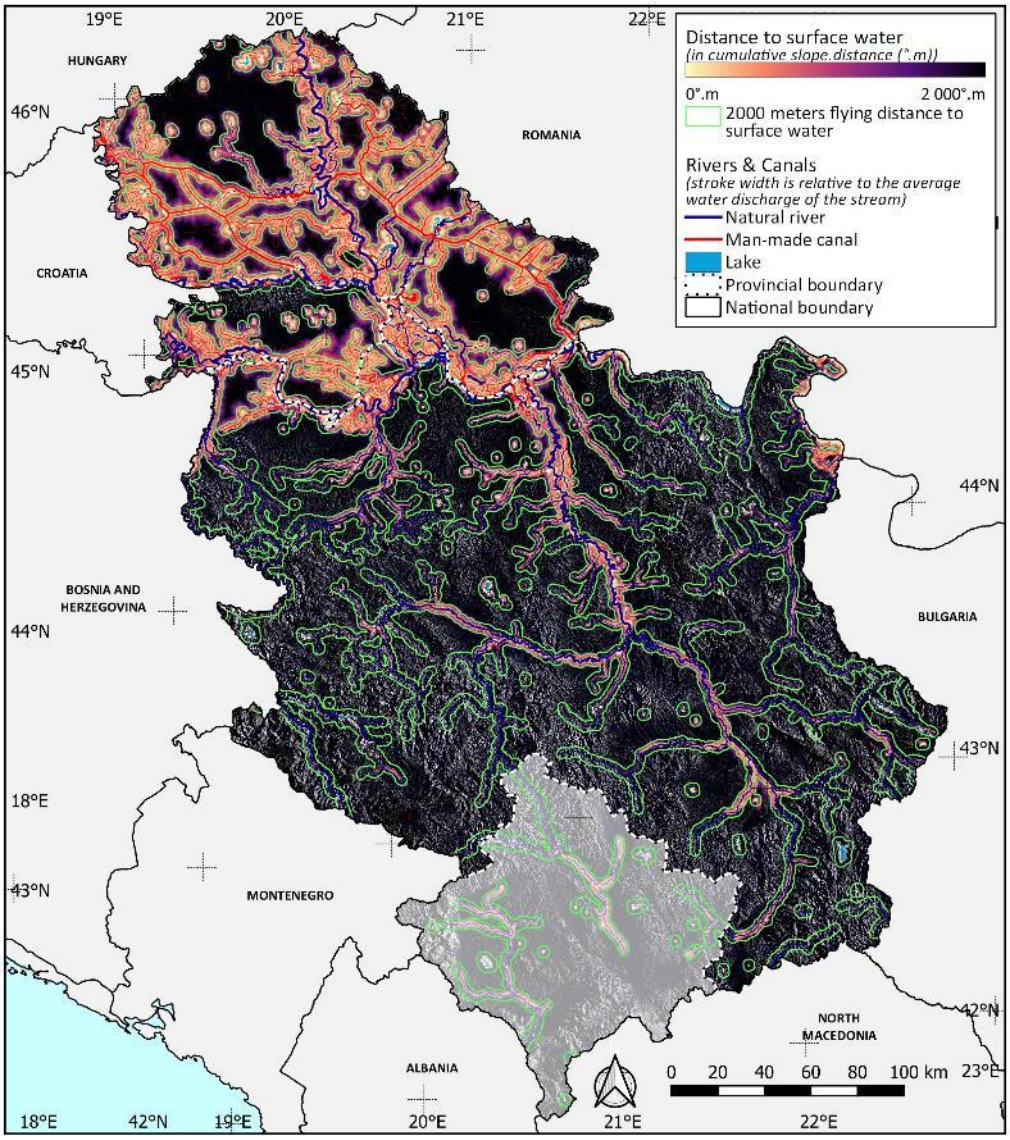

[14] The boundaries and names shown and the designations used on this map do not imply official endorsement or acceptance by the United Nations.

CURRENT CLIMATE

This section will outline the current climate of Serbia.

Summary

Köppen-Geiger climate classification - Serbia has a warm-summer humid continental climate (Dfb) according to the Köppen-Geiger climate classification.

Temperatures - The average temperature in Serbia varies from 0°C in January to 22°C in July. The monthly maximum and minimum temperatures follow the same pattern. Geographically, temperatures show an even distribution throughout the country during both the temperature increase and decrease periods.

Precipitation - The country experiences a rainy season from April to July, with peak precipitation occurring in May and June, with a monthly accumulated precipitation around 70 mm per month. The rest of the year (August to March) presents a baseline monthly accumulated precipitation between 40 to 50 mm per month. Precipitation intensity shows a steady increase from January to June, with a maximum of 6.2 mm/day, then remains relatively stable from June to August before increasing again up to 6.6 mm/day in September and October, before steadily decreasing until January. The monthly spatial distribution shows that precipitation and precipitation intensity are more pronounced in the hills of the south of Serbia than on the flatland of the north.

Wet days & dry spell - Wet days and very wet days increase from January to May-June, and then decrease until October, with September and October having less accumulated wet days (but more intense precipitation, see precipitation intensity). Dry spells are at their lowest during the wet season, increase until August, and then stay stable until October, before decreasing until April. The spatial distribution of wet days and very wet days is higher in the hills of the South of Serbia than in the flatland of the North, with very wet days being more common in the North during the peak of the wet season. The duration of dry spells is longer in the North and South valleys than in the Hilltops of the South.

Frost days, ice days, & chill hours - Frost days, ice days, and chill hours in Serbia peak in January and then steadily decrease until April-May where zero is reached. These indices resume their increase in September-October, and on average the first frost days and chill hours appear in October, while the first ice days appear in November. The monthly spatial distribution of these indices shows that they are more numerous and persist for a longer period on the higher altitudes of the south of the country.

Summer days & tropical nights - Summer days and tropical nights peak in August before steadily decreasing. There are no more tropical nights on average past October, and no more summer days on average past November. Summer days and tropical nights resume their increase in March and May, respectively, and steadily increase until August. Summer days and tropical nights are more numerous in the flat lands of the North and valleys of the South of the country. Tropical nights are more numerous in the Belgrade region during peak months (July and August) probably due to the high albedo and heat absorption capacity of artificial surfaces.

Degree days - Degree days in Serbia first appear in March and steadily increase until July, reaching close to 400-degree days. Degree days remain stable in July and August and then sharply decrease and to reach zero in December. The distribution of degree days is strongly related to topography, with higher values at low altitudes in the flat lands of the North and valleys of the South. This distribution remains constant throughout the year.

Water deficit - Water deficit in Serbia peaks in July and August at around 150 mm and steadily decreases until it is close to 0 mm in December and January, before increasing steadily back to its

maximum in July and August. The decrease period (August to December) is steeper than the increase period (January to July). The seasonal spatial distribution of the monthly accumulated water deficit is related to the topography, with high values in low altitude areas of the North and South. This distribution remains constant throughout the year.

Snowfall & snow depth - Snowfall typically begins in October and increases gradually until January, reaching slightly more than 30 mm of water equivalent per month, and then steadily decreases until May when no more snowfall occurs. Similarly, snow cover appears in October and increases until February, reaching slightly more than 30 mm of water equivalent, then sharply decreases until May when there is no more snow cover. The highest altitude areas of the Southeast and Southwest having the most snow. There is very little snowfall or snow depth north of the Sava-Danube axis, except for the top of the Fruška Gora range in January and February.

NDVI & LAI - the NDVI and LAI are at their minimum in January (2700 for NDVI and 2.3 for LAI) and then slowly increase, reaching their maximum in June and July, respectively. They then decrease towards their respective January levels, with LAI decreasing in a sigmoid shape and NDVI decreasing constantly. The distribution of NDVI and LAI is higher in higher altitudes where agriculture is less practical and the presence of forests is more significant. The South of the Sava-Danube axis has higher values of NDVI and LAI due to the presence of high altitudes and forests, with the Morava River valleys being cold spots. In contrast, the North of the Sava-Danube axis has lower and more evenly distributed values of NDVI and LAI, except in urban areas like Belgrade, where values remain low until June, and the top of Fruška Gora, where both indices are higher. Harvesting is noticeable as patches of sharp decreases in NDVI and LAI from June to September, starting from the Northeast.

Temperatures

This section provides an overview of the seasonal temperature variations in the Republic of Serbia, highlighting the following key metrics: average temperature (TG), maximum temperature (TX), minimum temperature (TN).

Figure 19 presents the current seasonal variations of monthly average, maximum, and minimum temperatures in the Republic of Serbia. The data in the chart represents a 30-year average (1990-2019).

Figure 19 – Current monthly variations of the monthly average, minimum and maximum temperatures
Data averaged over the 1990-2019 period. ***Light dotted line****: variable value from each weather station separately.* ***Dark full line:*** *median value of the variable.* ***In yellow:*** *monthly maximum temperature.* ***In green:*** *monthly average temperature.* ***In blue:*** *monthly minimum temperature.* ***In red dashed line:*** *variable value using ERA5 database. Data source: Republic Hydrometeorological Service of Serbia, HidMet (Republic Hydrometeorological Service of Serbia 2020) and ERA5 - ECMWF / Copernicus Climate Change Service (Muñoz Sabater 2019).*

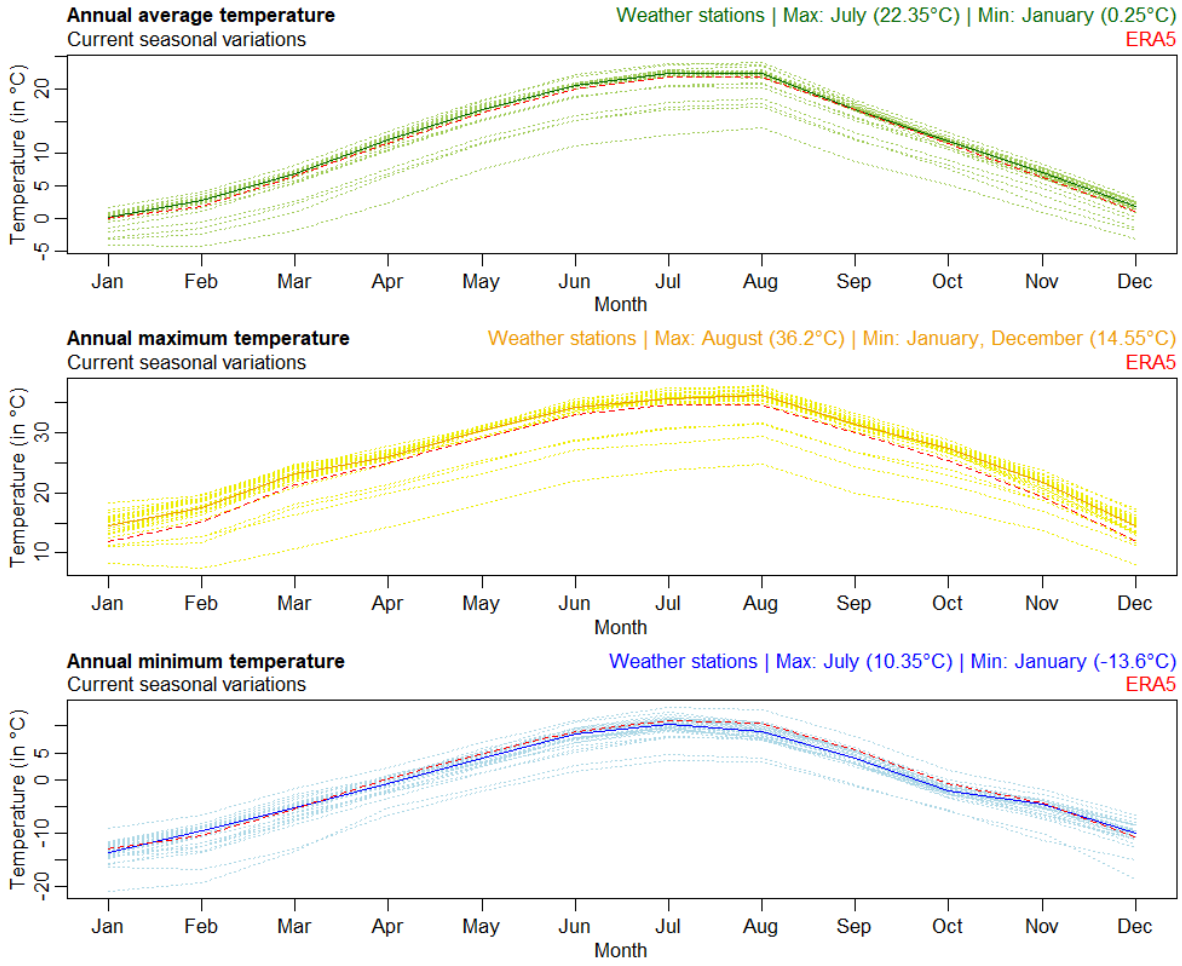

Over the 30-year period, the monthly average, minimum, and maximum temperatures in Serbia showed a steady increase, starting from a low point in January (TG around 0°C, TX around 14°C, TN around -13°C) and peaking in July and August (TG around 22°C, TX around 36°C, TN around 10°C), followed by a gradual decline through to January.

Figure 21 and Figure 20 illustrate the current spatial distribution of seasonal temperatures across Serbia. The average, maximum, and minimum temperatures show a constant distribution throughout the country during both the temperature increase period (January to July) and the temperature decrease period (August to December), with lower values at higher altitudes.

Figure 20 – current spatial distribution of monthly minimum and maximum temperatures[15]
*Data averaged over the 1990-2019 period**. In orange:** monthly maximum temperature, **In blue:** monthly minimum temperature. Data source: ERA5 - ECMWF / Copernicus Climate Change Service (Muñoz Sabater 2019).*

[15] The boundaries and names shown and the designations used on this map do not imply official endorsement or acceptance by the United Nations.

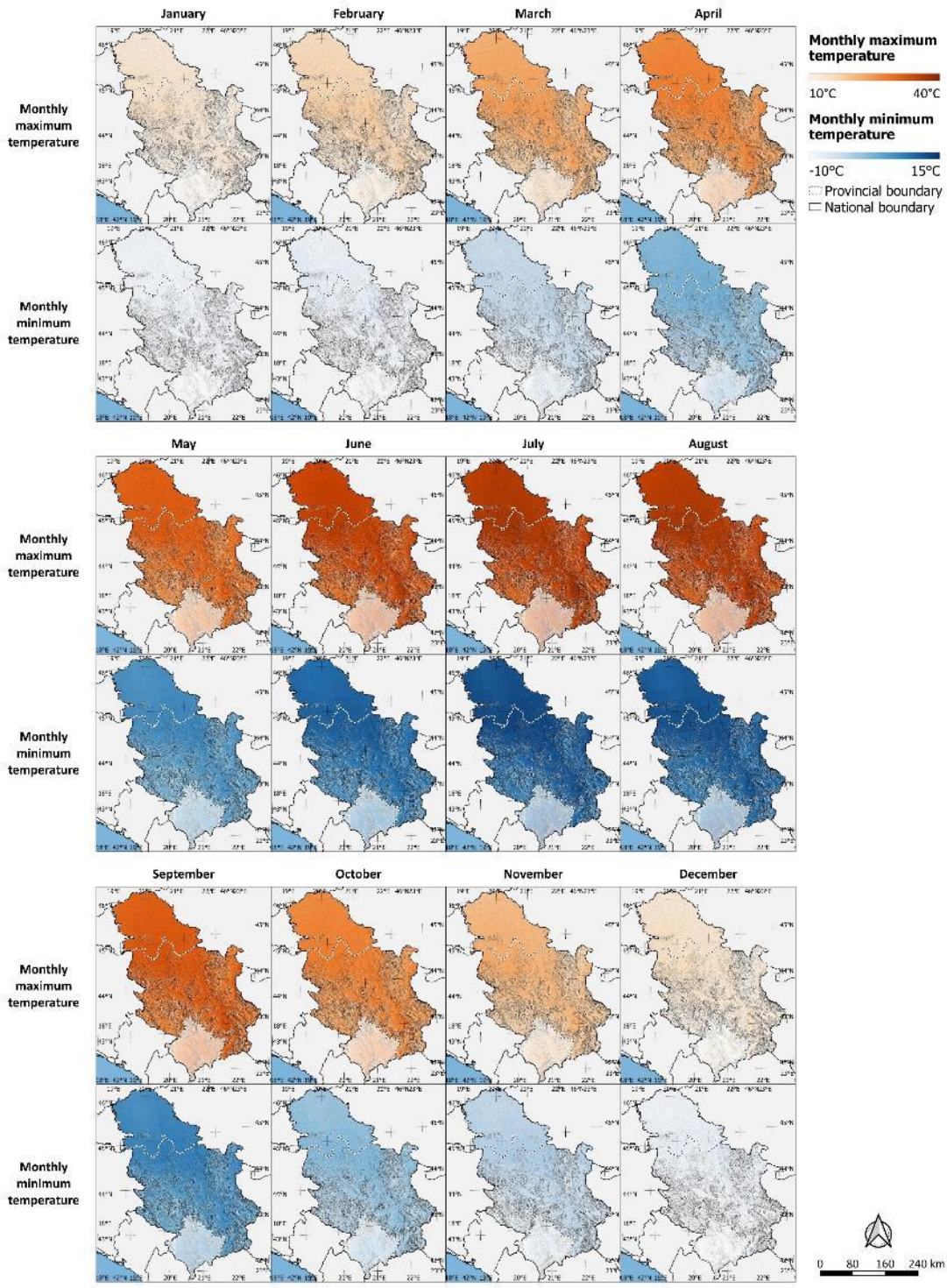

Figure 21 – Current spatial distribution of monthly average temperature[16]

Data averaged over the 1990-2019 period. Data source: ERA5 - ECMWF / Copernicus Climate Change Service (Muñoz Sabater 2019).

[16] The boundaries and names shown and the designations used on this map do not imply official endorsement or acceptance by the United Nations.

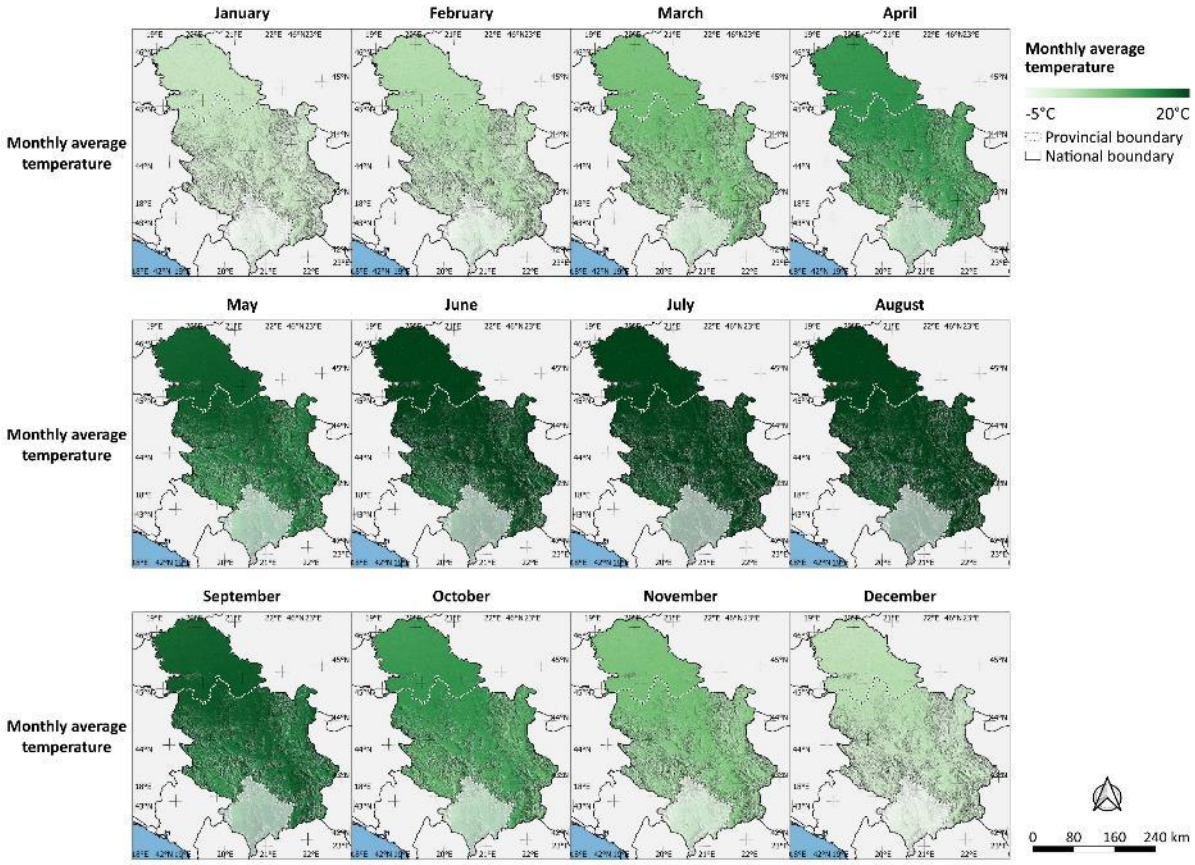
January
February
March
April
May
June
July
August
September
October
November
December
Monthly average temperature
Monthly average temperature
-5°C
20°C
Provincial boundary
National boundary
0 80 160 240 km

Precipitation

In this section, we will provide an overview of the current seasonal variations of precipitation in the Republic of Serbia. Our focus will be on two key metrics: accumulated precipitation (RR) and average precipitation intensity (RRx). Precipitation intensity is defined as the average amount of precipitation that falls on a rainy day. It is calculated by dividing the accumulated precipitation over a given period by the number of rainy days during that period. As we were unable to obtain daily data on precipitation from the local weather stations the analysis of historical trends of precipitation intensity was based on ERA5 data.

Figure 22 illustrates the current seasonal variations of monthly accumulated precipitation and average precipitation intensity in Serbia. The data in the chart represents a 30-year average (1990-2019) of RR and RRx.

Figure 22 – Current monthly variations of accumulated precipitation and average precipitation intensity *Data averaged over the 1990-2019 period.* ***In light blue:*** *accumulated precipitation for each weather station.* ***In dark blue full line:*** *median value of accumulated precipitation, calculated over all weather stations.* ***In red:*** *variable calculated with ERA5 data. Data source: ERA5 - ECMWF / Copernicus Climate Change Service (Muñoz Sabater 2019) and Republic Hydrometeorological Service of Serbia, HidMet (Republic Hydrometeorological Service of Serbia 2020).*

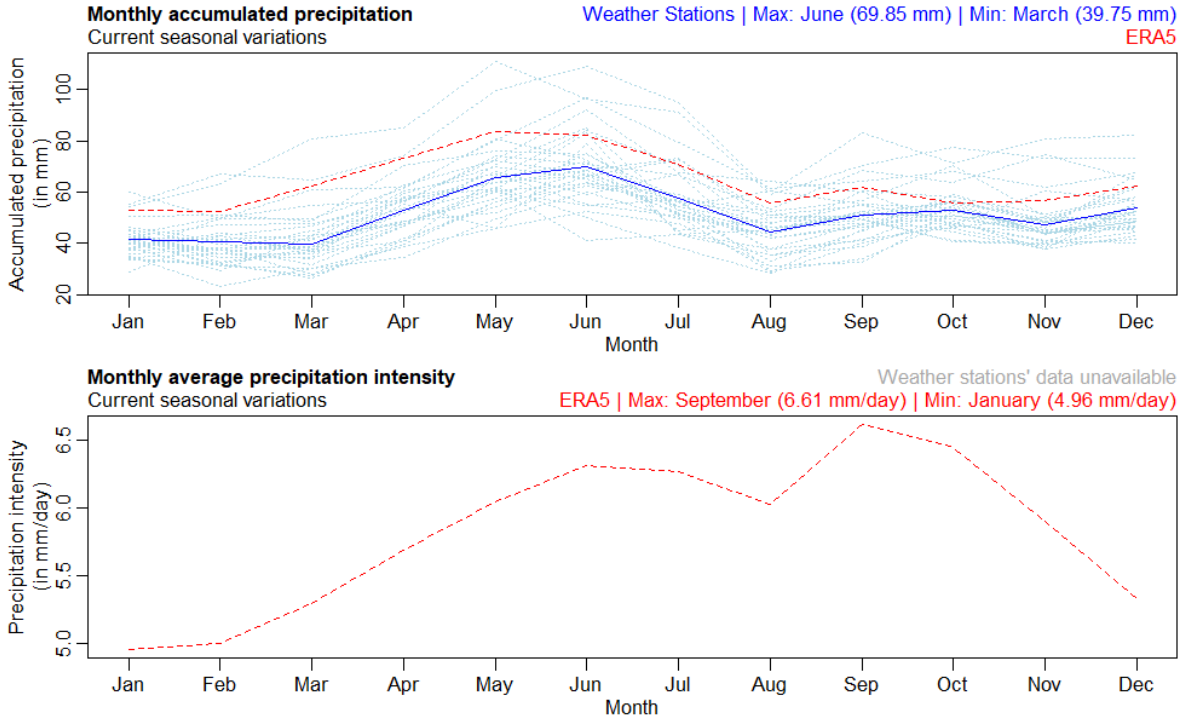

In Serbia, the rainy season occurs between April and July, peaking in May and June, with a monthly accumulated precipitation (RR) of around 70 mm. For the rest of the year (August to March), the country experiences a baseline monthly accumulated precipitation of between 40 to 50 mm.

The precipitation intensity shows a steady increase from 5 mm/day in January to 6.2 mm/day in June. It then remains relatively stable from June to August before increasing again to 6.6 mm/day during September and October. The September and October period is thus characterized by less accumulated precipitation than the rainy season (May-June), but more intense precipitations.

Figure 23 shows the monthly spatial distribution of accumulated precipitation and average precipitation intensity across Serbia. RR and RRx are more pronounced in the hills of the south than on the flatlands of the north, particularly during the rainy season (from April to July).**Error! Reference source not found.**

Figure 23 – Current spatial distribution of monthly accumulated precipitation and average precipitation intensity[17]

Data averaged over the 1990-2019 period. ***In blue:*** *monthly accumulated precipitation.* ***In red:*** *monthly average precipitation intensity. Data source: ERA5 - ECMWF / Copernicus Climate Change Service (Muñoz Sabater 2019).*

[17] The boundaries and names shown and the designations used on this map do not imply official endorsement or acceptance by the United Nations.

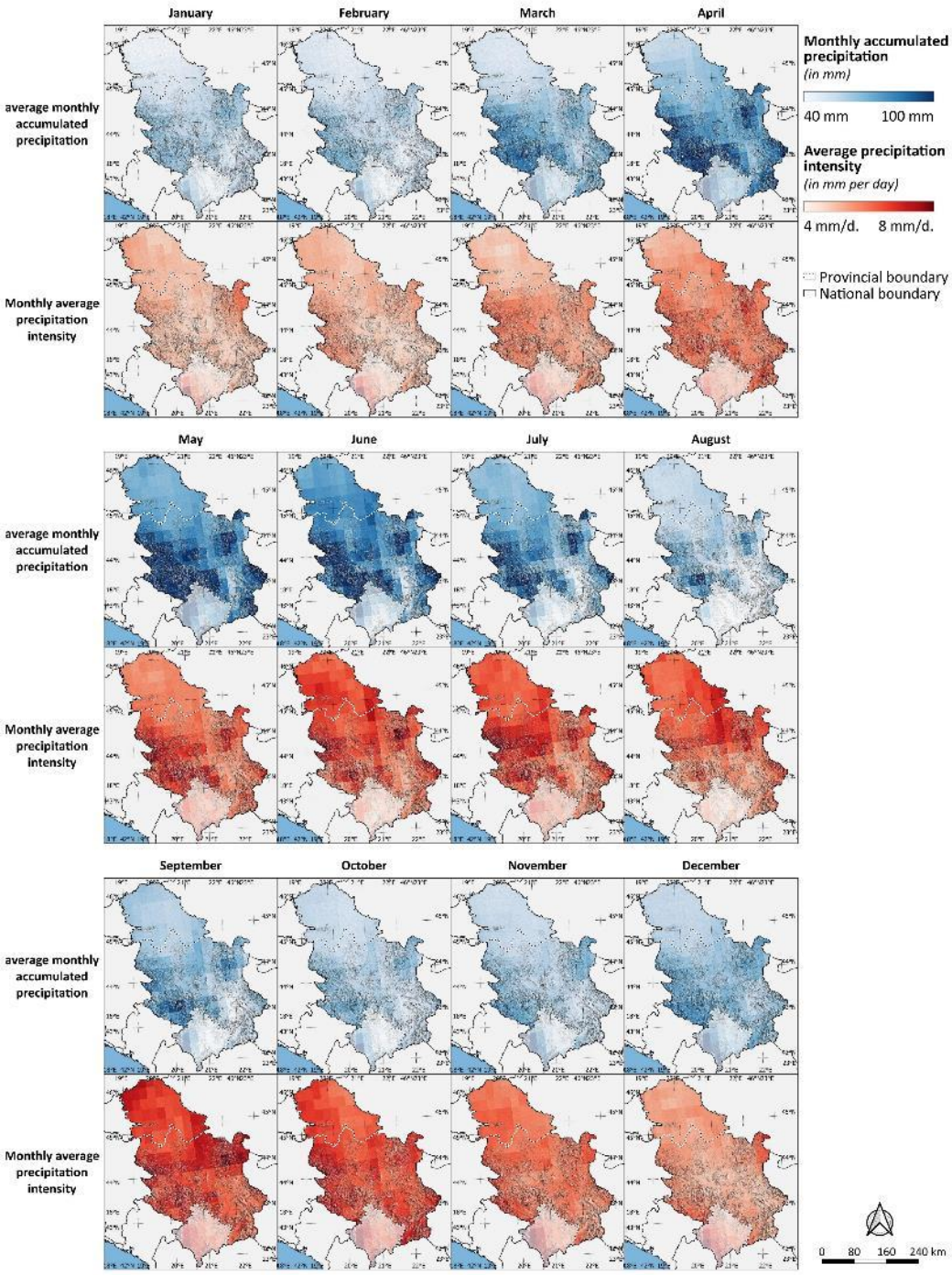
January
February
March
April
May
June
July
August
September
October
November
December
average monthly accumulated precipitation
Monthly average precipitation intensity
Monthly accumulated precipitation
(in mm)
40 mm
100 mm
Average precipitation intensity
(in mm per day)
4 mm/d.
8 mm/d.
Provincial boundary
National boundary
0
80
160
240 km

Wet days & dry spells

This section presents variations in wet days, very wet days, and the duration of the longest dry spell in the Republic of Serbia. Accumulated wet days (WD) are defined as the number of days over a given period where the accumulated precipitation is greater than 1 mm, while accumulated very wet days (VWD) defined as the number of days over a given period where the accumulated precipitation is greater than the 95th quantile of the daily accumulated precipitations over the period. The duration of the longest dry spell (DS) is defined as the largest number of consecutive days over a given period where the daily accumulated precipitation is below 1 mm.

As wet days, very wet days, and the duration of the longest dry spell are calculated at a daily level, this section uses ERA5 data for historical trends, as daily data from weather stations were not available.

Figure 24 – Current monthly variation of accumulated wet days, accumulated very wet days, and the duration of the longest dry spell.
Data averaged over the 1990-2019 period. ***In green:*** *monthly accumulated wet days.* ***In blue:*** *monthly accumulated very wet days.* ***In red:*** *duration of the longest dry spell of the month. Data source: ERA5 - ECMWF / Copernicus Climate Change Service (Muñoz Sabater 2019).*

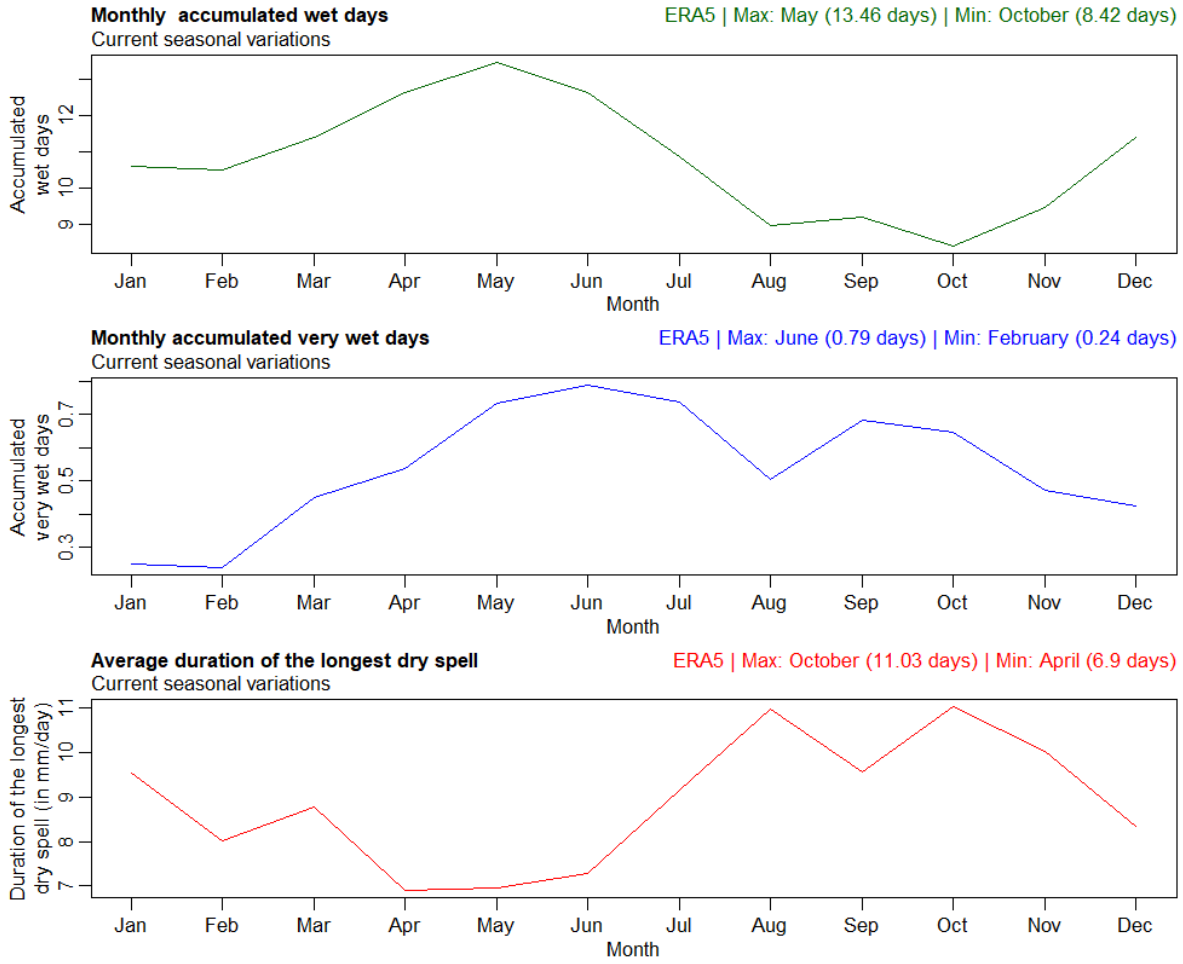

Figure 24 presents the current seasonal variations of WD, VWD, and DS averaged over 30 years (1990 to 2019). As expected, WD and VWD follow the increasing pattern of monthly accumulated precipitation from January (WD: 10.5 days, VWD: 0.2 days) until the rainy season in May-June, reaching

13 wet days and 0.8 very wet days per month. Both indices decrease from June to August. In September and October, while WD continues to decrease below its January level (reaching around 9 wet days), VWD starts to increase. This highlights the fact that September and October have fewer accumulated wet days, but the wet days that occur during these months are more intense (=very wet days), confirming the increase in precipitation intensity observed in Figure 22. After October, VWD decreases and WD increases to reach their respective January levels.

During the wet season, DS is at its lowest (around 7 days). It increases sharply until August, reaching 11 days, and stays stable until October (around 10-11 days), further confirming that September and October have fewer wet days but more intense ones. In November, DS steadily decreases until April.

The current spatial distribution of wet days, very wet days, and the duration of the longest dry spell for each month across Serbia is depicted in Figure 26 and Figure 25. Similar to RR and RRx, WD and VWD are more prevalent in the hills of the South of Serbia compared to the flatlands of the North. This difference is particularly noticeable during the wet season from April to July. Interestingly, during the peak of the wet season (June), very wet days become more frequent in the flatlands of the North than in the valleys of the South, while the hilltops of the South still experience a high number of very wet days.

Figure 25 – Current spatial distribution of the duration of the longest dry spell of the month[18]
Data averaged over the 1990-2019 period. Data source: ERA5 - ECMWF / Copernicus Climate Change Service (Muñoz Sabater 2019).

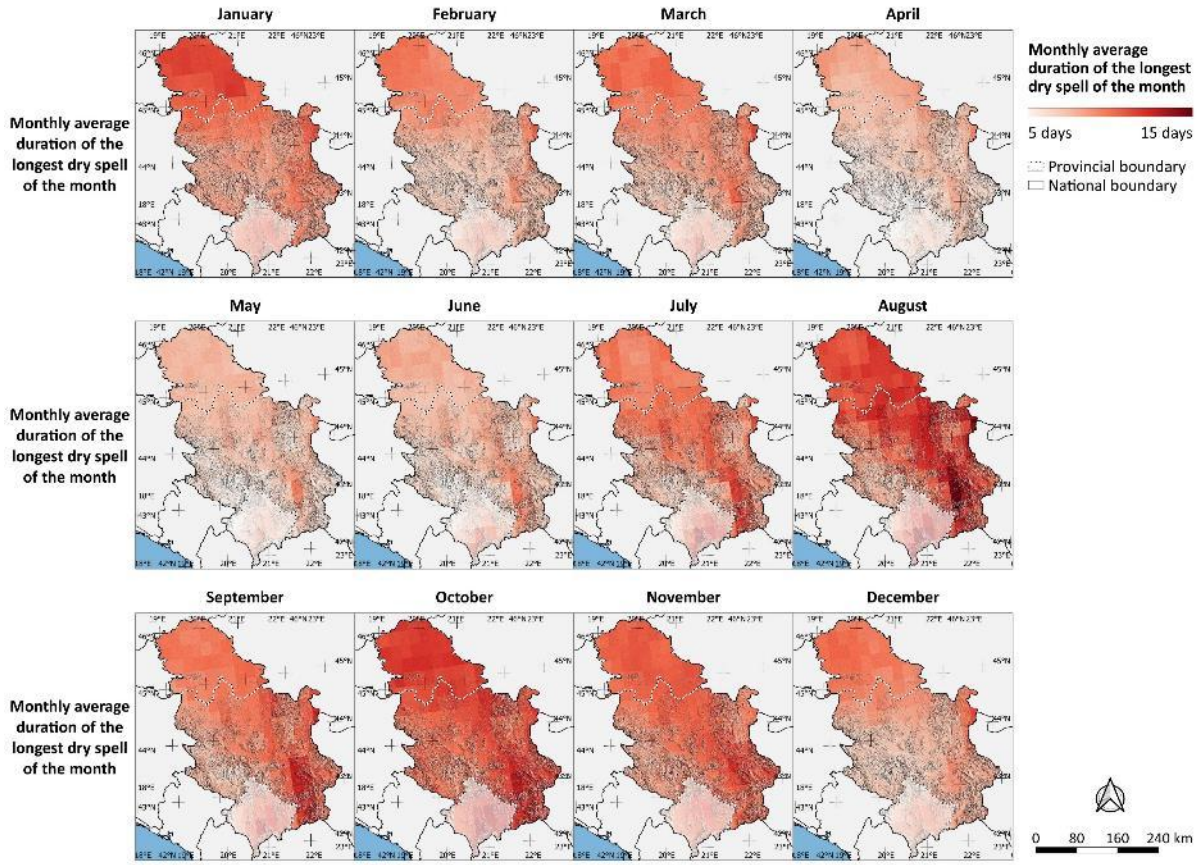

[18] The boundaries and names shown and the designations used on this map do not imply official endorsement or acceptance by the United Nations.

Figure 26 – Current spatial distribution of monthly accumulated wet days and very wet days[19]
*Data averaged over the 1990-2019 period**. In green:** monthly accumulated wet days. **In blue:** monthly accumulated very wet days. Data source: ERA5 - ECMWF / Copernicus Climate Change Service (Muñoz Sabater 2019).*

[19] The boundaries and names shown and the designations used on this map do not imply official endorsement or acceptance by the United Nations.

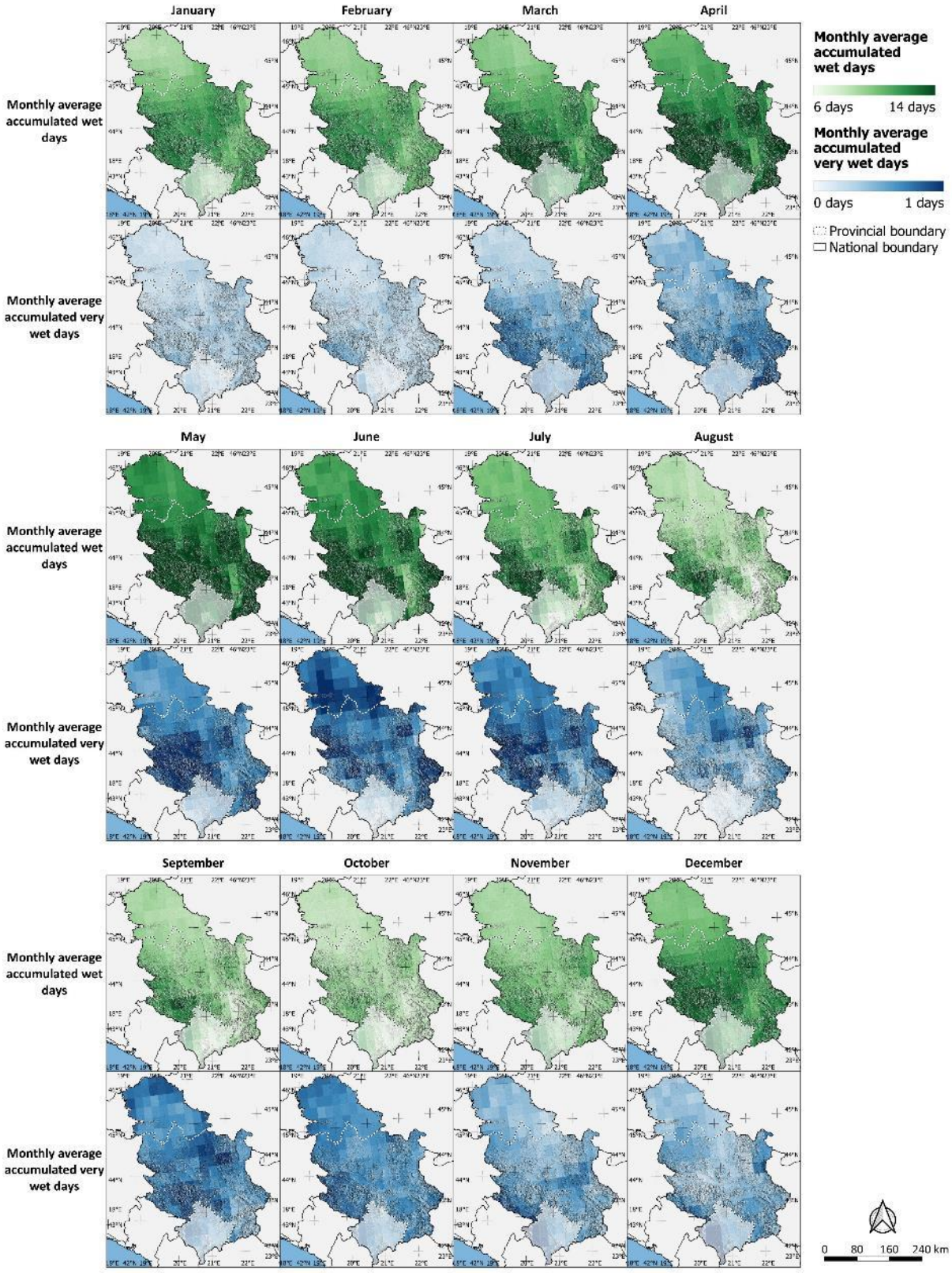
January
February
March
April
May
June
July
August
September
October
November
December
Monthly average accumulated wet days
Monthly average accumulated very wet days
Monthly average accumulated wet days
6 days
14 days
Monthly average accumulated very wet days
0 days
1 days
Provincial boundary
National boundary
0
80
160
240 km

Frost days, ice days & chill hours

In this section, we will explore the variations of frost days, ice days, and chill hours in the Republic of Serbia. Accumulated frost days (FD) are defined as the number of days over a given period when the daily minimum temperature is below 0°C, while accumulated ice days (ID) are defined as the number of days over a given period when the daily maximum temperature is below 0°C. Finally, accumulated chill hours (CH) are defined as the number of hours over a given period when the daily average temperature is below 0°C.

Since frost days, ice days, and chill hours are calculated at a daily or hourly scale, and daily data from weather stations were not available, this section will only present variables calculated using ERA5 data for historical trends. Moreover, as hourly predictions of average temperature were not available, the projected chill hours were defined as the number of days where the average daily temperature was below 0°C, multiplied by 24.

Figure 27 – Current monthly variations of frost days, ice days, and chill hours
*Data averaged over the 1990-2019 period**. In green:** monthly accumulated frost days. **In blue:** monthly accumulated ice days. **In red:** monthly accumulated chill hours. Data source: ERA5 - ECMWF / Copernicus Climate Change Service (Muñoz Sabater 2019).*

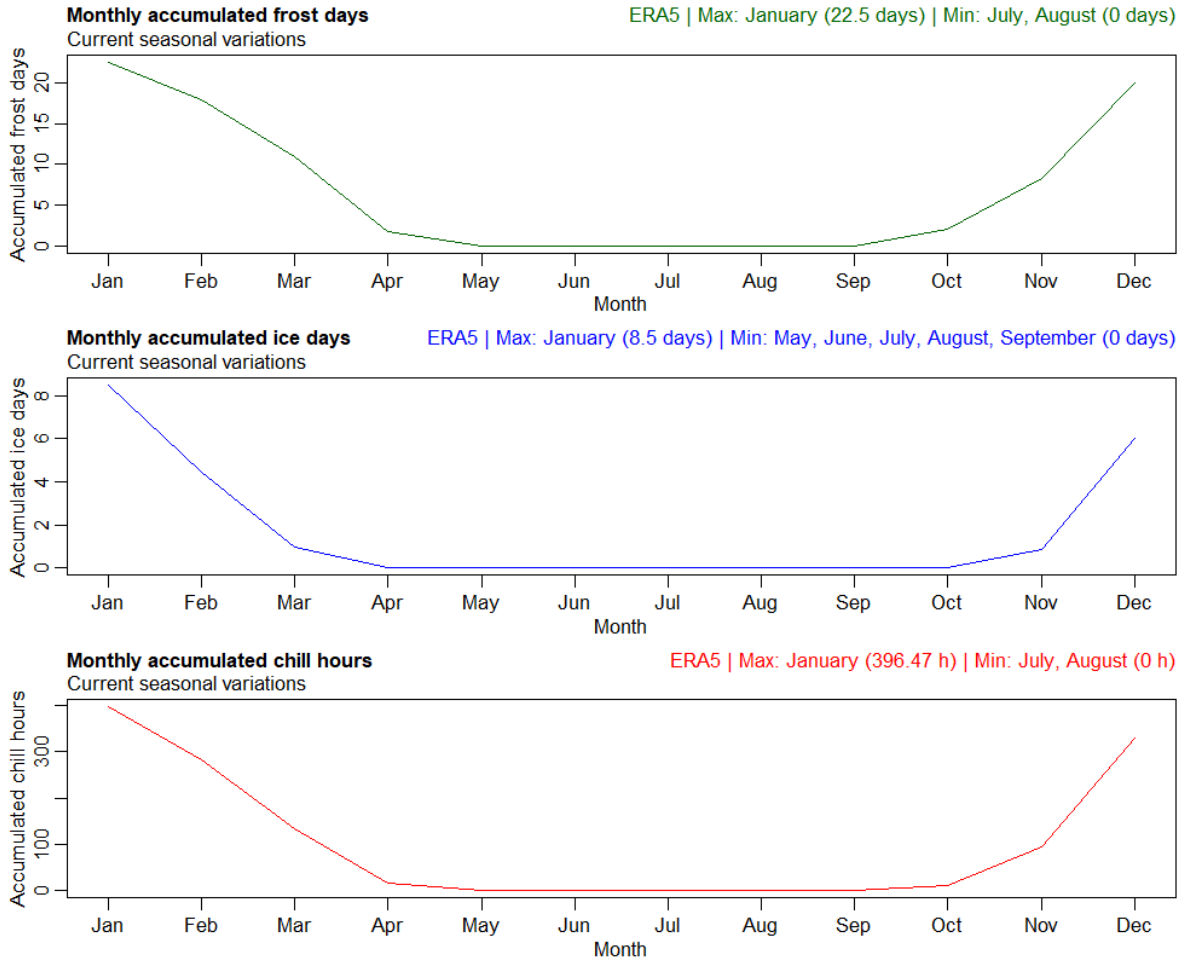

Figure 27 shows the current seasonal variation of frost days, ice days, and chill hours in the Republic of Serbia. FD, ID, and CH follow the same general pattern. The three indices peak in January (around 22 days for FD, 8 days for ID, and about 400h for CH). They then steadily decrease from January to April

- May. On average, there are no more ice days after March and no more chill hours and frost days after April. These indices reappear in September - October. On average, the first frost days and chill hours appear in October while the first ice days appear in November. These three indices then increase back until January.

The spatial distribution of frost days, ice days, and chill hours are illustrated in Figure 29 and Figure 28. As expected, these indices tend to be more frequent and long-lasting at higher elevations in the southern regions of the country. This trend is consistent with the pattern observed for minimum temperatures, indicating that the severity and duration of cold weather events are more pronounced in mountainous areas.

Figure 28 – Current spatial distribution of the monthly accumulated chill hours[20]
Data averaged over the 1990-2019 period. Data source: ERA5 - ECMWF / Copernicus Climate Change Service (Muñoz Sabater 2019).

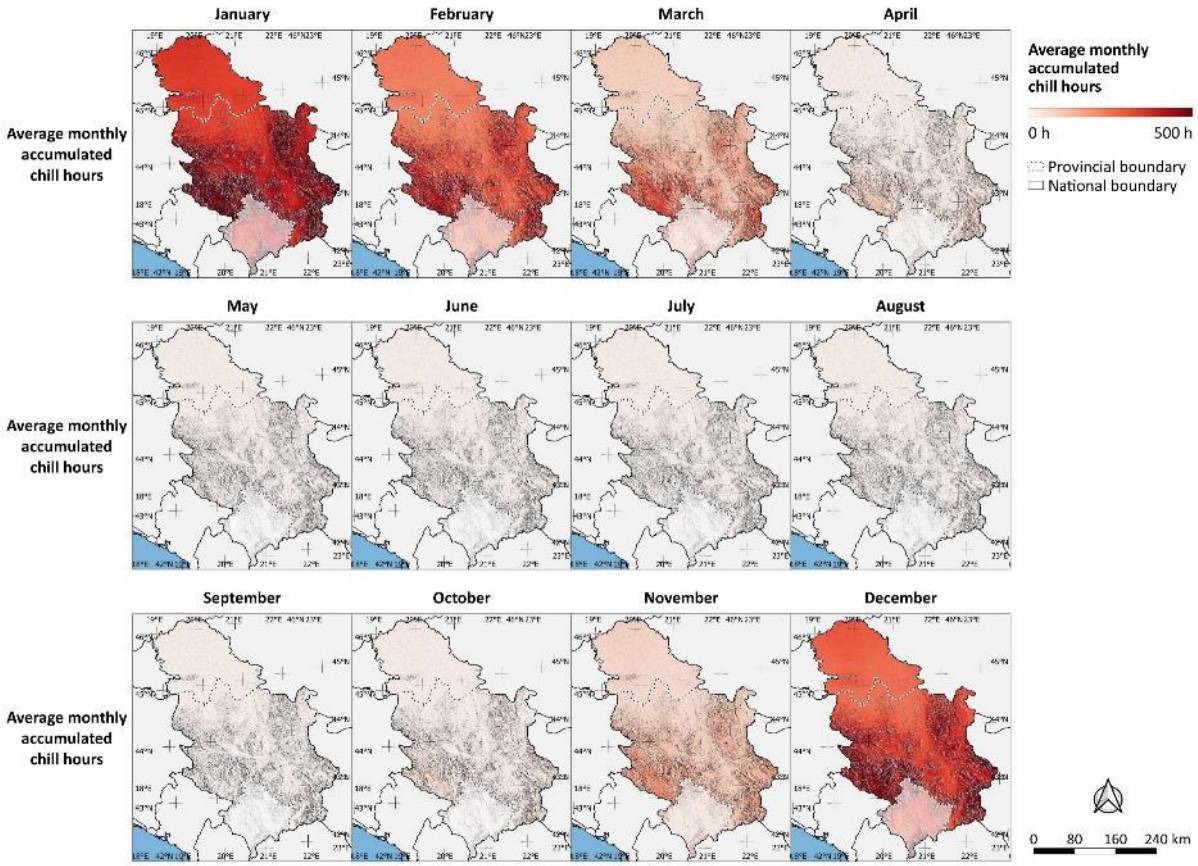

[20] The boundaries and names shown and the designations used on this map do not imply official endorsement or acceptance by the United Nations.

Figure 29 – Current spatial distribution of monthly accumulated frost days and ice days[21]
Data averaged over the 1990-2019 period. ***In green:*** *monthly accumulated frost days.* ***In blue:*** *Monthly accumulated ice days. Data source: ERA5 - ECMWF / Copernicus Climate Change Service (Muñoz Sabater 2019).*

[21] The boundaries and names shown and the designations used on this map do not imply official endorsement or acceptance by the United Nations.

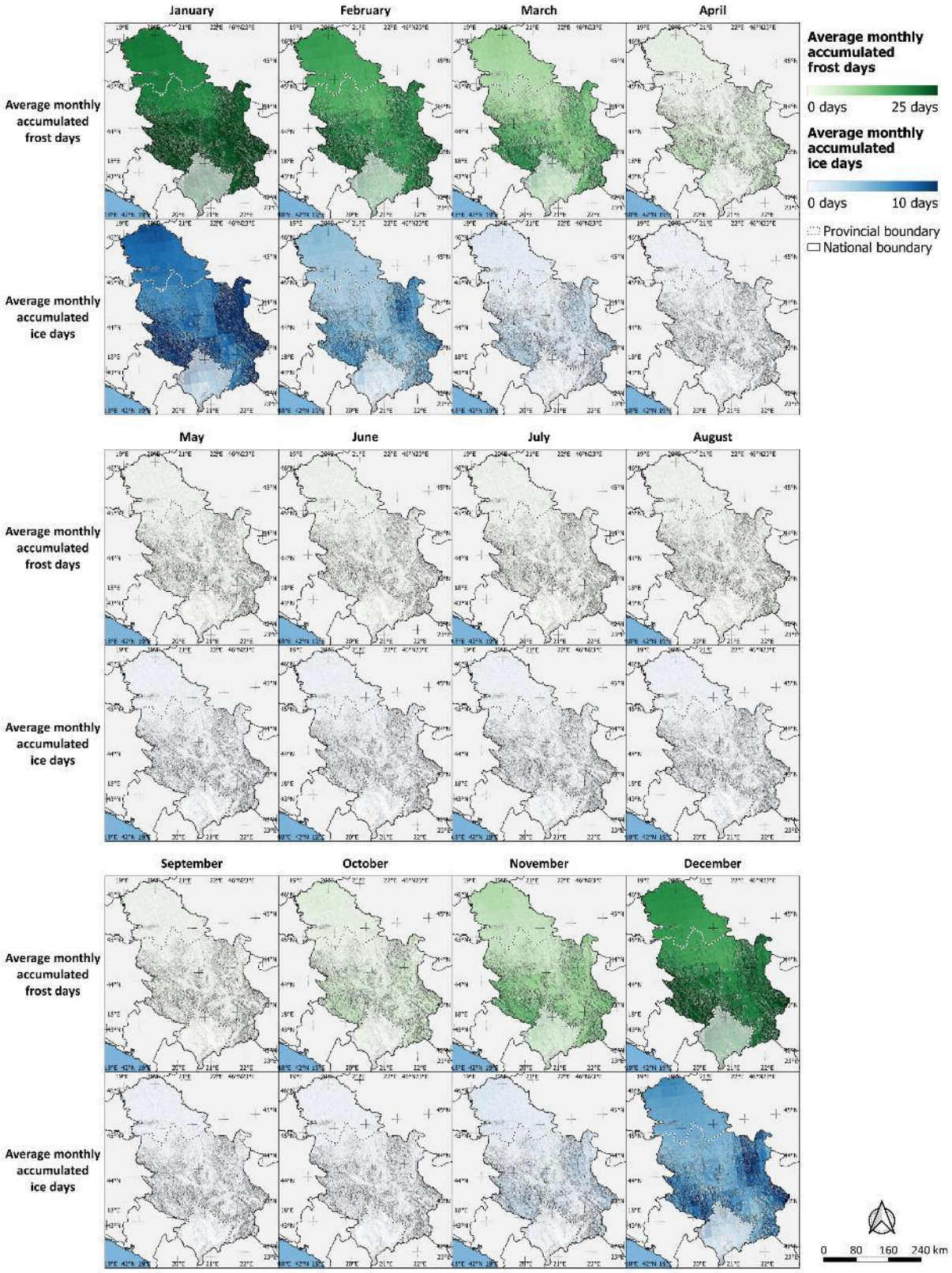
January
February
March
April
May
June
July
August
September
October
November
December
Average monthly accumulated frost days
Average monthly accumulated ice days
Average monthly accumulated frost days
0 days
25 days
Average monthly accumulated ice days
0 days
10 days
Provincial boundary
National boundary
0
80
160
240 km

Summer days & tropical nights

In this section, we'll examine the seasonal variations of summer days and tropical nights in the Republic of Serbia. Accumulated summer days (SD) are defined as the number of days over a given period when the daily maximum temperature exceeds 25°C, while accumulated tropical nights (TrN) are defined as the number of days over a given period when the daily minimum temperature is above 20°C.

Since accumulated summer days and tropical nights are calculated at a daily or hourly level, and daily weather station data wasn't available, we'll only present variables calculated using ERA5 data for historical trends.

Figure 30 shows the current seasonal variation of SD and TrN in the Republic of Serbia, averaged over 30 years (1990 to 2019).

Figure 30 – Current monthly variations of summer days and tropical nights
Data averaged over the 1990-2019 period. ***In green:*** *monthly accumulated summer days.* ***In red:*** *monthly accumulated tropical night. Data source: ERA5 - ECMWF / Copernicus Climate Change Service (Muñoz Sabater 2019).*

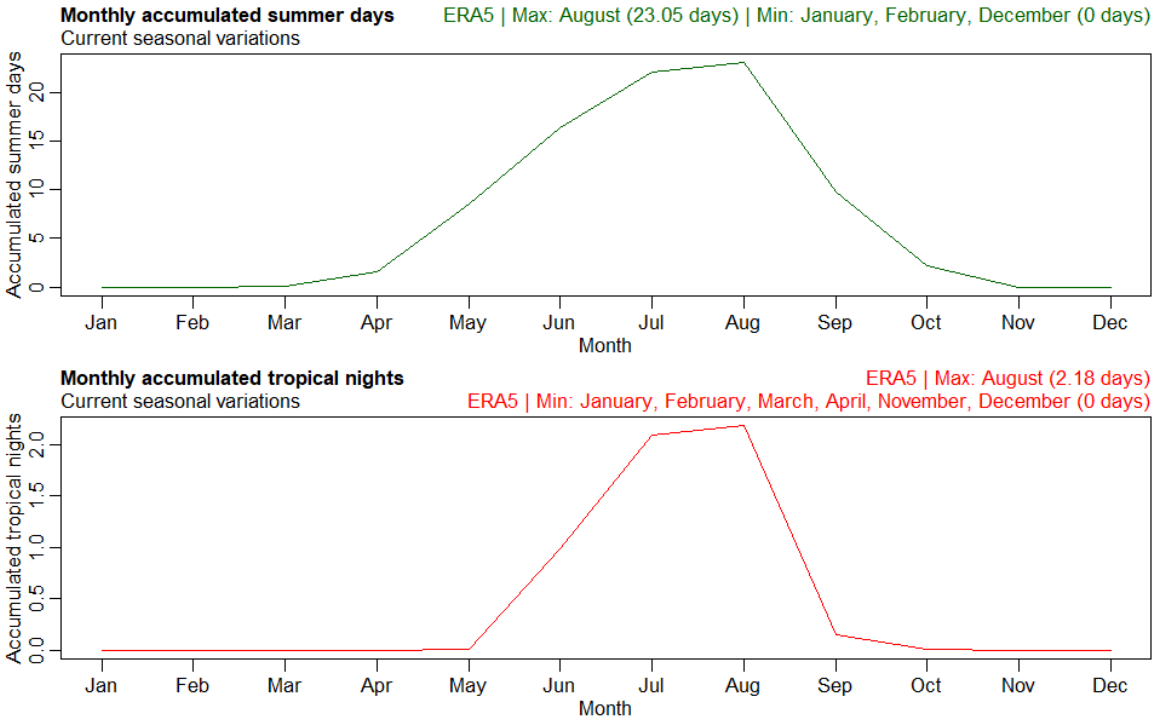

In Serbia, summer days and tropical nights peak in August with 23 days of summer and 2.2 days of tropical nights, before steadily decreasing. By October, there are no more tropical nights on average, and by November, there are no more summer days. However, summer days reappear in March and steadily increase until August, while tropical nights reappear in May and also steadily increase until August. It's worth noting that there are very few tropical nights in Serbia, with a maximum of 2.2 monthly in August.

The monthly spatial distribution of summer days and tropical nights throughout Serbia can be observed in Figure 31. These days tend to be more numerous and persist for a longer period in the flat lands of the North and in the valleys of the South, where the altitude is lower.

Notably, the Belgrade region experiences a higher number of tropical nights during the peak months of July and August. This may be attributed to the high albedo and heat absorption capacity of a large number of artificial surfaces present in the area (as seen in Figure 3).

Figure 31 – Current spatial distribution of monthly accumulated summer days and tropical nights[22].
Data averaged over the 1990-2019 period. ***In green:*** *summer days.* ***In red:*** *tropical nights. Data source: ERA5 - ECMWF / Copernicus Climate Change Service (Muñoz Sabater 2019).*

[22] The boundaries and names shown and the designations used on this map do not imply official endorsement or acceptance by the United Nations.

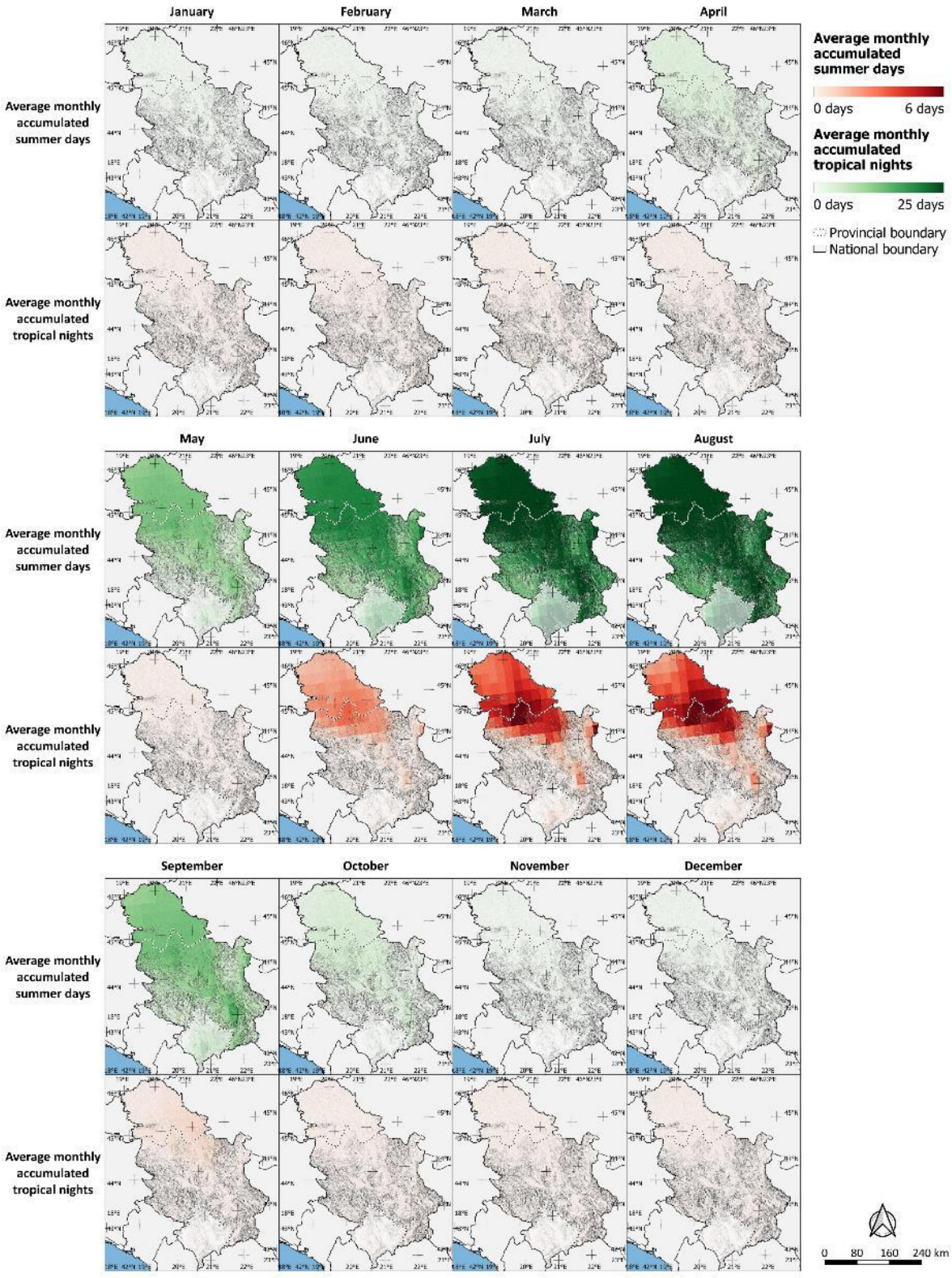

Degree days

In this section, we will examine the seasonal variation of accumulated degree days (DD) and hardiness zones (HZ) in the Republic of Serbia. Degree days are defined as the daily accumulated degree above 10°C and are calculated based on the daily mean temperature. They represent the amount of heat

accumulated throughout the day. As daily data from weather stations were not available, we have used ERA5 data for historical trends to calculate the degree days. H

Figure 32 presents the current seasonal variation of monthly accumulated degree days in the Republic of Serbia, which are averaged over 30 years (1990 to 2019).

Figure 32 – Current monthly variations of degree days

Data averaged over the 1990-2019 period. Data source: ERA5 - ECMWF / Copernicus Climate Change Service (Muñoz Sabater 2019)

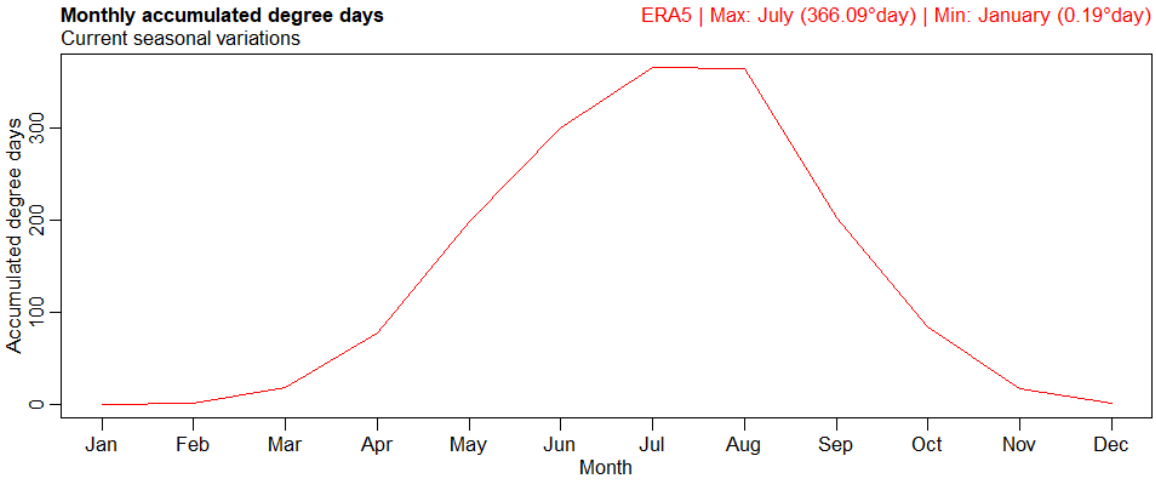

March marks the beginning of the first monthly accumulated degree days, as the daily mean temperature reaches 10 °C. The degree days then steadily increase from March to July, reaching almost 400-degree days. Throughout July and August, the degree days remain stable, before decreasing sharply until December, when they disappear entirely.

To observe the monthly spatial distribution of degree days across Serbia, refer in Figure 33. It is noteworthy that the distribution of degree days throughout the country is strongly related to its topography. The flatlands of the North and the valleys in the South experience higher values of degree days, which remain relatively constant throughout the year.

Figure 33 – Current spatial distribution of monthly accumulated degree days[23]

Data averaged over the 1990-2019 period. Data source: ERA5 - ECMWF / Copernicus Climate Change Service (Muñoz Sabater 2019).

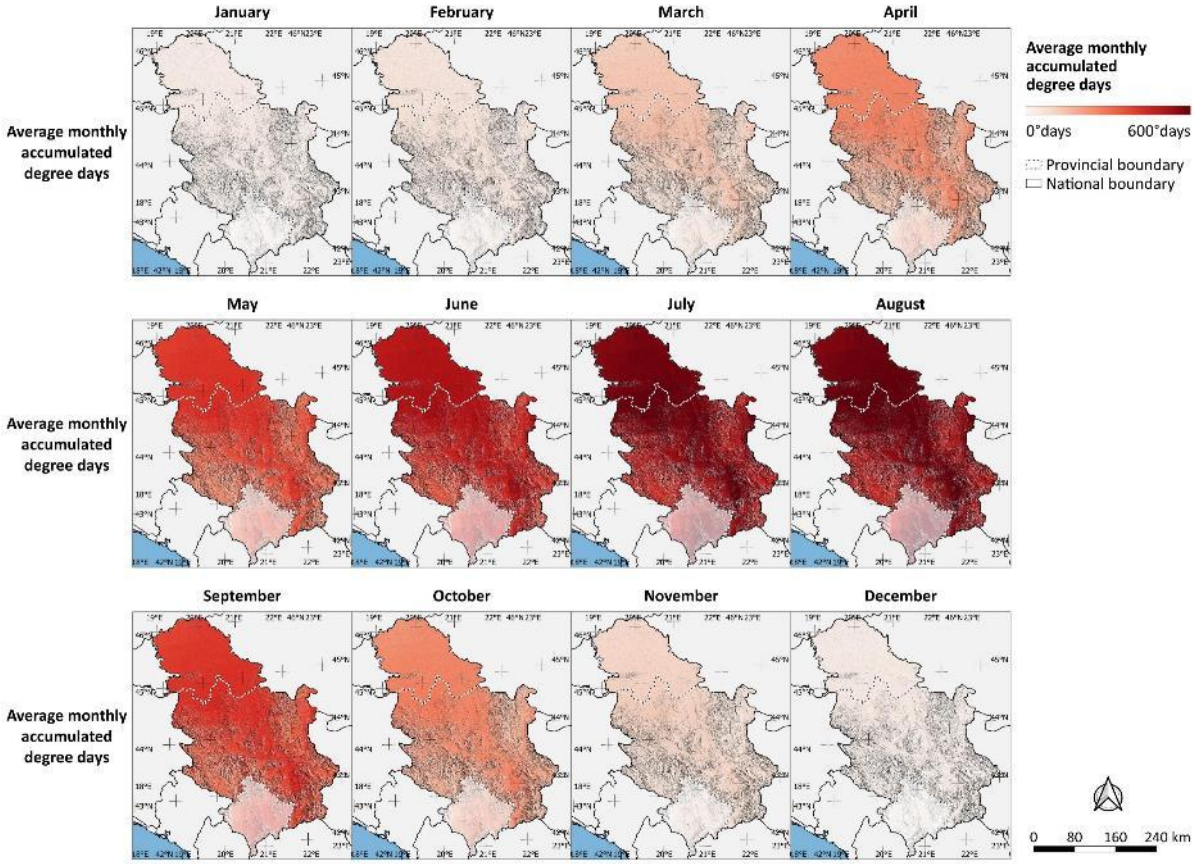

[23] The boundaries and names shown and the designations used on this map do not imply official endorsement or acceptance by the United Nations.

Water deficit

This section provides an overview of the accumulated water deficit in the Republic of Serbia. The water deficit (Wdef) is calculated as the difference between measured evapotranspiration (ET) and potential evapotranspiration (PET). It should be noted that ET and PET were not available in the weather stations dataset. Therefore, we used Terra Net Evapotranspiration to calculate the water deficit for this section.

Figure 34 illustrates the seasonal variation of the monthly accumulated water deficit in the Republic of Serbia.

Figure 34 – Current seasonal variation or monthly accumulated water deficit
Data averaged over the 2001-2019 period. Data source: NASA LP DAAC - EBMOD16A2.006: Terra Net Evapotranspiration (Running, Mu, and Zhao 2021).

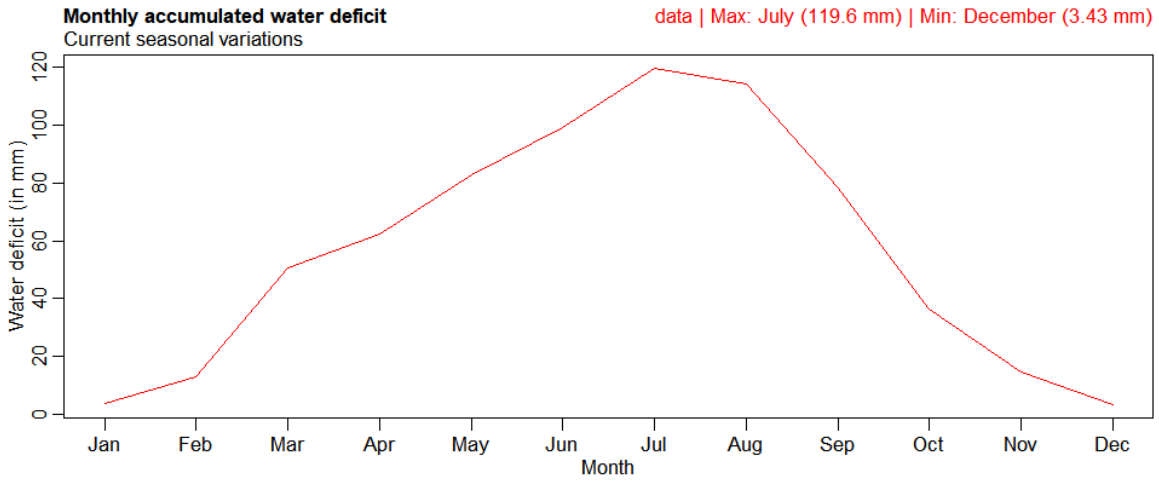

The monthly accumulated water deficit in the Republic of Serbia peaks during July and August, with values around 150 mm. It then steadily decreases until December-January, where the water deficit reaches close to 0 mm. The deficit then increases steadily back to its maximum during July-August. Notably, the decrease period from August to December is steeper than the increase period from January to July.

To observe the current seasonal spatial distribution of the monthly accumulated water deficit throughout Serbia, refer to Figure 35. The distribution of water deficit is strongly related to the country's topography. High water deficit values are visible in low altitude areas, such as the flatlands of the North and the valleys in the South. This distribution pattern remains constant throughout the year.

Figure 35 – Spatial distribution of the monthly accumulated water deficit in the Republic of Serbia[24].
Data averaged over the 2001-2019 period. Data source: NASA LP DAAC - EBMOD16A2.006: Terra Net Evapotranspiration (Running, Mu, and Zhao 2021).

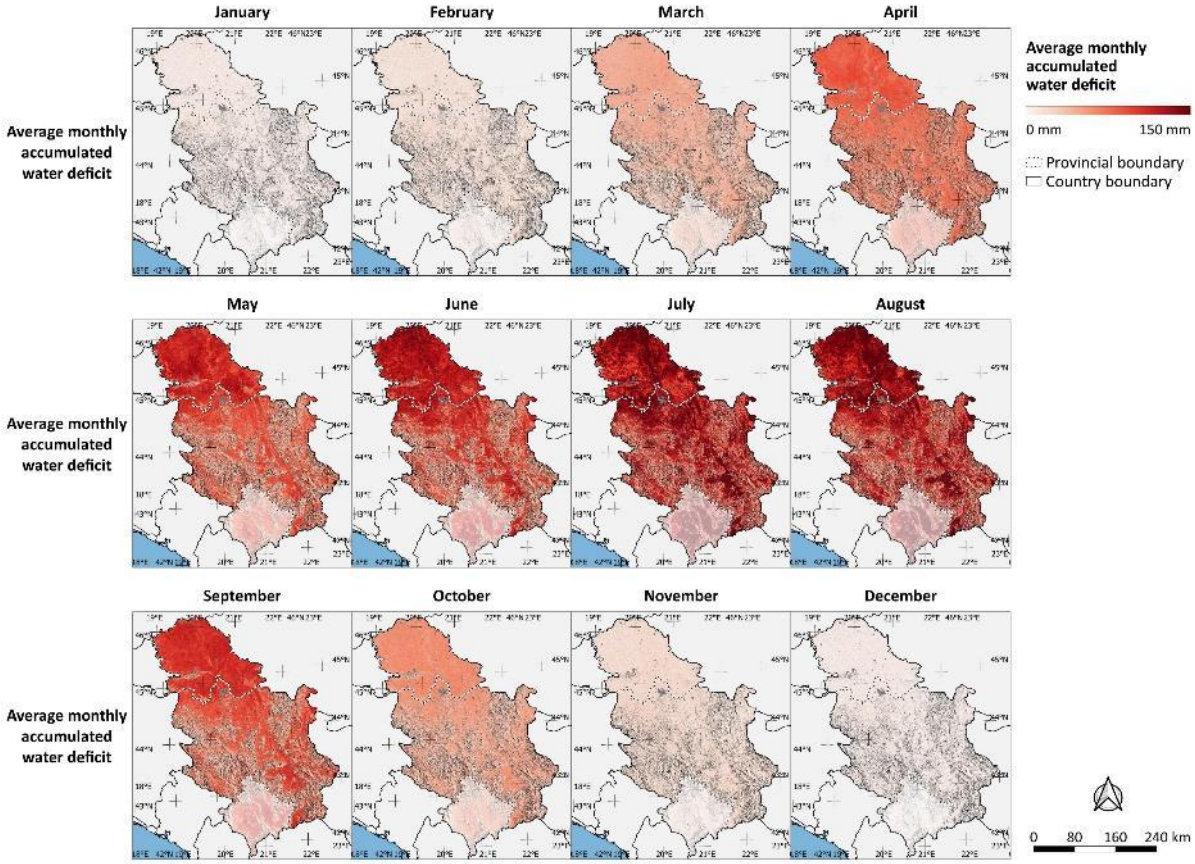

[24] The boundaries and names shown and the designations used on this map do not imply official endorsement or acceptance by the United Nations.

Snowfall & snow depth

This section provides an overview of two snow variables in the Republic of Serbia: Accumulated Snowfall (SnF) and Average Snow Depth (SnD). SnF represents the accumulated snowfall in mm of water equivalent, while SnD represents the average snow depth in mm of water equivalent.

It should be noted that snowfall and snow depth data were not available in the weather stations dataset. Therefore, we used GLDAS data to calculate these variables for this section.

Figure 36 illustrates the seasonal variation of snowfall and snow depth in the Republic of Serbia.

Figure 36 – Current seasonal variation of accumulated snowfall and average snow depth
Data averaged over the 2000-2019 period. ***In blue:*** *monthly accumulated snowfall.* ***In green:*** *monthly averaged snow depth. Data source: NASA GES DISC - GLDAS-2.1: Global Land Data Assimilation System (Rodell et al. 2004).*

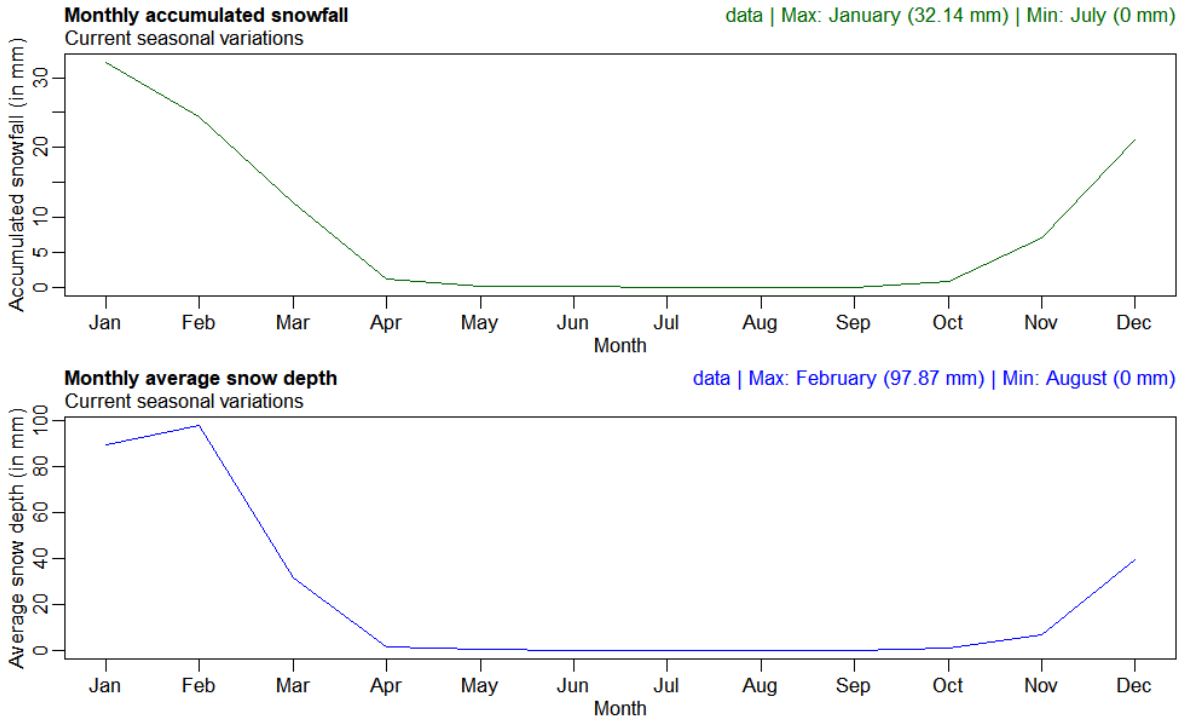

In the Republic of Serbia, the snowfall season starts in October and gradually intensifies until January, when it reaches slightly over 30 mm of water equivalent per month. Subsequently, it decreases steadily until May, when no more snowfall is observed. The trend of snow depth follows a similar pattern. Snow cover appears in Serbia with the first snowfall of October and then increases until February, when it reaches slightly over 30 mm of water equivalent. After that, it sharply decreases until May, when no more snow cover can be found.

Figure 39 displays the seasonal variation of the snowfall and snow depth in the Republic of Serbia. The spatial distribution of snowfall and snow depth during the snow season is primarily concentrated in the highest altitudes of the Southeast and Southwest regions. There is almost no snowfall or snow depth to the North of the Sava-Danube axis, except for the top of the Fruška Gora range during January and February.

Figure 37 – Spatial distribution of the current variation of accumulated snowfall and average snow depth[25]
*Data averaged over the 2000-2019 period**. In blue:** monthly accumulated snowfall. **In green:** monthly averaged snow depth. Data source: NASA GES DISC - GLDAS-2.1: Global Land Data Assimilation System (Rodell et al. 2004).*

[25] The boundaries and names shown and the designations used on this map do not imply official endorsement or acceptance by the United Nations.

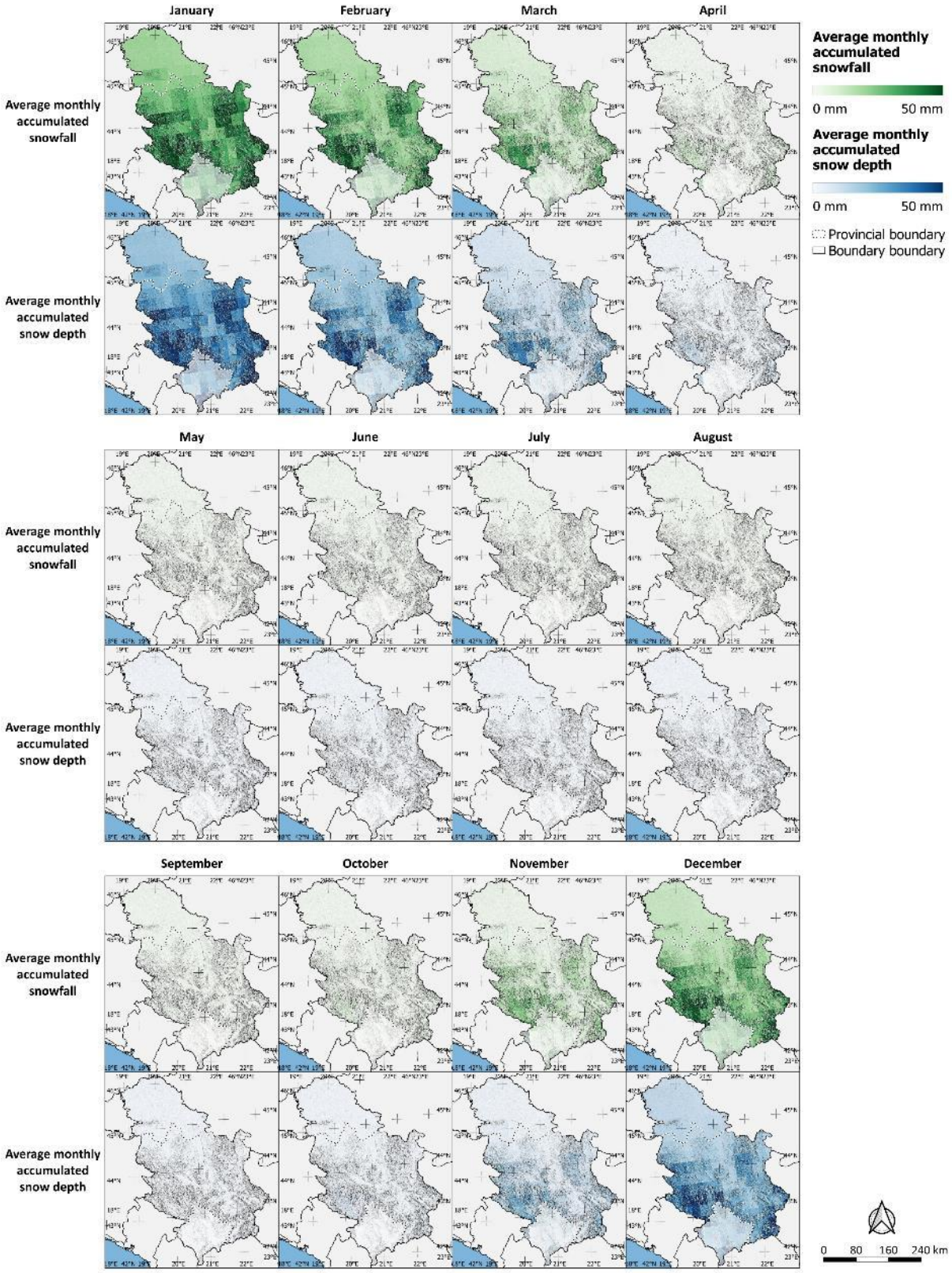

NDVI & LAI

In this section, we will present the variation of two important vegetation indices in the Republic of Serbia. These indices are Leaf Area Index (LAI) and Normalized Difference Vegetation Index (NDVI). LAI

is a dimensionless index that represents the ratio of canopy area to total area, while NDVI is a dimensionless spectral index that represents the amount of live green vegetation. These indices were calculated using the MODIS database.

Figure 38 presents the monthly variation of NDVI and LAI in the Republic of Serbia.

Figure 38 – Current seasonal variation of NDVI and LAI
*Data averaged over the 2001-2019 period**. In red:** NDVI. **In green:** LAI. Data source: NASA LP DAAC (Myneni, Knyazikhin, and Park 2015; Didan 2015).*

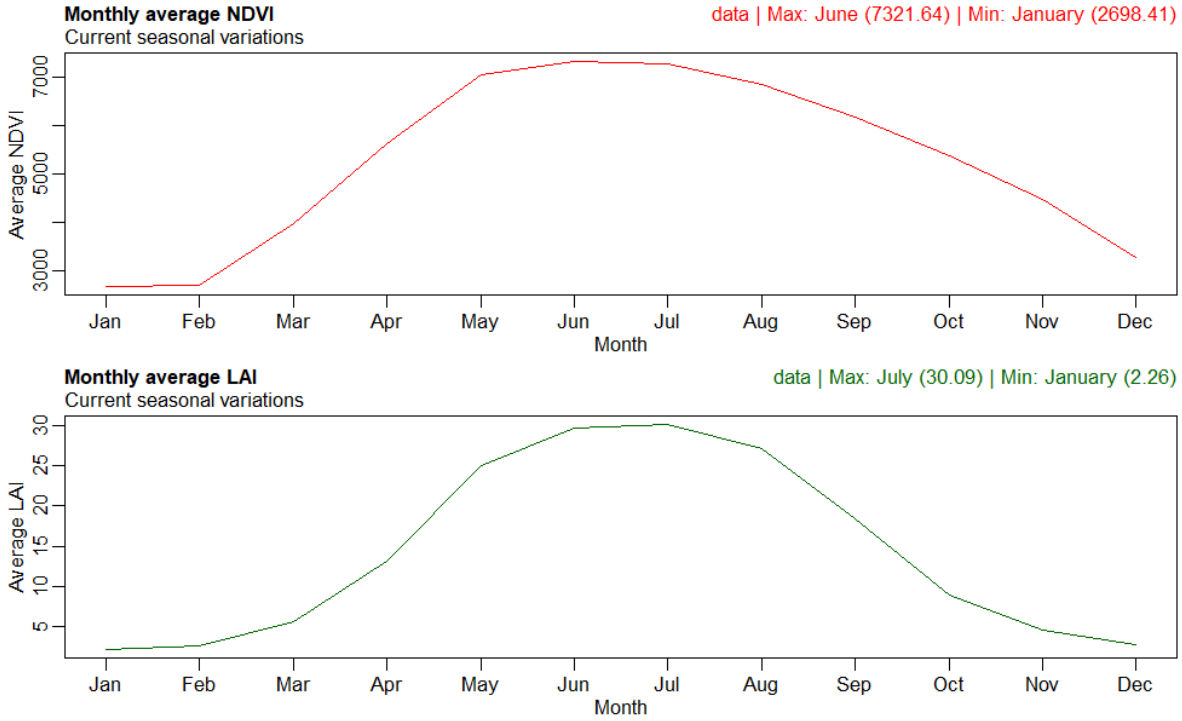

both NDVI and LAI reach their minimum in January, with NDVI at 2700 and LAI at 2.3. These indices gradually increase following a sigmoid shape and reach their maximum in June for NDVI (7300) and July for LAI (30). Both indices then decrease towards their respective January levels, with LAI decreasing in a sigmoid shape and NDVI decreasing constantly.

Figure 39 shows the seasonal spatial distribution of LAI and NDVI in the Republic of Serbia. The indices tend to be higher at higher altitudes, where agriculture is less practical and the presence of forests is more prominent. In terms of regionality, there is a clear difference between the North and South of the Sava-Danube axis. To the South, the high altitudes and the presence of forests push the LAI and NDVI to higher values, and the Morava rivers valleys are well-defined as NDVI and LAI cold spots. To the North of the Sava-Danube axis, the NDVI and LAI remain low and evenly distributed, except in large urban centers such as the Belgrade area, where NDVI and LAI stay lower than elsewhere until June. On top of the Fruška Gora range, both indices are higher. From June to September, harvesting is noticeable as patches of sharp decreases in NDVI and LAI, starting from the Northeast.

Figure 39 – Spatial distribution of the current monthly average NDVI and LAI[26]
Data averaged over the 2001-2019 period. Data source: NASA LP DAAC (Myneni, Knyazikhin, and Park 2015; Didan 2015).

[26] The boundaries and names shown and the designations used on this map do not imply official endorsement or acceptance by the United Nations.

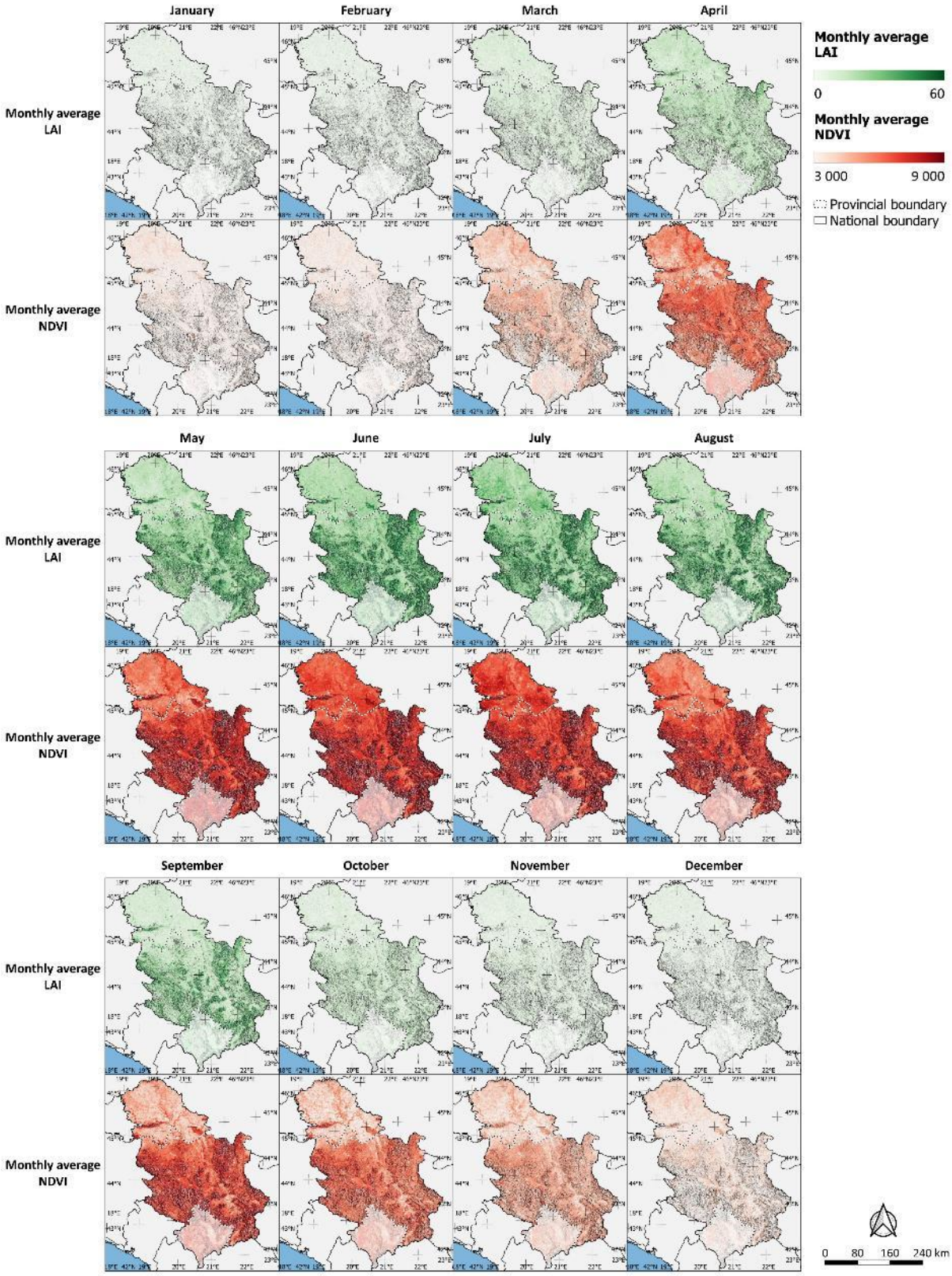
January
February
March
April
May
June
July
August
September
October
November
December
Monthly average LAI
Monthly average NDVI
Monthly average LAI
0
60
Monthly average NDVI
3 000
9 000
Provincial boundary
National boundary
0 80 160 240 km

HEAT STRESS TRENDS

This section will outline the past and future trends in heat stress related variables in Serbia

Summary

Temperatures - Over the last 40 years, Serbia has experienced a clear increase in annual average temperature, with an increase of +0.6°C per decade. The annual maximum temperature has also increased, while the annual minimum temperature has remained stable. Spatially, higher temperatures are distributed in low altitude areas such as the plains of the North and the valleys of the South. The projected data show a steady increase in average, maximum, and minimum temperature under both RCP4.5 and RCP8.5 scenarios. Average temperature is expected to increase at a rate of around +0.3°C/decade under RCP4.5 and +0.5°C/decade under RCP8.5. Maximum temperature is expected to increase at a rate of about +0.4°C/decade under RCP4.5 and +0.7°C/decade under RCP8.5. Minimum temperature is expected to increase at a rate of about +0.3°C/decade under RCP4.5 and +0.4°C/decade under RCP8.5.

Frost days, ice days & chill hours - Frost days, ice days and chill hours in Serbia have decreased in the last 40 years, with frost days decreasing by -7.7 days/decade, ice days decreasing by -2.6 days/decade, and chill hours decreasing by -111 hours/decade. The spatial distribution of these trends is constant, with higher altitudes in the south of the country showing more frost days, ice days, and chill hours. The projected trends for the next 40 years show that these indices will continue to decrease under both RCP4.5 and RCP8.5 scenarios, with frost days expected to decrease by -3 to -6 days/decade, ice days expected to decrease by -0.9 to -1.3 days/decade, and chill hours expected to decrease by -63 to -94 hours/decade.

Summer days & tropical nights - Historical trends show that summer days and tropical nights in Serbia have increased over the last 40 years, with summer days increasing by +7.2 days/decade and tropical nights increasing by +1.2 days/decade. These trends are expected to continue over the next 40 years under both RCP4.5 and RCP8.5 scenarios. The spatial distribution of these variables tends to be more numerous in the flat lands of the north and valleys of the south, with tropical nights being more numerous in the Belgrade region due to artificial surfaces. Under the RCP4.5 scenario, summer days is expected to increase by -5.1 days/decade, from 105 days in 2040 to 115 days in 2060, and tropical nights is expected to increase by 2.7 days/decade, from 12 days in 2040 to 18 days in 2060. Under the RCP8.5 scenario, summer days is expected to increase by +7.4 days/decade, from 111 days in 2040 to 115 days in 2060, and tropical nights is expected to increase by +6.6 days/decade, from 18 days in 2040 to 31 days in 2060.

Degree days & hardiness zones - The annually accumulated degree days in Serbia have increased by +79°days/decade in the last 40 years due to the increase of the average temperature, resulting in an increase of degree days from 1441°days in 1980 to 1747°days in 2019. However, the average hardiness zone in Serbia has remained around 7 due to stable annual minimum temperatures. The distribution of degree days and hardiness zones is strongly related to topography, with high values visible at low altitudes and lower values at high altitudes. The trend of increasing degree days is expected to continue for the next 40 years under both RCP4.5 and RCP8.5 scenarios, bringing degree days to 2044°days and 2238°days, respectively, by 2060. The average hardiness zone is expected to remain stable.

Temperatures

This section provides an overview of the past and future trends of temperatures in the Republic of Serbia, highlighting the following key metrics: average temperature (TG), maximum temperature (TX), minimum temperature (TN).

Figure 40 – Historical time series of annual average, minimum and maximum temperatures
Time series over 1980-2019 period. ***Light dotted line****: variable value from each weather station separately.* ***Dark full line:*** *median value of the variable.* ***In yellow:*** *monthly maximum temperature.* ***In green:*** *monthly average temperature.* ***In blue:*** *monthly minimum temperature.* ***In red dashed line:*** *variable value using ERA5 database.*
Data source: Republic Hydrometeorological Service of Serbia, HidMet (Republic Hydrometeorological Service of Serbia 2020) and ERA5 - ECMWF / Copernicus Climate Change Service (Muñoz Sabater 2019).

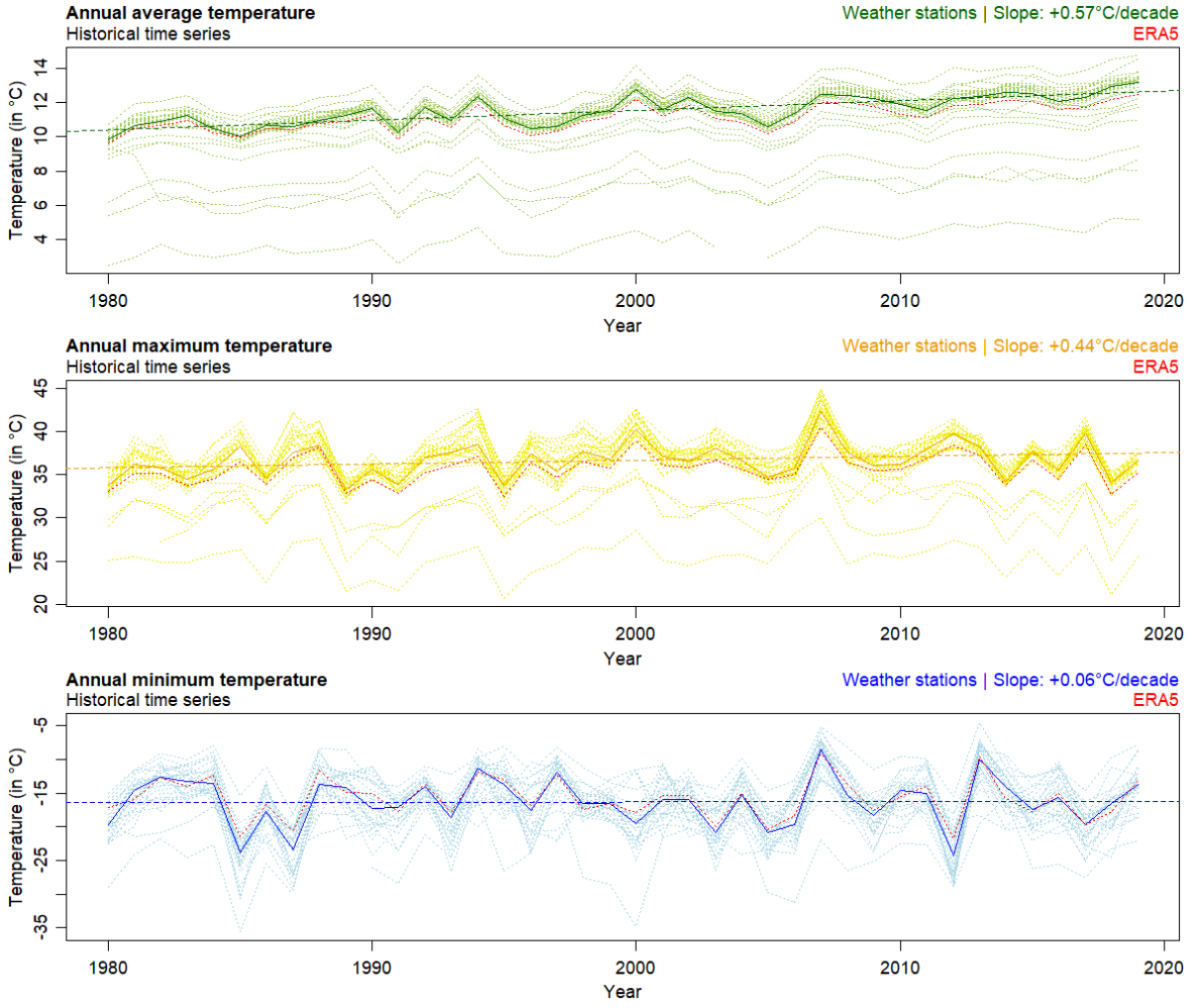

Table 3 – Characteristics of the trend of historical annual time series of average, minimum and maximum temperature (linear models)
Data source: Republic Hydrometeorological Service of Serbia, HidMet (Republic Hydrometeorological Service of Serbia 2020).

Variable	Slope	p-value	Adjusted R^2	Average value in 1980	Average value in 2019
TG	+0.57°C/decade	0.00	0.59	10.41°C	12.64°C
TX	+0.44°C/decade	0.10	0.04	35.79°C	37.53°C
TN	+0.06°C/decade	0.91	-0.03	-16.44°C	-16.21°C

Historical annual trends of average, minimum and maximum temperatures can be observed in Figure 40 and Table 3. Over the last 40 years, Serbia has experienced a significant increase in annual average temperature (TG) (+0.6 °C/decade), with the average temperature rising from around 10°C in 1980 to around 13°C in 2019. Despite small interannual variations ($p<0.05$, adj. $R2>0.5$), this upward trend is statistically significant. The annual maximum temperature (TX) also showed a slight increase (+0.4°C/decade), with the average maximum temperature rising from 36°C in 1980 to 37°C in 2019. However, the trend in annual minimum temperature (TN) remained stable with a slight increase (+0.06°C/decade), remaining around -16°C over the 1980-2019 period.

Figure 41 displays the spatial distribution of the trends in average, minimum, and maximum temperature across Serbia. The distribution remains constant over time, with temperatures generally higher at lower altitudes, particularly in the plains of the North and valleys of the South. This pattern holds true despite the steady increase in temperatures observed in the last 40 years.

Figure 41 – Historical spatial distribution of annual average, minimum and maximum temperatures[27]
*Data averaged over the 1980-2019 period, by decade**. In blue:** decadal averaged of the annually accumulated precipitation. **In orange:** decadal average of the annual average precipitation intensity. Data source: ERA5, ECMWF / Copernicus Climate Change Service (Muñoz Sabater 2019).*

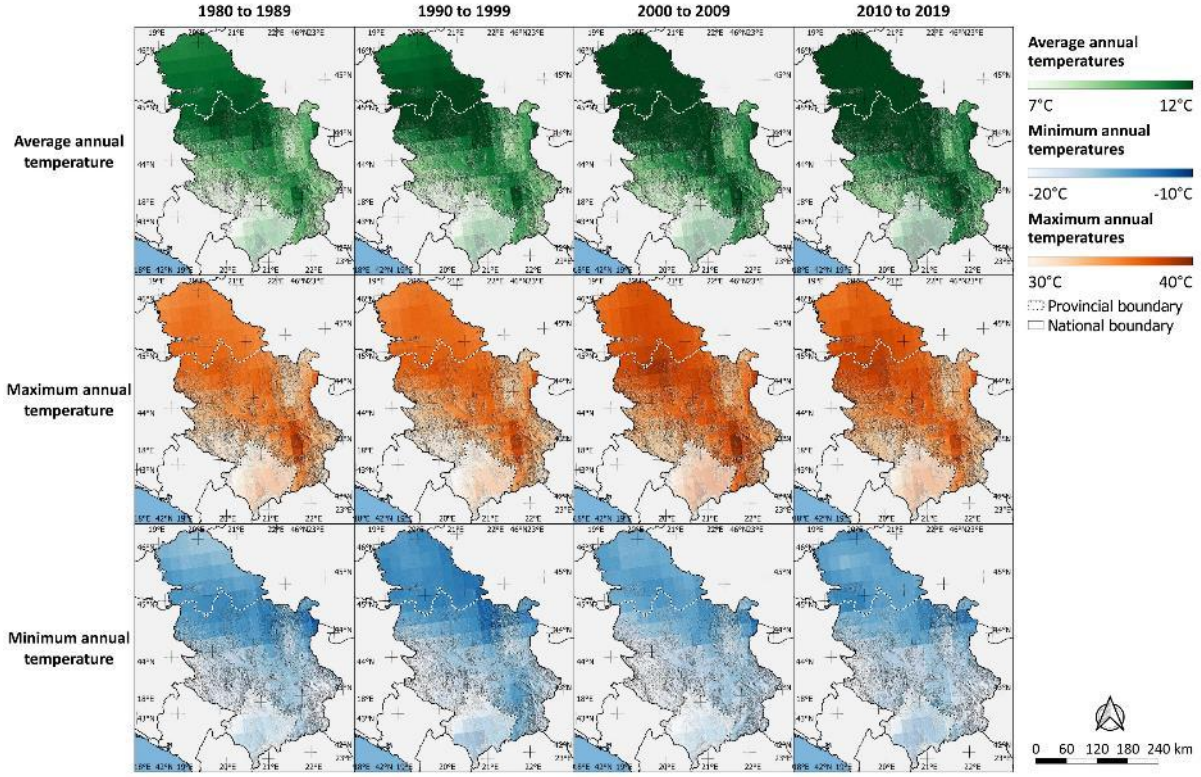

[27] The boundaries and names shown and the designations used on this map do not imply official endorsement or acceptance by the United Nations.

Figure 42 shows the projected trends for annual average, minimum, and maximum temperatures in Serbia under the RCP4.5 and RCP8.5 scenarios.

Figure 42 – Projected time series of the annual average, minimum and maximum temperatures
Time series over 2020-2060 period. Time series over 2020-2060 period. ***Pink dotted line****: variable value for each model separately under the RCP4.5 scenario.* ***grey dotted line****: variable value for each model separately under the RCP8.5 scenario.* ***Purple full line:*** *median value of the variable under RCP4.5 scenario.* ***Black full line:*** *median value of the variable under RCP8.5 scenario. Data source: NASA Earth Exchange - Global Daily Downscaled Climate Projections (NEX – GDDP) (Thrasher et al. 2012).*

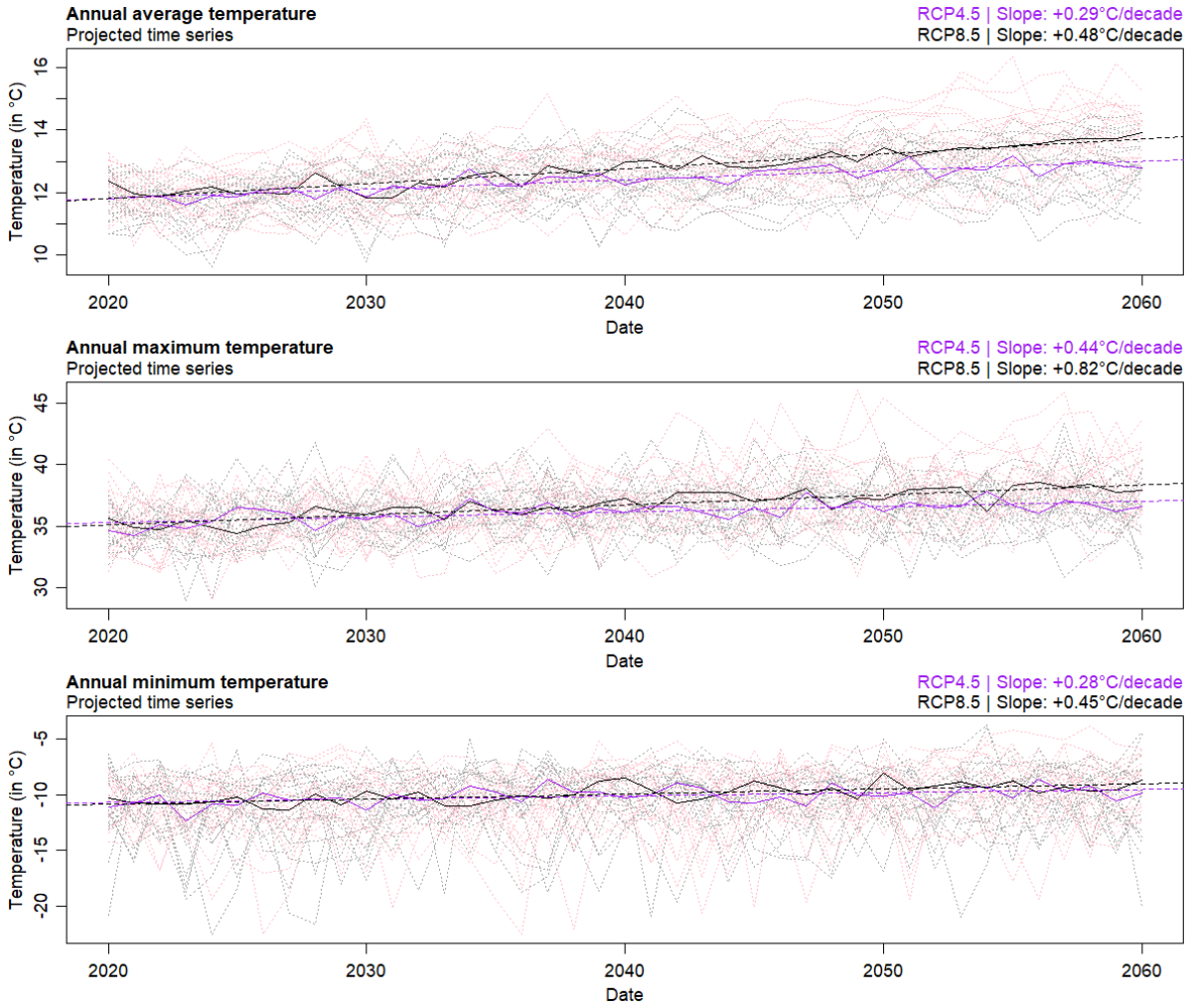

Similar to the historical data, the projected data expects a steady increase in all temperatures under both scenarios.

Under the RCP4.5 scenario, the annual average temperature is expected to increase at a rate of approximately +0.3°C/decade, and under the RCP8.5 scenario, the rate of increase is expected to be around +0.5°C/decade. This means that TG is projected to increase from around 12.4°C in 2040 to 13.0°C on average in 2060 under the RCP4.5 scenario, and from around 12.8°C in 2040 to 13.7°C in 2060 under the RCP8.5 scenario.

The annual maximum temperature is expected to increase at a rate of about +0.4°C/decade under RCP4.5 scenario, and +0.7°C/decade under RCP8.5 scenario. As a result, TX is projected to increase from around -36.2°C in 2040 to 37.0°C on average in 2060 under the RCP4.5 scenario, and from around 36.7°C in 2040 to 38.4°C in 2060 under the RCP8.5 scenario.

The annual minimum temperature is expected to increase at a rate of approximately +0.3°C/decade under RCP4.5 scenario, and +0.4°C/decade under RCP8.5 scenario. This means that TN is projected to increase from around -10.1°C in 2040 to -9.6°C on average in 2060 under the RCP4.5 scenario, and from around -9.9°C in 2040 to -9.0°C in 2060 under the RCP8.5 scenario.

Table 4 – Characteristics of the trend from projected time series of monthly average, minimum and maximum temperature under the RCP8.5 scenario (linear models)

Data source: Republic Hydrometeorological Service of Serbia, HidMet (Republic Hydrometeorological Service of Serbia 2020).

RCP4.5					
Variable	**Slope**	**p-value**	**Adjusted R^2**	**Average value in 2040**	**Average value in 2060**
TG	+0.29°C/decade	0.00	0.76	12.42°C	13.00°C
TX	+0.44°C/decade	0.00	0.41	36.16°C	37.03°C
TN	+0.28°C/decade	0.01	0.16	-10.14°C	-9.58°C
RCP8.5					
Variable	**Slope**	**p-value**	**Adjusted R^2**	**Average value in 2040**	**Average value in 2060**
TG	+0.48°C/decade	0.00	0.87	12.77°C	13.73°C
TX	+0.82°C/decade	0.00	0.74	36.72°C	38.37°C
TN	+0.45°C/decade	0.00	0.43	-9.93°C	-9.02°C

Frost days, ice days & chill hours

In this section, we will explore the past and future trends of frost days, ice days, and chill hours in the Republic of Serbia. Accumulated frost days (FD) are defined as the number of days over a given period when the daily minimum temperature is below 0°C, while accumulated ice days (ID) are defined as the number of days over a given period when the daily maximum temperature is below 0°C. Finally, accumulated chill hours (CH) are defined as the number of hours over a given period when the daily average temperature is below 0°C.

Since frost days, ice days, and chill hours are calculated at a daily or hourly scale, and daily data from weather stations were not available, this section will only present variables calculated using ERA5 data for historical trends.

Figure 43 and Table 5 present the historical annual trends on accumulated frost days, ice days, and chill hours.

Figure 43 – Historical annual time series of accumulated frost days, ice days and chill hours
Time series over 1980-2019 period. ***In green:*** *annually accumulated frost days.* ***In blue:*** *annually accumulated ice days.* ***In red:*** *annually accumulated chill hours. Data source: ERA5, ECMWF / Copernicus Climate Change Service (Muñoz Sabater 2019)*

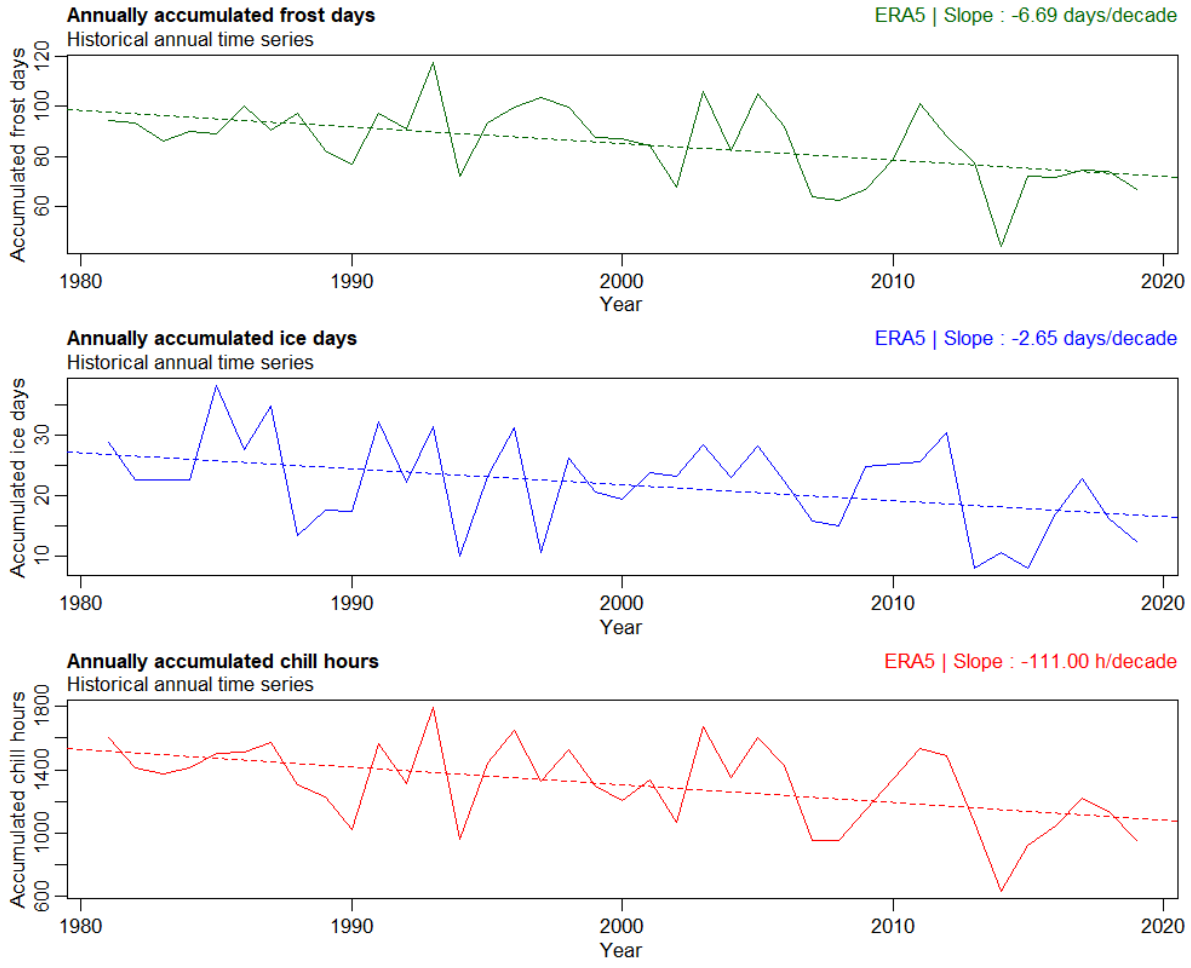

In Serbia, these indices have exhibited a general decreasing trend over the past 40 years. Specifically, frost days have decreased by an average of 7.7 days per decade, ice days have decreased by an average

of 2.6 days per decade, and chill hours have decreased by an average of 111 hours per decade. As a result, the average number of frost days decreased from 99 days in 1980 to 73 days in 2019, the average number of ice days decreased from 27 days in 1980 to 17 days in 2019, and the average number of chill hours decreased from 1526 hours in 1980 to 1093 hours in 2019.

Table 5 – Characteristics of the trend from historical annual times series of accumulated frost days, ice days and chill hours (linear models)
Data source: ERA5, ECMWF / Copernicus Climate Change Service (Muñoz Sabater 2019)

Variable	Slope	p-value	Adj. R^2	Average value in 1980	Average value in 2019
FD	*-6.69 days*	*0.00*	*0.24*	*99 days*	*73 days*
ID	*-2.65 days*	*0.01*	*0.14*	*27 days*	*17 days*
CH	*-111.00 h*	*0.00*	*0.22*	*1526 h*	*1093 h*

Figure 44 presents the spatial distribution of the trends in annually accumulated frost days, ice days, and chill hours throughout Serbia. The spatial distribution of these indices is consistent. Specifically, frost days, ice days, and chill hours are generally more prevalent at higher altitudes in the southern part of the country.

Figure 44 – Historical and projected decadal spatial distribution of annually accumulated frost days, ice days and chill hours[28]
*Data averaged over the 1980-2019 period, by decade**. In green:** annually accumulated frost days. **In blue:** annually accumulated ice days. **In red:** annually accumulated chill hours. Data source: ERA5, ECMWF / Copernicus Climate Change Service (Muñoz Sabater 2019)*

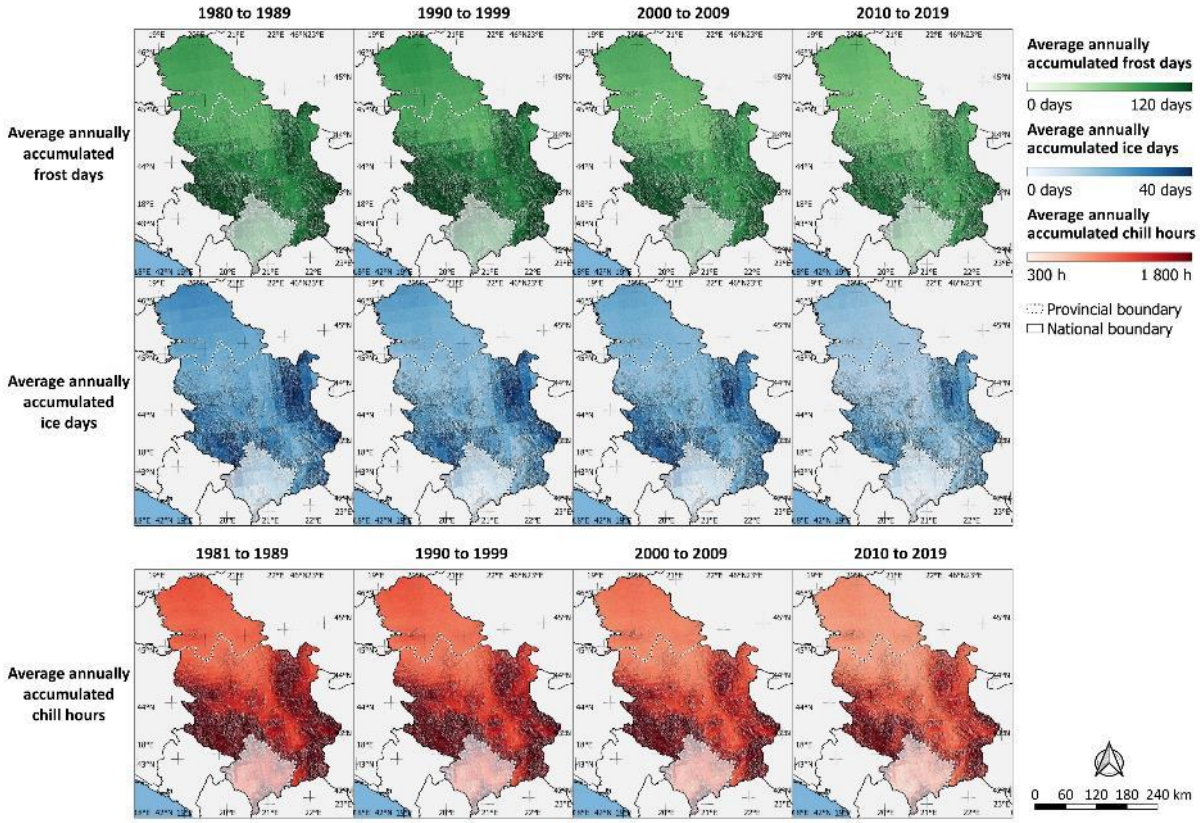

[28] The boundaries and names shown and the designations used on this map do not imply official endorsement or acceptance by the United Nations.

The projected annual trends in annually accumulated frost days, ice days, and chill hours, are presented in Figure 45 and

Table 6. Both scenarios predict a continued decrease in the number of frost days, ice days, and chill hours over the next 40 years.

Figure 45 – Projected annual time series of accumulated frost days, ice days, and chill hours
Time series over 2020-2060 period. Time series over 2020-2060 period. ***Pink dotted line****: variable value for each model separately under the RCP4.5 scenario.* ***grey dotted line****: variable value for each model separately under the RCP8.5 scenario.* ***Purple full line:*** *median value of the variable under RCP4.5 scenario.* ***Black full line:*** *median value of the variable under RCP8.5 scenario. Data source: NASA Earth Exchange - Global Daily Downscaled Climate Projections (NEX – GDDP) (Thrasher et al. 2012).*

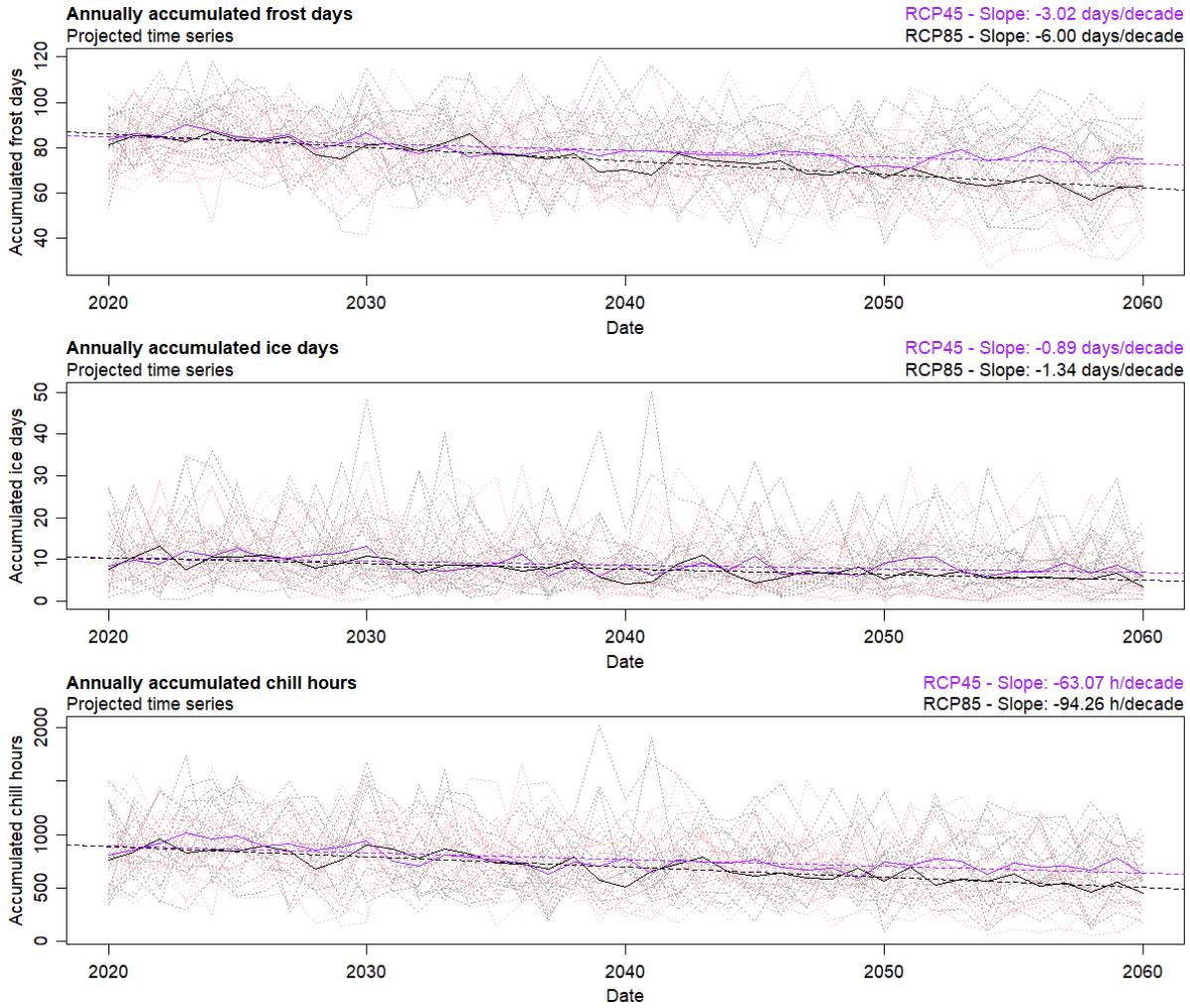

Under the RCP8.5 scenario, a more significant decrease is expected. Frost days are projected to decrease by an average of -6 days/decade, from 74 days in 2040 to 62 days in 2060. Ice days[29] are expected to decrease by an average of -1.3 days/decade, from 7.6 days in 2040 to 4.9 days in 2060. Chill hours[1] are also expected to decrease by an average of -94 hours/decade, from 697 hours in 2040 to 508 hours in 2060.

[29] It should be noted that the validation of the median models of the NEX ensemble for ice days and chill hours was uncertain under both scenario (RMSE: ID>0.7, CH>0.9, see Modelled data validation, below). Therefore, caution should be exercised when considering the projected accumulated ice days and accumulated chill hours in Serbia.

Under the RCP4.5 scenario, frost days are expected to decrease by an average of -3 days/decade, from 79 days in 2040 to 73 days in 2060. Similarly, ice days are projected to decrease by an average of -0.9 days/decade, from 8.6 days in 2040 to 6.8 days in 2060. Chill hours are also expected to decrease by an average of -63 hours/decade, from 769 hours in 2040 to 643 hours in 2060.

Table 6 – Characteristics of the trend from projected data for annually accumulated frost days, ice days and chill hours (linear models)

Data source: Second national communication of the Republic of Serbia under the United Nations framework convention on climate change (Rajkovic, Vujadinovic, and Vukovic 2013) and NASA Earth Exchange - Global Daily Downscaled Climate Projections (NEX – GDDP) (Thrasher et al. 2012).

RCP4.5					
Variable	**Slope**	**p-value**	**Adjusted R^2**	**Average value in 2040**	**Average value in 2060**
FD	-3.02 days/decade	0.00	0.59	78.90 days	72.86 days
ID	-0.89 days/decade	0.00	0.26	8.62 days	6.85 days
CH	-63.07 h/decade	0.00	0.53	769.19 h	643.05 h
RCP8.5					
Variable	**Slope**	**p-value**	**Adjusted R^2**	**Average value in 2040**	**Average value in 2060**
FD	-6.00 days/decade	0.00	0.83	74.15 days	62.15 days
ID	-1.34 days/decade	0.00	0.48	7.62 days	4.95 days
CH	-94.26 h/decade	0.00	0.71	696.99 h	508.47 h

Summer days & tropical nights

In this section, we'll examine the variations of summer days and tropical nights in the Republic of Serbia. Accumulated summer days (SD) are defined as the number of days over a given period when the daily maximum temperature exceeds 25°C, while accumulated tropical nights (TrN) are defined as the number of days over a given period when the daily minimum temperature is above 20°C.

Since accumulated summer days and tropical nights are calculated at a daily or hourly level, and daily weather station data wasn't available, we'll only present variables calculated using ERA5 data for historical trends.

The historical annual trends in accumulated summer days and tropical nights can be observed in Figure 56 and Table 13. Over the last 40 years in Serbia, there has been a general increase in the number of summer days and tropical nights, with an average increase of +7.2 days/decade for SD and +1.2 days/decade for TrN. This increase has led to an average of 94 summer days and 7 tropical nights in 2019, up from 66 summer days and 3 tropical nights in 1980.

Figure 46 – Historical annual time series of accumulated summer days and tropical nights
Time series over 1980-2019 period. ***In green:*** *annually accumulated summer days.* ***In red:*** *annually accumulated tropical nights. Data source: ERA5, ECMWF / Copernicus Climate Change Service (Muñoz Sabater 2019)*

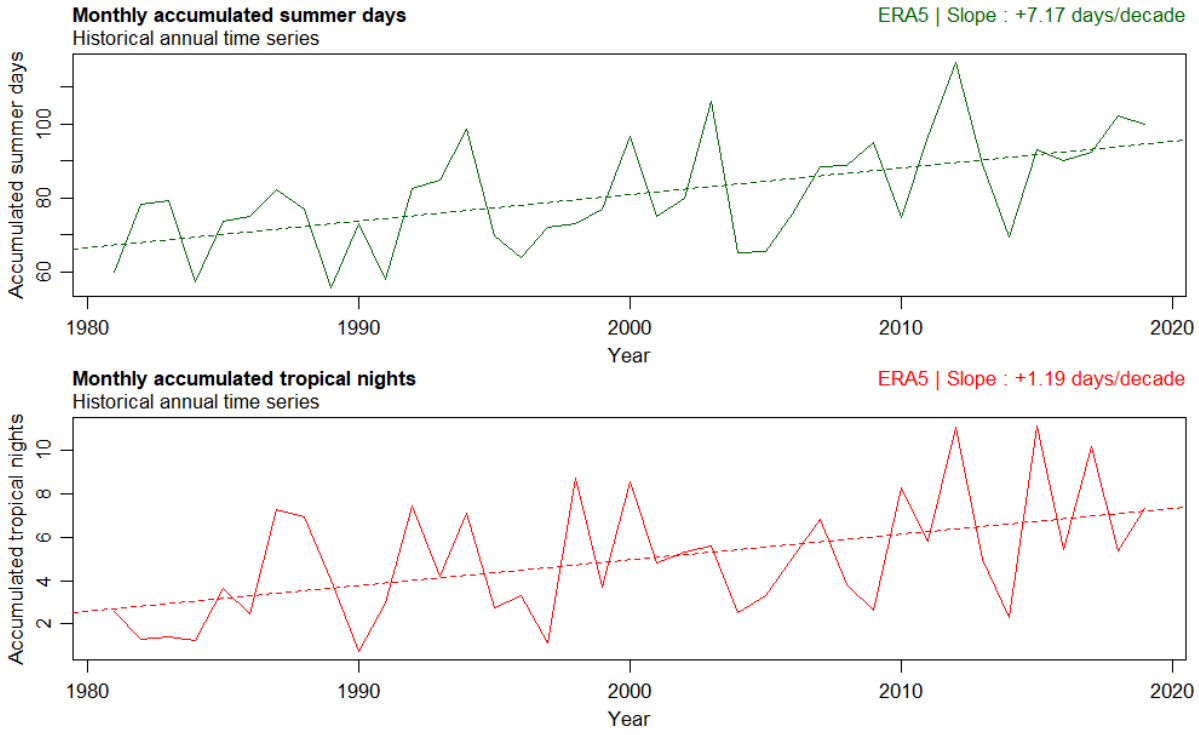

Table 7 – Characteristics of the trend from historical annual times series of accumulated frost days, ice days and chill hours (linear models)

Data source: ERA5, ECMWF / Copernicus Climate Change Service (Muñoz Sabater 2019)

Variable	Slope	p-value	Adj. R^2	Average value in 1980	Average value in 2019
SD	+7.17 days/decade	0.00	0.30	66.45 days	94.40 days
TrN	+1.19 days/decade	0.00	0.22	2.58 days	7.21 days

Refer to Figure 47 to observe the spatial distribution of annually accumulated summer days and tropical nights across Serbia. Over the last 40 years, the distribution of summer days and tropical nights has remained consistent. These variables tend to be more frequent and persistent for longer periods in the flat lands of the North of the country and in the valleys of the South, where the altitude is lower. Interestingly, tropical nights are more common in the Belgrade region, which is likely due to the high albedo and heat absorption capacity of the numerous artificial surfaces present in the area (see Figure 3).

Figure 47 – Historical and projected decadal spatial distribution of annually accumulated frost days, ice days and chill hours[30]

*Data averaged over the 1980-2019 period, by decade**. In green:** annually accumulated frost days. **In blue:** annually accumulated ice days. **In red:** annually accumulated chill hours. Data source: ERA5, ECMWF / Copernicus Climate Change Service (Muñoz Sabater 2019)*

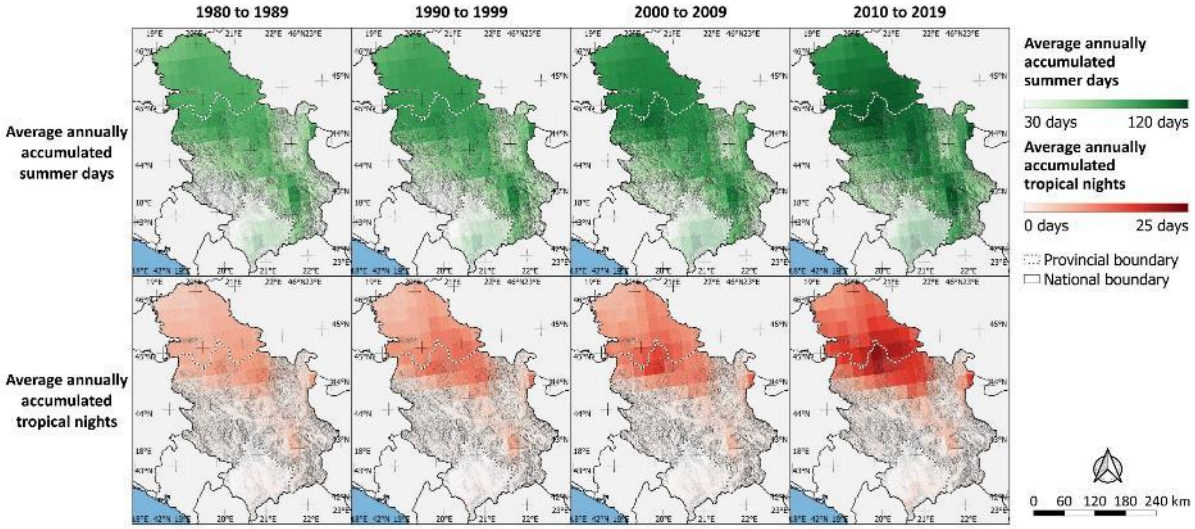

Figure 48 and Table 8 display the projected annual trends for the accumulation of summer days and tropical nights.

These trends are expected to continue increasing over the next 40 years. According to the NEX median model under the RCP4.5 scenario, the number of summer days is anticipated to increase by approximately -5.1 days per decade, reaching 115 days by 2060, up from 105 days in 2040. Meanwhile,

[30] The boundaries and names shown and the designations used on this map do not imply official endorsement or acceptance by the United Nations.

the number of tropical nights[31] is projected to increase by approximately 2.7 days per decade, with a rise from 12 days in 2040 to 18 days in 2060.

Table 8 – Characteristics of the trend from projected data for annually accumulated summer days and tropical nights (linear models)
Data source: Second national communication of the Republic of Serbia under the United Nations framework convention on climate change (Rajkovic, Vujadinovic, and Vukovic 2013) and NASA Earth Exchange - Global Daily Downscaled Climate Projections (NEX – GDDP) (Thrasher et al. 2012).

RCP4.5					
Variable	**Slope**	**p-value**	**Adjusted R^2**	**Average value in 2040**	**Average value in 2060**
SD	+5.11 days/decade	0.00	0.66	104.84 days	115.06 days
TrN	+2.79 days/decade	0.00	0.78	12.21 days	17.79 days
RCP8.5					
Variable	**Slope**	**p-value**	**Adjusted R^2**	**Average value in 2040**	**Average value in 2060**
FD	+7.43 days/decade	0.00	0.88	110.59 days	125.46 days
ID	+6.61 days/decade	0.00	0.92	18.01 days	31.23 days

The RCP8.5 scenario projects a steeper increase in both variables. The median model expects an increase of about +7.4 days/decade in SD, reaching 115 days by 2060, up from 111 days in 2040. Furthermore, the number of TrN is expected to increase by approximately +6.6 days per decade, rising from 18 days in 2040 to 31 days in 2060.

Figure 48 – Projected time series of annually accumulated summer days and tropical nights
*Time series over 2020-2060 period. Time series over 2020-2060 period. **Pink dotted line**: variable value for each model separately under the RCP4.5 scenario. **grey dotted line**: variable value for each model separately under the RCP8.5 scenario. **Purple full line:** median value of the variable under RCP4.5 scenario. **Black full line:** median value of the variable under RCP8.5 scenario. Data source: NASA Earth Exchange - Global Daily Downscaled Climate Projections (NEX – GDDP) (Thrasher et al. 2012).*

[31] It should be noted that the validation of the median models of the NEX ensemble tropical nights was uncertain under both scenario (RMSE>0.8, see Modelled data validation, below). Therefore, caution should be exercised when considering the projected accumulated tropical nights in Serbia.

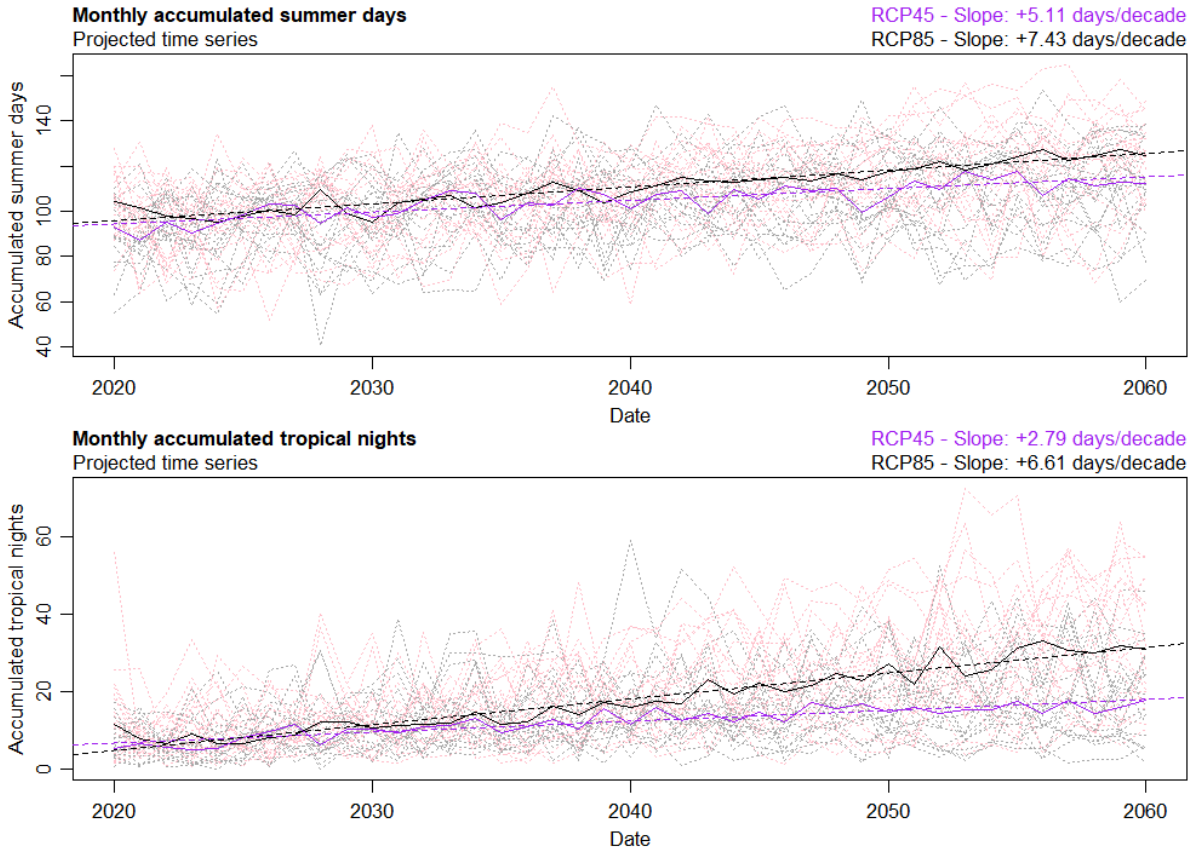
Monthly accumulated summer days
Projected time series
RCP45 - Slope: +5.11 days/decade
RCP85 - Slope: +7.43 days/decade
Accumulated summer days
40
60
80
100
140
2020
2030
2040
2050
2060
Date
Monthly accumulated tropical nights
Projected time series
RCP45 - Slope: +2.79 days/decade
RCP85 - Slope: +6.61 days/decade
Accumulated tropical nights
0
20
40
60
2020
2030
2040
2050
2060
Date

Degree days & hardiness zones

In this section, we will examine the past and future trends of accumulated degree days (DD) and hardiness zones (HZ) in the Republic of Serbia. Degree days are defined as the daily accumulated degree above 10°C and are calculated based on the daily mean temperature. They represent the amount of heat accumulated throughout the day. Hardiness zones represent the area where the annual minimum temperature falls within a predefined range established by the USDA[32]. These zones are defined on an annual basis, providing insight into the range of temperatures a specific area experiences over time. As daily data from weather stations were not available, we have used ERA5 data for historical trends to calculate the degree days.

Figure 49 and Table 9 provide insight into the historical annual trends of accumulated degree days and average hardiness zone in Serbia.

Figure 49 – Historical time series of the annual accumulated degree days and average hardiness zone
Time series over 1980-2019 period. ***In red:*** *ERA5.* ***In light blue:*** *variable from each weather stations.* ***In dark blue, full line:*** *annual median value over the weather stations data.* ***In dark blue, dashed line:*** *minimum and maximum value (respectively) over the weather stations data. Data source: ERA5, ECMWF / Copernicus Climate Change Service (Muñoz Sabater 2019)*

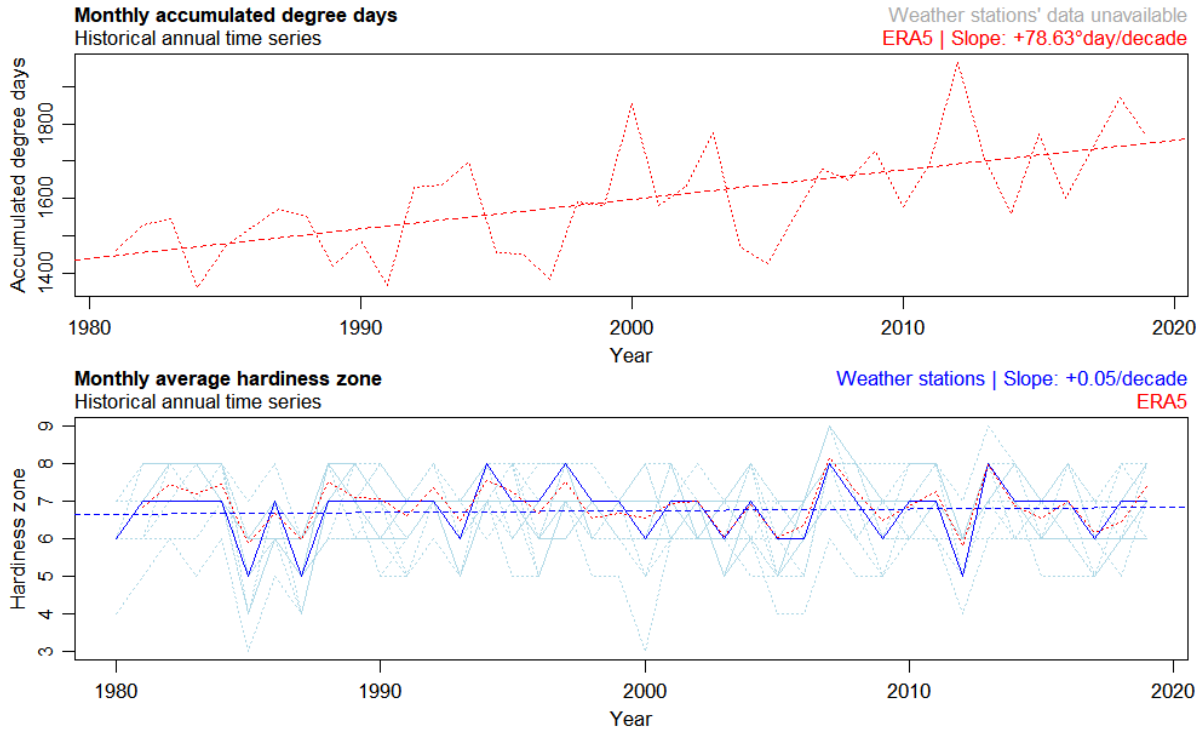

Accumulated degree days have generally increased over the past 40 years, with a rate of +79°days/decade. This increase can be attributed to the rising average temperature in Serbia, which has brought the average degree days from 1441°days in 1980 to 1747°days in 2019.

However, despite this increase in temperature, the annual minimum temperature has remained relatively stable over the same period (as shown in Figure 40). Consequently, the average hardiness

[32] https://planthardiness.ars.usda.gov/PHZMWeb/

zone in Serbia has not changed significantly, remaining around 7 over the past 40 years. This stability has been confirmed by both local weather station data and ERA5 data.

Table 9 – Characteristics of the trend from historical data for annually accumulated degree days and average hardiness zone (linear models)
Data source: ERA5, ECMWF / Copernicus Climate Change Service (Muñoz Sabater 2019)

Variable	Slope	p-value	Adj. R^2	Average value in 1980	Average value in 2019
DD	+78.63°days/decade	0.00	0.37	1440.79°days	1747.46°days
HZ	+0.05/decade	0.65	-0.02	6.66	6.84

Figure 50 provides a spatial representation of the trends on annually accumulated degree days and average hardiness zones. The distribution of annually accumulated degree days remains relatively constant throughout the period and is closely related to topography. High values can be observed at low altitudes, while low values are visible at high altitudes, reflecting the seasonal distribution pattern.

The spatial distribution of hardiness zones follows the pattern of minimum temperature distribution, with lower hardiness zones found at high altitudes and higher hardiness zones at low altitude. Interestingly, there is a 100 km wide band, oriented East-West, just South of the Sava Danube River axis, where the hardiness zone appears to be the highest.

Figure 50 – Historical and projected decadal spatial distribution of annually accumulated degree days and Hardiness zone[33]
*Data averaged over the 1980-2059 period, by decade**. In red:** degree days. **In color gradient (blue to red):** Hardiness zone. Data source: ERA5, ECMWF / Copernicus Climate Change Service (Muñoz Sabater 2019) and Second national communication of the Republic of Serbia under the United Nations framework convention on climate change (Rajkovic, Vujadinovic, and Vukovic 2013)*

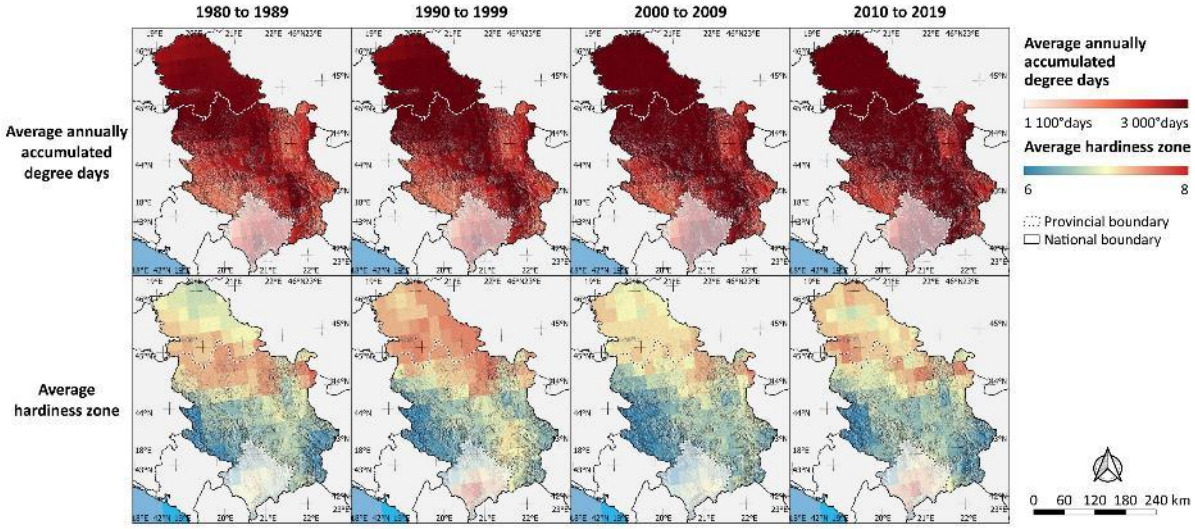

and Table 10 present the projected annual trends for annually accumulated degree days and average hardiness zones in Serbia. The annually accumulated degree days are expected to maintain their upward trend for the next 40 years, with projections indicating an increase of +72°days/decade under the RCP4.5 scenario and +120°days/decade under the RCP8.5 scenario. This increase is expected to

[33] The boundaries and names shown and the designations used on this map do not imply official endorsement or acceptance by the United Nations.

bring DD from 1900°days on average in 2040 to 2044°days on average in 2060 under the RCP4.5 scenario and from 1999°days in 2040 to 2238°days in 2060 under the RCP8.5 scenario.

The average hardiness zone is projected to remain stable in Serbia for the next 40 years.

Figure 51 – Projected annual time series of accumulated degree days and average hardiness zone
Time series over 2020-2060 period. Time series over 2020-2060 period. ***Pink dotted line****: variable value for each model separately under the RCP4.5 scenario.* ***grey dotted line****: variable value for each model separately under the RCP8.5 scenario.* ***Purple full line:*** *median value of the variable under RCP4.5 scenario.* ***Black full line:*** *median value of the variable under RCP8.5 scenario. Data source: NASA Earth Exchange - Global Daily Downscaled Climate Projections (NEX – GDDP) (Thrasher et al. 2012).*

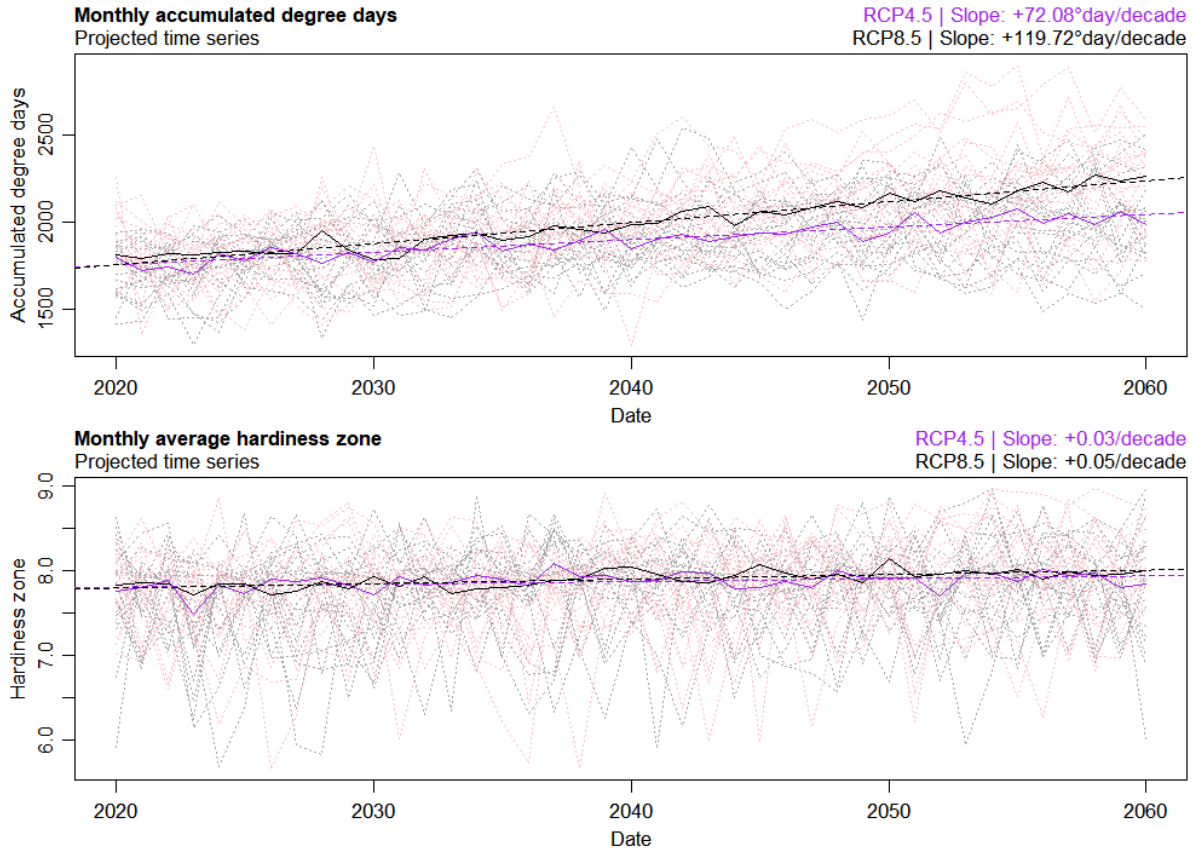

Table 10 – Characteristics of the trend from projected data for annually accumulated frost days, ice days and chill hours (linear models)
Data source: Second national communication of the Republic of Serbia under the United Nations framework convention on climate change (Rajkovic, Vujadinovic, and Vukovic 2013) and NASA Earth Exchange - Global Daily Downscaled Climate Projections (NEX – GDDP) (Thrasher et al. 2012).

RCP4.5					
Variable	**Slope**	**p-value**	**Adjusted R^2**	**Average value in 2040**	**Average value in 2060**
DD	+72.08°days/decade	0.00	0.80	1900.21°days	2044.38°days
HZ	+0.03/decade	0.02	0.11	7.88	7.94
RCP8.5					
Variable	**Slope**	**p-value**	**Adjusted R^2**	**Average value in 2040**	**Average value in 2060**
DD	+119.72°days/decade	0.00	0.92	1998.51°days	2237.94°days
HZ	+0.05/decade	0.00	0.43	7.90	8.01

WATER STRESS TRENDS

This section will outline the past and future trends in water stress related variables in Serbia

Summary

Precipitation - Over the past four decades, Serbia has experienced a wide range of variability in accumulated precipitation and precipitation intensity, resulting in a high degree of uncertainty. However, despite this variability, historical data suggests an increase in accumulated precipitation at a rate of +27 mm/decade, while precipitation intensity has remained relatively stable at around 6 mm/day. The spatial distribution of precipitation and precipitation intensity in Serbia is characterized by higher levels in the south's highlands and lower levels in the north and south valleys. Predicted data shows no significant changes in accumulated precipitation under the RCP4.5 scenario, while a decrease in precipitation is expected under the RCP8.5 scenario. Decadal variation in precipitation intensity is predicted to remain stable under both scenarios for the next 40 years.

Wet days & dry spells – as for precipitation the historical interannual variations range of wet days, very wet days and the duration of the longest dry spell are very large, and their trends are not very marked. Wet days and very wet days showed a slight increase over the last 40 years, while the duration of the longest dry spell stayed stable. Spatially, the distribution of these index remains constant, following the distribution of precipitations. The projected annual trends for these indices remain stable for the next 40 years under both scenarios, except for a small decrease in wet days under the RCP8.5 scenario.

Water deficit - Over the past 19 years, the country has experienced an increase in the annually accumulated water deficit, despite a large interannual variation ranging from 550 mm to 850 mm. On average, the water deficit has increased by 23 mm per decade, leading to an increased deficit from 665 mm in 2001 to 697 mm in 2019. The spatial distribution of the accumulated water deficit remained constant over the same period, with higher values observed at lower altitudes.

Precipitation variability - The standard deviation of the annually accumulated precipitation calculated over the previous 10 years (rolling window) has steadily increased over the past four decades, with a rate of (+24 mm/decade). Although the total amount of annual precipitation in Serbia appears to remain constant, the variability of the annual rainfall distribution is becoming more pronounced.

SPEI - Over the past 40 years, Serbia has experienced an increasing number of meteorological, agricultural, and hydrological drought events. The average amount of drought months per year has increased to a rate of +0.9 to +1.4 months per decade depending on the type of drought.

Snow - Over the last 20 years, Serbia has experienced a slight decrease in snowfall and snow depth (snowfall: -3.1 mm/decade, snow depth: -3 mm/decade), resulting in an average of 96 mm and 19 mm respectively in 2019, down from 102 mm and 25 mm in 2000. The distribution of snow cover and snowfall have remained consistent since 2000, with the highest quantity centered in the Southeast and Southwest at high altitudes, and, to a lesser extent on the Fruška Gora mountain range.

Precipitation

In this section, we will provide an overview of the past and present trends of precipitation in the Republic of Serbia. Our focus will be on two key metrics: accumulated precipitation (RR) and average precipitation intensity (RRx). Precipitation intensity is defined as the average amount of precipitation that falls on a rainy day. It is calculated by dividing the accumulated precipitation over a given period by the number of rainy days during that period. As we were unable to obtain daily data on precipitation from the local weather stations the analysis of historical trends of precipitation intensity was based on ERA5 data.

Figure 40 and Table 3 present the historical annual trends in accumulated precipitation in Serbia.

Figure 52 – Historical annual time series of accumulated precipitation and average precipitation intensity
Time series over 1980-2019 period. ***In light blue:*** *variable for each weather station.* ***In dark blue full line:*** *median value of the variable, calculated over all weather stations.* ***In dark blue dashed line:*** *minimum and maximum values of the variable, calculated over all weather stations.* ***In red:*** *variable calculated with ERA5 data. Data source: ERA5, ECMWF / Copernicus Climate Change Service (Muñoz Sabater 2019), Republic Hydrometeorological Service of Serbia, HidMet (Republic Hydrometeorological Service of Serbia 2020).*

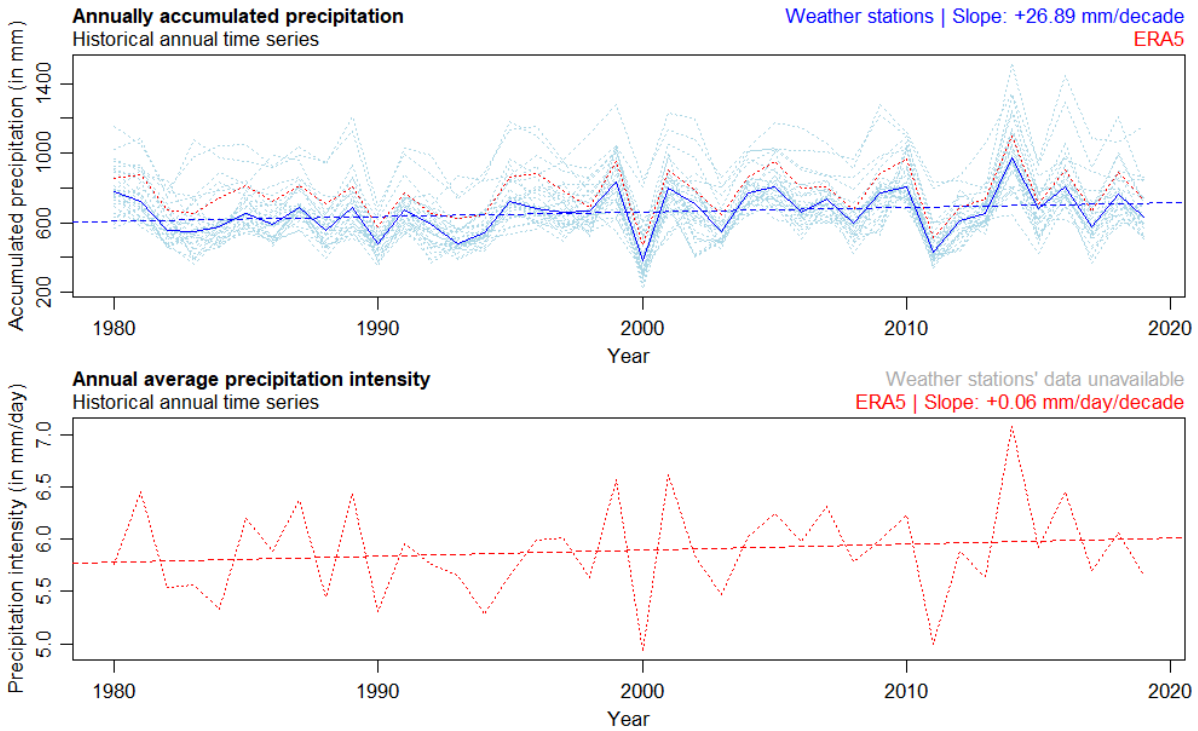

Table 11 – Characteristics of the trend from historical annual times series of accumulated precipitation and average precipitation intensity (linear models)
Data source: ERA5, ECMWF / Copernicus Climate Change Service (Muñoz Sabater 2019), Republic Hydrometeorological Service of Serbia, HidMet (Republic Hydrometeorological Service of Serbia 2020).

Variable	Slope	p-value	Adj. R^2	Average value in 1980	Average value in 2019
RR	+26.89 mm/dec.	0.11	0.04	606.62 mm	711.47 mm
RRx	+0.06 mm/day/dec.	0.37	0.00	5.78 mm/day	6.00 mm/day

Precipitation in Serbia has exhibited a wide range of variability over the last 40 years, with RR varying from about 300 mm in 2000 to 1100 mm in 2014, almost quadrupling during this period. Similarly, RRx has also varied, albeit to a lesser extent, ranging from 5 mm/day in 2000 to 7 mm/day in 2014. These

significant fluctuations make it challenging to model RR and RRx, resulting in a high level of uncertainty (p>>0.05; Adj. R2 close to 0). Therefore, any observed trends should be interpreted with caution.

Despite the aforementioned variability, there has been an increase in RR in Serbia over the last 40 years, with an average increase of +27 mm/decade. Specifically, the accumulated annual precipitation has risen from approximately 607 mm in 1980 to 711 mm in 2019.

In contrast, RRx's yearly variation has remained relatively stable around 6 mm/day on average, although the significant year-to-year variation as mentioned earlier.

The historical spatial distribution of annually accumulated precipitation and annual average precipitation intensity throughout Serbia can be observed in Figure 53. The spatial distribution appears to be constant for RR and RRx, with precipitation and precipitation intensity being higher in the southern highlands, particularly on mountain tops, and lower in the plains of the North and valleys of the South.

Figure 53 – Historical spatial distribution of annually accumulated precipitation and annual average precipitation intensity[34]

*Data averaged over the 1980-2019 period, by decade**. In blue:** decadal averaged of the annually accumulated precipitation. **In red:** decadal average of the annual average precipitation intensity. Data source: ERA5, ECMWF / Copernicus Climate Change Service (Muñoz Sabater 2019)*

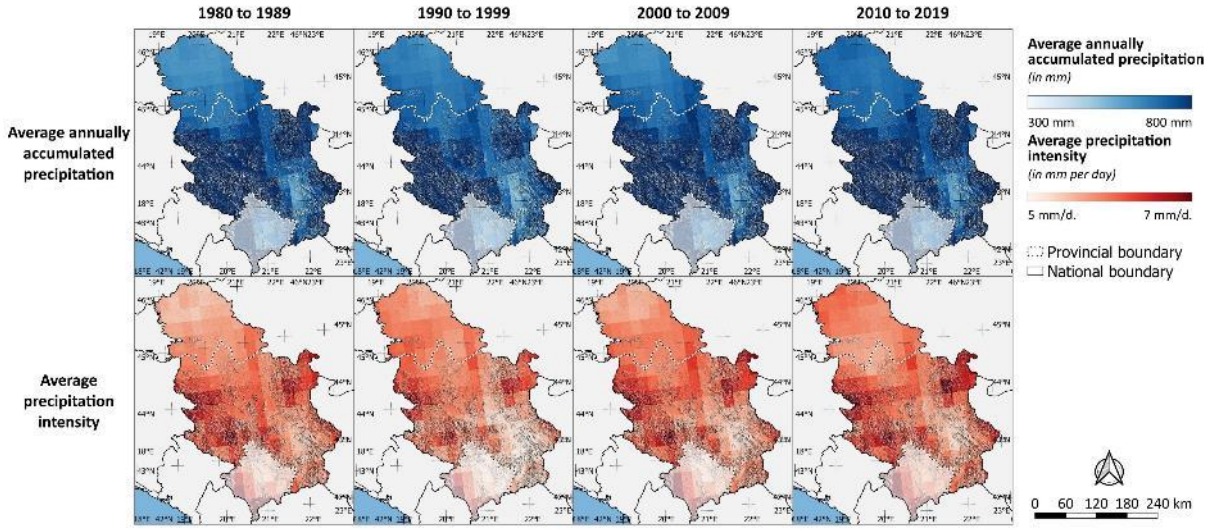

Figure 54 and Table 12 presents the projected annual trends for accumulated precipitation and average precipitation intensity in Serbia[35]. Under the RCP4.5 scenario, no significant variation predicted, with an increase of only +0.1 mm/decade. Annually accumulated precipitation it thus expects to remain stable around 720 mm per year. Under the RCP8.5 scenario, a decrease in precipitation of -14 mm/decade is predicted, which could bring the annually accumulated precipitation from an average of 726 mm in 2040 to 697 mm in 2060.

The NEX median models predict that RRx will remain stable for the next 40 years, with a level around 5.5 mm per rainy day under both the RCP4.5 and RCP8.5 scenarios.

[34] The boundaries and names shown and the designations used on this map do not imply official endorsement or acceptance by the United Nations.

[35] It should be noted that the validation of the median models of the NEX ensemble for accumulated precipitation and average precipitation intensity was uncertain under both scenario (RMSE: RR>0.9, RRx>1.1, see Modelled data validation, below). Therefore, caution should be exercised when considering the projected accumulated precipitation and average precipitation intensity in Serbia.

Figure 54 – Projected time series of the annual accumulated precipitation and average precipitation intensity *Time series over 2020-2060 period. Time series over 2020-2060 period.* ***Pink dotted line****: variable value for each model separately under the RCP4.5 scenario.* ***grey dotted line****: variable value for each model separately under the RCP8.5 scenario.* ***Purple full line:*** *median value of the variable under RCP4.5 scenario.* ***Black full line:*** *median value of the variable under RCP8.5 scenario. Data source: NASA Earth Exchange - Global Daily Downscaled Climate Projections (NEX – GDDP) (Thrasher et al. 2012).*

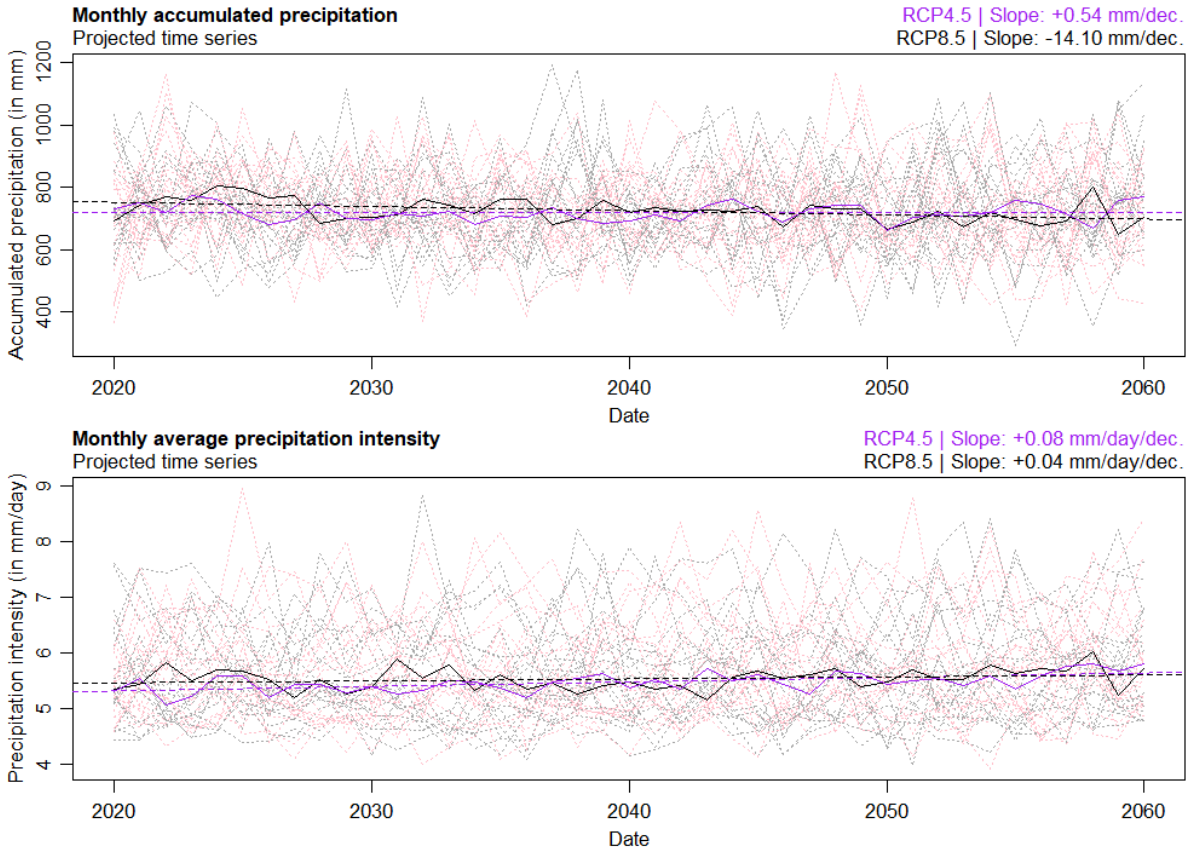

Table 12 – Characteristics of the trend from projected time series of monthly accumulated precipitation and average precipitation intensity under the RCP4.5 and RCP8.5 scenario (linear models)
Data source: NASA Earth Exchange - Global Daily Downscaled Climate Projections (NEX – GDDP) (Thrasher et al. 2012)

RCP4.5					
Variable	**Slope**	**p-value**	**Adjusted R^2**	**Average value in 2040**	**Average value in 2060**
RR	+0.54 mm/dec.	0.89	-0.03	719.85 mm	720.92 mm
RRx	+0.08 mm/day/dec.	0.00	0.30	5.47 mm/day	5.64 mm/day
RCP8.5					
Variable	**Slope**	**p-value**	**Adjusted R^2**	**Average value in 2040**	**Average value in 2060**
RR	-14.10 mm/dec.	0.00	0.17	725.63 mm	697.42 mm
RRx	+0.04 mm/day/dec.	0.17	0.02	5.53 mm/day	5.60 mm/day

Wet days & dry spell

This section presents the past and future trends in wet days, very wet days, and the duration of the longest dry spell in the Republic of Serbia. Accumulated wet days (WD) are defined as the number of days over a given period where the accumulated precipitation is greater than 1 mm, while accumulated very wet days (VWD) defined as the number of days over a given period where the accumulated precipitation is greater than the 95th quantile of the daily accumulated precipitations over the period. The duration of the longest dry spell (DS) is defined as the largest number of consecutive days over a given period where the daily accumulated precipitation is below 1 mm.

As wet days, very wet days, and the duration of the longest dry spell are calculated at a daily level, this section uses ERA5 data for historical trends, as daily data from weather stations were not available.

Figure 55 and Table 13 show the historical annual trends for accumulated wet days, accumulated very wet days, and the duration of the longest dry spell.

Figure 55 – Historical annual time series of the accumulated wet days, accumulated very wet days, and duration of the longest dry spell of the year

Time series over 1980-2019 period. ***In green:*** *annually accumulated wet days.* ***In blue:*** *annually accumulated very wet days.* ***In red:*** *duration of the longest dry spell of the year. Data source: ERA5, ECMWF / Copernicus Climate Change Service (Muñoz Sabater 2019)*

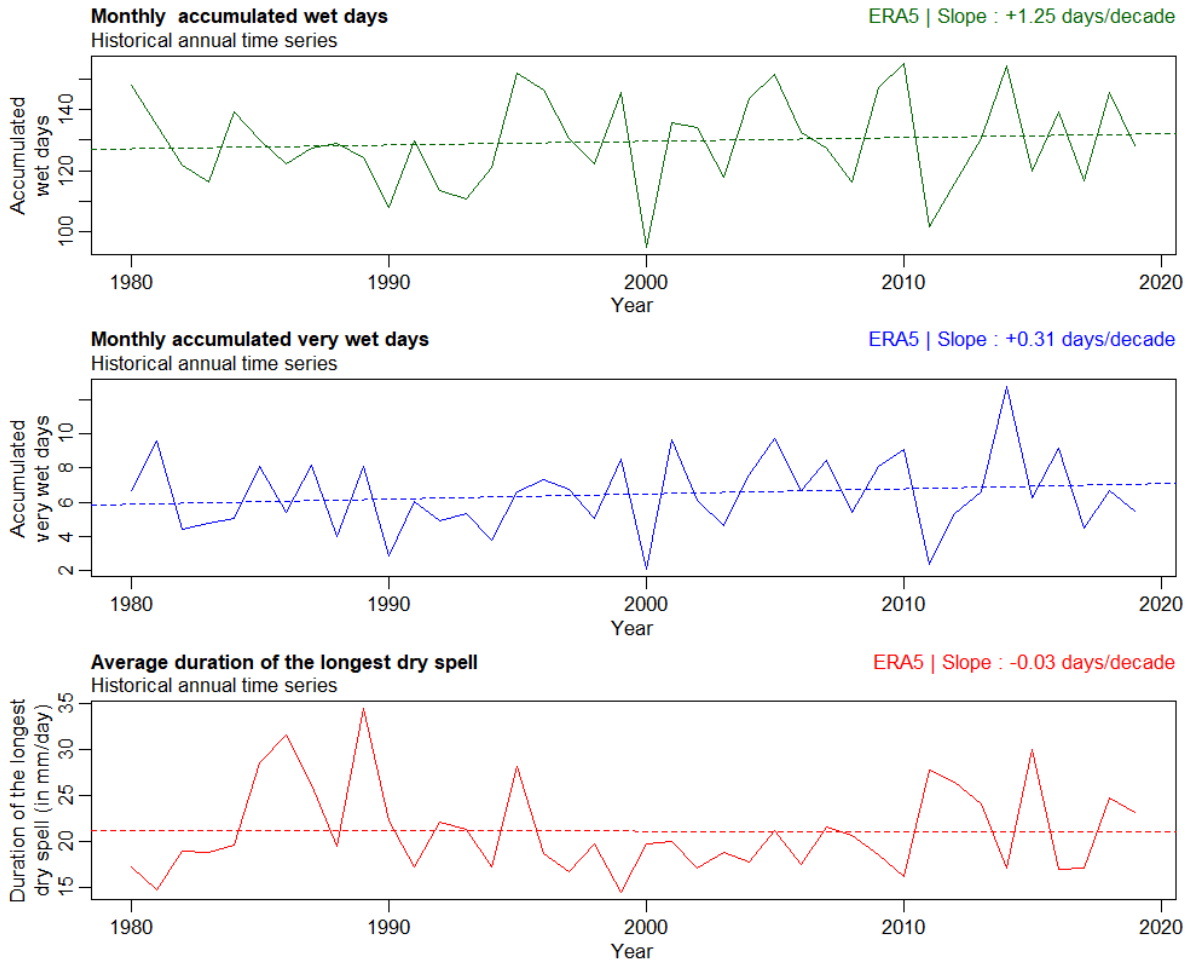

Table 13 – Characteristics of the trend from historical annual time series of the accumulated wet days, accumulated very wet days, and duration of the longest dry spell of the year (linear models)
Data source: ERA5, ECMWF / Copernicus Climate Change Service (Muñoz Sabater 2019)

Variable	Slope	p-value	Adj. R^2	Average value in 1980	Average value in 2019
WD	+1.25 days/dec.	0.54	-0.02	127 days	132 days
VWD	+0.31 days/dec.	0.32	0.00	5.86 days	7.06 days
DS	-0.03 days/dec.	0.97	-0.03	21.16 days	21.05 days

WD, VWD, and DS display large inter-annual variations (between 100 and 150 days for WD, between 2 and 12 days for VWD, and between 15 and 35 days for DS). Therefore, the trends presented here should be interpreted with caution. However, despite the variability, WD and VWD exhibited a slight increase over the past 40 years, with WD increasing by +1.25 days/decade and VWD increasing by +0.31 days/decade. This brings the total number of wet days from 127 in 1980 to 132 in 2019, and the number of very wet days from 6 in 1980 to 7 in 2019. On the other hand, the duration of the longest dry spell remained stable on average, with an average of 21 days.

The spatial distribution of the trends in accumulated wet days, accumulated very wet days, and the duration of the longest dry spell across Serbia is depicted in Figure 56.

Figure 56 – Historical decadal spatial distribution of annually accumulated wet days, very wet days, and the duration of the longest dry spell of the year[36]
Data averaged over the 1980-2059 period, by decade. Data source: ERA5, ECMWF / Copernicus Climate Change Service (Muñoz Sabater 2019)

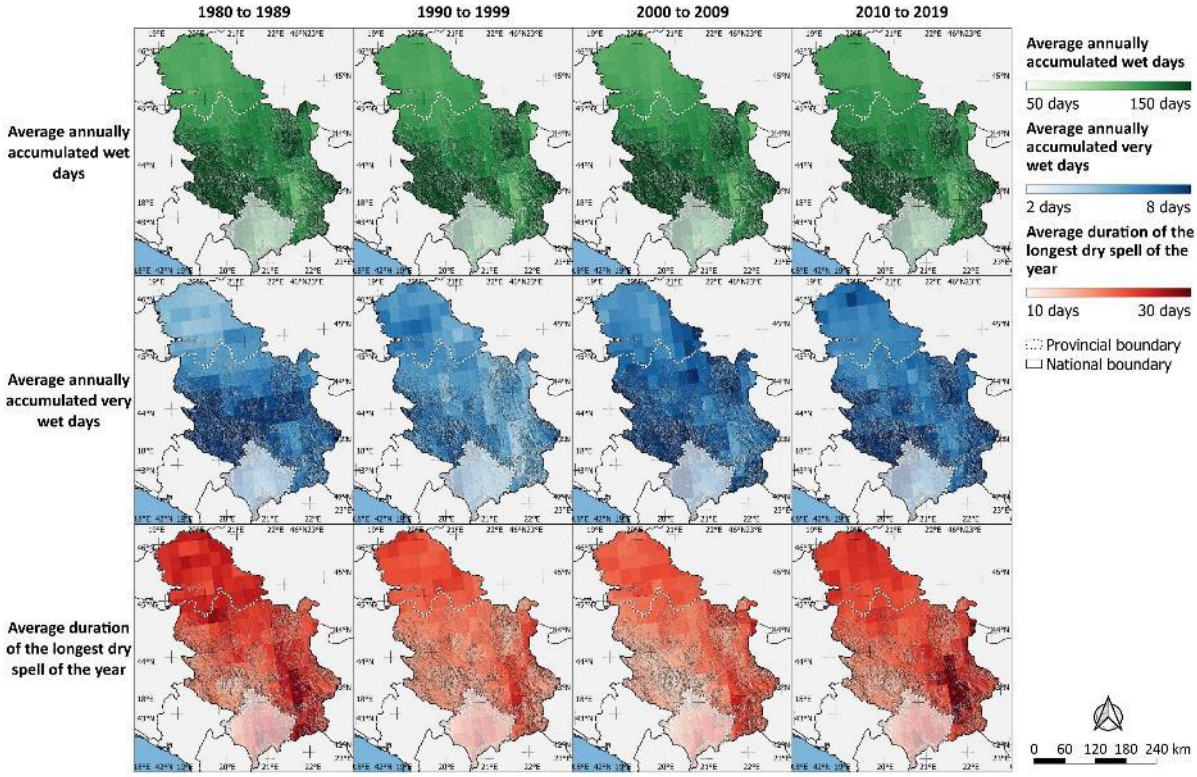

[36] The boundaries and names shown and the designations used on this map do not imply official endorsement or acceptance by the United Nations.

The distribution pattern seems to be constant for WD and VWD, with higher values observed in the highlands of the south, particularly on mountain tops, and lower values in the plains of the north and valleys of the south. The distribution for DS is also constant, but inverse, with lower values in the highlands of the south and higher values in the plains of the north and valleys of the south.

Projected annual trends on accumulated wet days, accumulated very wet days, and the duration of the longest dry spell can be seen in Figure 57 and Table 14[37]. Like projected precipitation, projected WD, VWD, and DS exhibit large projected inter-annual variations, with WD ranging between 80 and 200 days, VWD between 4 and 15 days, and DS between 10 and 50 days. It is thus important to note that the trends presented here should be interpreted with similar caution given the large variability.

Figure 57 – Projected annual time series of accumulated wet days, accumulated very wet days, and duration of the longest dry spell of the year

Time series over 2020-2060 period. Time series over 2020-2060 period. ***Pink dotted line****: variable value for each model separately under the RCP4.5 scenario.* ***grey dotted line****: variable value for each model separately under the RCP8.5 scenario.* ***Purple full line:*** *median value of the variable under RCP4.5 scenario.* ***Black full line:*** *median value of the variable under RCP8.5 scenario. Data source: NASA Earth Exchange - Global Daily Downscaled Climate Projections (NEX – GDDP) (Thrasher et al. 2012).*

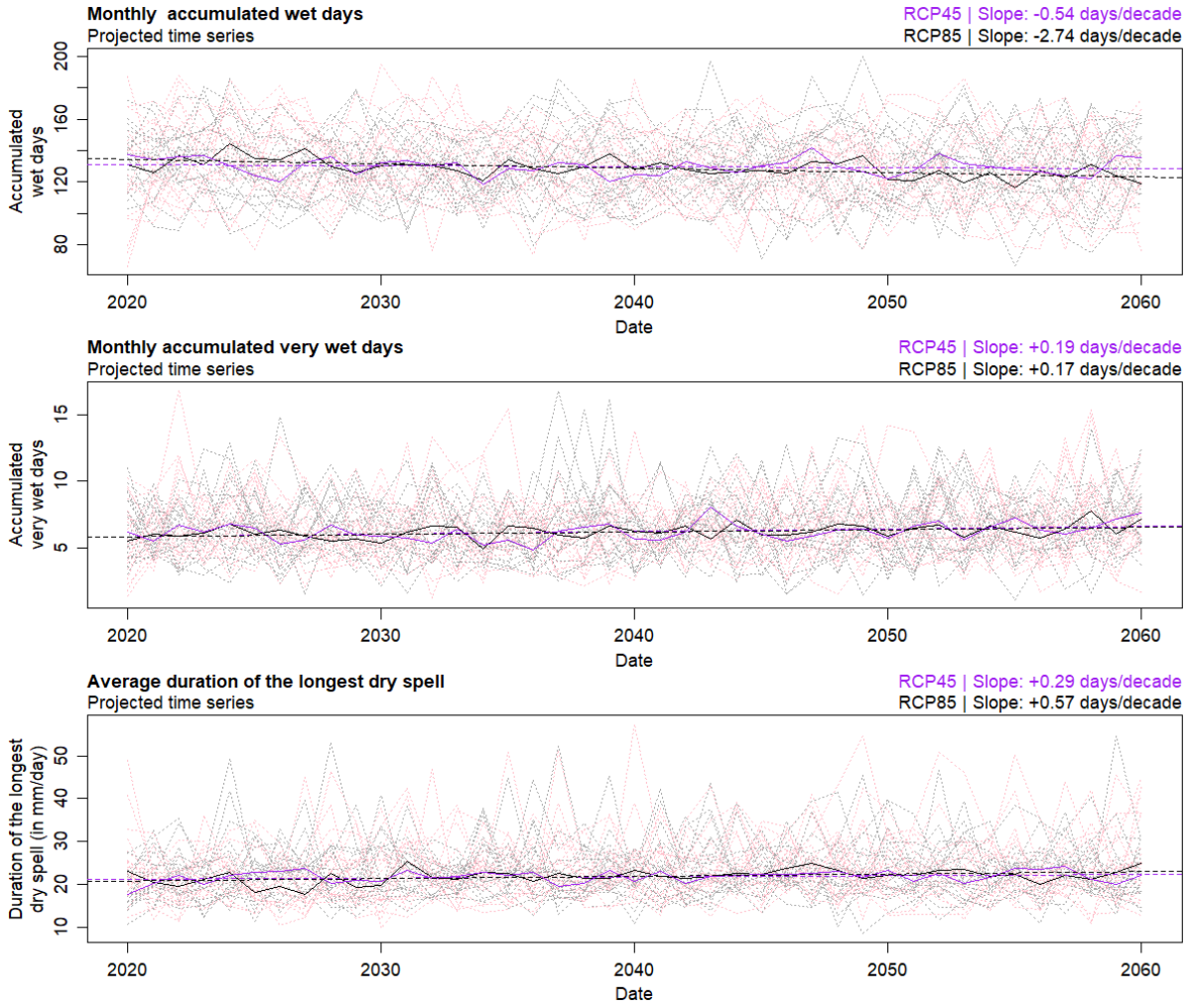

According to the NEX database, WD, VWD, and DS are expected to remain stable for the next 40 years under both scenarios, with WD averaging around 130 days, VWD around 6 days, and DS around 22 days. The only exception to this general trend is WD under the RCP8.5 scenario, which shows a small

[37] It should be noted that the validation of the median models of the NEX ensemble for accumulated wet days, accumulated very wet days and duration of the longest dry spell was uncertain under both scenario (RMSE: WD>1.1, VWD>1.0, DS>1.1 see Modelled data validation, below). Therefore, caution should be exercised when considering the projected accumulated wet days, accumulated very wet days and average duration of the longest dry spell in Serbia.

decrease of 3 days/decade, resulting in an average of 129 days in 2040 and 123 days in 2060. This trend confirms the decrease in accumulated precipitation observed in Figure 54 under the RCP8.5 scenario.

Table 14 – Characteristics of the trend from projected data for accumulated wet days, accumulated very wet days, and duration of the longest dry spell of the year (linear models)
Data source: NASA Earth Exchange - Global Daily Downscaled Climate Projections (NEX – GDDP) (Thrasher et al. 2012).

RCP4.5					
Variable	**Slope**	**p-value**	**Adjusted R^2**	**Average value in 2040**	**Average value in 2060**
WD	-0.54 days/decade	0.46	-0.01	130 days	129 days
VWD	+0.19 days/decade	0.03	0.09	6.22 days	6.60 days
DS	+0.29 days/decade	0.12	0.04	22 days	22 days
RCP8.5					
Variable	**Slope**	**p-value**	**Adjusted R^2**	**Average value in 2040**	**Average value in 2060**
WD	-2.74 days/decade	0.00	0.28	129 days	123 days
VWD	+0.17 days/decade	0.02	0.12	6.22 days	6.57 days
DS	+0.57 days/decade	0.01	0.15	22 days	23 days

Water deficit

This section provides an overview of the past trend of accumulated water deficit in the Republic of Serbia. The water deficit (Wdef) is calculated as the difference between measured evapotranspiration (ET) and potential evapotranspiration (PET). It should be noted that ET and PET were not available in the weather stations dataset. Therefore, we used Terra Net Evapotranspiration to calculate the water deficit for this section. Similarly, we were unable to find projected ET and PET data for Serbia, therefore no projected trend could be calculated.

Historical monthly accumulated water deficit can be observed in Figure 58 and Table 15. Despite large interannual variations (ranging from 550 mm to 850 mm), the annually accumulated water deficit in Serbia has increased on average over the last 19 years (+23 mm/decade). This increase has led to an average water deficit of 697 mm in 2019, up from 665 mm in 2001.

Figure 58 – Historical time series of annually accumulated water deficit
Time series over 2001-2019 period. Data source: NASA LP DAAC - EBMOD16A2.006: Terra Net Evapotranspiration (Running, Mu, and Zhao 2021).

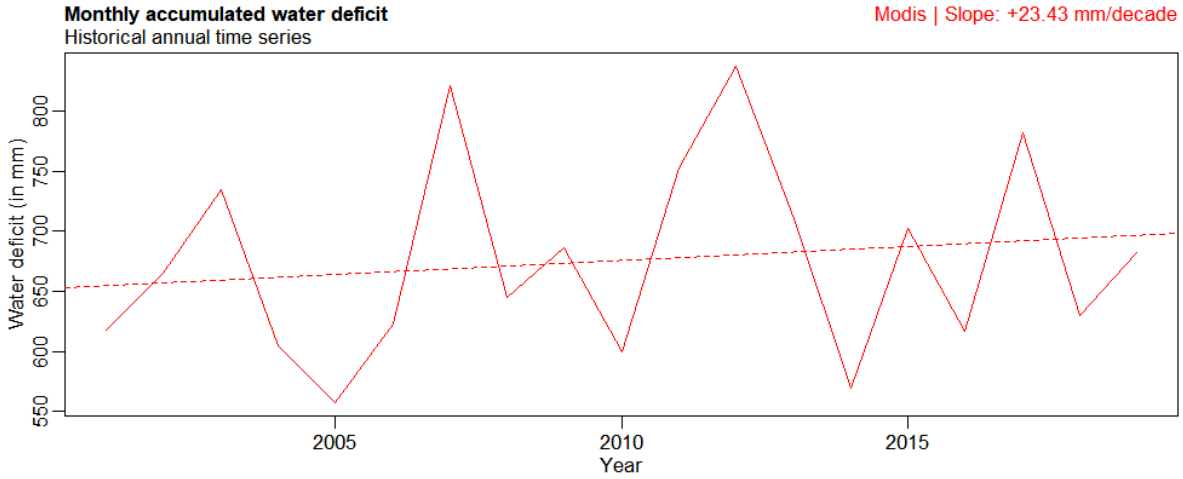

Table 15 – Characteristics of the trend from historical data for annually accumulated water deficit (linear models)
Data source: ERA5, ECMWF / Copernicus Climate Change Service (Muñoz Sabater 2019)

Variable	Slope	p-value	Adj. R^2	Average value in 1980	Average value in 2019
Wdef	+23.43 mm/decade	0.51	-0.03	605.35 mm	696.71 mm

The decadal spatial distribution of the annually accumulated water deficit throughout Serbia over the period 2001-2019 can be observed in Figure 59. The distribution of the annually accumulated water deficit has remained constant over the last 19 years, with higher values observed at lower altitudes.

Figure 59 – Historical decadal spatial distribution of annually accumulated water deficit[38]
Data averaged over the 2001-2019 period, by decade. Data source: NASA LP DAAC - EBMOD16A2.006: Terra Net Evapotranspiration (Running, Mu, and Zhao 2021).

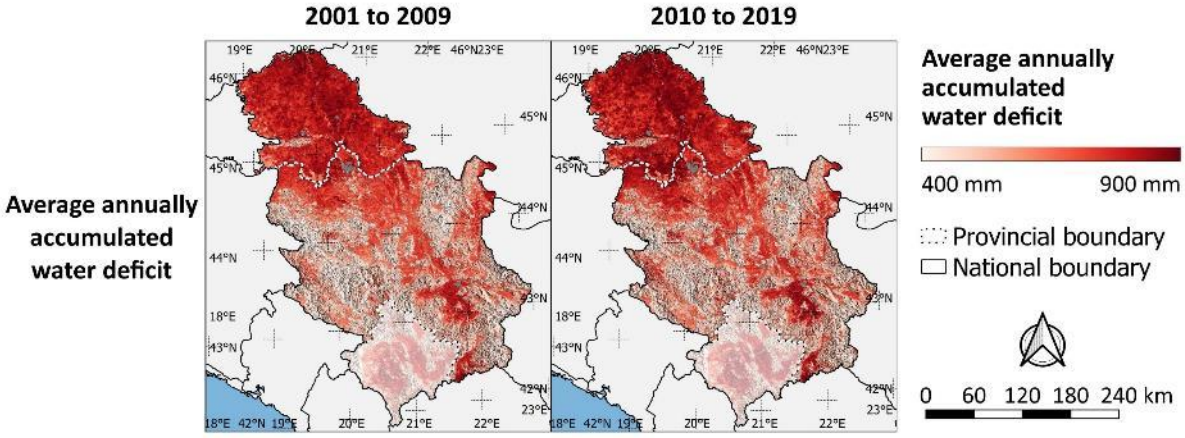

[38] The boundaries and names shown and the designations used on this map do not imply official endorsement or acceptance by the United Nations.

Precipitation variability

This section provides an overview of the past trend of variability of accumulated precipitation in the Republic of Serbia. The variability of accumulated precipitation (RRvar) will be represented by the standard deviation of the annually accumulated precipitation calculated over the previous 10 years, using a rolling window.

Figure 60 and Table 16 illustrate the historical standard deviation of annually accumulated precipitation. The RRvar has steadily increased over the past four decades, with a rate of (+24 mm/decade). As a result, the average standard deviation has risen from approximately 57 mm during the 1970-1980 period to 150 mm during the 2009-2019 period.

Figure 60 – Historical time series of standard deviation of the annually accumulated precipitation calculated over the previous 10 years (rolling window)

Time series over 1980-2019 period. Data source: Republic Hydrometeorological Service of Serbia, HidMet (Republic Hydrometeorological Service of Serbia 2020).

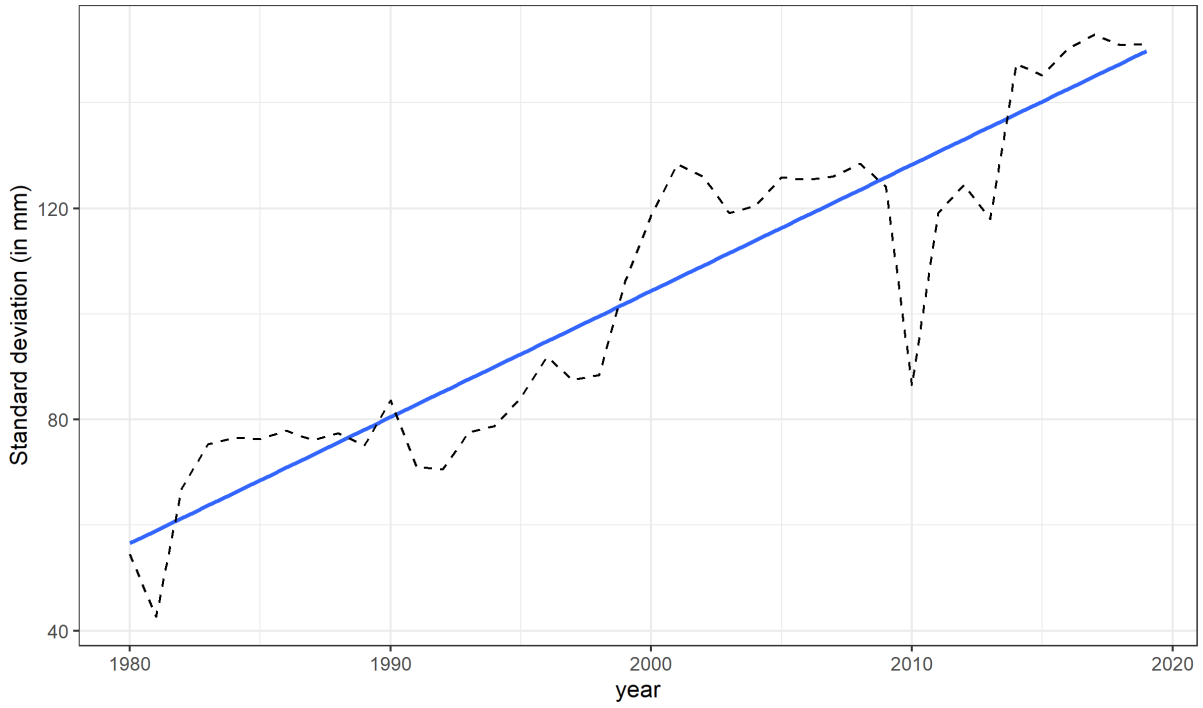

Table 16 – Characteristics of the trend from historical data for annually accumulated water deficit (linear models)

Data source: Republic Hydrometeorological Service of Serbia, HidMet (Republic Hydrometeorological Service of Serbia 2020).

Variable	Slope	p-value	Adj. R^2	Average value in 1980	Average value in 2019
RRvar	24 mm/decade	<0.001	0.85	57 mm	150 mm

SPEI

This section provides an overview of the past trends in the standardized precipitation evapotranspiration index (SPEI), which is a widely used tool for estimating droughts. The SPEI takes into account current precipitation, temperature, and potential evapotranspiration data, as well as the same data accumulated over a certain number of previous months. This information is then compared to data from the same period in previous years, resulting in a value that fluctuates around 0. When the SPEI falls below -1, it is generally considered a moderate drought period, while a value below -1.5 is typically considered a severe drought period.

SPEI is a highly flexible tool that can be adjusted to study different types of droughts[39] as the period of accumulated months can be specified. Meteorological droughts are typically studied using the 3-month accumulation SPEI, while agricultural droughts are often studied using the 6-month accumulation SPEI. Hydrological droughts are studied using the 9-month SPEI.

Over the past 40 years, Serbia has experienced an increasing number of meteorological, agricultural, and hydrological drought events. This trend is supported by the SPEI consistently falling below -1 or -1.5, as shown in Figure 61, Figure 62 and Figure 63. Conversely, wet periods have become less frequent, with SPEI rarely exceeding 1 or 1.5. The average amount of drought months per year has increased from +0.9 to +1.4 months per decade, depending on the type of drought (see Table 17).

Table 17 – Characteristics of the trend from historical data for annually accumulated water deficit (linear models)

Data source: Republic Hydrometeorological Service of Serbia, HidMet (Republic Hydrometeorological Service of Serbia 2020).

Variable	Slope	p-value	Average value in 1980	Average value in 2019
Number of meteorological drought months per year (3 months SPEI)	+0.94 months/decade	0.003	0.88 months	4.57 months
Number of agricultural drought months per year (6 months SPEI)	+1.05 months/decade	0.012	0.70 months	4.80 months
Number of hydrological drought months per year (9 months SPEI)	+1.45 months/decade	0.006	0.66 months	5.54 months

[39] Meteorological drought occurs when there is a prolonged period of below-normal precipitation, typically for a short period of time (usually 3 months). This type of drought impacts the availability of readily available water resources, including surface water and cisterns. Agricultural drought occurs when there is a prolonged period of below-normal precipitation, typically for a longer period of time (usually 6 months). Agricultural droughts have a significant impact on crop production, leading to reduced yields and economic losses. Finally, hydrological drought occurs when there is a prolonged period of below-normal precipitation, typically for a very long period of time (usually more than 6 months). This type of drought impacts watersheds, leading to reduced streamflow, depleted reservoirs, and dry wells. It often takes a long period of above-normal rainfall for the hydrological situation of the area to return to normal.

Figure 61 – Historical monthly time series of the 3 months SPEI

Time series over 1980-2019 period. Data source: Republic Hydrometeorological Service of Serbia, HidMet (Republic Hydrometeorological Service of Serbia 2020).

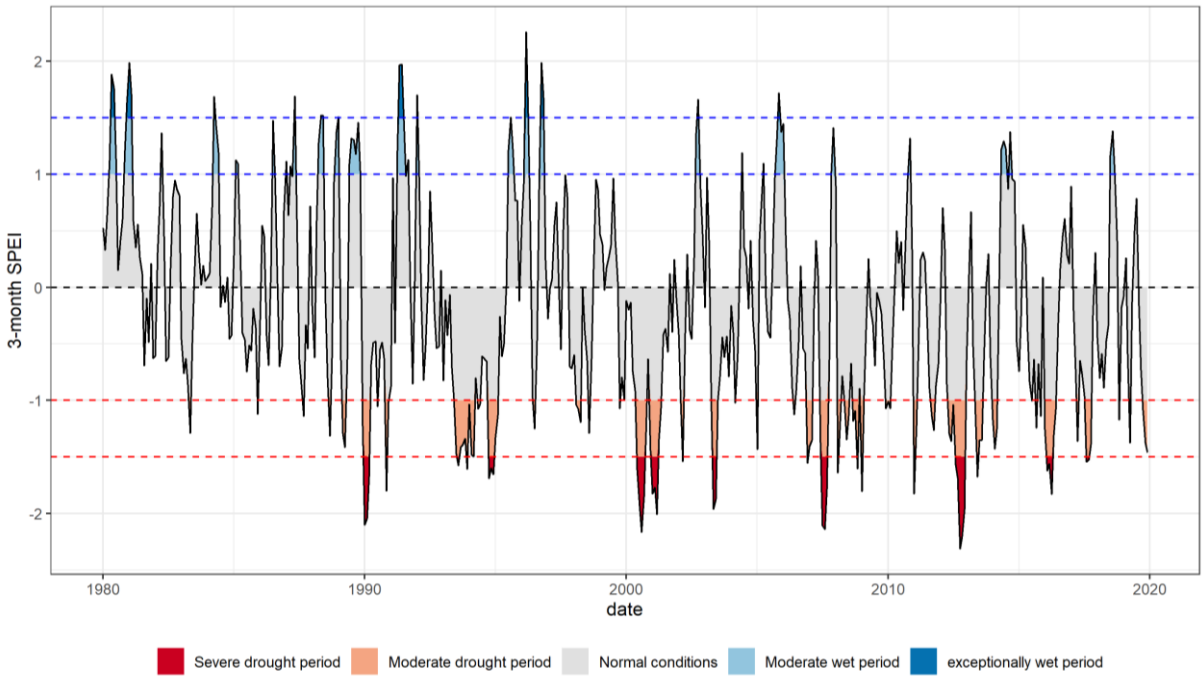

Figure 62 – Historical monthly time series of the 6 months SPEI

Time series over 1980-2019 period. Data source: Republic Hydrometeorological Service of Serbia, HidMet (Republic Hydrometeorological Service of Serbia 2020).

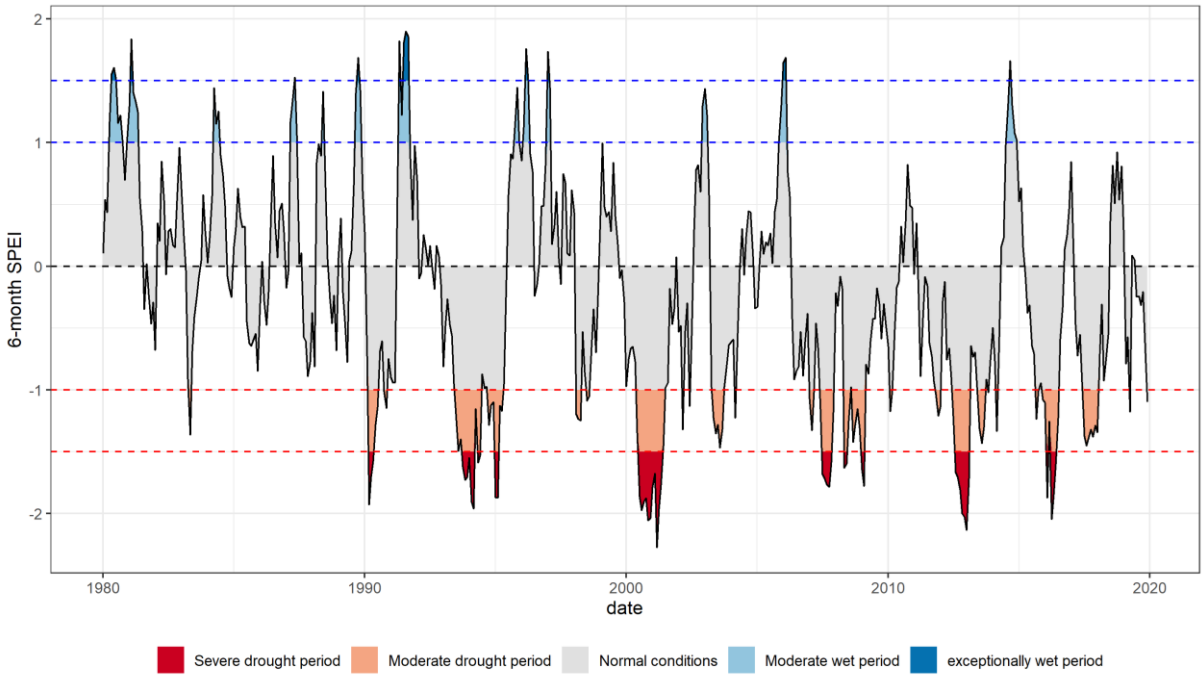

Figure 63 – Historical monthly time series of the 9 months SPEI

Time series over 1980-2019 period. Data source: Republic Hydrometeorological Service of Serbia, HidMet (Republic Hydrometeorological Service of Serbia 2020).

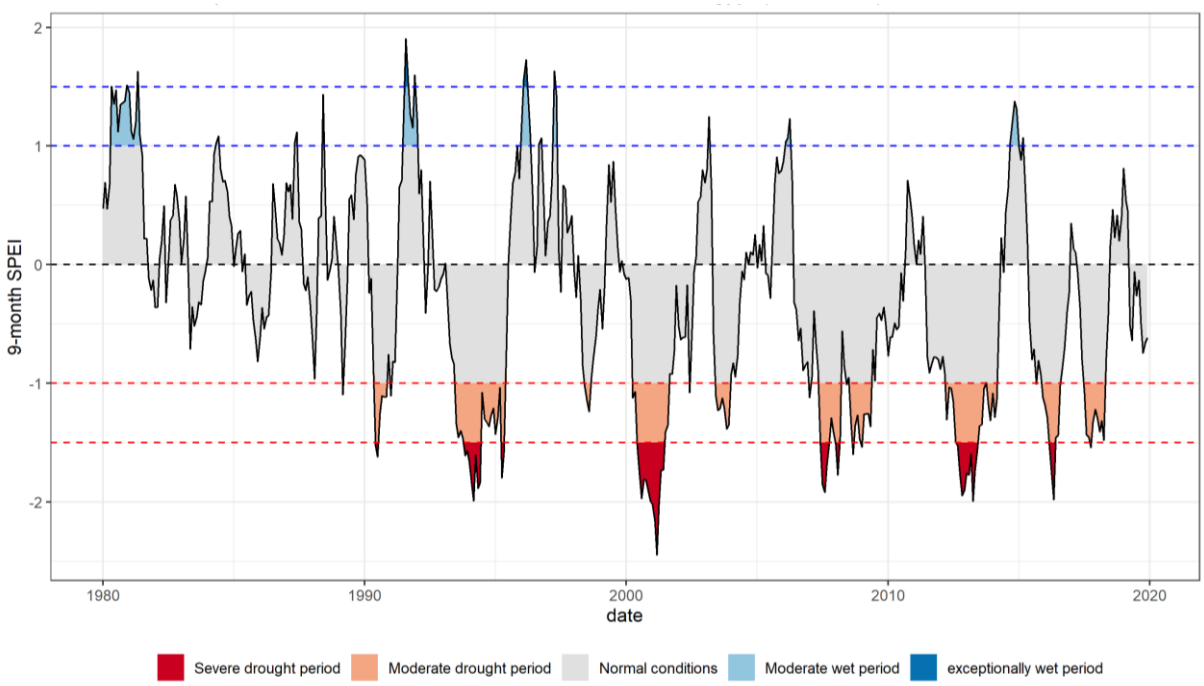

Snowfall & snow depth

This section provides an overview of the past trends of two snow variables in the Republic of Serbia: Accumulated Snowfall (SnF) and Average Snow Depth (SnD). SnF represents the accumulated snowfall in mm of water equivalent, while SnD represents the average snow depth in mm of water equivalent.

It should be noted that snowfall and snow depth data were not available in the weather stations dataset. Therefore, we used GLDAS data to calculate these variables for this section. Similarly, we were unable to find projected snowfall and snow depth data for Serbia, therefore no projected trend could be calculated.

Historical annual trends for these two snow indices in Serbia are presented in Figure 64 and Table 18.

Over the past two decades, there has been a slight decrease in the snowfall amount (SnF) and snow depth (SnD) in Serbia. Specifically, SnF has decreased by an average of -3.1 mm/decade, from 102 mm in 2000 to 96 mm in 2019. Meanwhile, SnD has decreased by an average of -3 mm/decade, from 25 mm in 2000 to 19 mm in 2019.

Figure 64 – Historical time series of annually accumulated snowfall and annually average snow depth
Data averaged over the 2000-2019 period. ***In blue:*** *annually accumulated snowfall.* ***In green:*** *annual average snow depth. Data source: NASA GES DISC - GLDAS-2.1: Global Land Data Assimilation System (Rodell et al. 2004).*

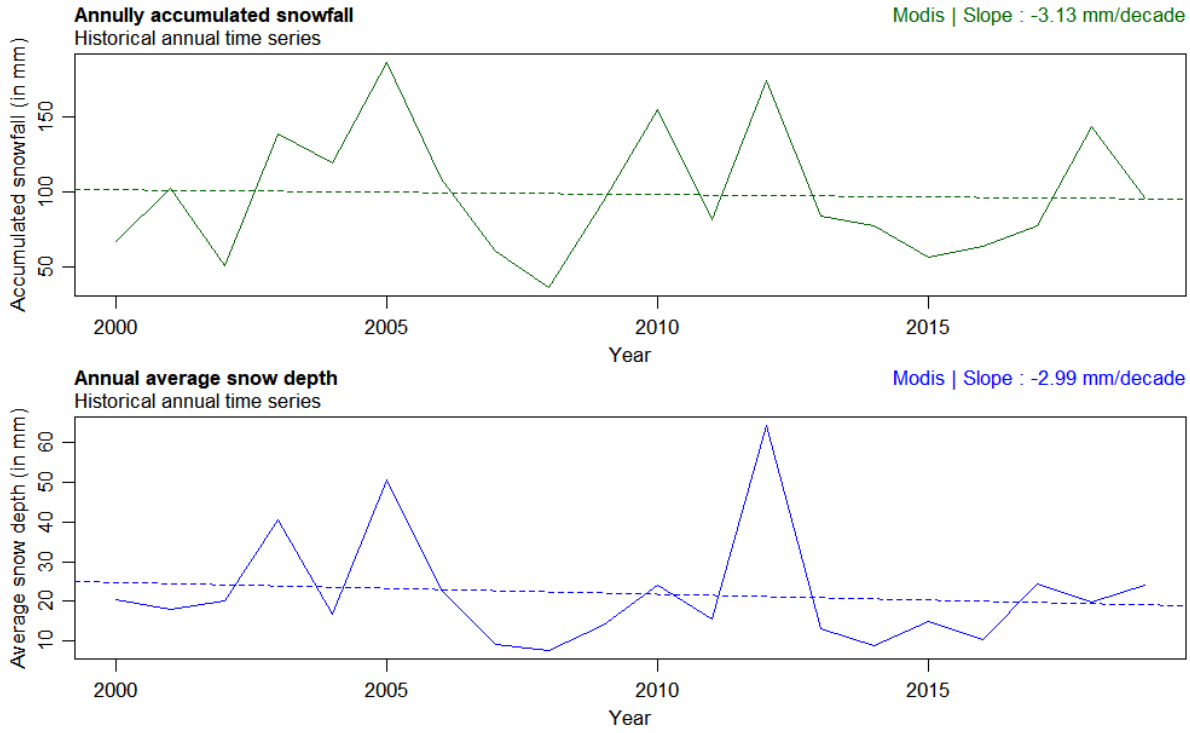

Table 18 – Characteristics of the trend from historical annual times series of accumulated frost days, ice days and chill hours (linear models)
Data source: ERA5, ECMWF / Copernicus Climate Change Service (Muñoz Sabater 2019)

Variable	Slope	p-value	Adj. R^2	Average value in 1980	Average value in 2019

SnF	-3.13 mm/decade	0.85	-0.05	107.98 mm	95.75 mm
SnD	-2.99 mm/decade	0.61	-0.04	30.80 mm	19.14 mm

Figure 65 provides the decadal spatial distribution of SnF and SnD for the period 2000-2019. The distribution of snow cover and snowfall has remained constant over the past two decades, with the highest values found at the highest altitudes in the Southeast and Southwest regions of the country, and a smaller amount of snowfall and snow depth on the Fruška Gora range.

Figure 65 – Historical decadal spatial distribution of annual average NDVI, LAI and vegetation productivity[40]. *Data averaged over the 2000-2019 period, by decade**. In blue:** annually accumulated snowfall. **In green:** annual average snow depth. Data source: NASA GES DISC - GLDAS-2.1: Global Land Data Assimilation System (Rodell et al. 2004).*

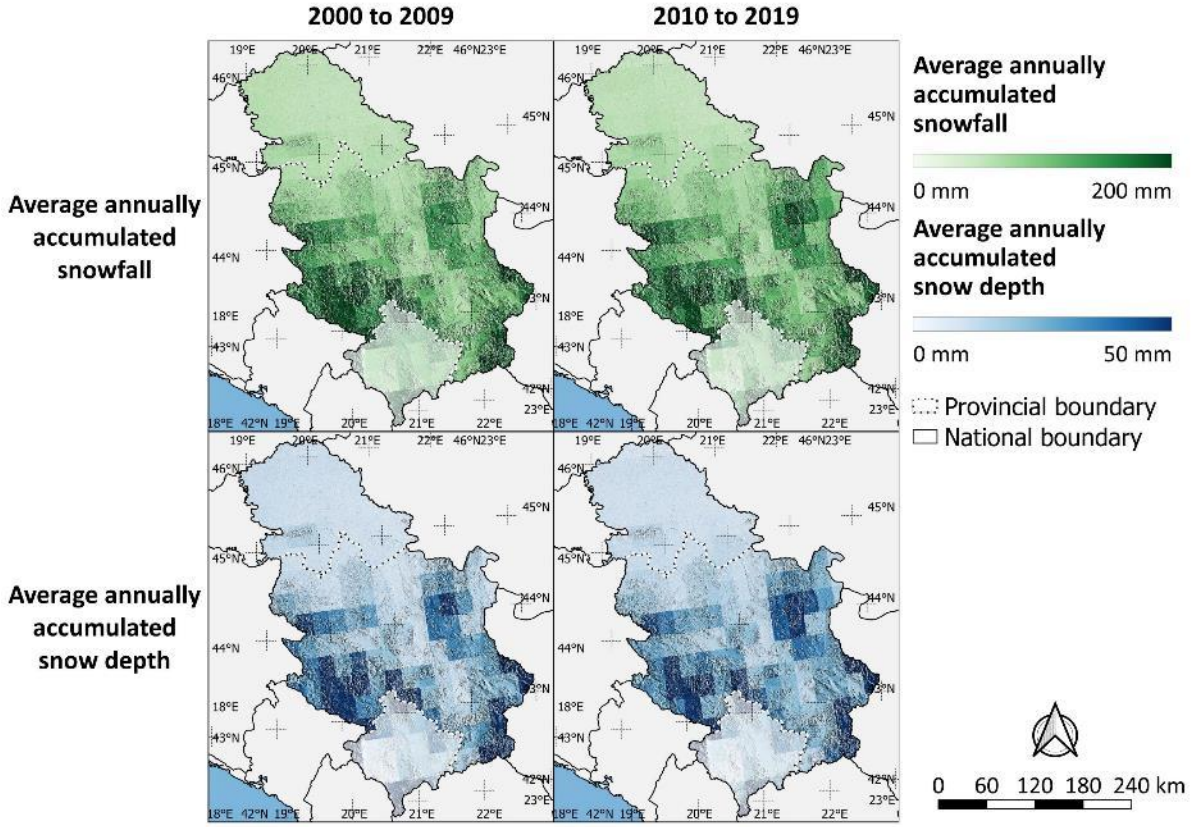

[40] The boundaries and names shown and the designations used on this map do not imply official endorsement or acceptance by the United Nations.

VEGETATION INDICES TRENDS

This section will outline the past trends of several vegetation indices in Serbia.

Summary

NDVI, LAI & Vegetation productivity index – NDVI, LAI & the vegetation productivity index have steadily increased since 2001 at a rate of +227/decade, +1.1/decade, and +1.0/decade, respectively. The very dry year of 2012 caused a noticeable decrease in all indices. The distribution of the vegetation indices remained constant during the study period, with higher values at higher altitudes and lower values at lower altitudes.

Start & length of the growing season - The start date of the growing season in Serbia has decreased slowly (-3 days/decade) while the length of the growing season has increased slowly (+2 days/decade), but year-to-year variability makes these trends uncertain. The growing season in Serbia begins on average on April 14 and lasts about 155 days, with differences some between the north and south of the country. In the south, the variables are evenly distributed, while in the north, the distribution is patCH due to variations in agricultural practices. The distribution of the growing season variable has not changed significantly over the observed periods.

Ellenberg's Quotient & Forest Aridity Index - Ellenberg's Quotient and Forest Aridity Index showed large year-to-year variations between 1980 and 2019, and no statistically significant trends could be ascertained. Under the RCP 8.5 scenario, both Ellenberg's Quotient and Forest Aridity Index are expected to increase significantly, while under the RCP 4.5 scenario, only Ellenberg's Quotient is expected to increase significantly. The historical trends of Ellenberg's Quotient and Forest Aridity Index at the district level were consistent with the country-level trends. The projected trends of Ellenberg's Quotient at the district level are all projected to show a statistically significant increase under both scenarios, while the projected trends of and Forest Aridity Index at the district level are all projected to show a statistically significant increase under the RCP 8.5 scenario, but only in certain districts under the RCP 4.5 scenario.

NDVI, LAI & Vegetation productivity index

This section focuses on the past trends of three vegetation indices in the Republic of Serbia: Leaf Area Index (LAI), Normalized Difference Vegetation Index (NDVI), and Vegetation Productivity (VP). LAI is a dimensionless index that represents the ratio of canopy area to total area. A higher LAI value indicates a larger canopy. NDVI is a dimensionless spectral index that represents the amount of live green vegetation. A higher NDVI value indicates a greener area. VP is an index that indicates the spatial distribution and change of vegetation cover. It is produced by the European Environment Agency (EEA) and is derived from remote sensing observed time series of vegetation indices[41].

As no projected data is available for LAI, NDVI, and VP, this section will solely focus on the historical trends of these indices.

Figure 66 and Table 19 show the historical annual trends on NDVI, LAI, and vegetation productivity.

Figure 66 – Historical time series of the annual average NDVI, LAI and vegetation productivity
Time series over 2001-2019 period. ***In red:*** *NDVI.* ***In green:*** *LAI.* ***In blue:*** *VPy. Data source: MODIS - NASA LP DAAC (Myneni, Knyazikhin, and Park 2015; Didan 2015) and European Environment Agency (EEA)*

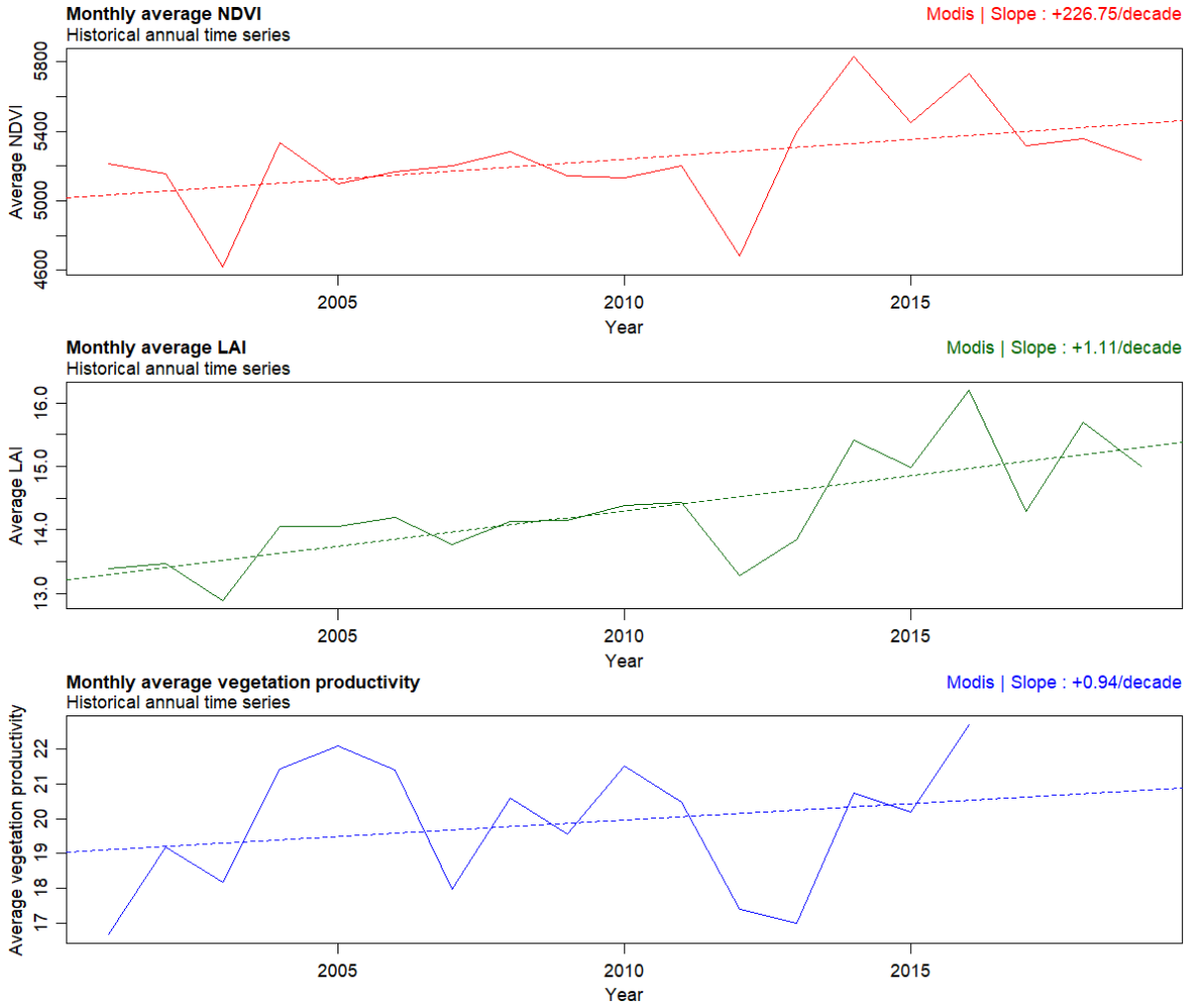

[41] https://www.eea.europa.eu/ds_resolveuid/IND-480-en

Table 19 – Characteristics of the trend from historical data for annual average NDVI, LAI, and vegetation productivity (linear models)
Data source: MODIS - NASA LP DAAC (Myneni, Knyazikhin, and Park 2015; Didan 2015) and European Environment Agency (EEA).

Variable	Slope	p-value	Adj. R^2	Average value in 1980	Average value in 2019
NDVI	+226.75/decade	0.05	0.16	4559.58	5443.92
LAI	+1.11/decade	0.00	0.51	10.98	15.29
VP	+0.94/decade	0.38	-0.01	17.14	20.80

Figure 67 – Historical decadal spatial distribution of annual average NDVI, LAI and vegetation productivity[42]
Data averaged over the 2001-2019 period, by decade. Data source: MODIS - NASA LP DAAC (Myneni, Knyazikhin, and Park 2015; Didan 2015) and European Environment Agency (EEA).

[42] The boundaries and names shown and the designations used on this map do not imply official endorsement or acceptance by the United Nations.

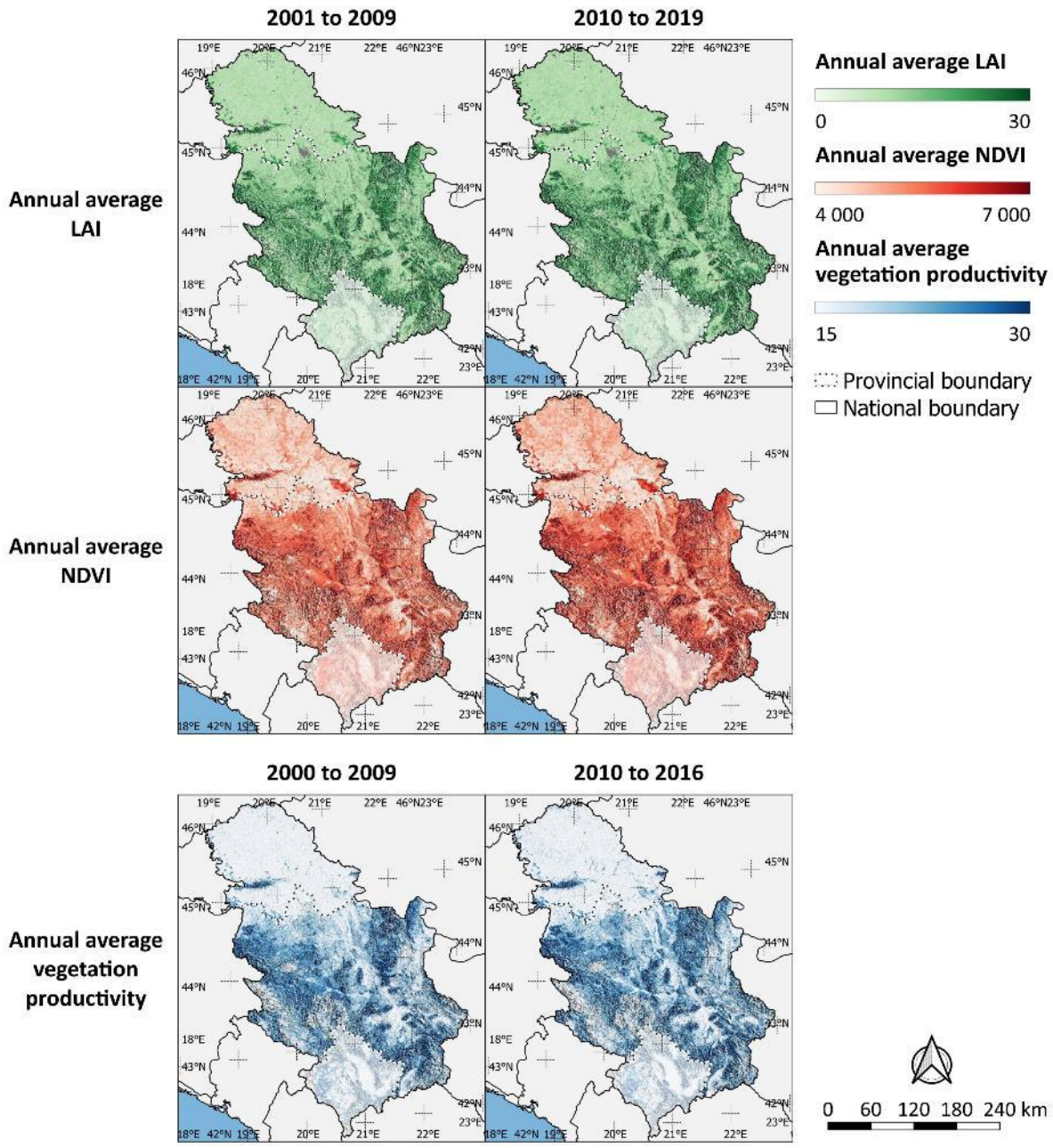

Since 2001, all vegetation indices have steadily increased (NDVI: +227/decade, LAI: +1.1/decade, VP: +1.0/decade). It is worth noting that the very dry year of 2012 is clearly visible in each index's time series as a significant decrease. However, no projected data on these indices is available, so only past trends can be presented.

Figure 67 shows the decadal spatial distribution of NDVI, LAI, and VP across the Republic of Serbia from 2001 to 2019. The analysis reveals a constant spatial pattern of the selected vegetation indices, with higher values observed at higher altitudes and lower values at lower altitudes. This pattern was consistent for all indices, with areas at high elevations generally exhibiting higher NDVI, LAI, and VP values compared to lower elevation areas. The difference in vegetation distribution across Serbia may contribute to this pattern, as forests are typically found on slopes and highlands (as shown in Figure 3).

Start & length of the growing season

In this section, we will present the past trends of two variables related to the growth season in the Republic of Serbia. These variables are the start date of the growing season (GS) and the length of the growing season (GL). GS represents the day of the year when vegetation starts to grow and is calculated by the European Environment Agency based on the Plant Phenology Index. The GL variable, on the other hand, represents the timespan between the start and end of the growing season and is also calculated by the European Environment Agency based on the Plant Phenology Index[43].

Historical annual trends on growing season variables can be observed in Figure 68 and Table 20.

Figure 68 – Historical time series of start date and length of the growing season
Time series over 2001-2016 period. ***In red:*** *start date of growing season.* ***In green:*** *length of the growing season. Data source: European Environment Agency (EEA).*

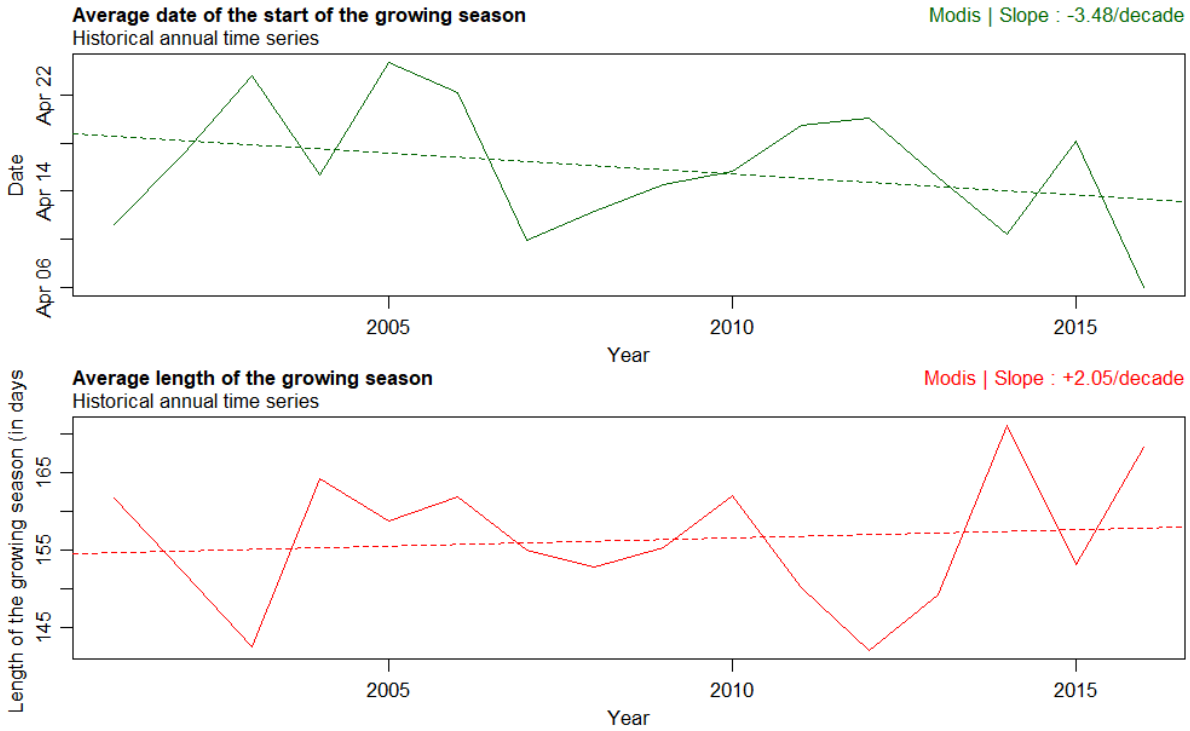

Table 20 – Historical trends characteristics for start date and length of the growing season (linear models)
Time series over 2001-2016 period. Data source: European Environment Agency (EEA).

Variable	Slope	p-value	Adj. R^2	Average value in 1980	Average value in 2019
GS	-3.48/decade	0.24	0.03	115.26	101.67
GL	+2.05/decade	0.67	-0.06	150.44	158.46

Despite observing a slow decrease in the start date of the growing season (approximately -3 days/decade) and a slow increase in the length of the growing season (about +2 days/decade), the high year-to-year variability of both indices makes these trends uncertain (p>>0.05; adj. R2 close to 0). The start of the growing season in the Republic of Serbia, on average, is around the 14th of April, and it lasts for approximately 155 days.

[43] https://www.eea.europa.eu/data-and-maps/data/annual-start-of-vegetation-growing

The historical decadal spatial distribution of GS and GL throughout the Republic of Serbia over the period 2001-2016 can be observed in Figure 69.

Figure 69 – Historical spatial distribution of start date and length of the growing season[44]
Data averaged over the 2001-2010 and 2010-2016 periods. Data source: European Environment Agency (EEA) .

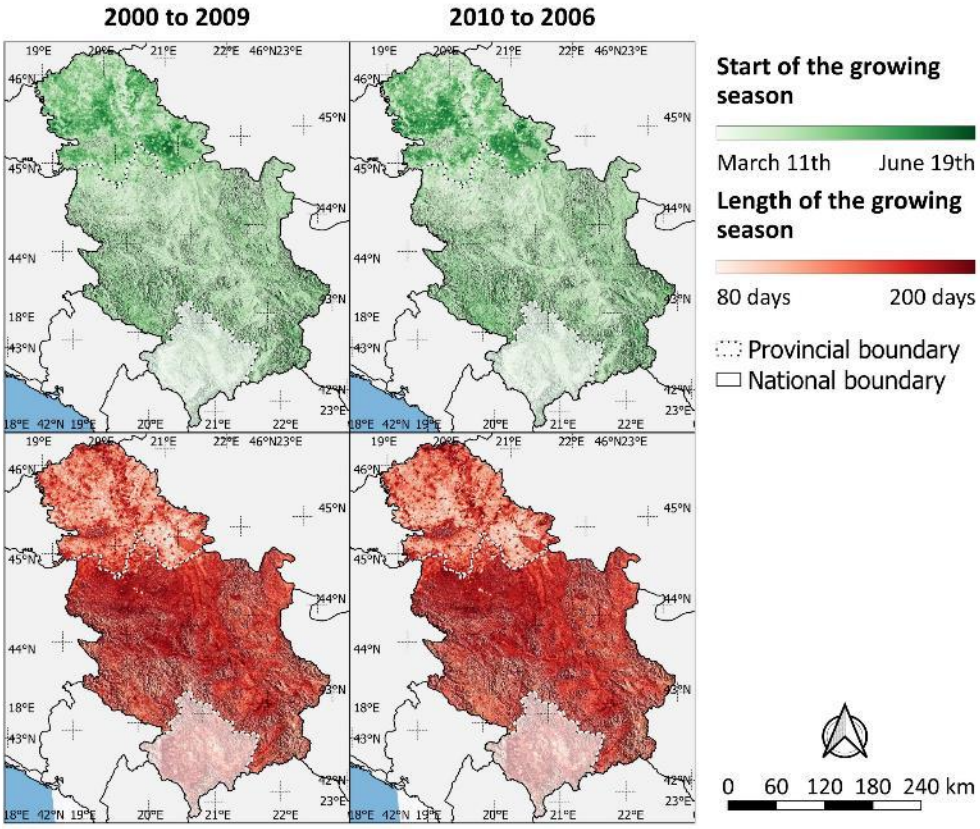

There is a clear regional difference in the distribution of the two growing season variables in the Republic of Serbia. South of the Sava-Danube axis, both variables are evenly distributed with a slightly later start and shorter length of the growing season observed at higher altitudes. In the northern part of the country, where agriculture is the dominant land use, the start and length of the growing season are strongly related to the crop calendar, leading to a patchy distribution of the variables. The distribution is influenced by the type of crops grown and the agricultural practices employed. Despite the two periods of observation, there was no noticeable change in the distribution of the growing season variables across the country.

[44] The boundaries and names shown and the designations used on this map do not imply official endorsement or acceptance by the United Nations.

Ellenberg's Quotient & Forest Aridity Index

This section will present the historical variation of Ellenberg's Quotient (EQ) and Forest Aridity Index (FAI) in the Republic of Serbia. The forest aridity index and Ellenberg's quotient as define in Miletić et al. (2021), are given as follow:

The forest aridity index (FAI) (Führer et al. 2011) is defined as:

$$FAI = \frac{100 \times \frac{T_{VII} + T_{VIII}}{2}}{P_V + P_{VI} + 2 \times P_{VII} + P_{VIII}}$$

Where T_{VII} is the average temperature during the month of July, T_{VIII} is the average temperature during the month of August, P_V is the accumulated precipitation during the month of May, P_{VI} is the accumulated precipitation during the month of June, P_{VII} is the accumulated precipitation during the month of July and P_{VIII} is the accumulated precipitation during the month of August. Temperatures are given in °C, and precipitations in mm. FAI considers the average temperature of the critical months (July and August) and precipitation during the main growth cycle (May to July), as well as precipitation during the critical months (July and August)

Ellenberg's (1988) quotient (EQ) is defined as:

$$EQ = \left(\frac{T_{max.\ month}}{P_{annual}}\right) * 1000$$

Where $T_{max.\ month}$ is the average temperature of the warmest month (in °C) and P_{annual} is the annually accumulated precipitation (in mm).

The validation process was hindered due to the limited number of data couples available during the overlap period, as FAI and EQ are calculated annually. With only 14 data couples available, the sample size was not sufficient for a proper validation to be conducted.

Figure 70 displays historical trends for Ellenberg's Quotient (EQ) and Forest Aridity Index (FAI) between 1980 and 2019. Both indices showed significant year-to-year variations during this time, with EQ ranging from 21.50°C/mm in 2014 to 60.76°C/mm in 2000, and FAI ranging from 3.63°C/mm in 2014 to 16.13°C/mm in 2000. No statistically significant trends were thus observed for either index (p value = 0.87 for EQ and 0.79 for FAI). Therefore, these indices are considered constant, with an average value of 33.99°C/mm for EQ and 7.71°C/mm for FAI.

Figure 71 illustrates projected annual trends in temperature under two different scenarios: RCP 8.5 and RCP 4.5. Both scenarios predict a statistically significant increase in EQ and FAI. Under RCP 8.5, EQ and FAI are expected to increase at rates of +1.88°C/mm.decade and +0.42°C/mm.decade, respectively. This result in an average EQ of 38.98°C/mm and an average FAI of 8.27°C/mm in 2060, compared to averages of 31.48°C/mm and 6.58°C/mm in 2020. Under RCP 4.5, only EQ is expected to show a statistically significant increasing trend, with an increase rate of +0.75°C/mm.decade, resulting in an average EQ of 36.16°C/mm in 2060. FAI is projected to remain stable around 7.30°C/mm during the same period.

Figure 70 – Historical annual time series of Ellenberg's Quotient and Forest Aridity Index
Time series over 1980-2019 period. ***Blue plot:*** *Ellenberg's Quotient.* ***Green plot:*** *Forest Aridity Index* *Data source: Serbia NAP - Advancing Medium And Long-Term Adaptation Planning In The Republic Of Serbia (United Nations Development Programme (UNDP) and Serbian Ministry of Agriculture Forestry and Water Management n.d.)*

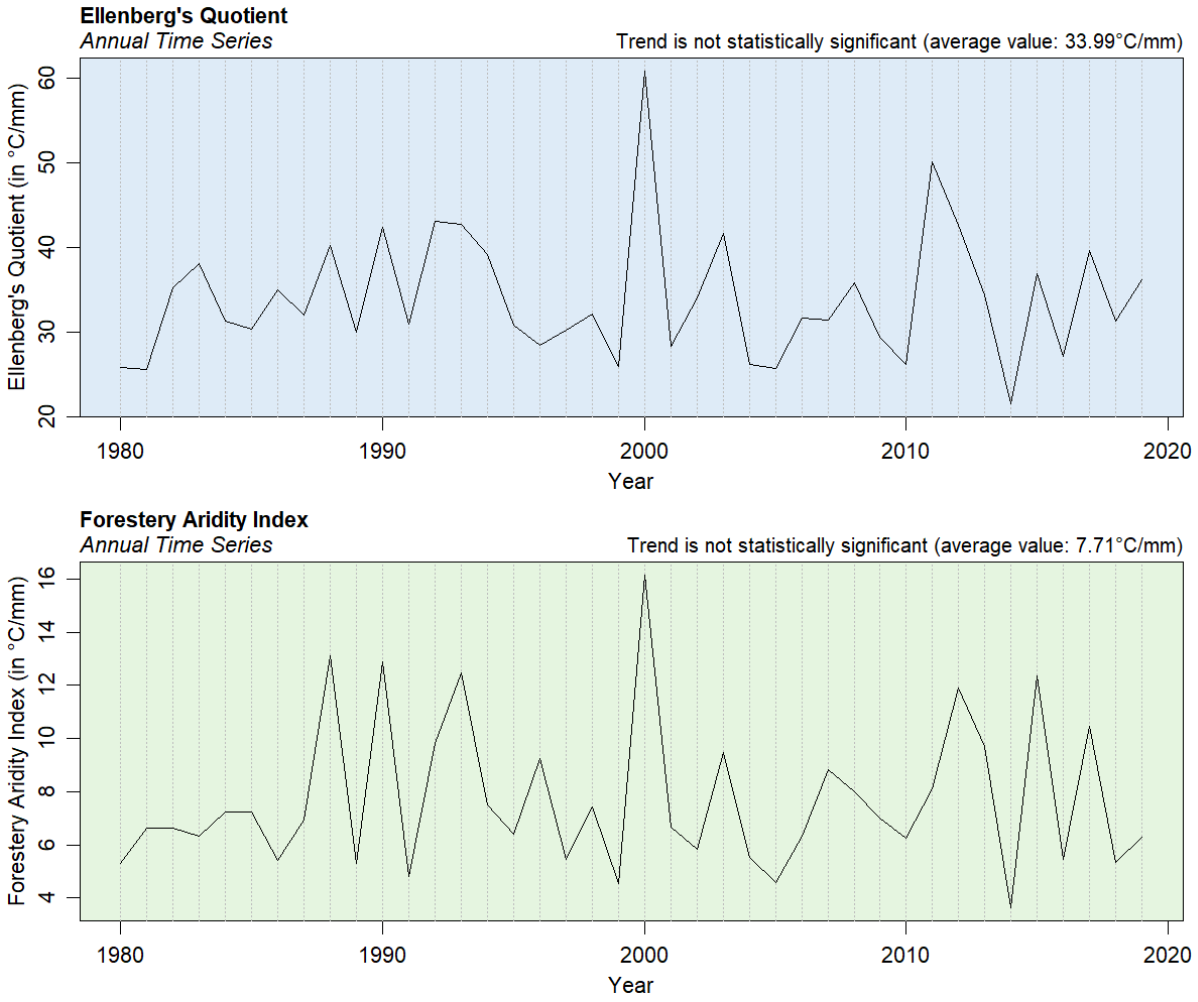

Figure 72, Figure 73, and Figure 74 present historical trends of Ellenberg's Quotient (EQ) at the district level. These trends align with the country-level EQ trend, as none of the districts exhibit a statistically significant trend. Across districts, the average EQ value ranged from 24.26°C/mm in Zlatiborski to 44.30°C/mm in Severno-banatski.

Figure 71 – Projected annual time series of Ellenberg's Quotient and Forest Aridity Index
Time series over 1980-2019 period. ***Blue plot:*** *Ellenberg's Quotient.* ***Green plot:*** *Forest Aridity Index.* ***Green full line:*** *data under RCP 4.5 scenario, median model.* ***Orange dotted line:*** *data under RCP 8.5 scenario, individual model.* ***Green full line:*** *data under RCP 4.5 scenario, median model.* ***Orange dotted line:*** *data under RCP 8.5 scenario, individual model. Data source: NASA Earth Exchange - Global Daily Downscaled Climate Projections (NEX – GDDP) (Thrasher et al. 2012).*

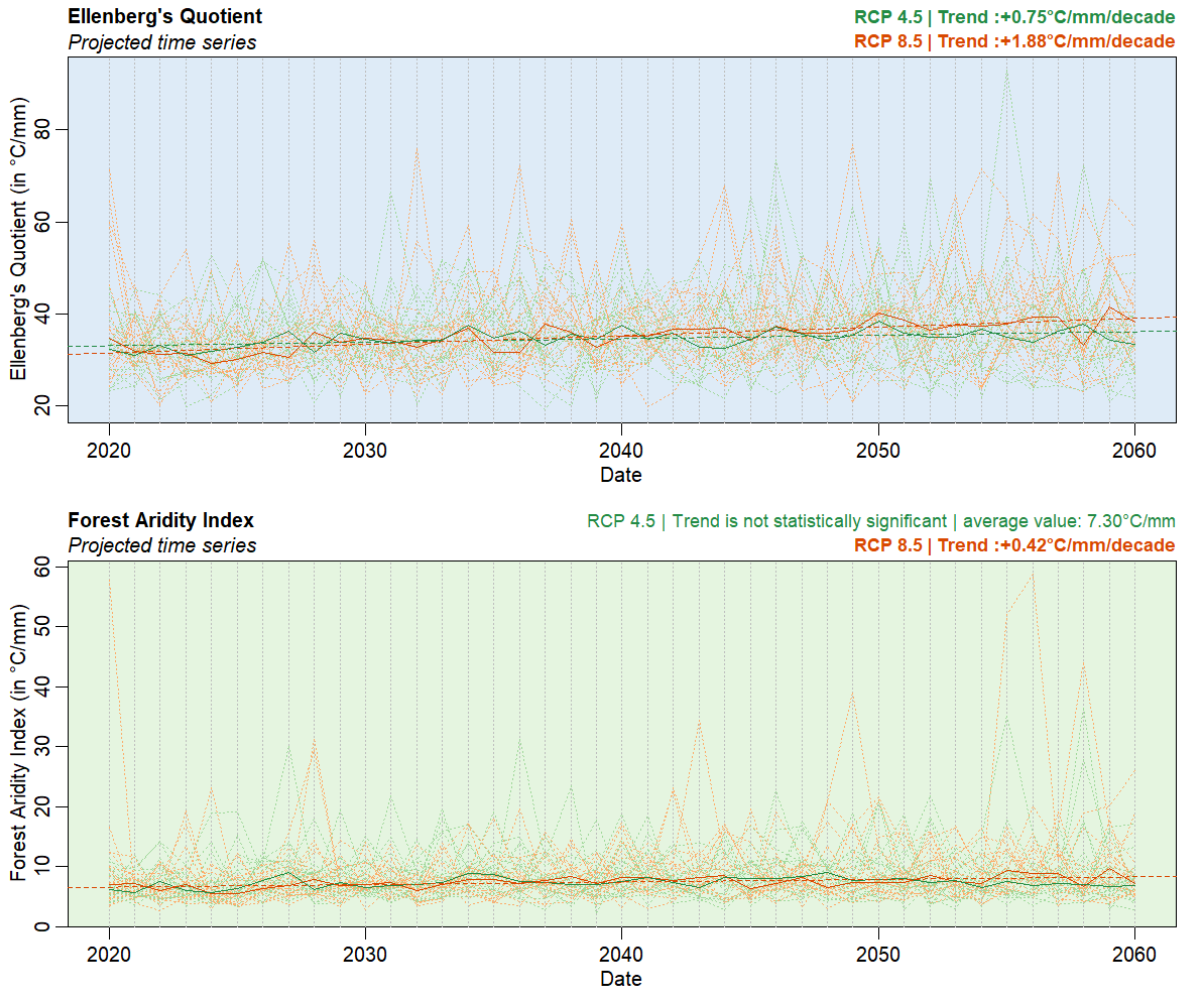

Figure 72 – Historical time series of Ellenberg's Quotient at the district level (Borski to Moravicki)
Time series over 1980-2019 period. Data source: Serbia NAP - Advancing Medium And Long-Term Adaptation Planning In The Republic Of Serbia (United Nations Development Programme (UNDP) and Serbian Ministry of Agriculture Forestry and Water Management n.d.)

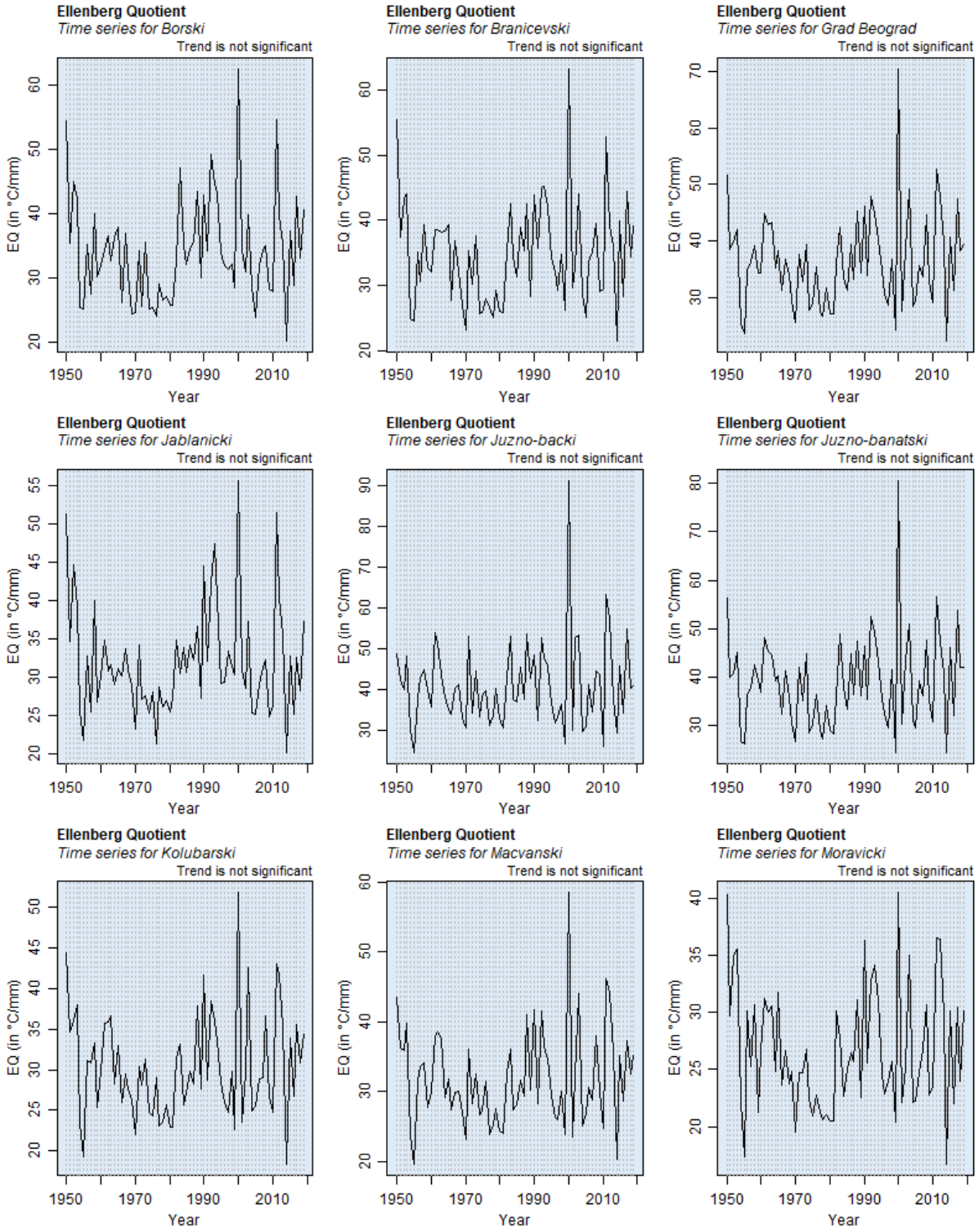

Figure 73 – Historical time series of Ellenberg's Quotient at the district level (Nisavski to Severno-Banatski)
Time series over 1980-2019 period. Data source: Serbia NAP - Advancing Medium And Long-Term Adaptation Planning In The Republic Of Serbia (United Nations Development Programme (UNDP) and Serbian Ministry of Agriculture Forestry and Water Management n.d.)

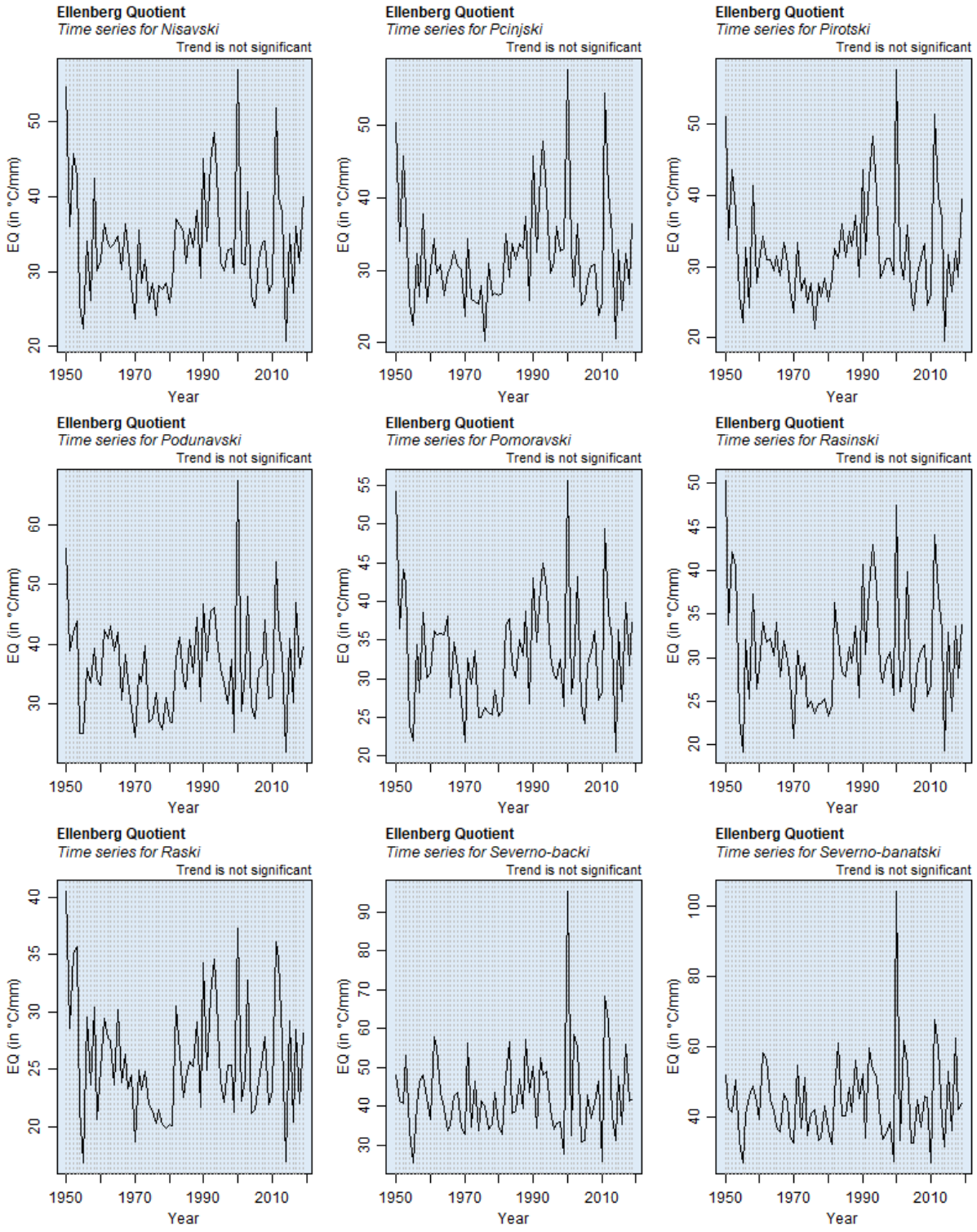

Figure 74 – Historical time series of Ellenberg's Quotient at the district level (Srednje-Banatski to Zlatiborski)
Time series over 1980-2019 period. Data source: Serbia NAP - Advancing Medium And Long-Term Adaptation Planning In The Republic Of Serbia (United Nations Development Programme (UNDP) and Serbian Ministry of Agriculture Forestry and Water Management n.d.)

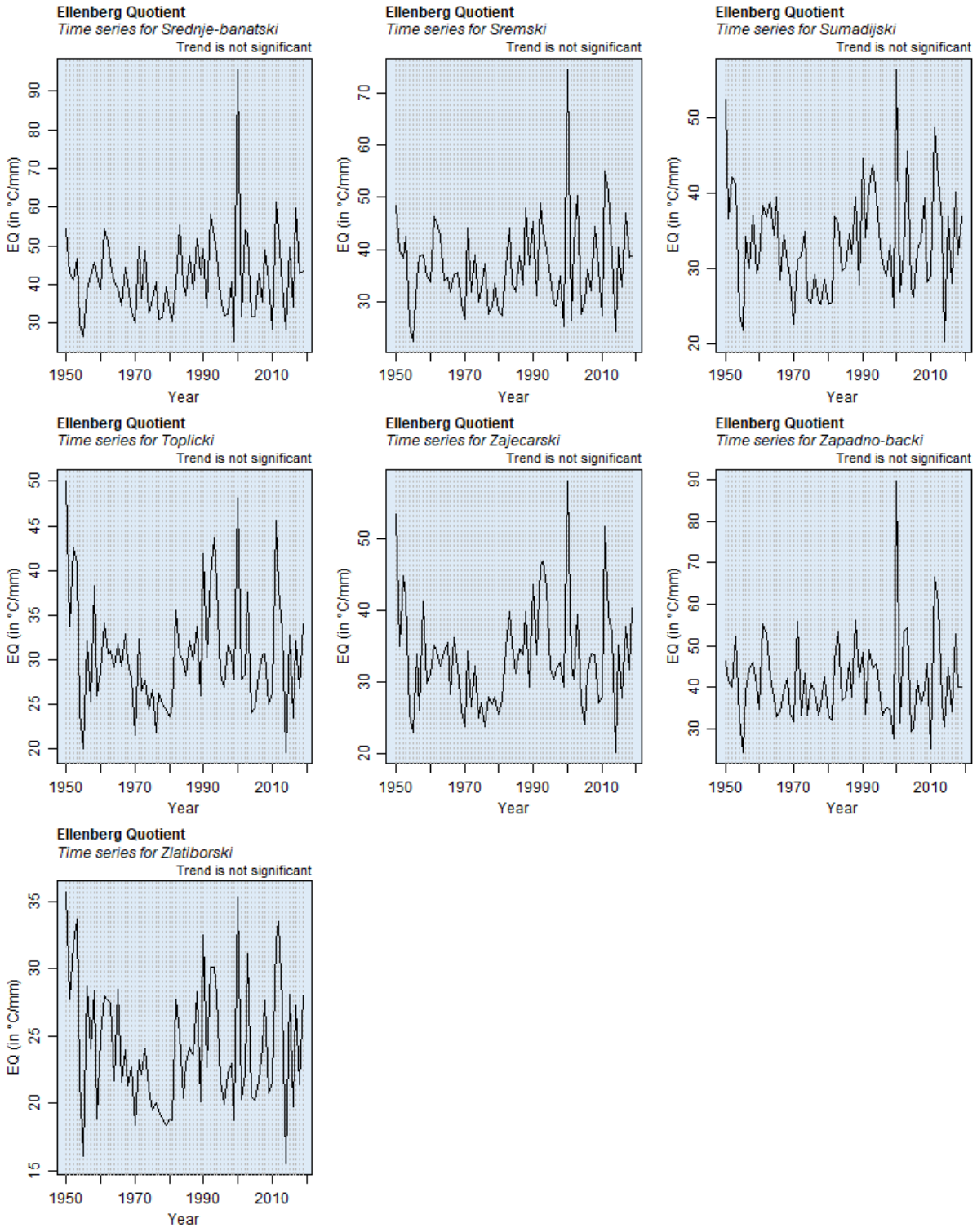

Historical trends of Forest Aridity Index at the district level can be observed in Figure 75, Figure 76 and Figure 77.

Figure 75 – Historical time series of Forest Aridity Index at the district level (Borski to Moravicki)
Time series over 1980-2019 period. Data source: Serbia NAP - Advancing Medium And Long-Term Adaptation Planning In The Republic Of Serbia (United Nations Development Programme (UNDP) and Serbian Ministry of Agriculture Forestry and Water Management n.d.)

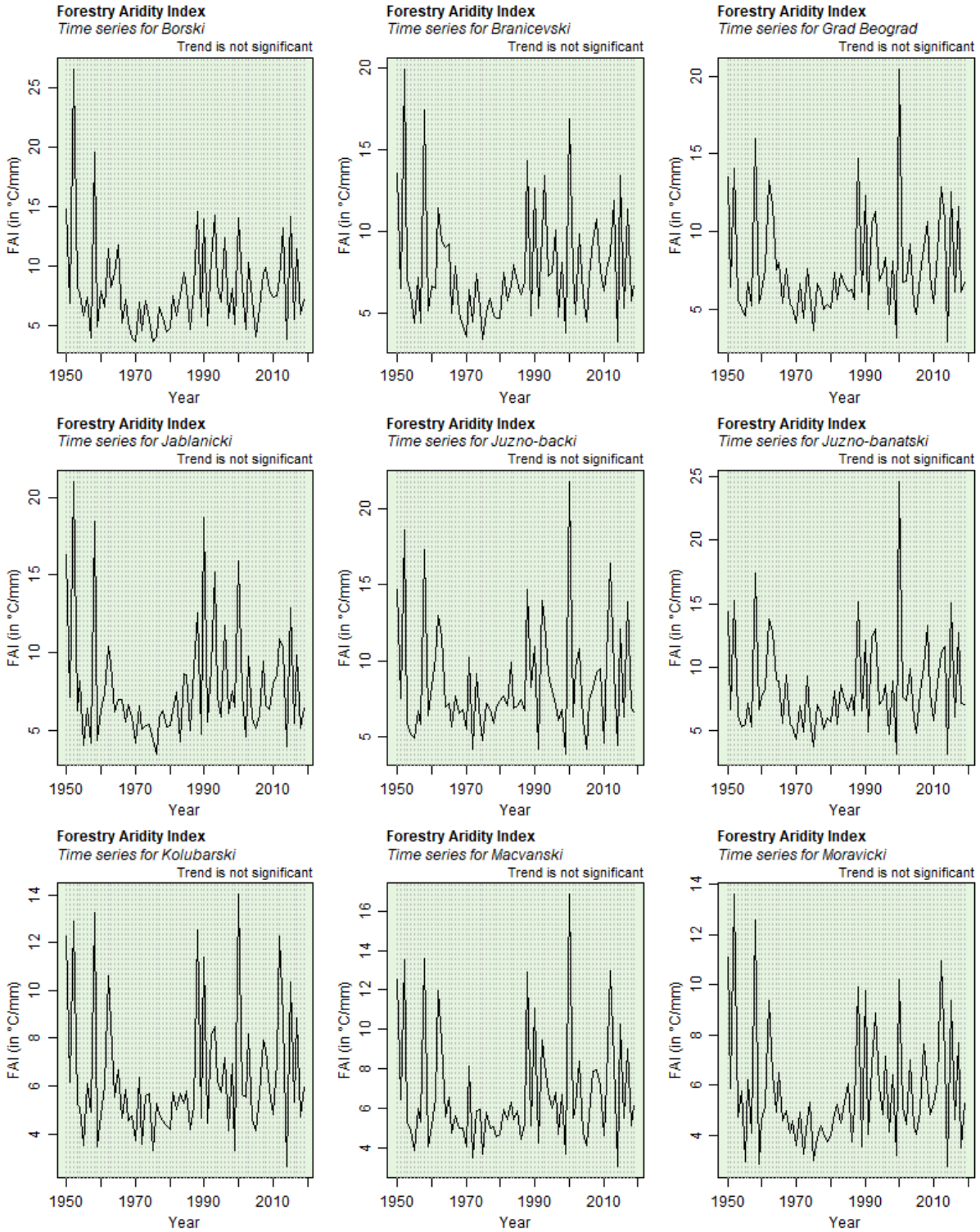

Figure 76 – Historical time series of Forest Aridity Index at the district level (Nisavski to Severno-Banatski)
Time series over 1980-2019 period. Data source: Serbia NAP - Advancing Medium And Long-Term Adaptation Planning In The Republic Of Serbia (United Nations Development Programme (UNDP) and Serbian Ministry of Agriculture Forestry and Water Management n.d.)

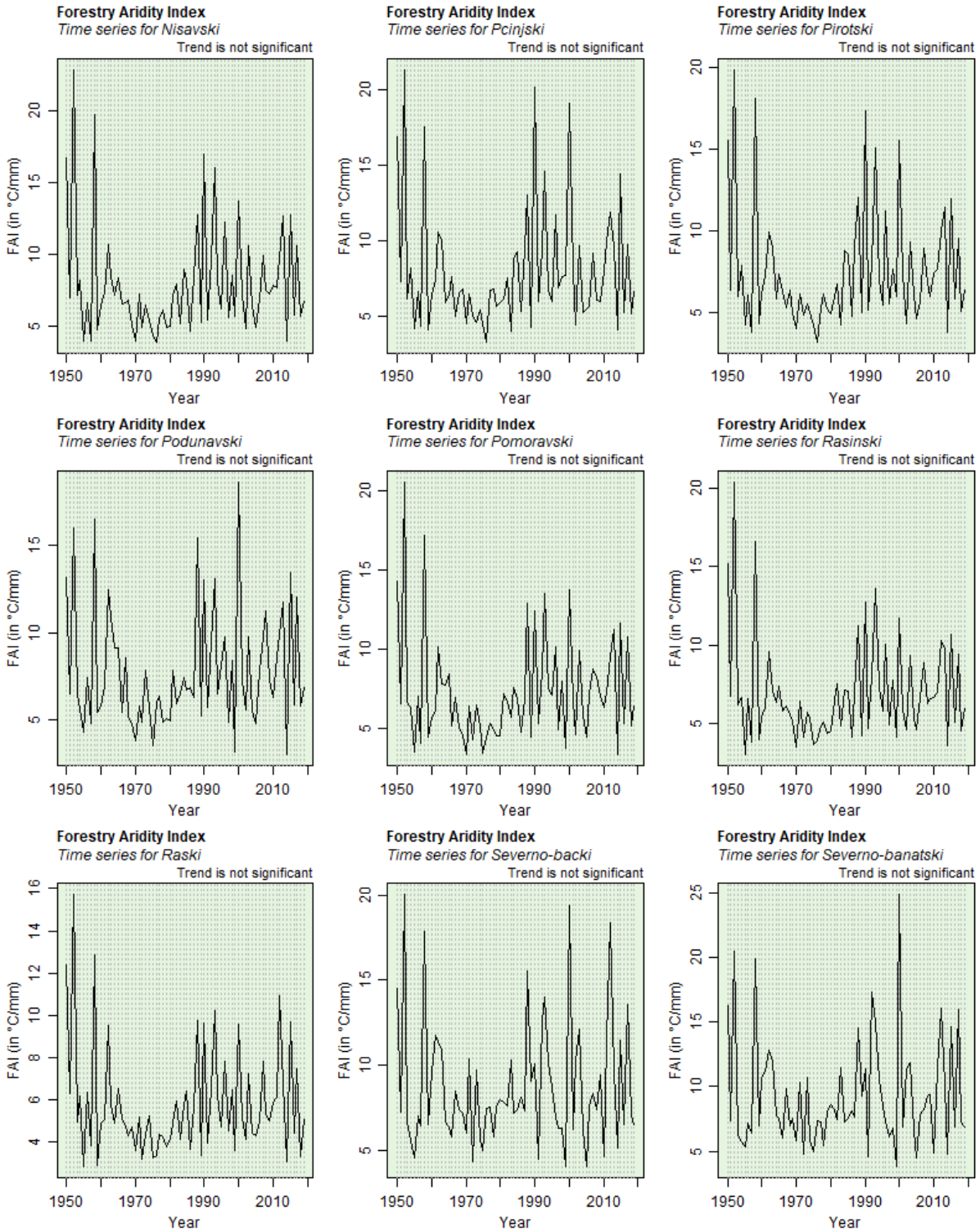

Figure 77 – Historical time series of Forest Aridity Index at the district level (Srednje-Banatski to Zlatiborski)
Time series over 1980-2019 period. Data source: Serbia NAP - Advancing Medium And Long-Term Adaptation Planning In The Republic Of Serbia (United Nations Development Programme (UNDP) and Serbian Ministry of Agriculture Forestry and Water Management n.d.)

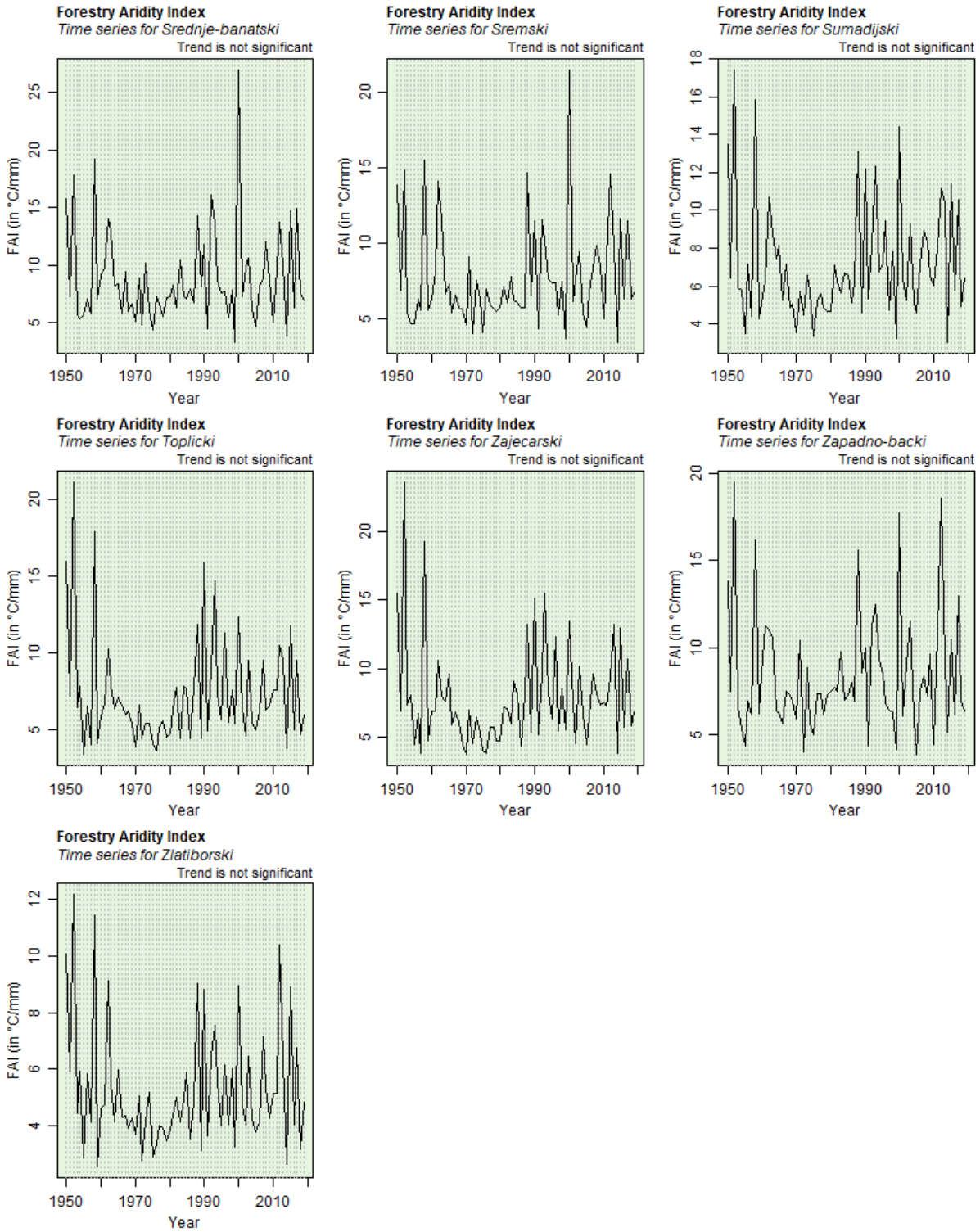

Similar to the country-level trend, none of the districts exhibit a statistically significant trend in the historical trends of Forest Aridity Index (FAI) at the district level. The average FAI value across districts ranged from 5.27°C/mm in Zlatiborski to 9.22°C/mm in Severno-banatski.

Figure 78, Figure 79, Figure 80 display the projected trends of Ellenberg's Quotient (EQ) at the district level. Under both RCP 4.5 and RCP 8.5 scenarios, all districts are projected to experience a statistically significant increase in EQ between 2020 and 2060. The average increase in EQ is anticipated to range from +0.45°C/mm/decade in Moravicki to +1.13°C/mm/decade in Pcinjski under the RCP 4.5 scenario and from +1.37°C/mm/decade in Macvanski to +2.49°C/mm/decade in Pcinjski under the RCP 8.5 scenario.

Figure 78 – Projected time series of Ellenberg's Quotient at the district level (Borski to Moravicki)
Time series over 2020-2060 period. Data source: NASA Earth Exchange - Global Daily Downscaled Climate Projections (NEX – GDDP) (Thrasher et al. 2012).

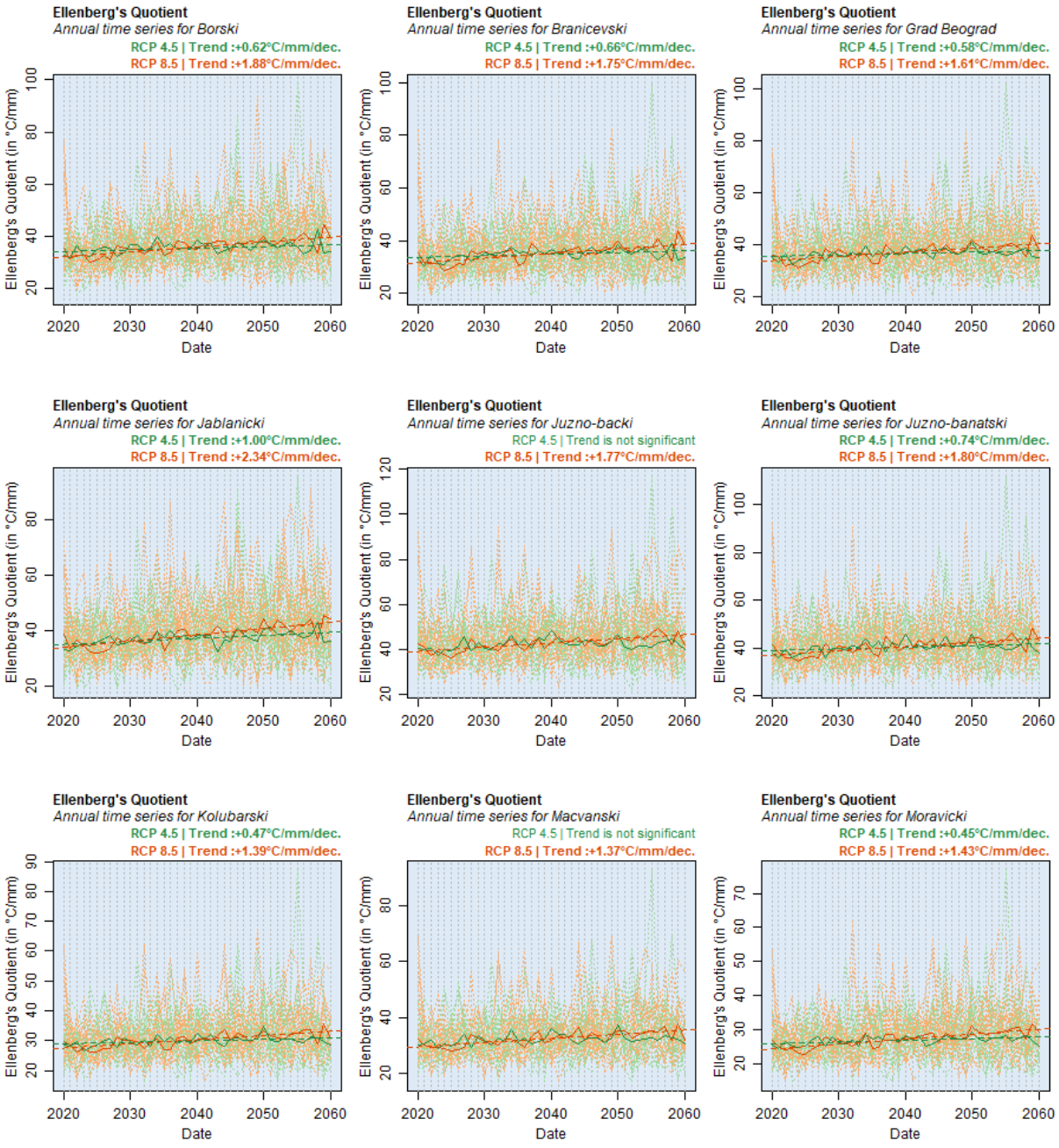

Figure 79 – Projected time series of Ellenberg's Quotient at the district level (Nisavski to Severno-Banatski)
Time series over 2020-2060 period. Data source: NASA Earth Exchange - Global Daily Downscaled Climate Projections (NEX – GDDP) (Thrasher et al. 2012).

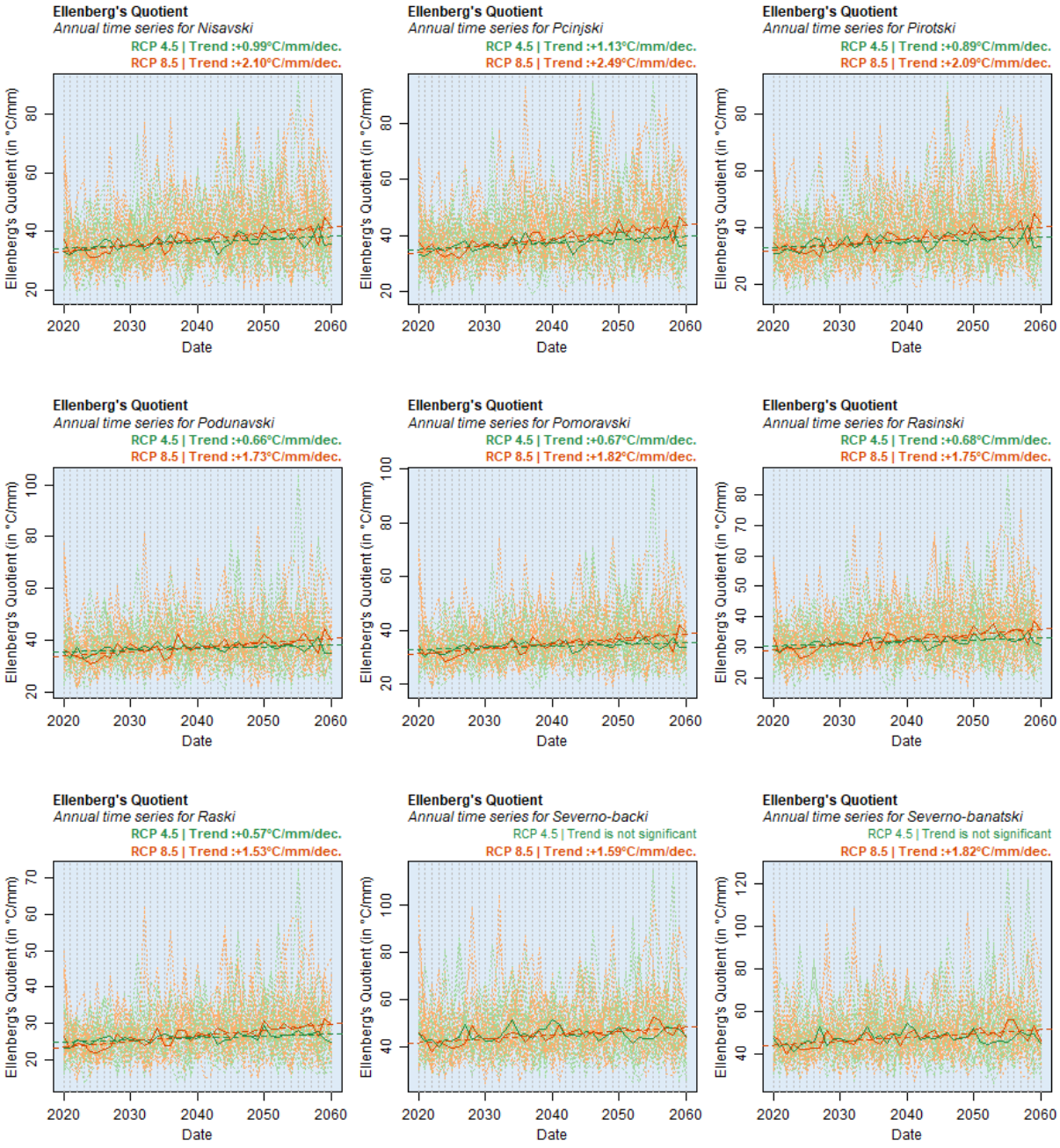

Figure 80 – Projected time series of Ellenberg's Quotient at the district level (Srednje-Banatski to Zlatiborski)
Time series over 2020-2060 period. Data source: NASA Earth Exchange - Global Daily Downscaled Climate Projections (NEX – GDDP) (Thrasher et al. 2012).

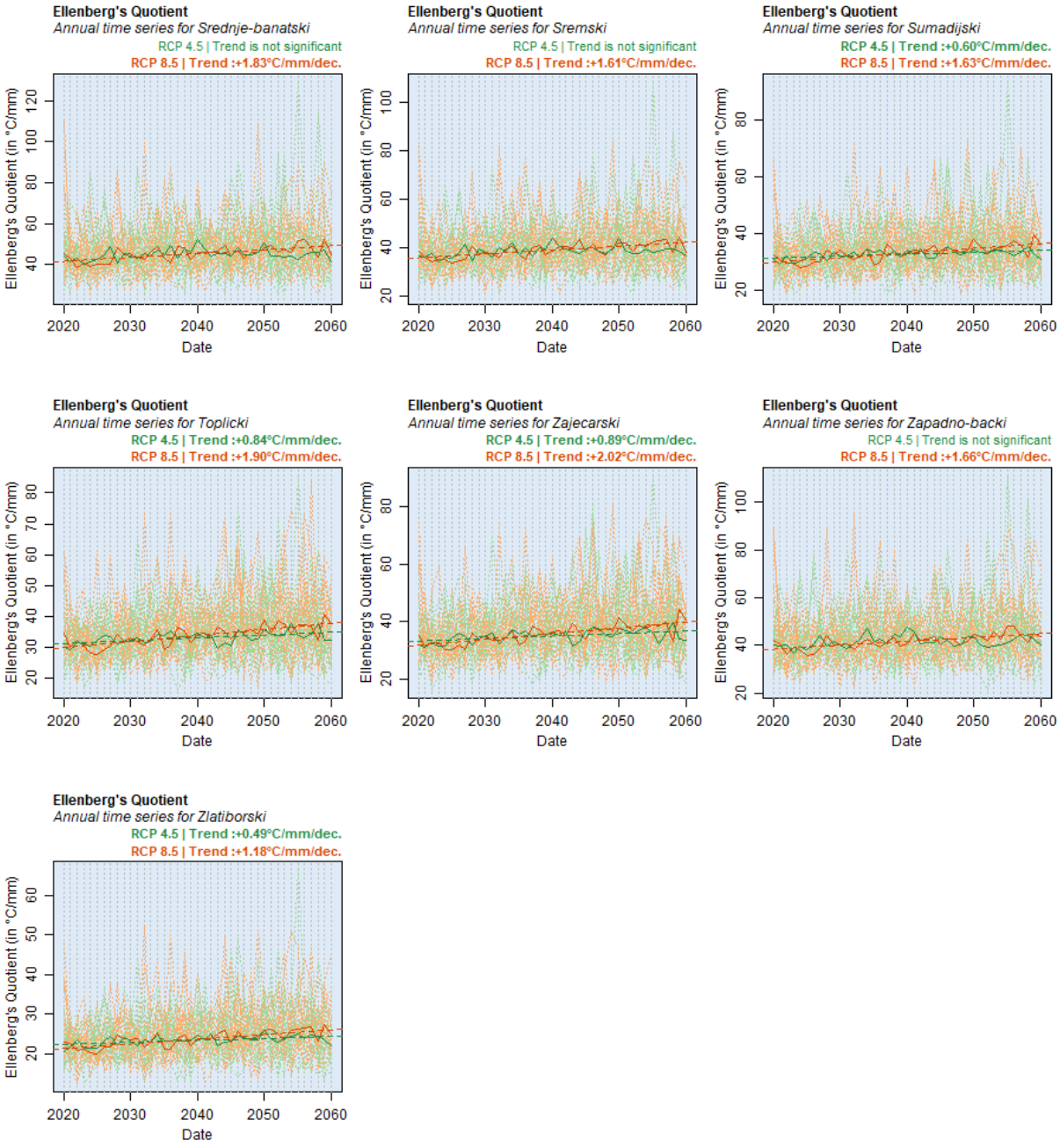

Figure 81, Figure 82, Figure 83 present the projected trends of the Forest Aridity Index (FAI) at the district level. Under the RCP 8.5 scenario, all districts are projected to experience a statistically significant increase in FAI between 2020 and 2060. The average increase in FAI is expected to range from +0.33°C/mm.decade in Kolubarski to +0.53°C/mm/decade in Pcinjski. In contrast, under the RCP 4.5 scenario, only Severno-backi, Severno-banatski, and Zlatiborski are projected to experience a statistically significant increase in FAI.

Figure 81 – Projected time series of Forest Aridity Index at the district level (Borski to Moravicki)
Time series over 2020-2060 period. Data source: NASA Earth Exchange - Global Daily Downscaled Climate Projections (NEX – GDDP) (Thrasher et al. 2012).

Figure 82 – Projected time series of Forest Aridity Index at the district level (Nisavski to Severno-Banatski)
Time series over 2020-2060 period. Data source: NASA Earth Exchange - Global Daily Downscaled Climate Projections (NEX – GDDP) (Thrasher et al. 2012).

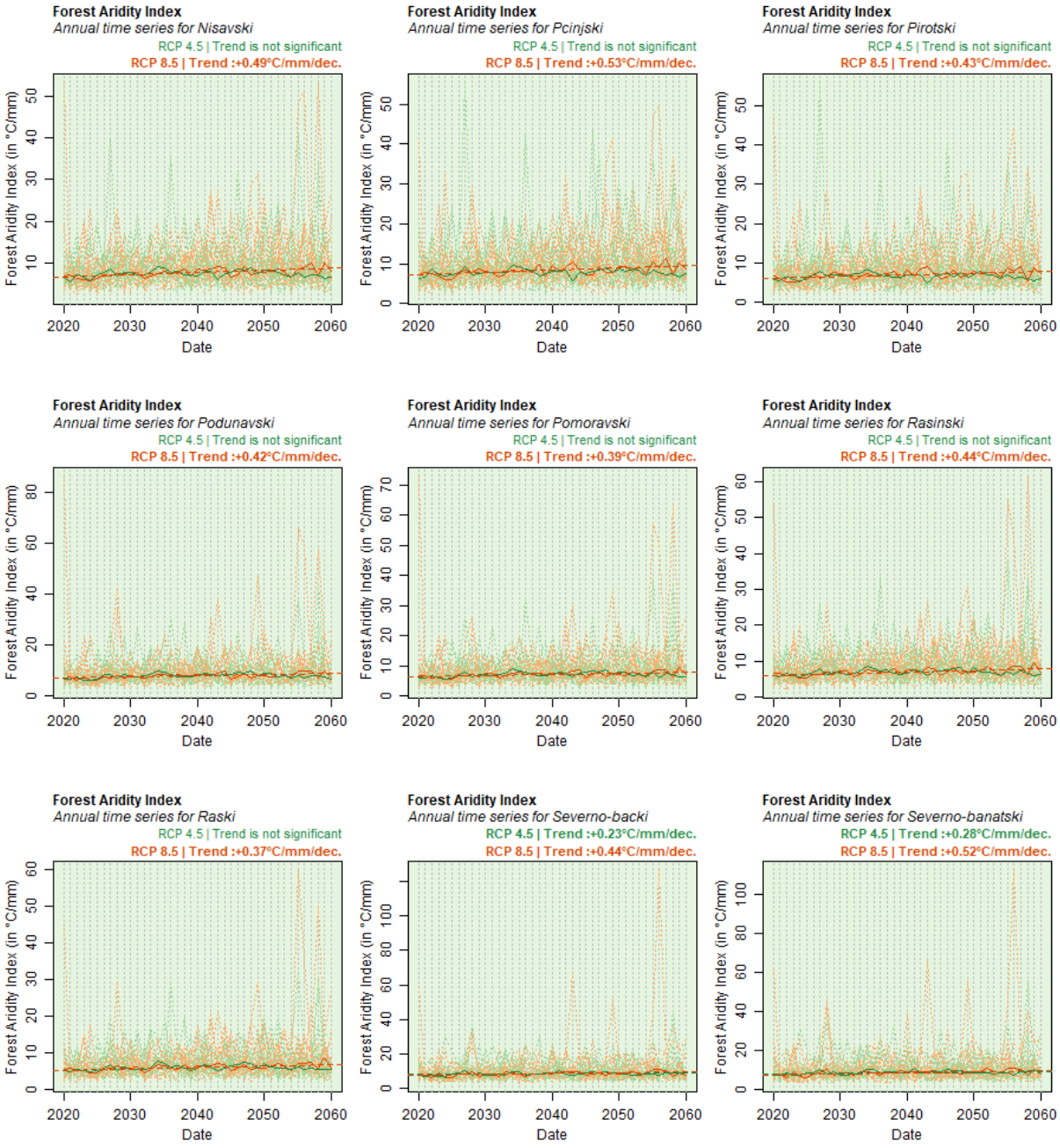

Figure 83 – Projected time series of Forest Aridity Index at the district level (Srednje-Banatski to Zlatiborski)
Time series over 2020-2060 period. Data source: NASA Earth Exchange - Global Daily Downscaled Climate Projections (NEX – GDDP) (Thrasher et al. 2012).

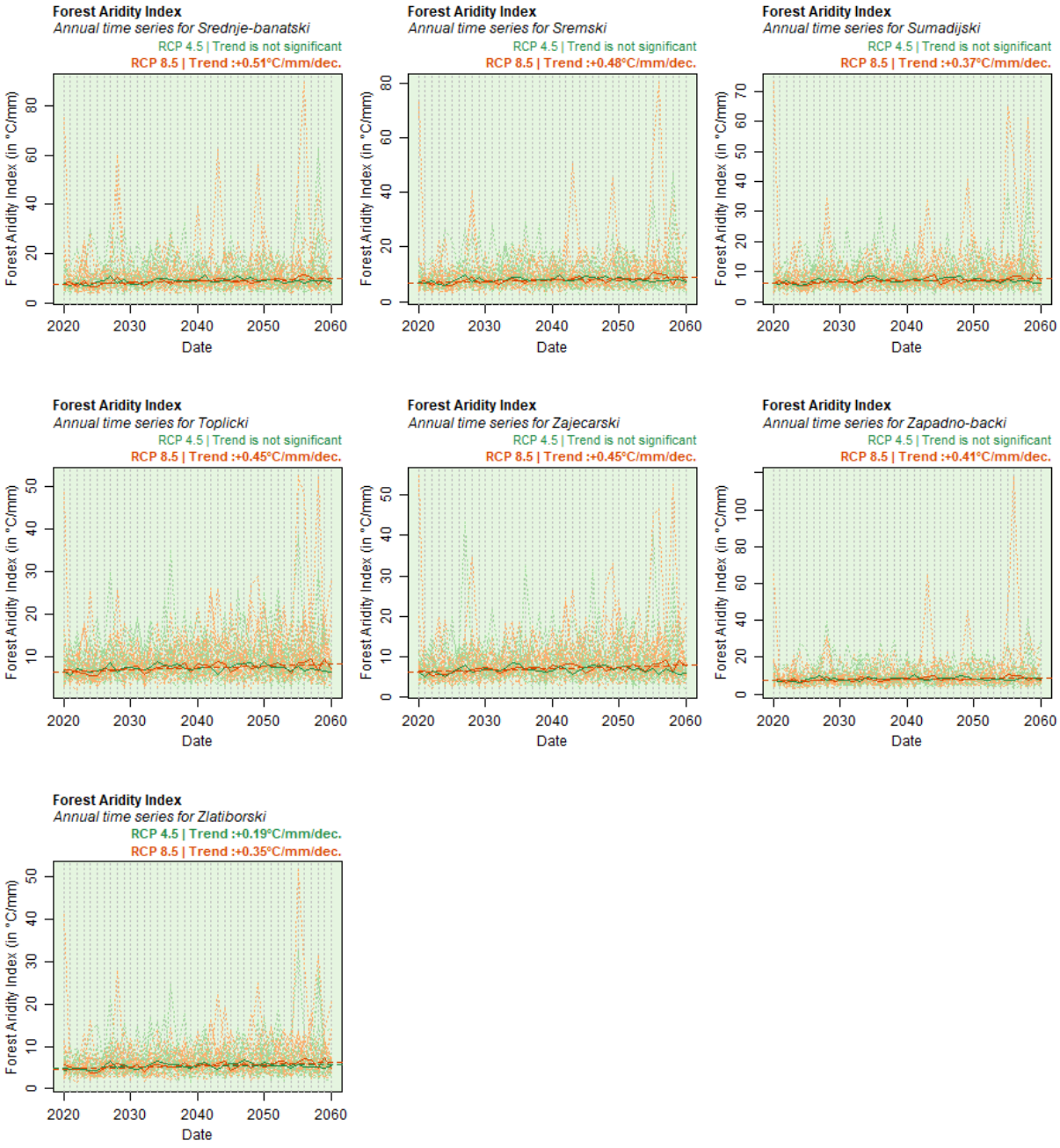

ANNUAL VARIATION OF THE MONTHLY VALUES

This section will present the annual variation of the monthly value of the studied variables.

Temperatures

The historical trends of monthly average, minimum, and maximum temperatures can be observed in Figure 84, Figure 85, Figure 86 and Table 21. In most months, an increase in all three temperatures can be observed. The critical months with the largest increase in TG are November (+1.0°C/decade), April (+0.8°C/decade), and June (+0.8°C/decade). For TX, the largest increase is observed in February (+1.3°C/decade), April (+1.0°C/decade), and November (+0.9°C/decade). For TN, critical months are November (+0.9°C/decade), August (+0.7°C/decade), and July (+0.6°C/decade).

Overall, November appears to be the month with the clearest increase for all three temperatures.

The monthly projected trends of average, minimum, and maximum temperatures can be observed in Figure 87, Figure 88, Figure 89, Table 22 and Table 23. Under both scenarios, most months are projected to experience an increase in all three temperatures, with steeper increases expected under the RCP8.5 scenario. The critical months with the largest increase in TG are August (+0.4°C/decade), September (+0.4°C/decade), and October (+0.3°C/decade) under RCP4.5 scenario and August (+0.7°C/decade), July (+0.7°C/decade), and September (+0.6°C/decade) under RCP8.5 scenario. For TX, the largest increase is expected in October (+0.5°C/decade), July (+0.5°C/decade), and June (+0.5°C/decade) under RCP4.5 scenario and August (+0.8°C/decade), July (+0.8°C/decade), and September (+0.7°C/decade) under RCP8.5 scenario. Finally, for TN, critical months are September (+0.4°C/decade), March (+0.4°C/decade), and October (+0.4°C/decade) under RCP4.5 scenario and August (+0.5°C/decade), September (+0.5°C/decade), and January (+0.5°C/decade) under RCP8.5 scenario.

Overall, the months at the end of the summer and the beginning of fall (July, August, September) are projected to experience the highest increase in temperatures.

Figure 84 – Historical time series of monthly average temperatures

Time series over 1980-2019 period. ***Light green dotted line****: variable value from each weather station separately.* ***Dark green full line:*** *median value of the variable.* ***Red dashed line:*** *variable value using ERA5 database. Data source: Republic Hydrometeorological Service of Serbia, HidMet (Republic Hydrometeorological Service of Serbia 2020) and ERA5 - ECMWF / Copernicus Climate Change Service (Muñoz Sabater 2019).*

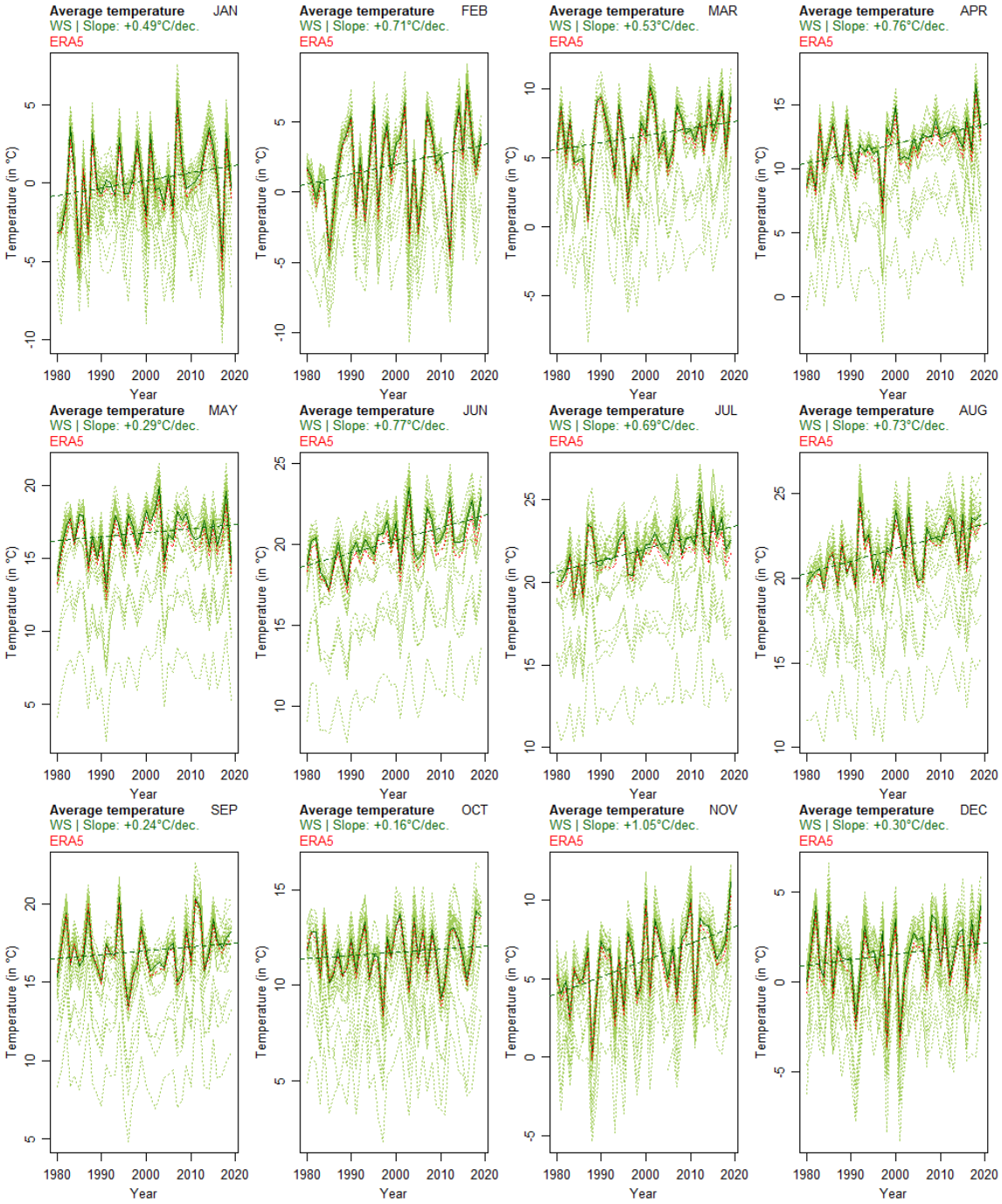

Figure 85 – Historical time series of monthly maximum temperatures

Time series over 1980-2019 period. ***Yellow dotted line****: variable value from each weather station separately.* ***Orange full line:*** *median value of the variable.* ***Red dashed line:*** *variable value using ERA5 database. Data source: Republic Hydrometeorological Service of Serbia, HidMet (Republic Hydrometeorological Service of Serbia 2020) and ERA5 - ECMWF / Copernicus Climate Change Service (Muñoz Sabater 2019).*

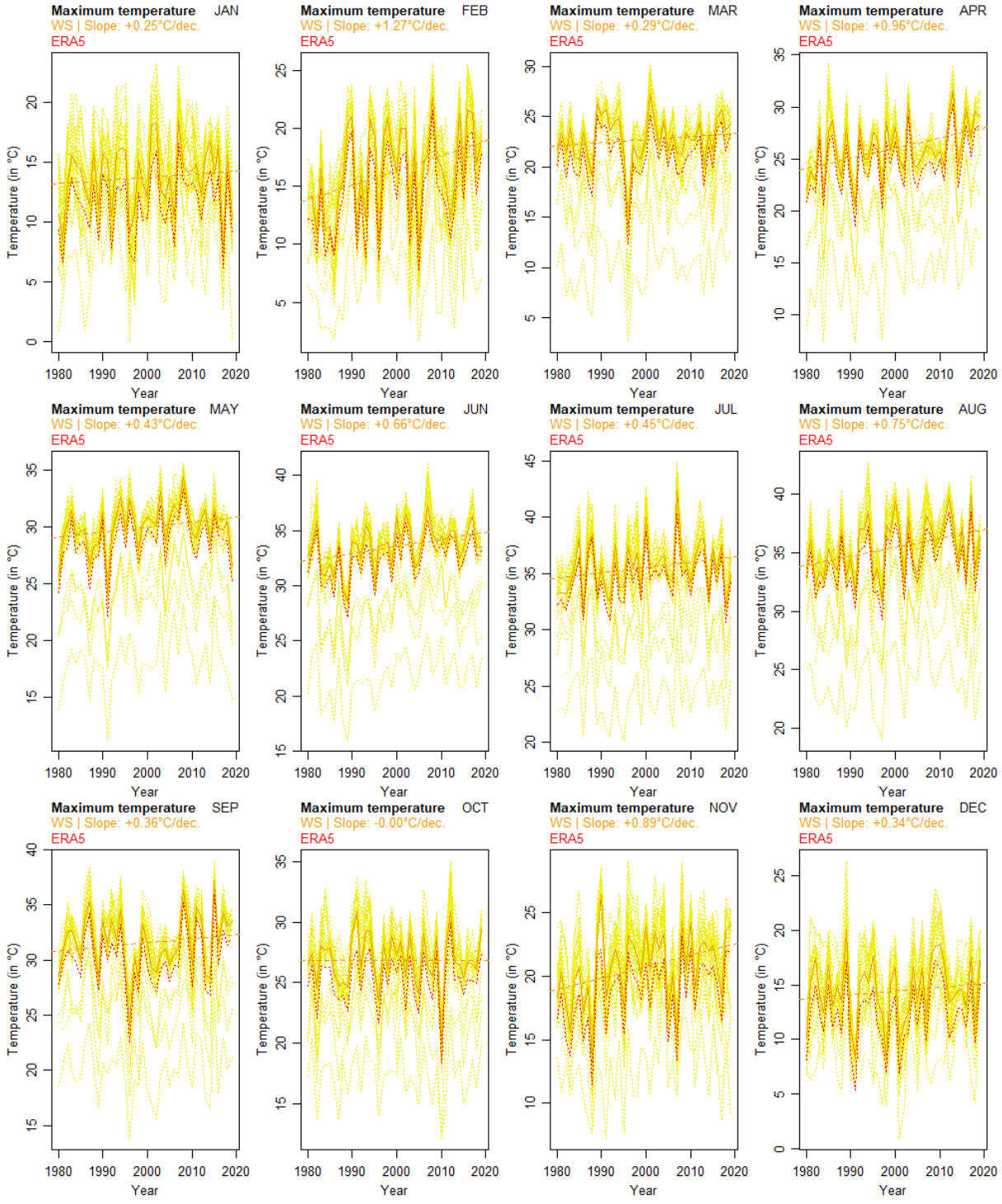

Figure 86 – Historical time series of monthly minimum temperatures

Time series over 1980-2019 period. ***Light blue dotted line****: variable value from each weather station separately.* ***Dark blue full line:*** *median value of the variable.* ***Red dashed line:*** *variable value using ERA5 database. Data source: Republic Hydrometeorological Service of Serbia, HidMet (Republic Hydrometeorological Service of Serbia 2020) and ERA5 - ECMWF / Copernicus Climate Change Service (Muñoz Sabater 2019).*

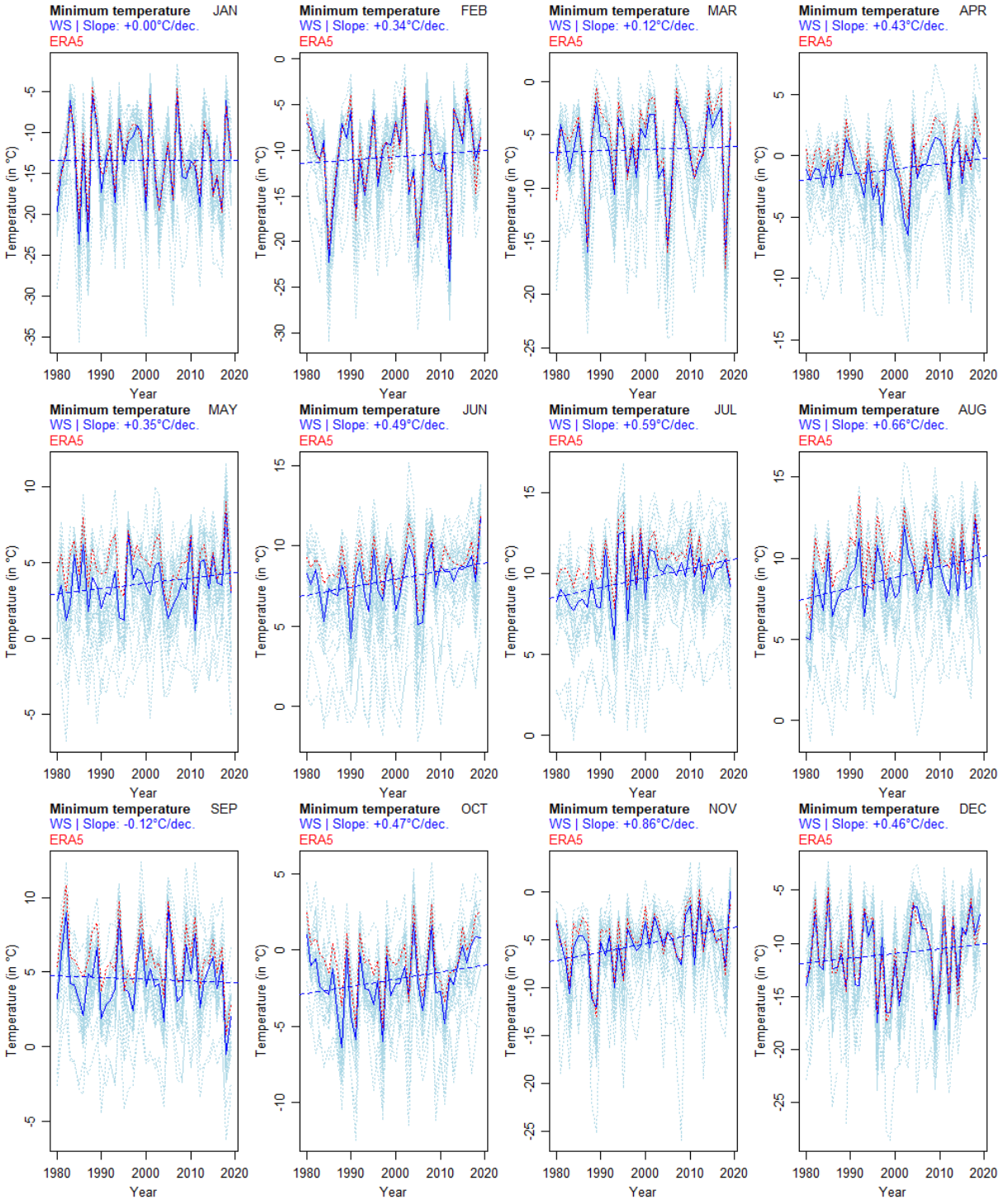

Table 21 – Characteristics of the trends from the historical time series of the monthly average, minimum and maximum temperatures (linear models)

***In green**: Monthly average temperature. **In yellow:** monthly maximum temperature. **In blue:** monthly minimum temperature. Data source: Republic Hydrometeorological Service of Serbia, HidMet (Republic Hydrometeorological Service of Serbia 2020).*

Variable	Month	Slope	p-value	Adjusted R^2	Average value in 1980	Average value in 2019
TG	January	+0.49°C/dec.	0.12	0.04	-0.79°C	1.11°C
TG	February	+0.71°C/dec.	0.08	0.05	0.55°C	3.33°C
TG	March	+0.53°C/dec.	0.07	0.06	5.55°C	7.62°C
TG	April	+0.76°C/dec.	0.00	0.23	10.39°C	13.36°C
TG	May	+0.29°C/dec.	0.16	0.03	16.19°C	17.30°C
TG	June	+0.77°C/dec.	0.00	0.36	18.72°C	21.73°C
TG	July	+0.69°C/dec.	0.00	0.35	20.64°C	23.35°C
TG	August	+0.73°C/dec.	0.00	0.29	20.27°C	23.12°C
TG	September	+0.24°C/dec.	0.27	0.01	16.51°C	17.44°C
TG	October	+0.16°C/dec.	0.38	-0.01	11.41°C	12.04°C
TG	November	+1.05°C/dec.	0.00	0.25	4.10°C	8.19°C
TG	December	+0.30°C/dec.	0.24	0.01	0.92°C	2.10°C
TX	January	+0.25°C/dec.	0.51	-0.01	13.23°C	14.21°C
TX	February	+1.27°C/dec.	0.01	0.13	13.82°C	18.78°C
TX	March	+0.29°C/dec.	0.36	0.00	22.14°C	23.29°C
TX	April	+0.96°C/dec.	0.01	0.16	24.10°C	27.86°C
TX	May	+0.43°C/dec.	0.12	0.04	29.09°C	30.77°C
TX	June	+0.66°C/dec.	0.01	0.13	32.23°C	34.79°C
TX	July	+0.45°C/dec.	0.16	0.03	34.64°C	36.39°C
TX	August	+0.75°C/dec.	0.02	0.11	33.91°C	36.85°C
TX	September	+0.36°C/dec.	0.32	0.00	30.82°C	32.24°C
TX	October	-0.00°C/dec.	0.99	-0.03	26.87°C	26.85°C
TX	November	+0.89°C/dec.	0.02	0.11	18.96°C	22.43°C
TX	December	+0.34°C/dec.	0.39	-0.01	13.75°C	15.09°C
TN	January	+0.00°C/dec.	1.00	-0.03	-13.42°C	-13.41°C
TN	February	+0.34°C/dec.	0.61	-0.02	-11.35°C	-10.04°C
TN	March	+0.12°C/dec.	0.81	-0.02	-6.63°C	-6.16°C
TN	April	+0.43°C/dec.	0.12	0.04	-1.97°C	-0.31°C
TN	May	+0.35°C/dec.	0.14	0.03	2.94°C	4.30°C
TN	June	+0.49°C/dec.	0.02	0.12	6.93°C	8.86°C
TN	July	+0.59°C/dec.	0.00	0.17	8.56°C	10.85°C
TN	August	+0.66°C/dec.	0.00	0.18	7.48°C	10.04°C
TN	September	-0.12°C/dec.	0.67	-0.02	4.76°C	4.27°C
TN	October	+0.47°C/dec.	0.09	0.05	-2.86°C	-1.02°C
TN	November	+0.86°C/dec.	0.02	0.12	-7.22°C	-3.85°C
TN	December	+0.46°C/dec.	0.35	0.00	-11.89°C	-10.09°C

Figure 87 – Projected time series of monthly average temperature

Time series over 2020-2060 period. ***Pink dotted line****: variable value for each model separately under the RCP4.5 scenario.* ***grey dotted line****: variable value for each model separately under the RCP8.5 scenario.* ***Purple full line:*** *median value of the variable under RCP4.5 scenario.* ***Black full line:*** *median value of the variable under RCP8.5 scenario. Data source: NASA Earth Exchange - Global Daily Downscaled Climate Projections (NEX – GDDP) (Thrasher et al. 2012).*

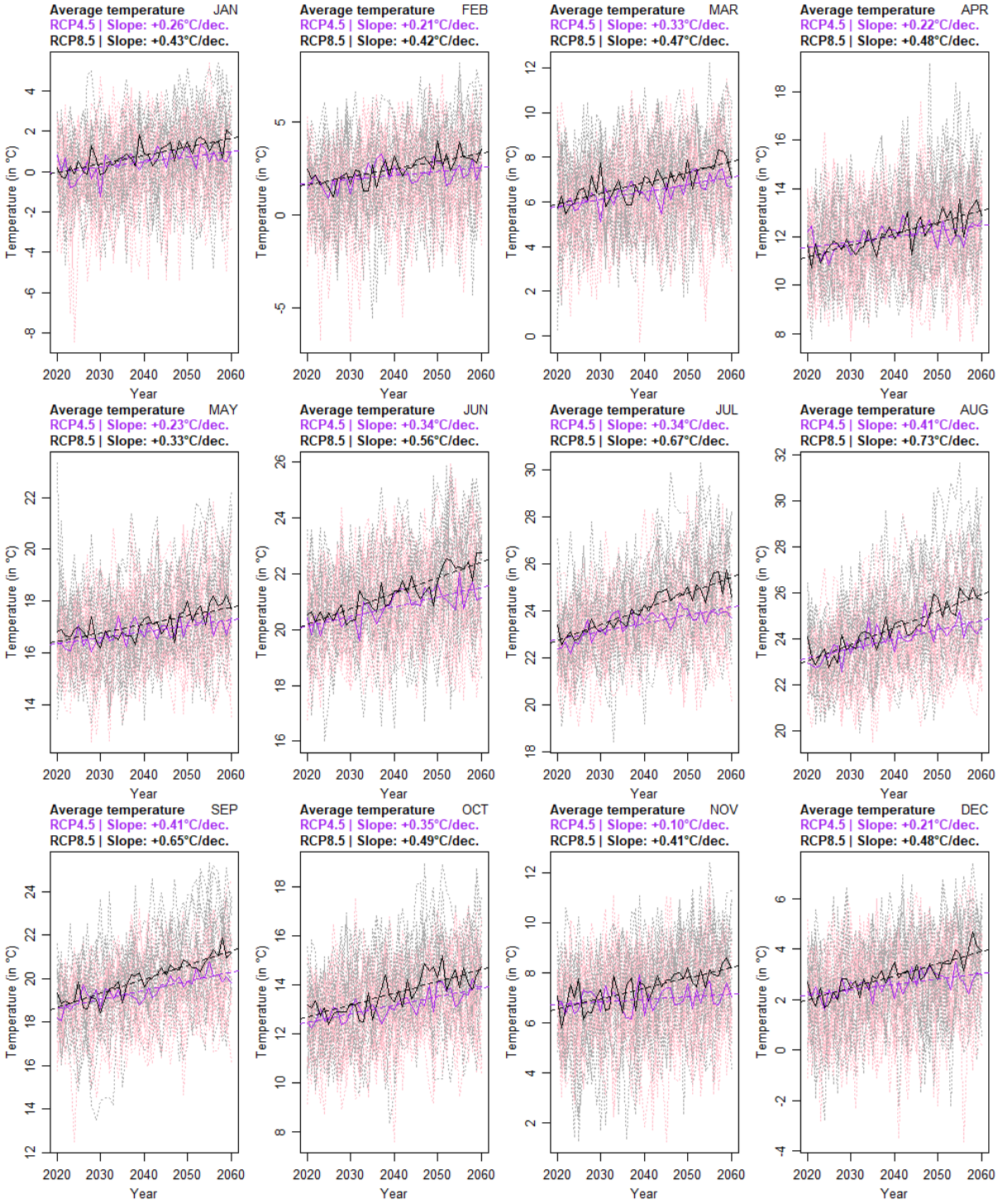

Figure 88 – Projected time series of monthly maximum temperature

Time series over 2020-2060 period. ***Pink dotted line****: variable value for each model separately under the RCP4.5 scenario.* ***grey dotted line****: variable value for each model separately under the RCP8.5 scenario.* ***Purple full line:*** *median value of the variable under RCP4.5 scenario.* ***Black full line:*** *median value of the variable under RCP8.5 scenario. Data source: NASA Earth Exchange - Global Daily Downscaled Climate Projections (NEX – GDDP) (Thrasher et al. 2012).*

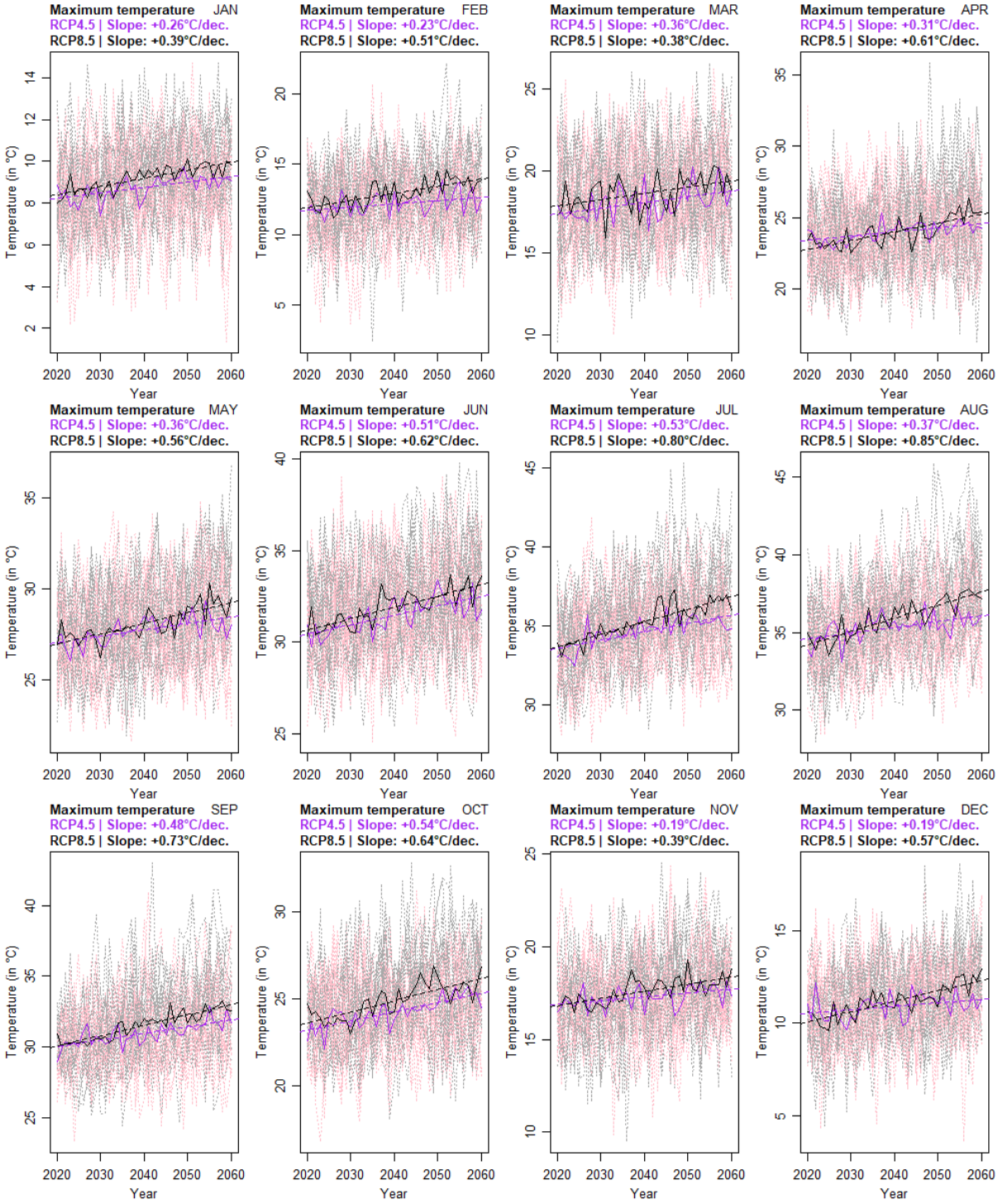

Figure 89 – Projected time series of monthly minimum temperatures

Time series over 2020-2060 period. ***Pink dotted line****: variable value for each model separately under the RCP4.5 scenario.* ***grey dotted line****: variable value for each model separately under the RCP8.5 scenario.* ***Purple full line:*** *median value of the variable under RCP4.5 scenario.* ***Black full line:*** *median value of the variable under RCP8.5 scenario. Data source: NASA Earth Exchange - Global Daily Downscaled Climate Projections (NEX – GDDP) (Thrasher et al. 2012).*

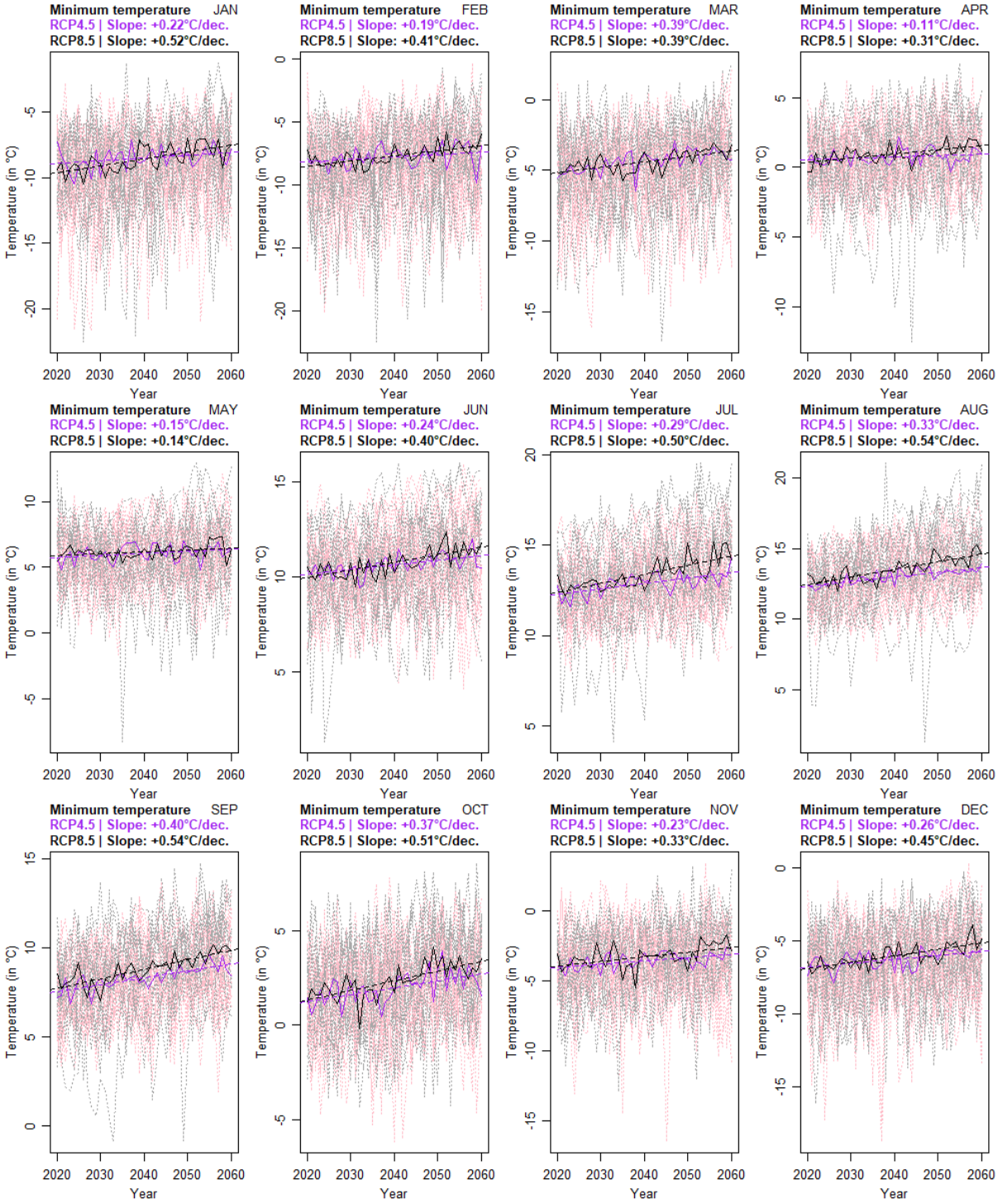

Table 22 – Characteristics of the trend from projected time series of monthly average, minimum and maximum temperature under the RCP4.5 scenario (linear models)

Data source: NASA Earth Exchange - Global Daily Downscaled Climate Projections (NEX – GDDP) (Thrasher et al. 2012).

RCP4.5						
Variable	**Month**	**Slope**	**p-value**	**Adj. R^2**	**Average value in 2040**	**Average value in 2060**
TG	January	+0.26°C/dec.	0.00	0.27	0.49°C	1.01°C
TG	February	+0.21°C/dec.	0.00	0.18	2.14°C	2.57°C
TG	March	+0.33°C/dec.	0.00	0.47	6.44°C	7.09°C
TG	April	+0.22°C/dec.	0.00	0.27	12.01°C	12.45°C
TG	May	+0.23°C/dec.	0.00	0.40	16.81°C	17.28°C
TG	June	+0.34°C/dec.	0.00	0.54	20.81°C	21.50°C
TG	July	+0.34°C/dec.	0.00	0.55	23.47°C	24.16°C
TG	August	+0.41°C/dec.	0.00	0.53	23.99°C	24.81°C
TG	September	+0.41°C/dec.	0.00	0.67	19.45°C	20.27°C
TG	October	+0.35°C/dec.	0.00	0.59	13.18°C	13.87°C
TG	November	+0.10°C/dec.	0.08	0.05	6.97°C	7.17°C
TG	December	+0.21°C/dec.	0.00	0.33	2.62°C	3.03°C
TX	January	+0.26°C/dec.	0.00	0.35	8.75°C	9.27°C
TX	February	+0.23°C/dec.	0.01	0.13	12.21°C	12.68°C
TX	March	+0.36°C/dec.	0.00	0.18	18.09°C	18.81°C
TX	April	+0.31°C/dec.	0.00	0.34	23.98°C	24.59°C
TX	May	+0.36°C/dec.	0.00	0.38	27.75°C	28.48°C
TX	June	+0.51°C/dec.	0.00	0.45	31.45°C	32.48°C
TX	July	+0.53°C/dec.	0.00	0.51	34.61°C	35.66°C
TX	August	+0.37°C/dec.	0.00	0.27	35.35°C	36.08°C
TX	September	+0.48°C/dec.	0.00	0.50	30.95°C	31.91°C
TX	October	+0.54°C/dec.	0.00	0.60	24.25°C	25.32°C
TX	November	+0.19°C/dec.	0.01	0.15	17.29°C	17.68°C
TX	December	+0.19°C/dec.	0.02	0.11	10.92°C	11.31°C
TN	January	+0.22°C/dec.	0.03	0.09	-8.50°C	-8.06°C
TN	February	+0.19°C/dec.	0.07	0.06	-7.76°C	-7.38°C
TN	March	+0.39°C/dec.	0.00	0.40	-4.38°C	-3.60°C
TN	April	+0.11°C/dec.	0.13	0.03	0.74°C	0.95°C
TN	May	+0.15°C/dec.	0.06	0.06	6.06°C	6.35°C
TN	June	+0.24°C/dec.	0.00	0.28	10.63°C	11.11°C
TN	July	+0.29°C/dec.	0.00	0.37	12.87°C	13.45°C
TN	August	+0.33°C/dec.	0.00	0.58	13.01°C	13.67°C
TN	September	+0.40°C/dec.	0.00	0.57	8.30°C	9.11°C
TN	October	+0.37°C/dec.	0.00	0.29	1.97°C	2.71°C
TN	November	+0.23°C/dec.	0.00	0.24	-3.55°C	-3.09°C
TN	December	+0.26°C/dec.	0.00	0.23	-6.25°C	-5.72°C

Table 23 – Characteristics of the trend from projected time series of monthly average, minimum and maximum temperature under the RCP8.5 scenario (linear models)

Data source: NASA Earth Exchange - Global Daily Downscaled Climate Projections (NEX – GDDP) (Thrasher et al. 2012).

RCP8.5						
Variable	**Month**	**Slope**	**p-value**	**Adj. R^2**	**Average value in 2040**	**Average value in 2060**
TG	January	+0.43°C/dec.	0.00	0.61	0.81°C	1.66°C
TG	February	+0.42°C/dec.	0.00	0.51	2.48°C	3.32°C
TG	March	+0.47°C/dec.	0.00	0.57	6.84°C	7.79°C
TG	April	+0.48°C/dec.	0.00	0.63	12.13°C	13.08°C
TG	May	+0.33°C/dec.	0.00	0.52	17.11°C	17.77°C
TG	June	+0.56°C/dec.	0.00	0.76	21.29°C	22.40°C
TG	July	+0.67°C/dec.	0.00	0.84	24.06°C	25.40°C
TG	August	+0.73°C/dec.	0.00	0.81	24.48°C	25.93°C
TG	September	+0.65°C/dec.	0.00	0.82	19.97°C	21.26°C
TG	October	+0.49°C/dec.	0.00	0.59	13.66°C	14.64°C
TG	November	+0.41°C/dec.	0.00	0.53	7.41°C	8.24°C
TG	December	+0.48°C/dec.	0.00	0.72	2.96°C	3.92°C
TX	January	+0.39°C/dec.	0.00	0.64	9.18°C	9.96°C
TX	February	+0.51°C/dec.	0.00	0.44	12.95°C	13.96°C
TX	March	+0.38°C/dec.	0.00	0.18	18.65°C	19.42°C
TX	April	+0.61°C/dec.	0.00	0.53	23.99°C	25.21°C
TX	May	+0.56°C/dec.	0.00	0.57	28.10°C	29.22°C
TX	June	+0.62°C/dec.	0.00	0.63	31.91°C	33.15°C
TX	July	+0.80°C/dec.	0.00	0.73	35.26°C	36.86°C
TX	August	+0.85°C/dec.	0.00	0.75	35.91°C	37.61°C
TX	September	+0.73°C/dec.	0.00	0.81	31.53°C	32.98°C
TX	October	+0.64°C/dec.	0.00	0.58	24.90°C	26.19°C
TX	November	+0.39°C/dec.	0.00	0.46	17.62°C	18.40°C
TX	December	+0.57°C/dec.	0.00	0.66	11.20°C	12.33°C
TN	January	+0.52°C/dec.	0.00	0.41	-8.56°C	-7.51°C
TN	February	+0.41°C/dec.	0.00	0.37	-7.68°C	-6.86°C
TN	March	+0.39°C/dec.	0.00	0.40	-4.39°C	-3.60°C
TN	April	+0.31°C/dec.	0.00	0.32	0.95°C	1.57°C
TN	May	+0.14°C/dec.	0.04	0.08	6.17°C	6.46°C
TN	June	+0.40°C/dec.	0.00	0.48	10.74°C	11.55°C
TN	July	+0.50°C/dec.	0.00	0.55	13.37°C	14.36°C
TN	August	+0.54°C/dec.	0.00	0.63	13.54°C	14.62°C
TN	September	+0.54°C/dec.	0.00	0.66	8.80°C	9.87°C
TN	October	+0.51°C/dec.	0.00	0.49	2.35°C	3.36°C
TN	November	+0.33°C/dec.	0.00	0.23	-3.24°C	-2.58°C
TN	December	+0.45°C/dec.	0.00	0.50	-6.02°C	-5.13°C

Precipitation

The historical trends of monthly accumulated precipitation and monthly average precipitation intensity are depicted in Figure 90 and Figure 91 and Table 24. However, it is important to note that the trends should be interpreted with caution due to their poor quality, with an adjusted R2 << 0.5 and p-value >> 0.05. The majority of the months showed a slight increase in RR, with slopes lower than 5 mm per decade and large interannual and geographic variation, ranging up to 200 and 300 mm, respectively.

For local weather stations, the critical months with the most significant increase in RR were May (+7 mm/decade), October (+5 mm/decade), and February (+4 mm/decade). Similarly, a mild increase in RRx was observed for most months, with the largest increase occurring in September (+0.25 mm/day/decade), May (+0.22 mm/day/decade), and December (+0.14 mm/day/decade). However, the trends in precipitation intensity also exhibited poor quality, with an adjusted R2 << 0.5 and p-value >> 0.05, and large interannual variation up to 10 mm/day.

The projected trends of monthly accumulated precipitation and average precipitation intensity are shown in Figure 92, Figure 93, Table 25 and Table 26. According to the RCP4.5 scenario, most months are predicted to have a very mild variation of RR, ranging from +2 mm/decade to -2 mm/decade. The only exception is June, which is predicted to decrease by -4 mm/decade. Similarly, under the RCP8.5 scenario, trends are expected to be comparable, with variations between +2 mm/decade to -2 mm/decade. However, July is predicted to have a more significant decrease in RR, with -6 mm/decade.

Regarding RRx, most months under both scenarios are predicted to have a mild variation, ranging from +0.1 mm per wet day/decade to -0.2 mm per wet day/decade.

Figure 90 – Historical monthly time series of accumulated precipitation

Time series over 1980-2019 period. ***Light blue dotted line****: variable value from each weather station separately.* ***Dark blue full line:*** *median value of the variable.* ***Red dashed line:*** *variable value using ERA5 database. Data source: Republic Hydrometeorological Service of Serbia, HidMet (Republic Hydrometeorological Service of Serbia 2020) and ERA5 - ECMWF / Copernicus Climate Change Service (Muñoz Sabater 2019).*

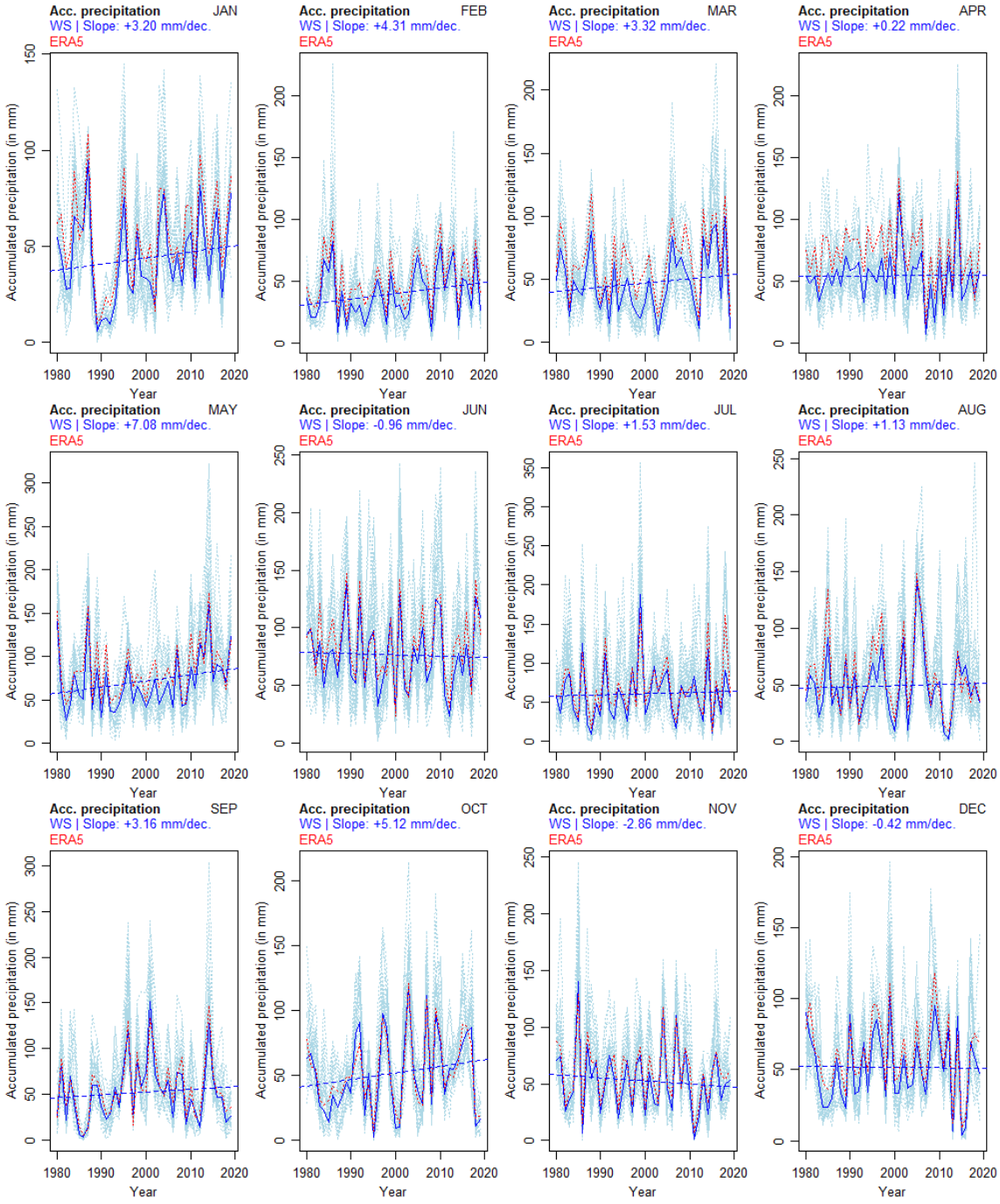

Figure 91 – Historical monthly time series of average precipitation intensity

Time series over 1980-2019 period. ***Red dashed line:*** *variable value using ERA5 database. Data source: ERA5 - ECMWF / Copernicus Climate Change Service (Muñoz Sabater 2019).*

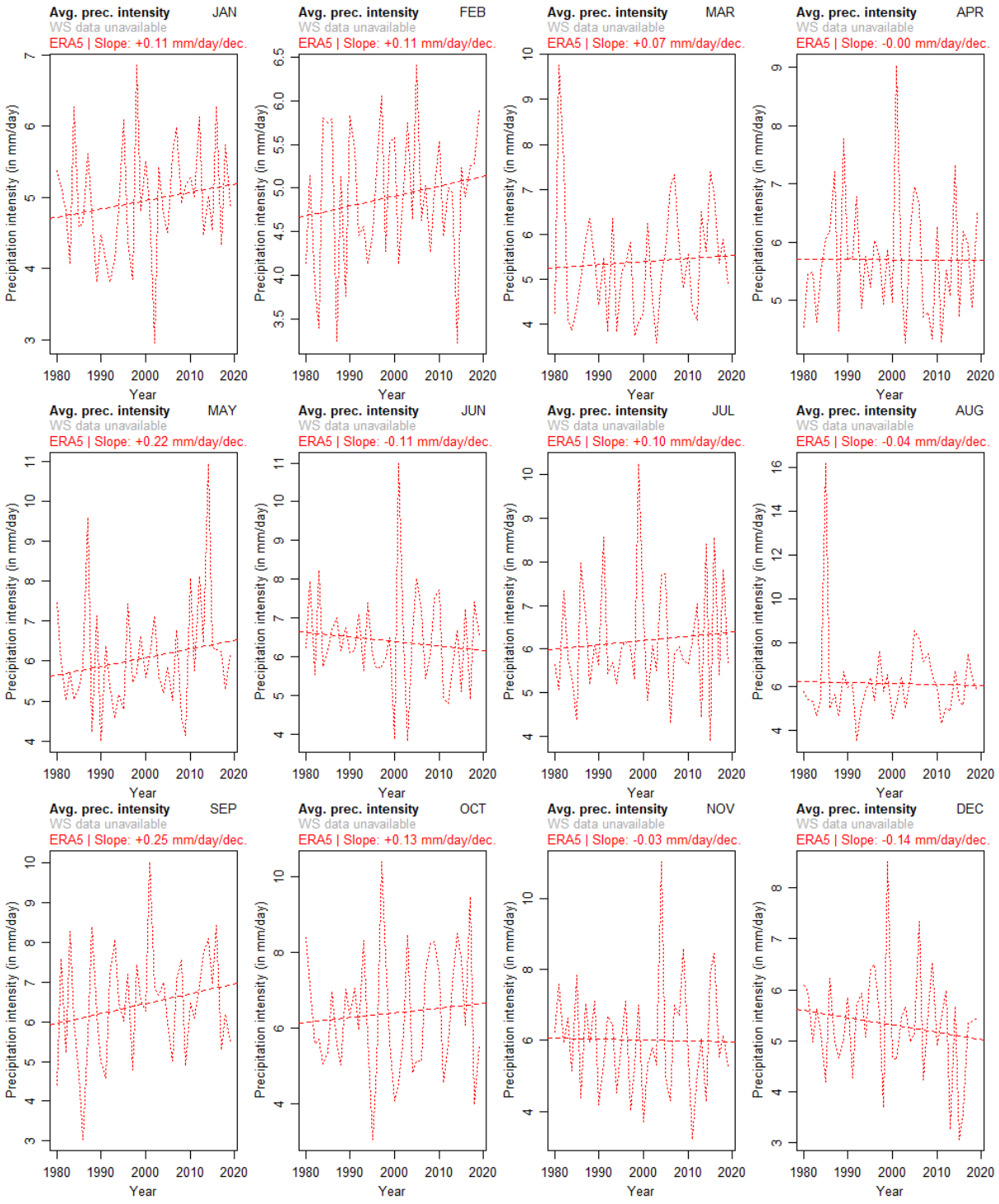

Table 24 – Characteristics of the trends from the historical time series of the monthly accumulated precipitation and monthly average precipitation intensity (linear models)

Data source: Republic Hydrometeorological Service of Serbia, HidMet (Republic Hydrometeorological Service of Serbia 2020) and ERA5 - ECMWF / Copernicus Climate Change Service (Muñoz Sabater 2019).

Variable	Month	Slope	p-value	Adj. R^2	Average value in 1980	Average value in 2019
RR	January	+3.20 mm/dec.	0.29	0.00	37.64 mm	50.12 mm
RR	February	+4.31 mm/dec.	0.13	0.03	31.59 mm	48.42 mm
RR	March	+3.32 mm/dec.	0.33	0.00	40.35 mm	53.31 mm
RR	April	+0.22 mm/dec.	0.94	-0.03	53.52 mm	54.38 mm
RR	May	+7.08 mm/dec.	0.12	0.04	57.40 mm	85.02 mm
RR	June	-0.96 mm/dec.	0.82	-0.02	78.64 mm	74.89 mm
RR	July	+1.53 mm/dec.	0.76	-0.02	57.50 mm	63.46 mm
RR	August	+1.13 mm/dec.	0.78	-0.02	46.79 mm	51.18 mm
RR	September	+3.16 mm/dec.	0.49	-0.01	46.38 mm	58.72 mm
RR	October	+5.12 mm/dec.	0.23	0.01	41.37 mm	61.34 mm
RR	November	-2.86 mm/dec.	0.48	-0.01	58.30 mm	47.15 mm
RR	December	-0.42 mm/dec.	0.91	-0.03	52.59 mm	50.94 mm
RRx	January	+0.11 mm/day/dec.	0.31	0.00	4.72 mm/day	5.17 mm/day
RRx	February	+0.11 mm/day/dec.	0.30	0.00	4.68 mm/day	5.12 mm/day
RRx	March	+0.07 mm/day/dec.	0.70	-0.02	5.25 mm/day	5.52 mm/day
RRx	April	-0.00 mm/day/dec.	0.98	-0.03	5.71 mm/day	5.69 mm/day
RRx	May	+0.22 mm/day/dec.	0.27	0.01	5.64 mm/day	6.49 mm/day
RRx	June	-0.11 mm/day/dec.	0.52	-0.01	6.62 mm/day	6.17 mm/day
RRx	July	+0.10 mm/day/dec.	0.60	-0.02	6.00 mm/day	6.38 mm/day
RRx	August	-0.04 mm/day/dec.	0.88	-0.03	6.22 mm/day	6.05 mm/day
RRx	September	+0.25 mm/day/dec.	0.20	0.02	5.96 mm/day	6.92 mm/day
RRx	October	+0.13 mm/day/dec.	0.58	-0.02	6.13 mm/day	6.62 mm/day
RRx	November	-0.03 mm/day/dec.	0.89	-0.03	6.08 mm/day	5.96 mm/day
RRx	December	-0.14 mm/day/dec.	0.33	0.00	5.59 mm/day	5.04 mm/day

Figure 92 – Projected time series of monthly accumulated precipitation

Time series over 2020-2060 period. ***Pink dotted line****: variable value for each model separately under the RCP4.5 scenario.* ***grey dotted line****: variable value for each model separately under the RCP8.5 scenario.* ***Purple full line:*** *median value of the variable under RCP4.5 scenario.* ***Black full line:*** *median value of the variable under RCP8.5 scenario. Data source: NASA Earth Exchange - Global Daily Downscaled Climate Projections (NEX – GDDP) (Thrasher et al. 2012).*

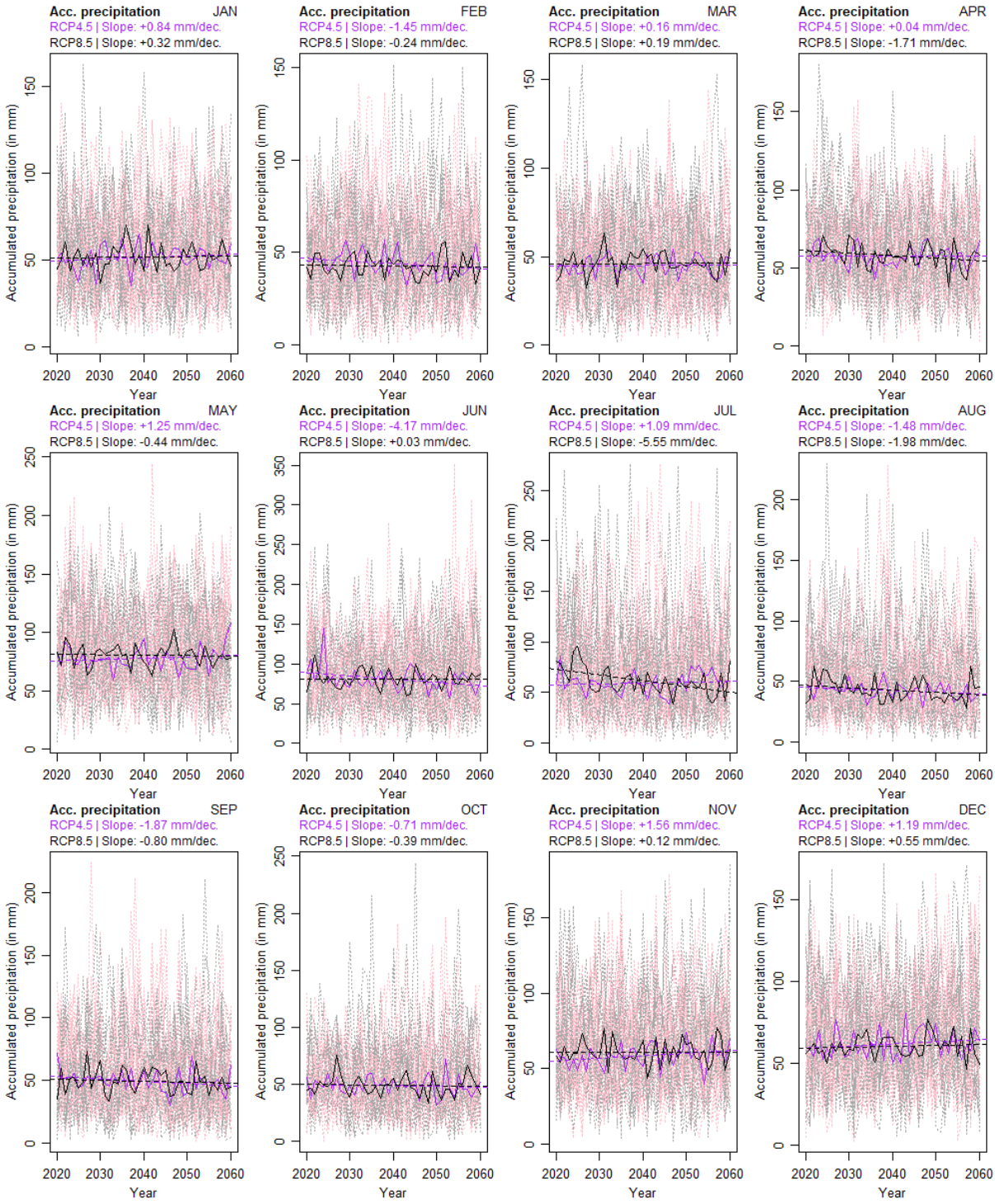

Figure 93 – Projected time series of monthly average precipitation intensity

Time series over 2020-2060 period. ***Pink dotted line****: variable value for each model separately under the RCP4.5 scenario.* ***grey dotted line****: variable value for each model separately under the RCP8.5 scenario.* ***Purple full line:*** *median value of the variable under RCP4.5 scenario.* ***Black full line:*** *median value of the variable under RCP8.5 scenario. Data source: NASA Earth Exchange - Global Daily Downscaled Climate Projections (NEX – GDDP) (Thrasher et al. 2012).*

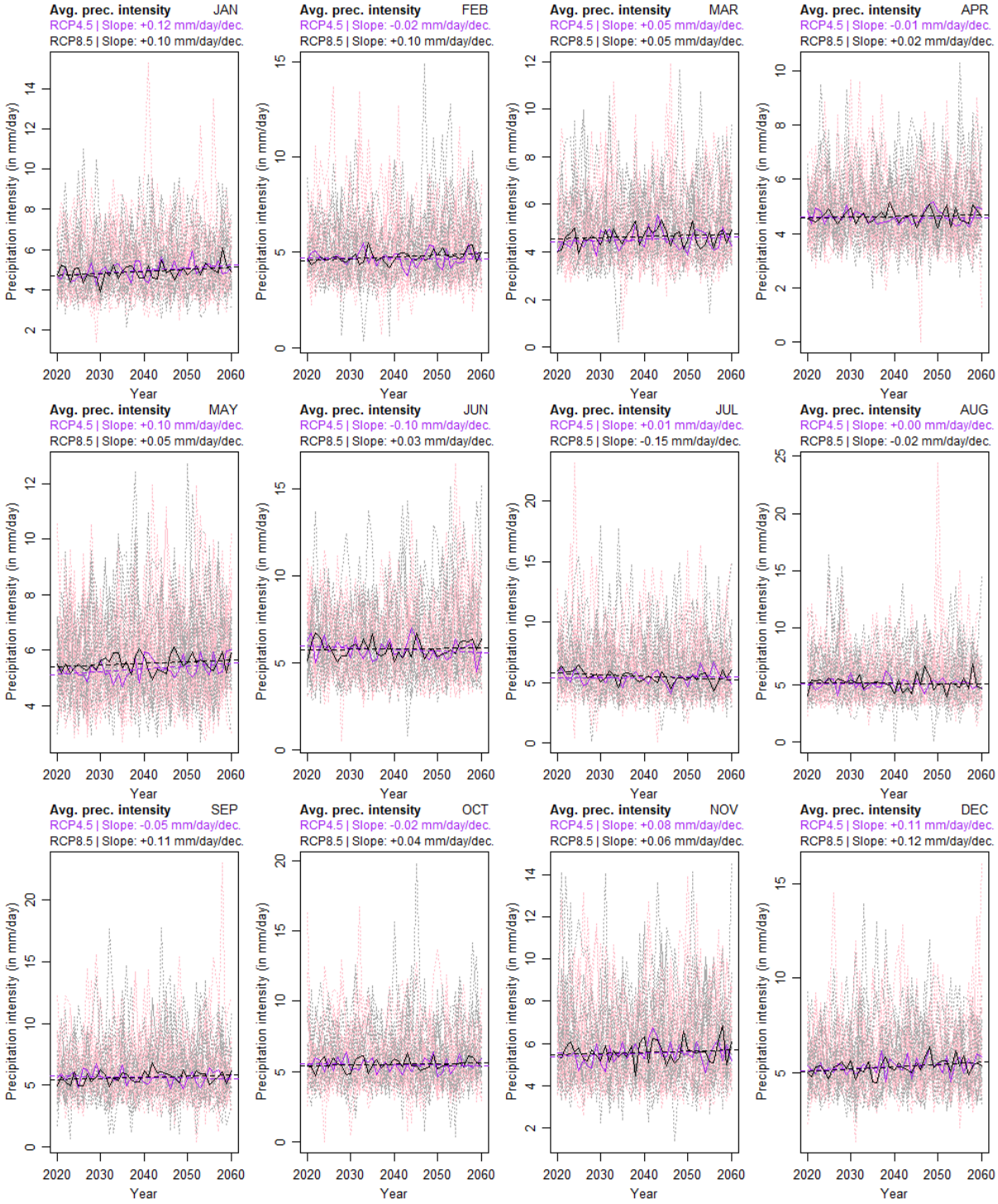

Table 25 – Characteristics of the trend from projected time series of monthly accumulated precipitation and monthly average precipitation intensity under the RCP4.5 scenario (linear models)

Data source: NASA Earth Exchange - Global Daily Downscaled Climate Projections (NEX – GDDP) (Thrasher et al. 2012).

RCP4.5						
Variable	**Month**	**Slope**	**p-value**	**Adj. R^2**	**Average value in 2040**	**Average value in 2060**
RR	January	+0.84 mm/dec.	0.34	0.00	51.33 mm	53.00 mm
RR	February	-1.45 mm/dec.	0.08	0.05	44.10 mm	41.20 mm
RR	March	+0.16 mm/dec.	0.83	-0.02	44.80 mm	45.11 mm
RR	April	+0.04 mm/dec.	0.97	-0.03	57.44 mm	57.52 mm
RR	May	+1.25 mm/dec.	0.34	0.00	77.63 mm	80.13 mm
RR	June	-4.17 mm/dec.	0.03	0.09	81.29 mm	72.96 mm
RR	July	+1.09 mm/dec.	0.43	-0.01	59.10 mm	61.28 mm
RR	August	-1.48 mm/dec.	0.09	0.05	42.58 mm	39.62 mm
RR	September	-1.87 mm/dec.	0.10	0.04	49.30 mm	45.57 mm
RR	October	-0.71 mm/dec.	0.51	-0.01	49.01 mm	47.59 mm
RR	November	+1.56 mm/dec.	0.12	0.04	58.45 mm	61.57 mm
RR	December	+1.19 mm/dec.	0.29	0.00	61.84 mm	64.23 mm
RRx	January	+0.12 mm/day/dec.	0.01	0.13	4.95 mm/day	5.19 mm/day
RRx	February	-0.02 mm/day/dec.	0.73	-0.02	4.68 mm/day	4.65 mm/day
RRx	March	+0.05 mm/day/dec.	0.37	0.00	4.51 mm/day	4.61 mm/day
RRx	April	-0.01 mm/day/dec.	0.76	-0.02	4.60 mm/day	4.58 mm/day
RRx	May	+0.10 mm/day/dec.	0.02	0.10	5.33 mm/day	5.54 mm/day
RRx	June	-0.10 mm/day/dec.	0.16	0.03	5.79 mm/day	5.59 mm/day
RRx	July	+0.01 mm/day/dec.	0.86	-0.02	5.43 mm/day	5.46 mm/day
RRx	August	+0.00 mm/day/dec.	0.94	-0.03	5.08 mm/day	5.09 mm/day
RRx	September	-0.05 mm/day/dec.	0.42	-0.01	5.63 mm/day	5.52 mm/day
RRx	October	-0.02 mm/day/dec.	0.75	-0.02	5.48 mm/day	5.45 mm/day
RRx	November	+0.08 mm/day/dec.	0.21	0.02	5.53 mm/day	5.69 mm/day
RRx	December	+0.11 mm/day/dec.	0.04	0.08	5.34 mm/day	5.57 mm/day

Table 26 – Characteristics of the trend from projected time series of monthly accumulated precipitation and monthly average precipitation intensity under the RCP8.5 scenario (linear models)

Data source: NASA Earth Exchange - Global Daily Downscaled Climate Projections (NEX – GDDP) (Thrasher et al. 2012).

RCP8.5						
Variable	**Month**	**Slope**	**p-value**	**Adj. R^2**	**Average value in 2040**	**Average value in 2060**
RR	January	+0.32 mm/dec.	0.74	-0.02	51.78 mm	52.43 mm
RR	February	-0.24 mm/dec.	0.76	-0.02	42.48 mm	41.99 mm
RR	March	+0.19 mm/dec.	0.82	-0.02	46.23 mm	46.62 mm
RR	April	-1.71 mm/dec.	0.09	0.05	57.95 mm	54.54 mm
RR	May	-0.44 mm/dec.	0.70	-0.02	80.27 mm	79.40 mm
RR	June	+0.03 mm/dec.	0.99	-0.03	80.98 mm	81.03 mm
RR	July	-5.55 mm/dec.	0.00	0.22	61.50 mm	50.40 mm
RR	August	-1.98 mm/dec.	0.11	0.04	43.22 mm	39.26 mm
RR	September	-0.80 mm/dec.	0.53	-0.02	49.23 mm	47.63 mm
RR	October	-0.39 mm/dec.	0.74	-0.02	48.96 mm	48.18 mm
RR	November	+0.12 mm/dec.	0.91	-0.03	60.70 mm	60.94 mm
RR	December	+0.55 mm/dec.	0.55	-0.02	60.25 mm	61.35 mm
RRx	January	+0.10 mm/day/dec.	0.03	0.09	4.90 mm/day	5.10 mm/day
RRx	February	+0.10 mm/day/dec.	0.01	0.16	4.75 mm/day	4.95 mm/day
RRx	March	+0.05 mm/day/dec.	0.34	0.00	4.63 mm/day	4.73 mm/day
RRx	April	+0.02 mm/day/dec.	0.48	-0.01	4.63 mm/day	4.68 mm/day
RRx	May	+0.05 mm/day/dec.	0.16	0.03	5.52 mm/day	5.63 mm/day
RRx	June	+0.03 mm/day/dec.	0.64	-0.02	5.83 mm/day	5.88 mm/day
RRx	July	-0.15 mm/day/dec.	0.02	0.12	5.51 mm/day	5.21 mm/day
RRx	August	-0.02 mm/day/dec.	0.83	-0.02	5.15 mm/day	5.11 mm/day
RRx	September	+0.11 mm/day/dec.	0.08	0.05	5.65 mm/day	5.86 mm/day
RRx	October	+0.04 mm/day/dec.	0.46	-0.01	5.53 mm/day	5.61 mm/day
RRx	November	+0.06 mm/day/dec.	0.39	-0.01	5.59 mm/day	5.71 mm/day
RRx	December	+0.12 mm/day/dec.	0.02	0.11	5.30 mm/day	5.55 mm/day

Wet days & dry spell

Figure 94, Figure 95, Figure 96 and Table 27 a visualization of the historical trends of monthly accumulated wet days, accumulated very wet days and the duration of the longest dry spell. On average, most of the monthly values remained stable despite a large interannual variation. The variation in WD ranged from -0.6 days/decade to +0.7 days/decade, while VWD ranged from -0.1 days/decade to +0.1 days/decade, and DS varied from -1 day/decade to -1 day/decade.

Figure 97, Figure 98 and Figure 99, Table 28 and Table 29 depict the projected trends for accumulated wet days, accumulated very wet days, and the duration of the longest dry spell at a monthly scale. Despite a large interannual variation, most of the monthly values are predicted to remain stable on average under both scenarios. WD is predicted to vary between -0.6 days/decade to +0.2 days/decade, VWD between -0.1 days/decade and no variation, and DS is predicted to vary between -0.4 day/decade and +0.1 day/decade.

Figure 94 – Historic time series of the monthly accumulated wet days

Time series over 1980-2019 period. Data source: ERA5, ECMWF / Copernicus Climate Change Service (Muñoz Sabater 2019), Republic Hydrometeorological Service of Serbia.

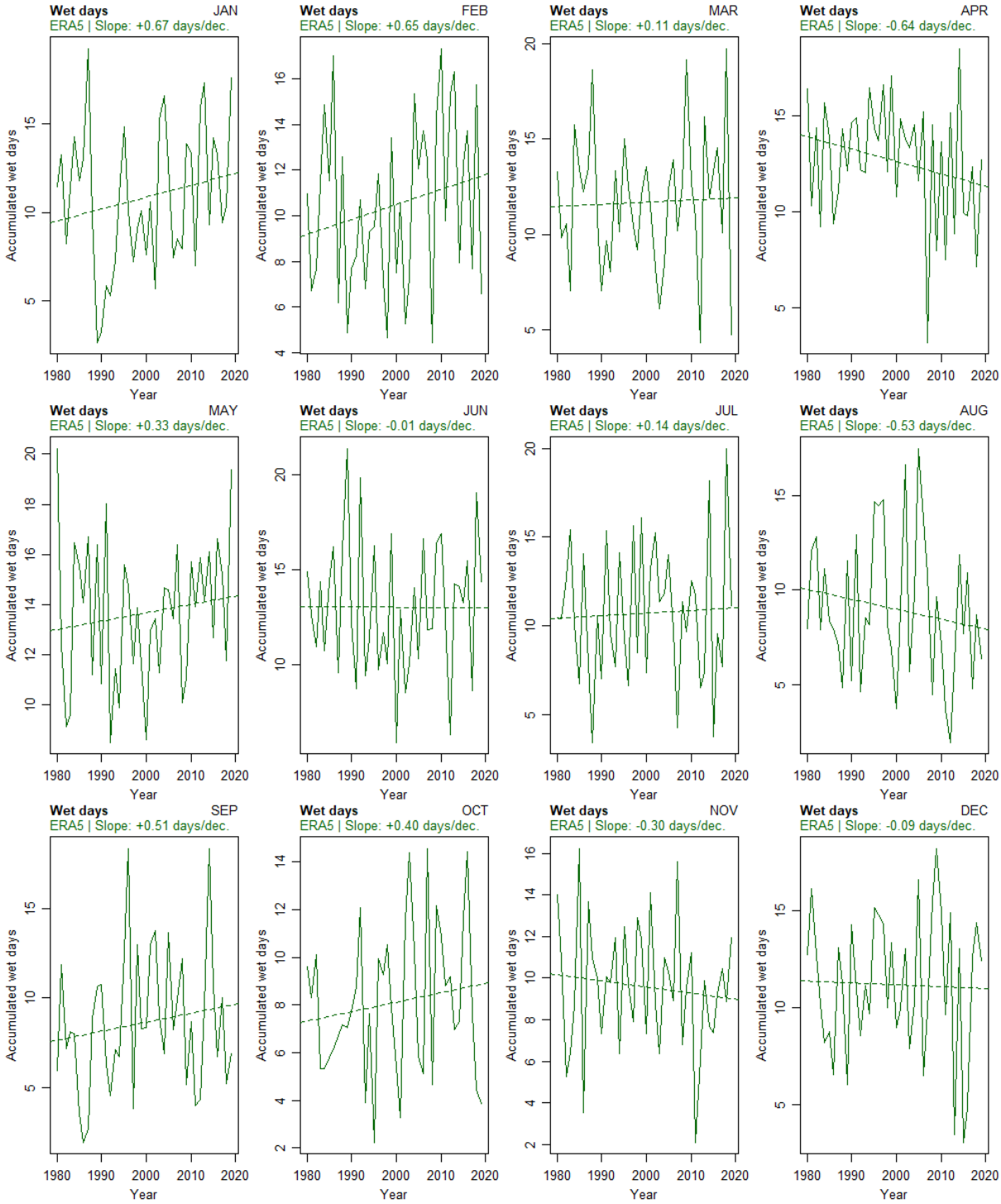

Figure 95 – Historic time series of the monthly accumulated very wet days

Time series over 1980-2019 period. Data source: ERA5, ECMWF / Copernicus Climate Change Service (Muñoz Sabater 2019), Republic Hydrometeorological Service of Serbia

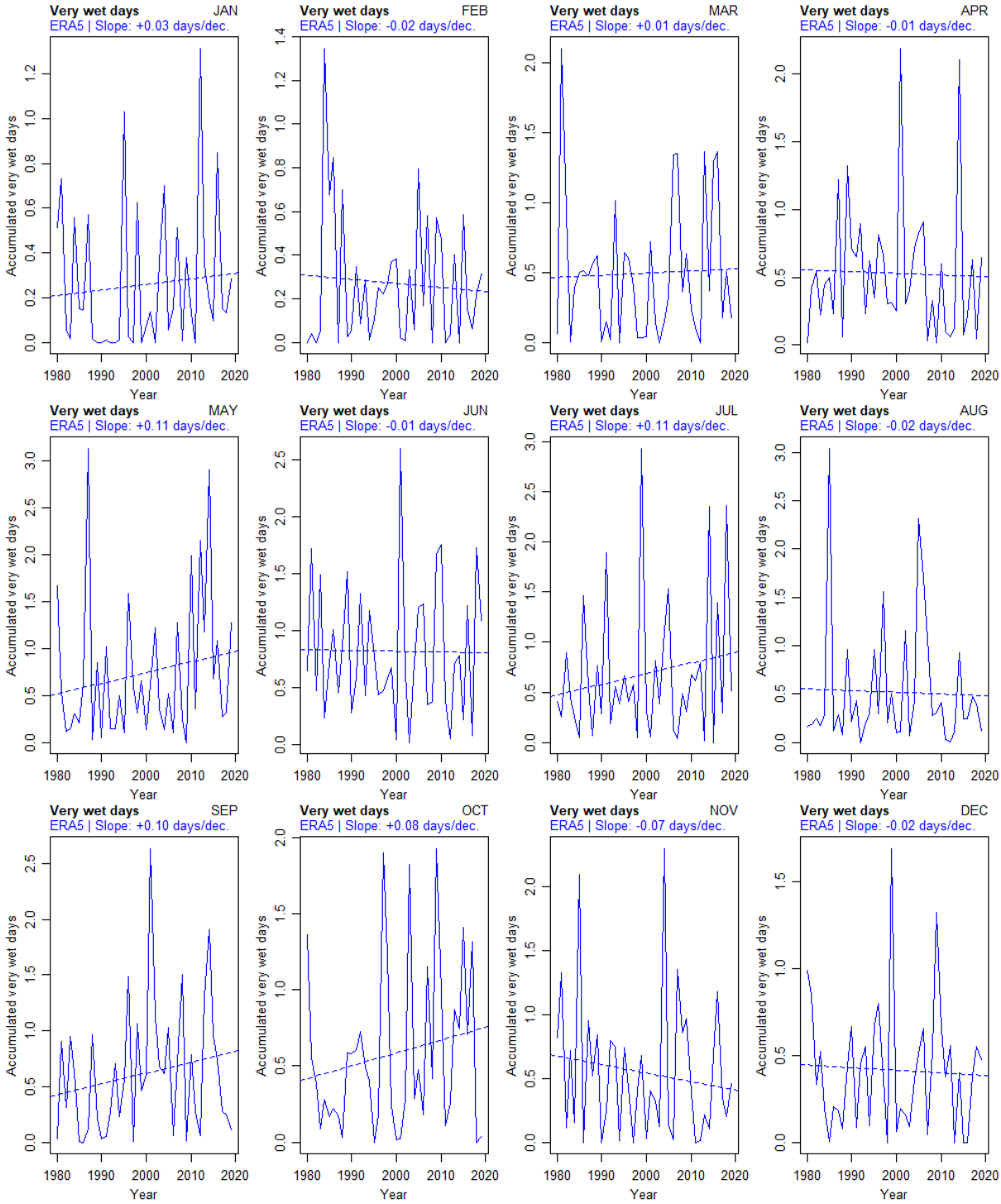

Figure 96 – Historic time series of the duration of the longest dry spell of the month

Time series over 1980-2019 period. Data source: ERA5, ECMWF / Copernicus Climate Change Service (Muñoz Sabater 2019), Republic Hydrometeorological Service of Serbia.

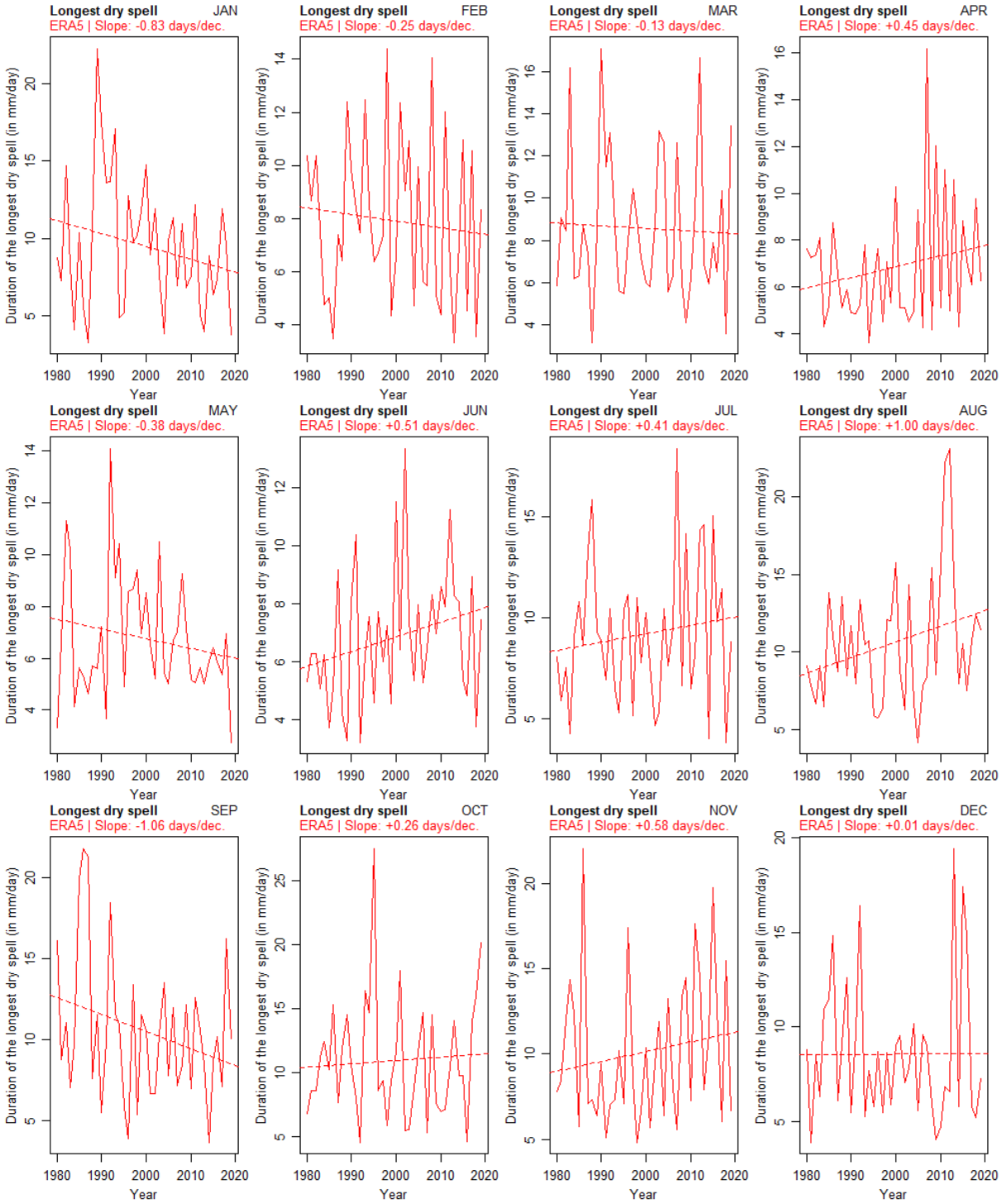

Table 27 - Characteristics of the trends from the historical time series of the monthly accumulated wet days, very wet days, and the duration of the longest dry spell of the month (linear models)
***In green**: Monthly accumulated wet days. **In blue:** monthly accumulated very wet days. **In red:** duration of the longest dry spell of the month. Data source: ERA5, ECMWF / Copernicus Climate Change Service (Muñoz Sabater 2019), Republic Hydrometeorological Service of Serbia.*

Variable	Month	Slope	p-value	Adjusted R^2	Average value in 1980	Average value in 2019
WD	January	+0.67 days/dec.	0.23	0.01	9.53 days	12.13 days
WD	February	+0.65 days/dec.	0.20	0.02	9.20 days	11.75 days
WD	March	+0.11 days/dec.	0.82	-0.02	11.45 days	11.89 days
WD	April	-0.64 days/dec.	0.14	0.03	13.90 days	11.39 days
WD	May	+0.33 days/dec.	0.41	-0.01	13.00 days	14.28 days
WD	June	-0.01 days/dec.	0.99	-0.03	13.03 days	13.00 days
WD	July	+0.14 days/dec.	0.79	-0.02	10.42 days	10.97 days
WD	August	-0.53 days/dec.	0.31	0.00	10.04 days	7.99 days
WD	September	+0.51 days/dec.	0.34	0.00	7.61 days	9.61 days
WD	October	+0.40 days/dec.	0.36	0.00	7.32 days	8.88 days
WD	November	-0.30 days/dec.	0.49	-0.01	10.17 days	9.01 days
WD	December	-0.09 days/dec.	0.85	-0.03	11.38 days	11.01 days
VWD	January	+0.03 days/dec.	0.56	-0.02	0.21 days	0.31 days
VWD	February	-0.02 days/dec.	0.66	-0.02	0.31 days	0.23 days
VWD	March	+0.01 days/dec.	0.83	-0.03	0.46 days	0.52 days
VWD	April	-0.01 days/dec.	0.86	-0.03	0.55 days	0.50 days
VWD	May	+0.11 days/dec.	0.28	0.00	0.51 days	0.96 days
VWD	June	-0.01 days/dec.	0.94	-0.03	0.83 days	0.81 days
VWD	July	+0.11 days/dec.	0.28	0.01	0.47 days	0.89 days
VWD	August	-0.02 days/dec.	0.85	-0.03	0.55 days	0.48 days
VWD	September	+0.10 days/dec.	0.24	0.01	0.43 days	0.80 days
VWD	October	+0.08 days/dec.	0.26	0.01	0.42 days	0.75 days
VWD	November	-0.07 days/dec.	0.38	-0.01	0.67 days	0.41 days
VWD	December	-0.02 days/dec.	0.77	-0.02	0.44 days	0.38 days
DS	January	-0.83 days/dec.	0.15	0.03	11.16 days	7.92 days
DS	February	-0.25 days/dec.	0.56	-0.02	8.41 days	7.45 days
DS	March	-0.13 days/dec.	0.79	-0.02	8.84 days	8.33 days
DS	April	+0.45 days/dec.	0.21	0.02	5.94 days	7.71 days
DS	May	-0.38 days/dec.	0.26	0.01	7.51 days	6.05 days
DS	June	+0.51 days/dec.	0.11	0.04	5.85 days	7.82 days
DS	July	+0.41 days/dec.	0.40	-0.01	8.38 days	9.99 days
DS	August	+1.00 days/dec.	0.08	0.06	8.65 days	12.56 days
DS	September	-1.06 days/dec.	0.08	0.05	12.61 days	8.49 days
DS	October	+0.26 days/dec.	0.69	-0.02	10.44 days	11.45 days
DS	November	+0.58 days/dec.	0.33	0.00	8.98 days	11.25 days
DS	December	+0.01 days/dec.	0.99	-0.03	8.56 days	8.59 days

Figure 97 – Projected time series of the monthly accumulated wet days

Time series over 2020-2060 period. ***Pink dotted line****: variable value for each model separately under the RCP4.5 scenario.* ***grey dotted line****: variable value for each model separately under the RCP8.5 scenario.* ***Purple full line:*** *median value of the variable under RCP4.5 scenario.* ***Black full line:*** *median value of the variable under RCP8.5 scenario. Data source: NASA Earth Exchange - Global Daily Downscaled Climate Projections (NEX – GDDP) (Thrasher et al. 2012).*

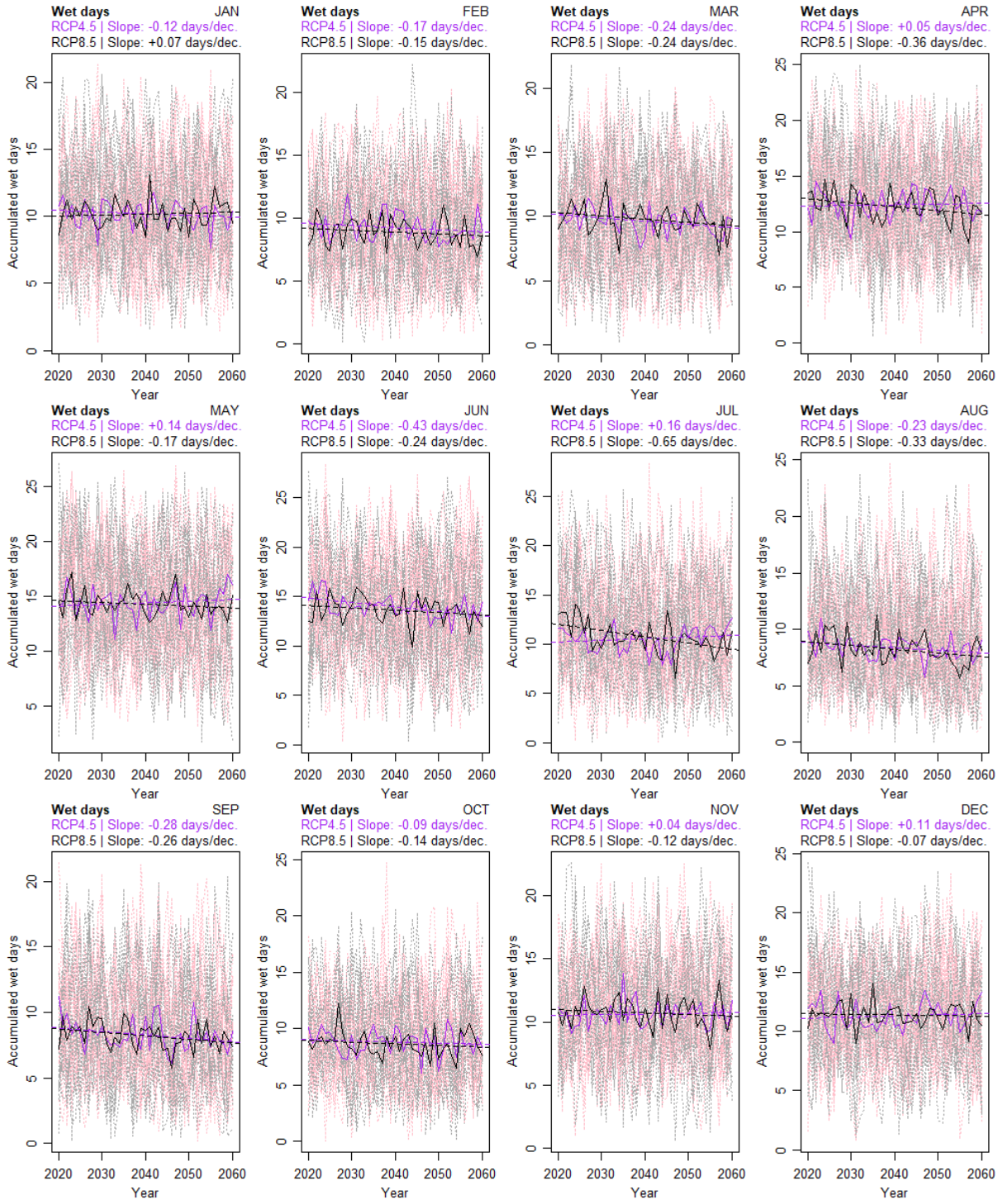

Figure 98 – Projected time series of the monthly accumulated very wet days

Time series over 2020-2060 period. ***Pink dotted line****: variable value for each model separately under the RCP4.5 scenario.* ***grey dotted line****: variable value for each model separately under the RCP8.5 scenario.* ***Purple full line:*** *median value of the variable under RCP4.5 scenario.* ***Black full line:*** *median value of the variable under RCP8.5 scenario. Data source: NASA Earth Exchange - Global Daily Downscaled Climate Projections (NEX – GDDP) (Thrasher et al. 2012).*

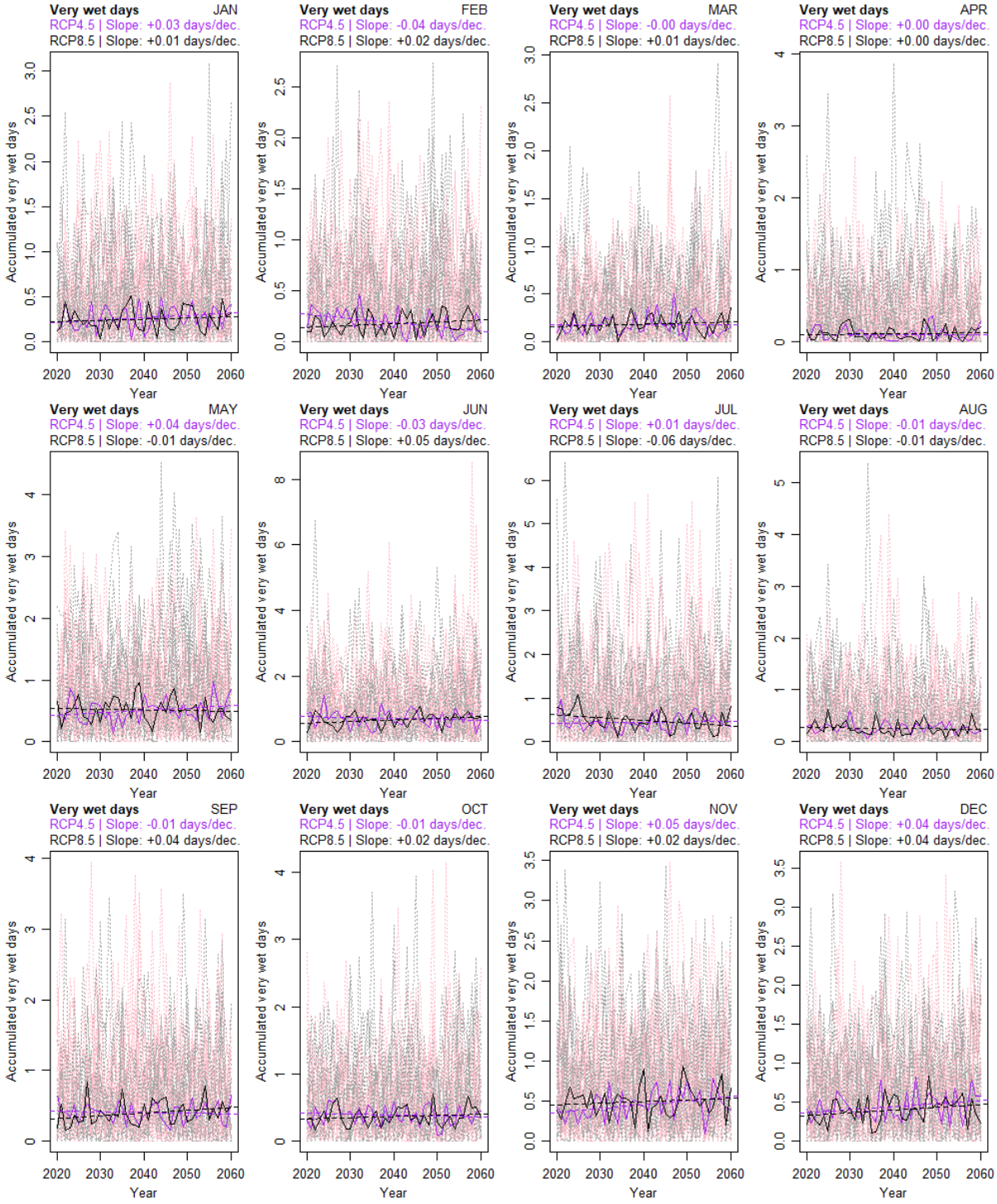

Figure 99 – Historic time series of the duration of the longest dry spell of the month

Time series over 2020-2060 period. ***Pink dotted line****: variable value for each model separately under the RCP4.5 scenario.* ***grey dotted line****: variable value for each model separately under the RCP8.5 scenario.* ***Purple full line:*** *median value of the variable under RCP4.5 scenario.* ***Black full line:*** *median value of the variable under RCP8.5 scenario. Data source: NASA Earth Exchange - Global Daily Downscaled Climate Projections (NEX – GDDP) (Thrasher et al. 2012).*

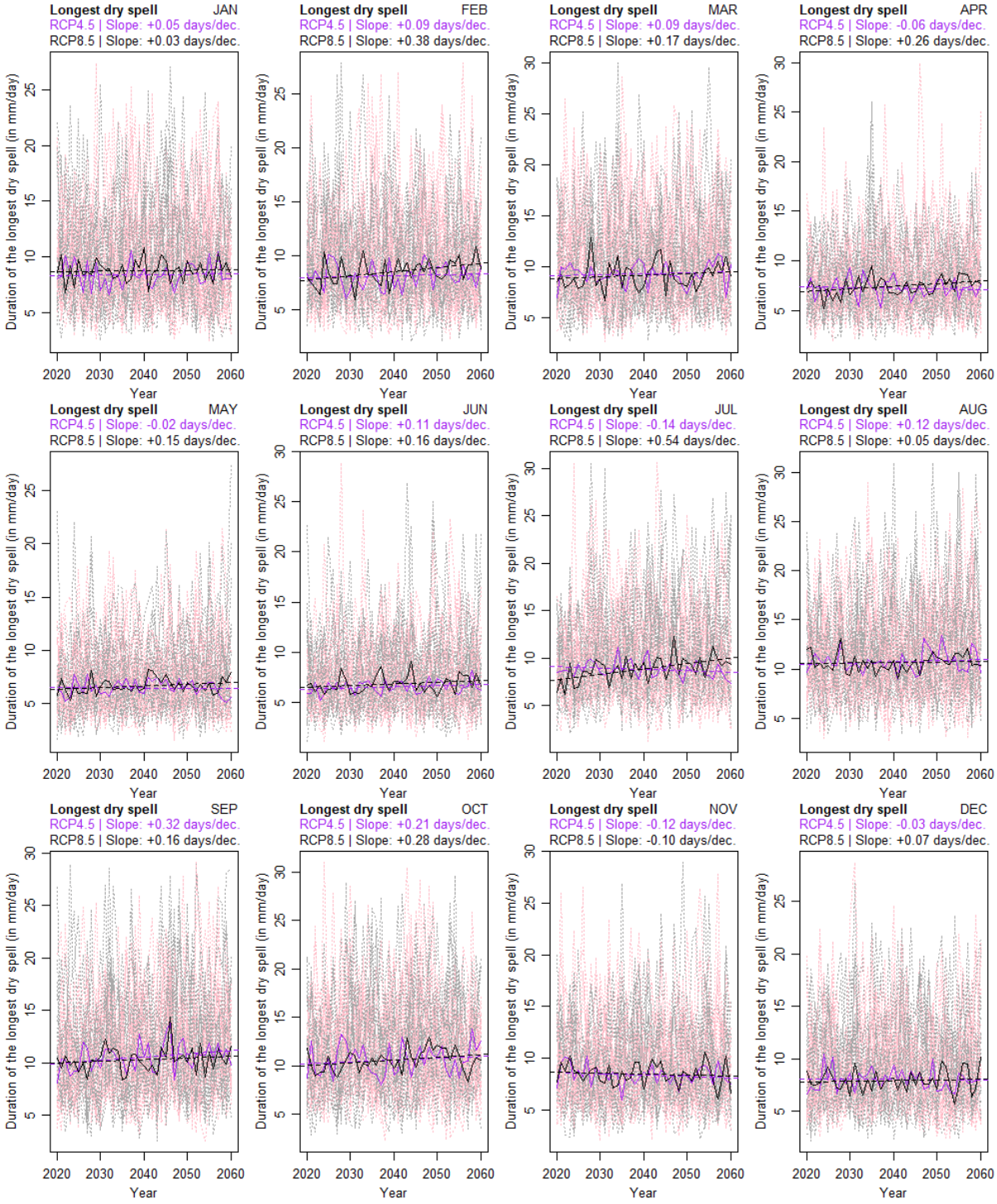

Table 28 – Characteristics of the trend from projected time series of monthly accumulated wet days, very wet days, and the duration of the longest dry spell of the month under the RCP4.5 scenario (linear models)
Data source: NASA Earth Exchange - Global Daily Downscaled Climate Projections (NEX – GDDP) (Thrasher et al. 2012).

RCP4.5						
Variable	**Month**	**Slope**	**p-value**	**R^2**	**Average value in 2040**	**Average value in 2060**
WD	January	-0.12 days/dec.	0.33	0.00	10.19 days	9.94 days
WD	February	-0.17 days/dec.	0.21	0.01	9.28 days	8.94 days
WD	March	-0.24 days/dec.	0.07	0.06	9.65 days	9.17 days
WD	April	+0.05 days/dec.	0.75	-0.02	12.44 days	12.54 days
WD	May	+0.14 days/dec.	0.44	-0.01	14.38 days	14.66 days
WD	June	-0.43 days/dec.	0.00	0.19	13.97 days	13.10 days
WD	July	+0.16 days/dec.	0.33	0.00	10.54 days	10.86 days
WD	August	-0.23 days/dec.	0.07	0.06	8.35 days	7.89 days
WD	September	-0.28 days/dec.	0.07	0.06	8.30 days	7.74 days
WD	October	-0.09 days/dec.	0.54	-0.02	8.82 days	8.64 days
WD	November	+0.04 days/dec.	0.78	-0.02	10.64 days	10.71 days
WD	December	+0.11 days/dec.	0.45	-0.01	11.30 days	11.53 days
VWD	January	+0.03 days/dec.	0.12	0.04	0.27 days	0.32 days
VWD	February	-0.04 days/dec.	0.00	0.18	0.19 days	0.11 days
VWD	March	-0.00 days/dec.	0.92	-0.03	0.18 days	0.18 days
VWD	April	+0.00 days/dec.	0.99	-0.03	0.11 days	0.11 days
VWD	May	+0.04 days/dec.	0.11	0.04	0.51 days	0.58 days
VWD	June	-0.03 days/dec.	0.42	-0.01	0.70 days	0.64 days
VWD	July	+0.01 days/dec.	0.73	-0.02	0.44 days	0.46 days
VWD	August	-0.01 days/dec.	0.53	-0.02	0.26 days	0.24 days
VWD	September	-0.01 days/dec.	0.65	-0.02	0.40 days	0.39 days
VWD	October	-0.01 days/dec.	0.50	-0.01	0.39 days	0.36 days
VWD	November	+0.05 days/dec.	0.04	0.08	0.46 days	0.55 days
VWD	December	+0.04 days/dec.	0.10	0.04	0.44 days	0.52 days
DS	January	+0.05 days/dec.	0.74	-0.02	8.39 days	8.48 days
DS	February	+0.09 days/dec.	0.56	-0.02	8.12 days	8.30 days
DS	March	+0.09 days/dec.	0.55	-0.02	9.31 days	9.48 days
DS	April	-0.06 days/dec.	0.62	-0.02	7.25 days	7.12 days
DS	May	-0.02 days/dec.	0.82	-0.02	6.49 days	6.45 days
DS	June	+0.11 days/dec.	0.17	0.02	6.54 days	6.77 days
DS	July	-0.14 days/dec.	0.21	0.02	8.81 days	8.53 days
DS	August	+0.12 days/dec.	0.41	-0.01	10.75 days	10.99 days
DS	September	+0.40°C/dec.	0.00	0.57	8.30 days	9.11 days
DS	October	+0.37°C/dec.	0.00	0.29	1.97 days	2.71 days
DS	November	+0.23°C/dec.	0.00	0.24	-3.55 days	-3.09 days
DS	December	+0.26°C/dec.	0.00	0.23	-6.25 days	-5.72 days

Table 29 – Characteristics of the trend from projected time series of monthly accumulated wet days, very wet days, and the duration of the longest dry spell of the month under the RCP8.5 scenario (linear models)
Data source: NASA Earth Exchange - Global Daily Downscaled Climate Projections (NEX – GDDP) (Thrasher et al. 2012).

RCP8.5						
Variable	**Month**	**Slope**	**p-value**	**R^2**	**Average value in 2040**	**Average value in 2060**
WD	January	+0.07 days/dec.	0.62	-0.02	10.18 days	10.31 days
WD	February	-0.15 days/dec.	0.29	0.00	8.90 days	8.59 days
WD	March	-0.24 days/dec.	0.10	0.04	9.78 days	9.29 days
WD	April	-0.36 days/dec.	0.04	0.08	12.26 days	11.53 days
WD	May	-0.17 days/dec.	0.26	0.01	14.29 days	13.95 days
WD	June	-0.24 days/dec.	0.18	0.02	13.62 days	13.15 days
WD	July	-0.65 days/dec.	0.00	0.22	10.79 days	9.50 days
WD	August	-0.33 days/dec.	0.05	0.07	8.24 days	7.58 days
WD	September	-0.26 days/dec.	0.06	0.06	8.22 days	7.71 days
WD	October	-0.14 days/dec.	0.36	0.00	8.64 days	8.37 days
WD	November	-0.12 days/dec.	0.42	-0.01	10.70 days	10.45 days
WD	December	-0.07 days/dec.	0.59	-0.02	11.38 days	11.24 days
VWD	January	+0.01 days/dec.	0.46	-0.01	0.25 days	0.27 days
VWD	February	+0.02 days/dec.	0.17	0.02	0.18 days	0.21 days
VWD	March	+0.01 days/dec.	0.32	0.00	0.18 days	0.21 days
VWD	April	+0.00 days/dec.	0.75	-0.02	0.11 days	0.12 days
VWD	May	-0.01 days/dec.	0.69	-0.02	0.52 days	0.50 days
VWD	June	+0.05 days/dec.	0.07	0.06	0.67 days	0.76 days
VWD	July	-0.06 days/dec.	0.03	0.10	0.49 days	0.36 days
VWD	August	-0.01 days/dec.	0.51	-0.01	0.25 days	0.23 days
VWD	September	+0.04 days/dec.	0.10	0.05	0.40 days	0.47 days
VWD	October	+0.02 days/dec.	0.41	-0.01	0.37 days	0.40 days
VWD	November	+0.02 days/dec.	0.38	0.00	0.50 days	0.54 days
VWD	December	+0.04 days/dec.	0.10	0.04	0.40 days	0.47 days
DS	January	+0.03 days/dec.	0.83	-0.02	8.77 days	8.82 days
DS	February	+0.38 days/dec.	0.01	0.14	8.52 days	9.28 days
DS	March	+0.17 days/dec.	0.35	0.00	9.15 days	9.48 days
DS	April	+0.26 days/dec.	0.03	0.10	7.43 days	7.94 days
DS	May	+0.15 days/dec.	0.11	0.04	6.69 days	6.99 days
DS	June	+0.16 days/dec.	0.15	0.03	6.85 days	7.16 days
DS	July	+0.54 days/dec.	0.00	0.24	8.87 days	9.95 days
DS	August	+0.05 days/dec.	0.69	-0.02	10.63 days	10.73 days
DS	September	+0.16 days/dec.	0.31	0.00	10.32 days	10.64 days
DS	October	+0.28 days/dec.	0.05	0.07	10.59 days	11.15 days
DS	November	-0.10 days/dec.	0.46	-0.01	8.46 days	8.25 days
DS	December	+0.07 days/dec.	0.61	-0.02	7.92 days	8.06 days

Frost days, ice days & chill hours

The trends of monthly accumulated frost days (FD), ice days (ID), and chill hours (CH) are presented in Figure 100, Figure 101, Figure 102 and Table 30. Overall, a decreasing trend in FD, ID, and CH was observed for most months. Notably, the largest decrease in FD occurred in November (-2.1 days/decade), October (-1.7 days/decade), and January (-1.2 days/decade), while the largest decrease in ID was observed in February (-1 day/decade), December (-0.6 days/decade), and January (-0.5 days/decade). The largest decrease in CH was observed in February (-34 h/decade), November (-30 h/decade), and January (-16 h/decade).

Projected trends for FD, ID, and CH under the NEX median model for RCP4.5 and RCP8.5 scenarios are presented in Figure 103, Figure 104, Figure 105, Table 31, and Table 32. Overall, a decreasing trend in FD, ID, and CH was also projected for most months under both scenarios. For RCP4.5, the largest decrease in FD was projected for March (-0.9 days/decade), December (-0.6 days/decade), and January (-0.4 days/decade). For RCP8.5, the largest decrease in FD was projected for December (-1.6 days/decade), February (-1.4 days/decade), and January (-1.3 days/decade).

For ID, the largest decrease under RCP4.5 was projected for January (-0.5 days/decade), December (-0.2 days/decade), and February (-0.2 days/decade), while for RCP8.5, the largest decrease was projected for January (-0.6 days/decade), February (-0.3 days/decade), and December (-0.3 days/decade). For CH, the largest decrease under RCP4.5 was projected for January (-23 h/decade), December (-17 h/decade), and February (-13 h/decade), while for RCP8.5, the largest decrease was projected for January (-34 h/decade), February (-27 h/decade), and March (-7 h/decade).

Figure 100 – Historical monthly time series of accumulated frost days

Time series over 1980-2019 period. Data source: ERA5, ECMWF / Copernicus Climate Change Service (Muñoz Sabater 2019)

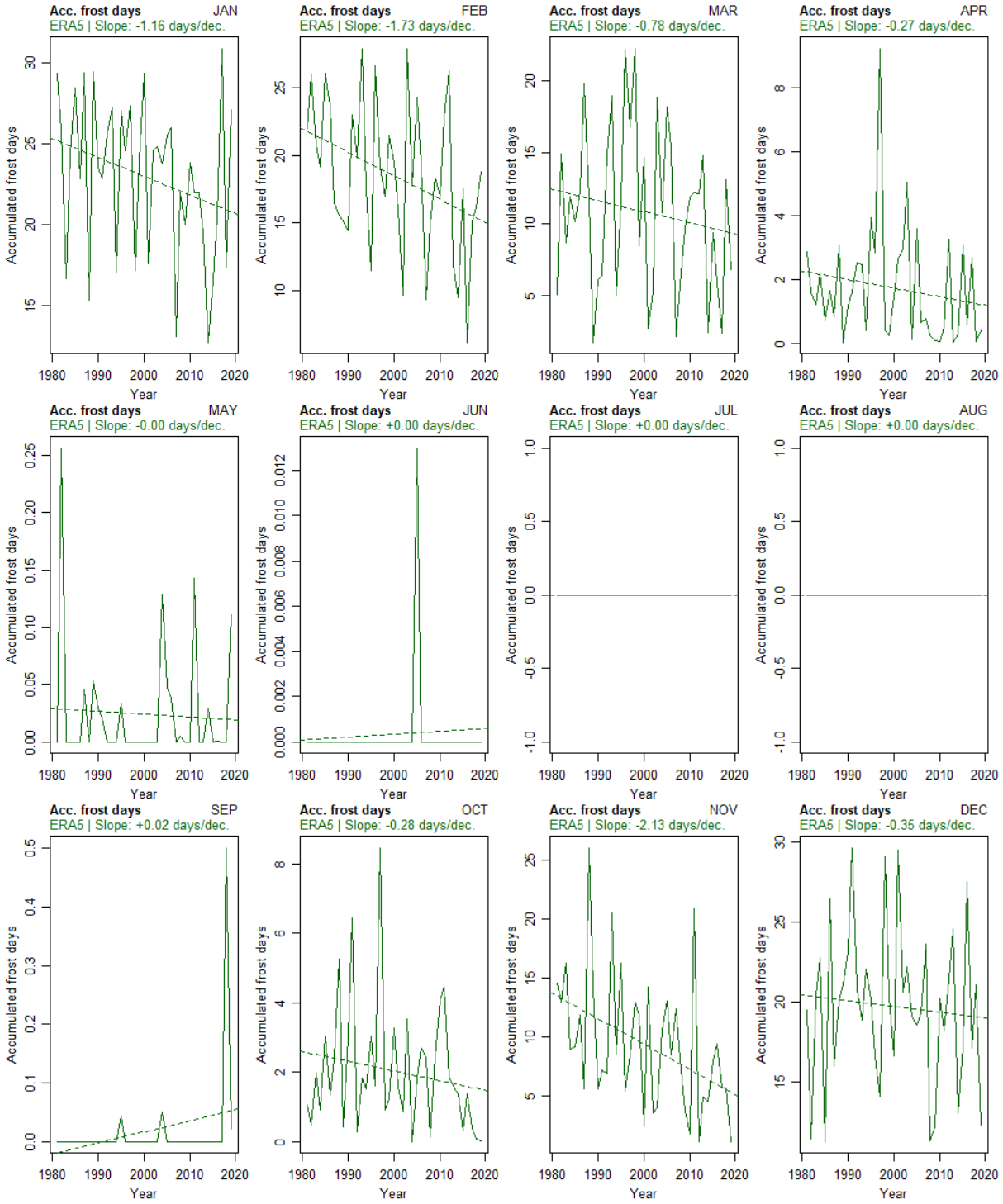

Figure 101 – Historical monthly time series of accumulated ice days

Time series over 1980-2019 period. Data source: ERA5, ECMWF / Copernicus Climate Change Service (Muñoz Sabater 2019)

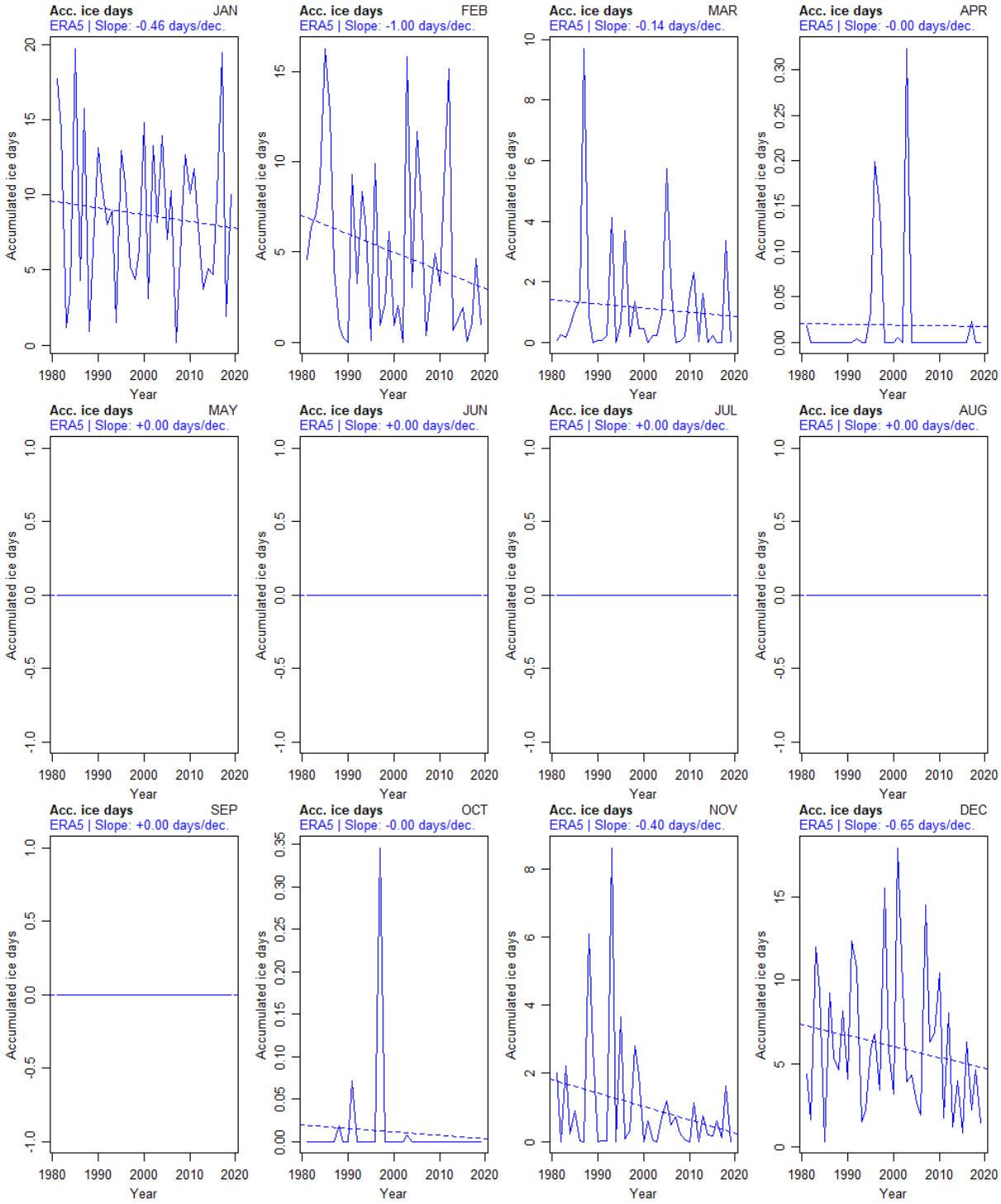

Figure 102 – Historical monthly time series of accumulated chill hours

Time series over 1980-2019 period. Data source: ERA5, ECMWF / Copernicus Climate Change Service (Muñoz Sabater 2019)

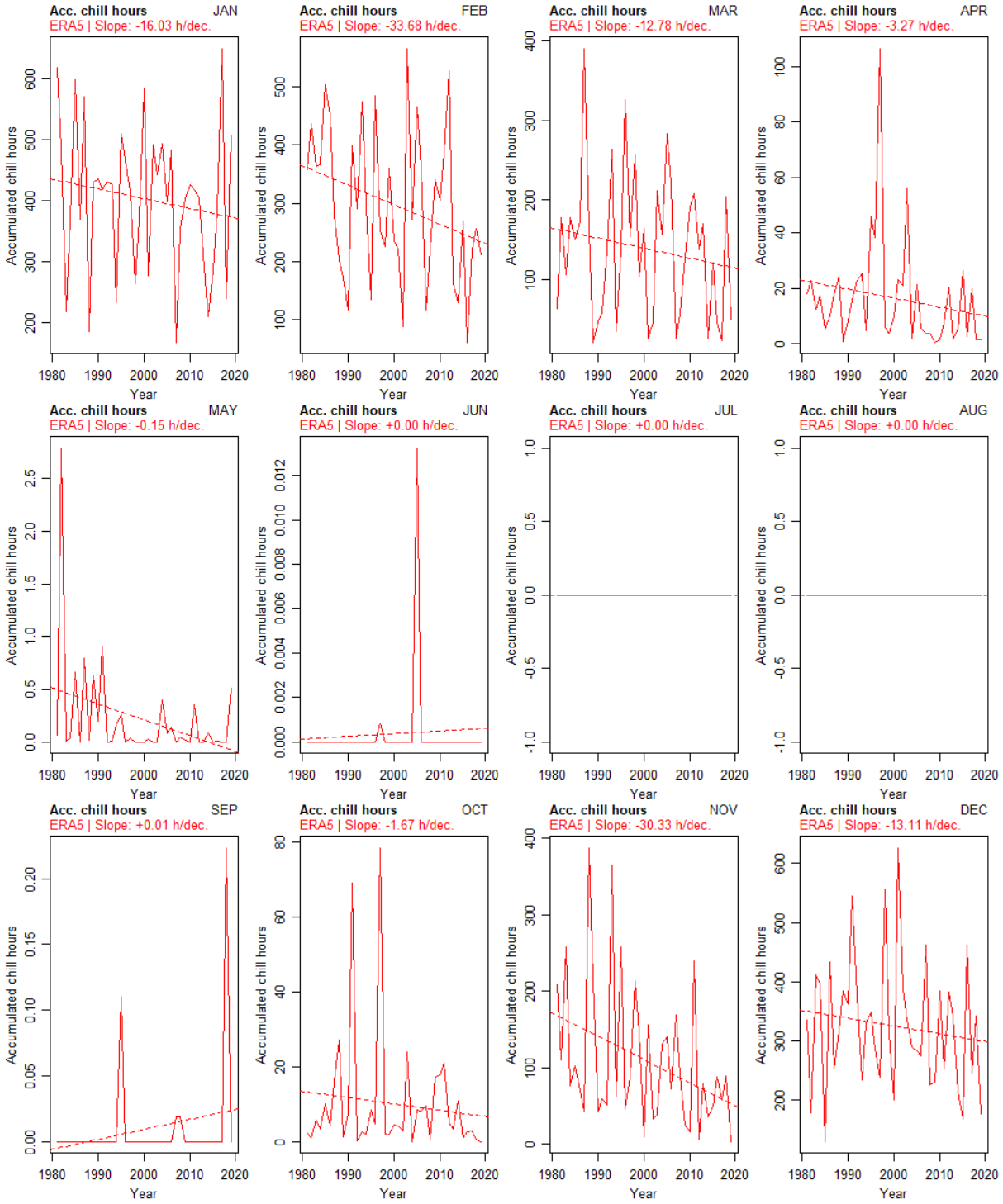

Table 30 – Characteristics of the trends from the historical time series of the monthly accumulated of frost days, ice days, and chill hours (linear models)

***In green**: Monthly accumulated frost days. **In blue:** monthly accumulated ice days. **In red:** monthly accumulated chill hours. Data source: ERA5, ECMWF / Copernicus Climate Change Service (Muñoz Sabater 2019).*

Variable	Month	Slope	p-value	Adjusted R^2	Average value in 1980	Average value in 2019
FD	January	-1.16 days/dec.	0.09	0.05	25.30 days	20.79 days
FD	February	-1.73 days/dec.	0.02	0.11	21.97 days	15.22 days
FD	March	-0.78 days/dec.	0.34	0.00	12.42 days	9.37 days
FD	April	-0.27 days/dec.	0.30	0.00	2.26 days	1.20 days
FD	May	-0.00 days/dec.	0.72	-0.02	0.03 days	0.02 days
FD	June	+0.00 days/dec.	0.66	-0.02	0.00 days	0.00 days
FD	July	+0.00 days/dec.	NA	NA	0.00 days	0.00 days
FD	August	+0.00 days/dec.	NA	NA	0.00 days	0.00 days
FD	September	+0.02 days/dec.	0.10	0.05	-0.02 days	0.05 days
FD	October	-0.28 days/dec.	0.29	0.00	2.59 days	1.51 days
FD	November	-2.13 days/dec.	0.01	0.16	13.65 days	5.33 days
FD	December	-0.35 days/dec.	0.62	-0.02	20.45 days	19.09 days
ID	January	-0.46 days/dec.	0.55	-0.02	9.61 days	7.82 days
ID	February	-1.00 days/dec.	0.14	0.03	7.00 days	3.09 days
ID	March	-0.14 days/dec.	0.62	-0.02	1.40 days	0.86 days
ID	April	-0.00 days/dec.	0.93	-0.03	0.02 days	0.02 days
ID	May	+0.00 days/dec.	NA	NA	0.00 days	0.00 days
ID	June	+0.00 days/dec.	NA	NA	0.00 days	0.00 days
ID	July	+0.00 days/dec.	NA	NA	0.00 days	0.00 days
ID	August	+0.00 days/dec.	NA	NA	0.00 days	0.00 days
ID	September	+0.00 days/dec.	NA	NA	0.00 days	0.00 days
ID	October	-0.00 days/dec.	0.64	-0.02	0.02 days	0.00 days
ID	November	-0.40 days/dec.	0.12	0.04	1.83 days	0.28 days
ID	December	-0.65 days/dec.	0.30	0.00	7.33 days	4.79 days
CH	January	-16.03 h/dec.	0.36	0.00	435.60 h	373.10 h
CH	February	-33.68 h/dec.	0.07	0.06	364.36 h	233.03 h
CH	March	-12.78 h/dec.	0.33	0.00	164.63 h	114.78 h
CH	April	-3.27 h/dec.	0.25	0.01	22.98 h	10.23 h
CH	May	-0.15 h/dec.	0.03	0.10	0.51 h	-0.07 h
CH	June	+0.00 h/dec.	0.68	-0.02	0.00 h	0.00 h
CH	July	+0.00 h/dec.	NA	NA	0.00 h	0.00 h
CH	August	+0.00 h/dec.	NA	NA	0.00 h	0.00 h
CH	September	+0.01 h/dec.	0.18	0.02	-0.01 h	0.02 h
CH	October	-1.67 h/dec.	0.49	-0.01	13.39 h	6.87 h
CH	November	-30.33 h/dec.	0.02	0.11	171.85 h	53.57 h
CH	December	-13.11 h/dec.	0.41	-0.01	352.54 h	301.41 h

Figure 103 – Projected time series of the monthly accumulated frost days

Time series over 2020-2060 period. ***Pink dotted line****: variable value for each model separately under the RCP4.5 scenario.* ***grey dotted line****: variable value for each model separately under the RCP8.5 scenario.* ***Purple full line:*** *median value of the variable under RCP4.5 scenario.* ***Black full line:*** *median value of the variable under RCP8.5 scenario. Data source: NASA Earth Exchange - Global Daily Downscaled Climate Projections (NEX – GDDP) (Thrasher et al. 2012).*

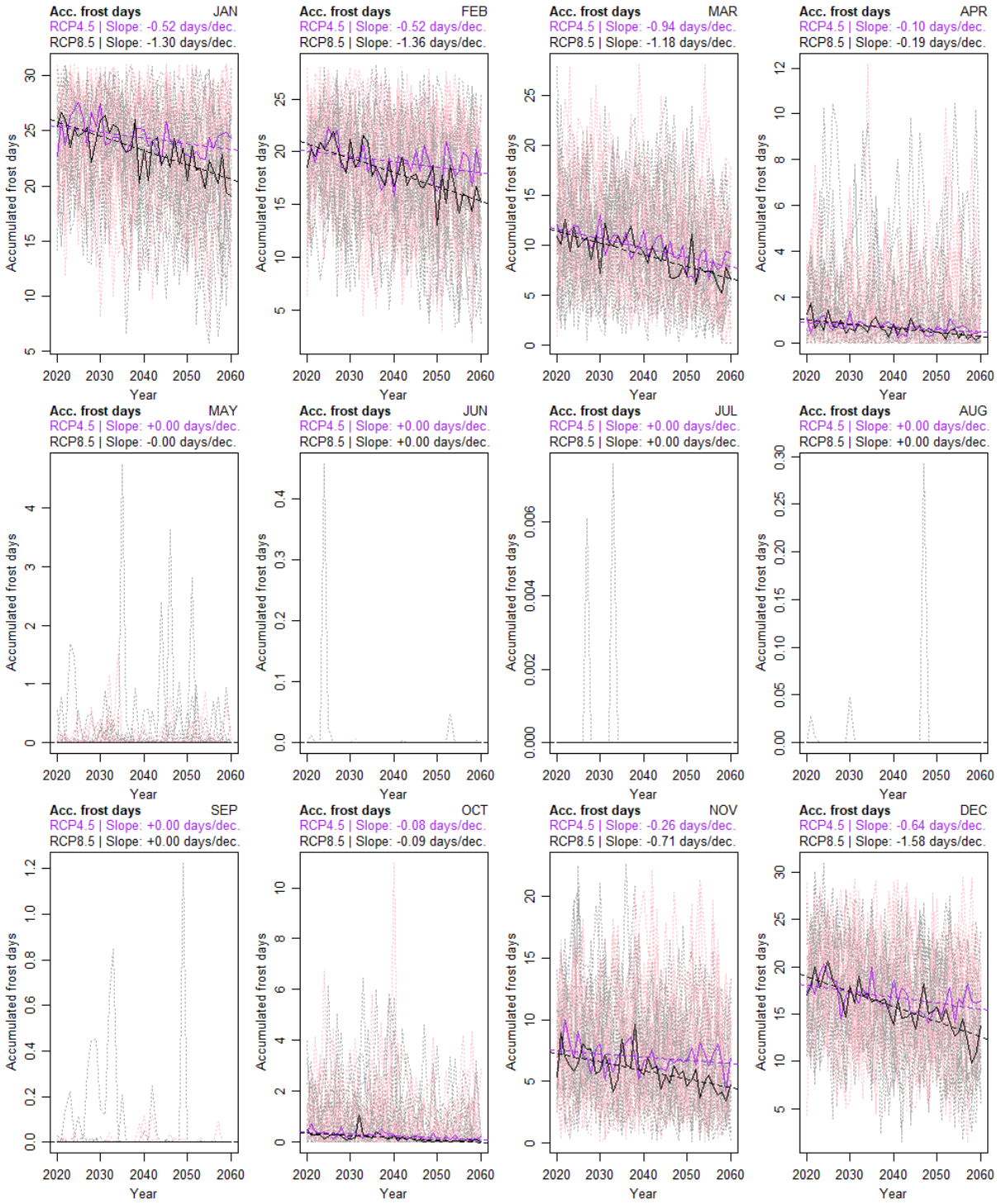

Figure 104 – Projected time series of the monthly accumulated ice days

Time series over 2020-2060 period. ***Pink dotted line****: variable value for each model separately under the RCP4.5 scenario.* ***grey dotted line****: variable value for each model separately under the RCP8.5 scenario.* ***Purple full line:*** *median value of the variable under RCP4.5 scenario.* ***Black full line:*** *median value of the variable under RCP8.5 scenario. Data source: NASA Earth Exchange - Global Daily Downscaled Climate Projections (NEX – GDDP) (Thrasher et al. 2012).*

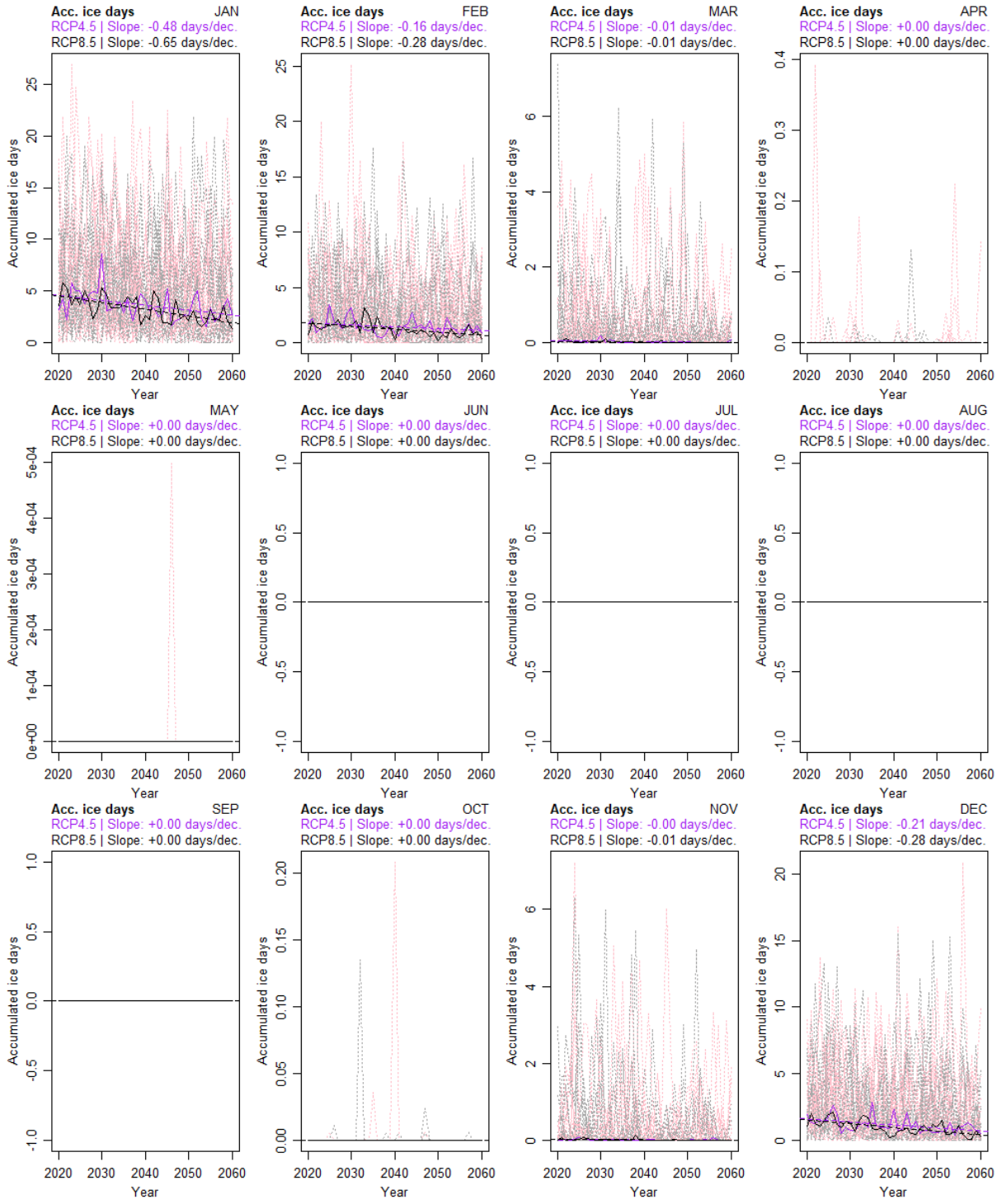

Figure 105 – Projected time series of the monthly accumulated chill hours

Time series over 2020-2060 period. ***Pink dotted line****: variable value for each model separately under the RCP4.5 scenario.* ***grey dotted line****: variable value for each model separately under the RCP8.5 scenario.* ***Purple full line:*** *median value of the variable under RCP4.5 scenario.* ***Black full line:*** *median value of the variable under RCP8.5 scenario. Data source: NASA Earth Exchange - Global Daily Downscaled Climate Projections (NEX – GDDP) (Thrasher et al. 2012).*

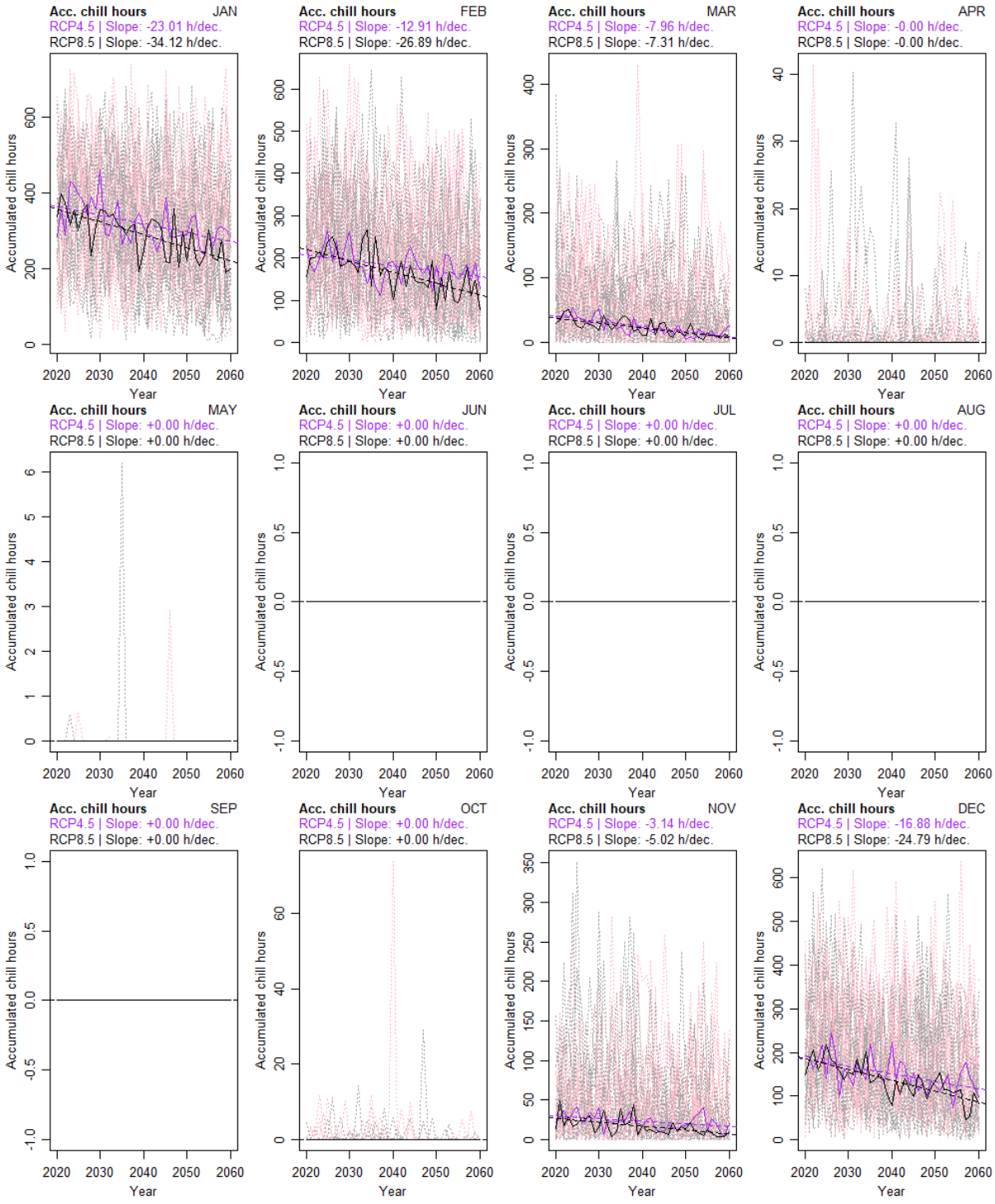

Table 31 – Characteristics of the trend from projected time series of monthly accumulated wet days, very wet days, and the duration of the longest dry spell of the month under the RCP4.5 scenario (linear models)
Data source: NASA Earth Exchange - Global Daily Downscaled Climate Projections (NEX – GDDP) (Thrasher et al. 2012).

RCP4.5						
Variable	**Month**	**Slope**	**p-value**	**R^2**	**Average value in 2040**	**Average value in 2060**
FD	January	-0.52 days/dec.	0.00	0.18	24.32 days	23.28 days
FD	February	-0.52 days/dec.	0.01	0.13	19.06 days	18.03 days
FD	March	-0.94 days/dec.	0.00	0.49	9.73 days	7.85 days
FD	April	-0.10 days/dec.	0.00	0.17	0.71 days	0.51 days
FD	May	+0.00 days/dec.	0.33	0.00	0.00 days	0.00 days
FD	June	+0.00 days/dec.	NA	NA	0.00 days	0.00 days
FD	July	+0.00 days/dec.	NA	NA	0.00 days	0.00 days
FD	August	+0.00 days/dec.	NA	NA	0.00 days	0.00 days
FD	September	+0.00 days/dec.	NA	NA	0.00 days	0.00 days
FD	October	-0.08 days/dec.	0.00	0.36	0.25 days	0.09 days
FD	November	-0.26 days/dec.	0.06	0.06	6.94 days	6.41 days
FD	December	-0.64 days/dec.	0.00	0.23	16.76 days	15.48 days
ID	January	-0.48 days/dec.	0.01	0.16	3.61 days	2.66 days
ID	February	-0.16 days/dec.	0.06	0.06	1.47 days	1.14 days
ID	March	-0.01 days/dec.	0.01	0.13	0.02 days	0.00 days
ID	April	+0.00 days/dec.	NA	NA	0.00 days	0.00 days
ID	May	+0.00 days/dec.	NA	NA	0.00 days	0.00 days
ID	June	+0.00 days/dec.	NA	NA	0.00 days	0.00 days
ID	July	+0.00 days/dec.	NA	NA	0.00 days	0.00 days
ID	August	+0.00 days/dec.	NA	NA	0.00 days	0.00 days
ID	September	+0.00 days/dec.	NA	NA	0.00 days	0.00 days
ID	October	+0.00 days/dec.	NA	NA	0.00 days	0.00 days
ID	November	-0.00 days/dec.	0.17	0.02	0.02 days	0.01 days
ID	December	-0.21 days/dec.	0.00	0.17	1.16 days	0.74 days
CH	January	-23.01 h/dec.	0.00	0.25	317.98 h	271.97 h
CH	February	-12.91 h/dec.	0.01	0.16	181.46 h	155.64 h
CH	March	-7.96 h/dec.	0.00	0.54	24.92 h	9.01 h
CH	April	-0.00 h/dec.	0.05	0.07	0.00 h	0.00 h
CH	May	+0.00 h/dec.	NA	NA	0.00 h	0.00 h
CH	June	+0.00 h/dec.	NA	NA	0.00 h	0.00 h
CH	July	+0.00 h/dec.	NA	NA	0.00 h	0.00 h
CH	August	+0.00 h/dec.	NA	NA	0.00 h	0.00 h
CH	September	+0.00 h/dec.	NA	NA	0.00 h	0.00 h
CH	October	+0.00 h/dec.	NA	NA	0.00 h	0.00 h
CH	November	-3.14 h/dec.	0.01	0.14	23.11 h	16.84 h
CH	December	-16.88 h/dec.	0.00	0.27	151.86 h	118.10 h

Table 32 – Characteristics of the trend from projected time series of monthly accumulated wet days, very wet days, and the duration of the longest dry spell of the month under the RCP8.5 scenario (linear models)
Data source: NASA Earth Exchange - Global Daily Downscaled Climate Projections (NEX – GDDP) (Thrasher et al. 2012).

RCP8.5						
Variable	**Month**	**Slope**	**p-value**	**R^2**	**Average value in 2040**	**Average value in 2060**
FD	January	-1.30 days/dec.	0.00	0.55	23.22 days	20.61 days
FD	February	-1.36 days/dec.	0.00	0.58	18.05 days	15.33 days
FD	March	-1.18 days/dec.	0.00	0.54	9.03 days	6.67 days
FD	April	-0.19 days/dec.	0.00	0.41	0.66 days	0.28 days
FD	May	-0.00 days/dec.	0.11	0.04	0.00 days	0.00 days
FD	June	+0.00 days/dec.	NA	NA	0.00 days	0.00 days
FD	July	+0.00 days/dec.	NA	NA	0.00 days	0.00 days
FD	August	+0.00 days/dec.	NA	NA	0.00 days	0.00 days
FD	September	+0.00 days/dec.	NA	NA	0.00 days	0.00 days
FD	October	-0.09 days/dec.	0.00	0.30	0.18 days	0.00 days
FD	November	-0.71 days/dec.	0.00	0.36	5.86 days	4.44 days
FD	December	-1.58 days/dec.	0.00	0.65	15.78 days	12.62 days
ID	January	-0.65 days/dec.	0.00	0.41	3.28 days	1.98 days
ID	February	-0.28 days/dec.	0.00	0.27	1.22 days	0.67 days
ID	March	-0.01 days/dec.	0.00	0.20	0.02 days	0.00 days
ID	April	+0.00 days/dec.	NA	NA	0.00 days	0.00 days
ID	May	+0.00 days/dec.	NA	NA	0.00 days	0.00 days
ID	June	+0.00 days/dec.	NA	NA	0.00 days	0.00 days
ID	July	+0.00 days/dec.	NA	NA	0.00 days	0.00 days
ID	August	+0.00 days/dec.	NA	NA	0.00 days	0.00 days
ID	September	+0.00 days/dec.	NA	NA	0.00 days	0.00 days
ID	October	+0.00 days/dec.	NA	NA	0.00 days	0.00 days
ID	November	-0.01 days/dec.	0.01	0.14	0.01 days	0.00 days
ID	December	-0.28 days/dec.	0.00	0.39	0.98 days	0.42 days
CH	January	-34.12 h/dec.	0.00	0.47	290.68 days	222.44 days
CH	February	-26.89 h/dec.	0.00	0.43	167.23 days	113.45 days
CH	March	-7.31 h/dec.	0.00	0.49	23.00 days	8.37 days
CH	April	-0.00 h/dec.	0.13	0.03	0.00 days	0.00 days
CH	May	+0.00 h/dec.	NA	NA	0.00 days	0.00 days
CH	June	+0.00 h/dec.	NA	NA	0.00 days	0.00 days
CH	July	+0.00 h/dec.	NA	NA	0.00 days	0.00 days
CH	August	+0.00 h/dec.	NA	NA	0.00 days	0.00 days
CH	September	+0.00 h/dec.	NA	NA	0.00 days	0.00 days
CH	October	+0.00 h/dec.	NA	NA	0.00 days	0.00 days
CH	November	-5.02 h/dec.	0.00	0.27	16.79 days	6.75 days
CH	December	+0.07 days/dec.	0.61	-0.02	7.92 days	8.06 days

Summer days & tropical nights

The historical trends of monthly accumulated summer days and tropical nights can be observed in Figure 106, Figure 107, and Table 33. Overall, there has been an increase in SD and TrN for most of the months. The critical months for these indicators are the hottest months, from June to September, with the largest increases in SD for June (+2.0 days/decade), July (+1.7 days/decade), and August (+1.6 days/decade), and the largest increase in TrN for August (+0.4 days/decade), June (+0.4 days/decade), and July (+0.3 days/decade).

The projected trends of monthly accumulated summer days and tropical nights can be observed in Figure 108, Figure 109, Table 34 and Table 35. Under the RCP4.5 scenario, the NEX median model shows that the largest increases in SD will occur during the months of September (+1.2 days/decade), June (+0.8 days/decade), and July (+0.6 days/decade). On the other hand, under the RCP8.5 scenario, the largest increase in SD can be observed for the months of September (+2.1 days/decade), June (+1.6 days/decade), and May (+1.3 days/decade).

Regarding TrN, under the RCP4.5 scenario, the NEX median model shows that the largest increase will occur during the months of August (+1.5 days/decade), July (+1.3 days/decade), and June (+0.1 days/decade). Similarly, under the RCP8.5 scenario, the largest increase in TrN can be observed for the months of August (+2.6 days/decade), July (+2.5 days/decade), and June (+0.6 days/decade).

In summary, the critical months for SD and TrN are the hottest months, from June to September.

Figure 106 – Historical monthly time series of accumulated summer days

Time series over 1980-2019 period. Data source: ERA5, ECMWF / Copernicus Climate Change Service (Muñoz Sabater 2019)

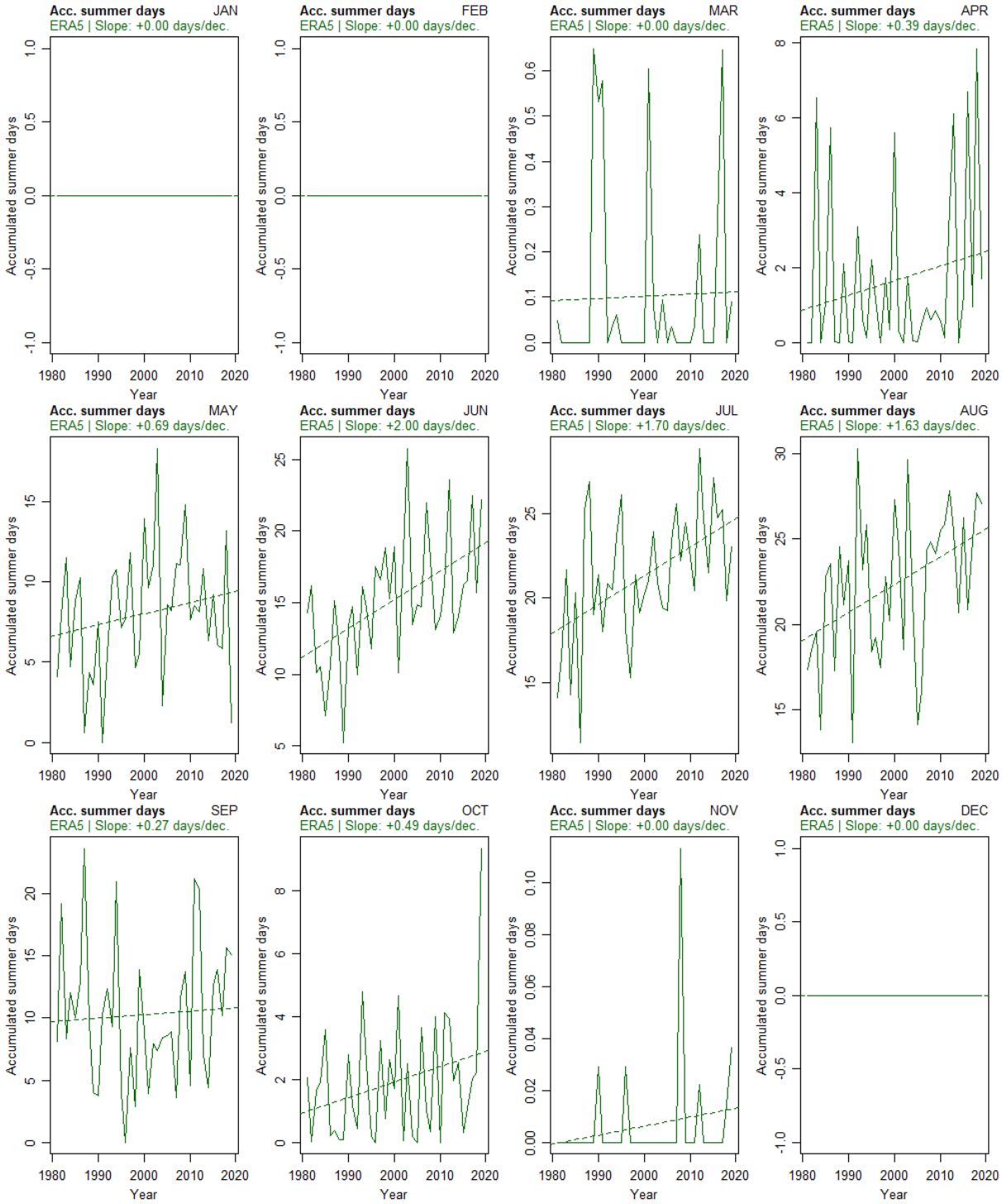

Figure 107 – Historical monthly time series of accumulated tropical nights

Time series over 1980-2019 period. Data source: ERA5, ECMWF / Copernicus Climate Change Service (Muñoz Sabater 2019)

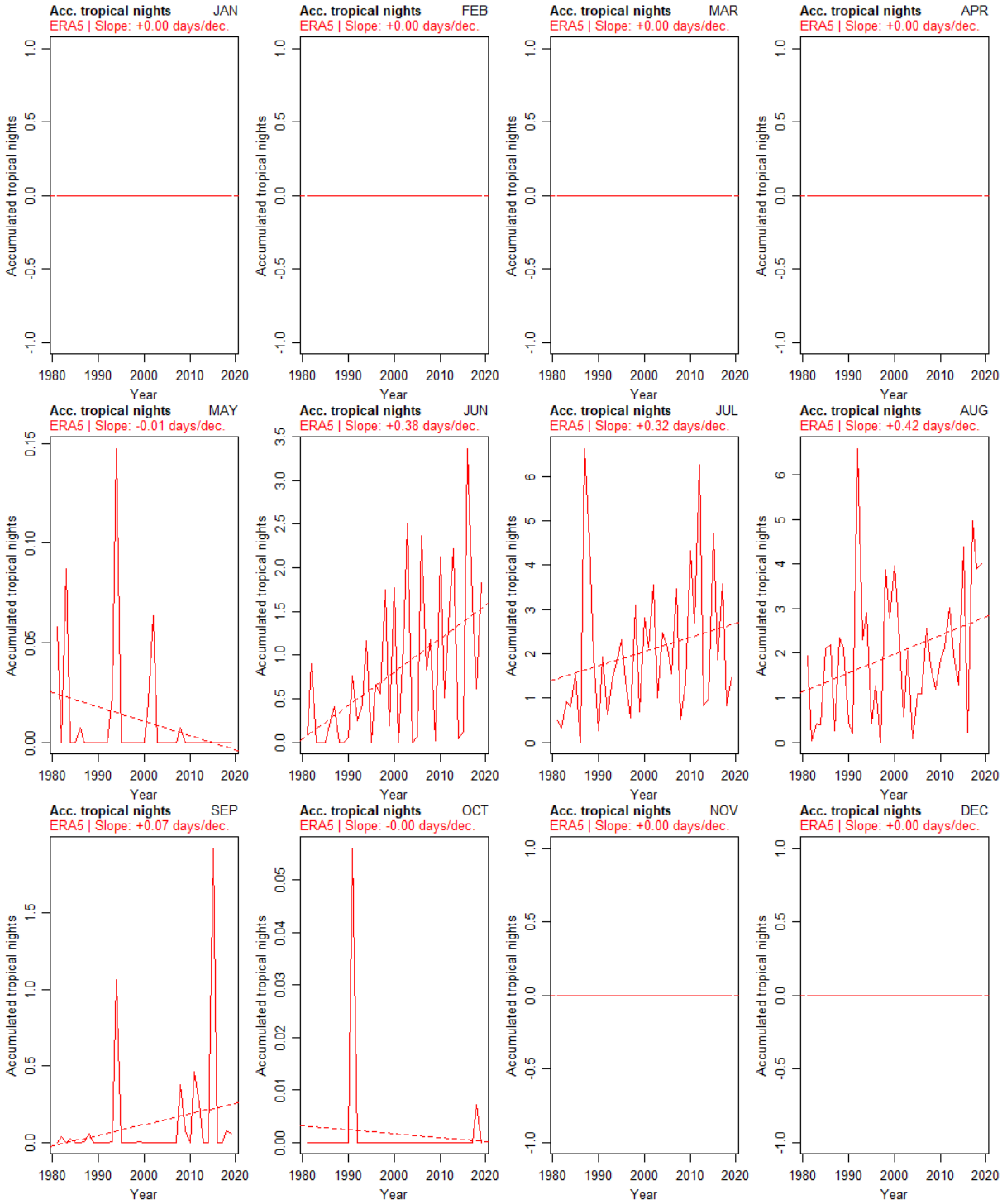

Table 33 – Characteristics of the trends from the historical time series of the monthly accumulated of summer days and tropical nights (linear models)

***In green**: Monthly accumulated summer days. **In red:** monthly accumulated tropical nights. Data source: ERA5, ECMWF / Copernicus Climate Change Service (Muñoz Sabater 2019).*

Variable	Month	Slope	p-value	Adjusted R^2	Average value in 1980	Average value in 2019
SD	January	+0.00 days/dec.	NA	NA	0.00 days	0.00 days
SD	February	+0.00 days/dec.	NA	NA	0.00 days	0.00 days
SD	March	+0.00 days/dec.	0.87	-0.03	0.09 days	0.11 days
SD	April	+0.39 days/dec.	0.23	0.01	0.86 days	2.39 days
SD	May	+0.69 days/dec.	0.23	0.01	6.64 days	9.32 days
SD	June	+2.00 days/dec.	0.00	0.25	11.21 days	19.00 days
SD	July	+1.70 days/dec.	0.00	0.24	17.94 days	24.56 days
SD	August	+1.63 days/dec.	0.01	0.16	19.05 days	25.40 days
SD	September	+0.27 days/dec.	0.74	-0.02	9.74 days	10.77 days
SD	October	+0.49 days/dec.	0.07	0.06	0.92 days	2.83 days
SD	November	+0.00 days/dec.	0.22	0.01	0.00 days	0.01 days
SD	December	+0.00 days/dec.	NA	NA	0.00 days	0.00 days
TrN	January	+0.00 days/dec.	NA	NA	0.00 days	0.00 days
TrN	February	+0.00 days/dec.	NA	NA	0.00 days	0.00 days
TrN	March	+0.00 days/dec.	NA	NA	0.00 days	0.00 days
TrN	April	+0.00 days/dec.	NA	NA	0.00 days	0.00 days
TrN	May	-0.01 days/dec.	0.09	0.05	0.02 days	0.00 days
TrN	June	+0.38 days/dec.	0.00	0.22	0.04 days	1.53 days
TrN	July	+0.32 days/dec.	0.16	0.03	1.41 days	2.65 days
TrN	August	+0.42 days/dec.	0.05	0.07	1.14 days	2.78 days
TrN	September	+0.07 days/dec.	0.16	0.03	-0.03 days	0.25 days
TrN	October	-0.00 days/dec.	0.56	-0.02	0.00 days	0.00 days
TrN	November	+0.00 days/dec.	NA	NA	0.00 days	0.00 days
TrN	December	+0.00 days/dec.	NA	NA	0.00 days	0.00 days

Figure 108 – Historical monthly time series of accumulated summer days

Time series over 2020-2060 period. ***Pink dotted line****: variable value for each model separately under the RCP4.5 scenario.* ***grey dotted line****: variable value for each model separately under the RCP8.5 scenario.* ***Purple full line:*** *median value of the variable under RCP4.5 scenario.* ***Black full line:*** *median value of the variable under RCP8.5 scenario. Data source: NASA Earth Exchange - Global Daily Downscaled Climate Projections (NEX – GDDP) (Thrasher et al. 2012).*

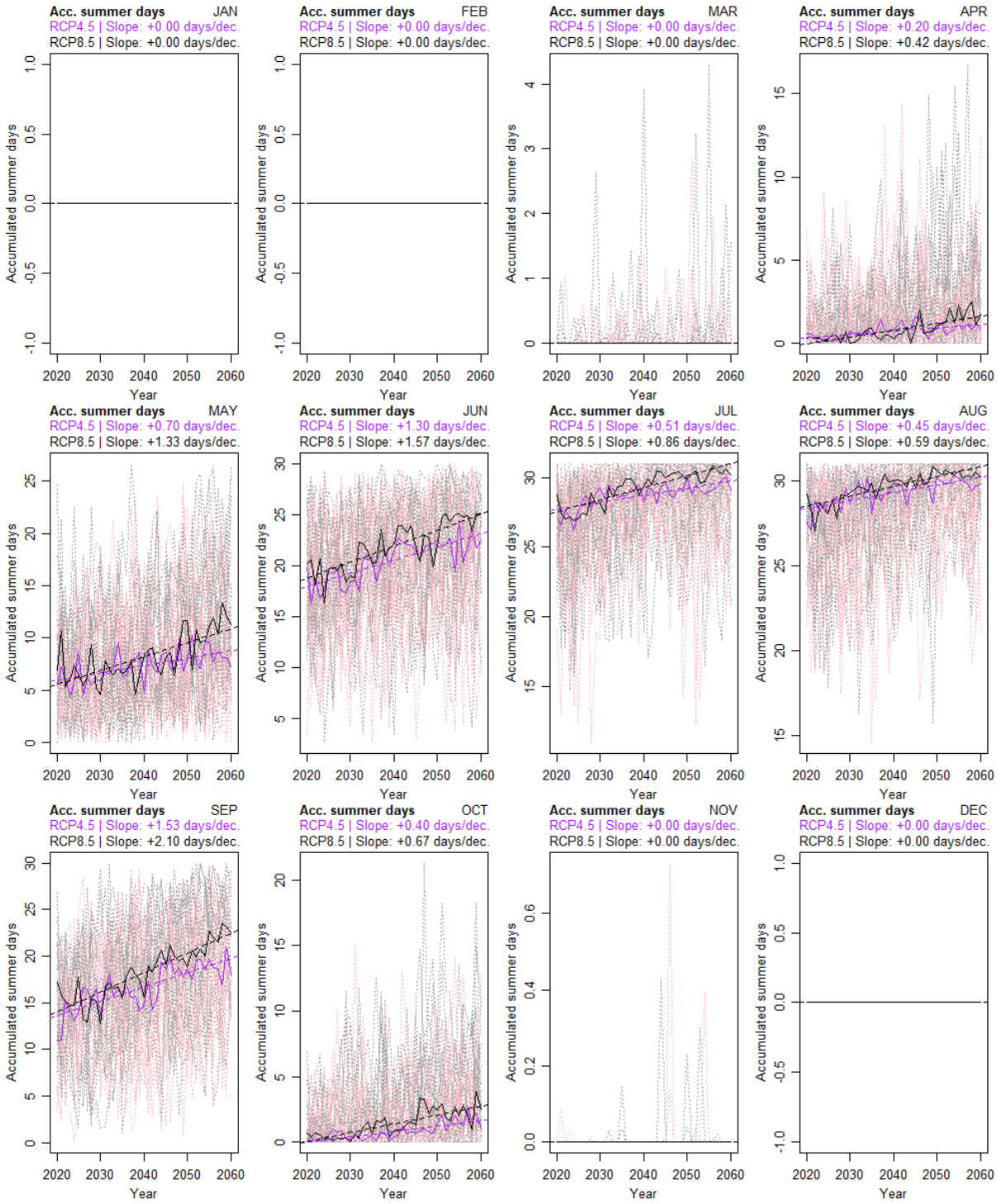

Figure 109 – Historical monthly time series of accumulated tropical nights

Time series over 2020-2060 period. ***Pink dotted line****: variable value for each model separately under the RCP4.5 scenario.* ***grey dotted line****: variable value for each model separately under the RCP8.5 scenario.* ***Purple full line:*** *median value of the variable under RCP4.5 scenario.* ***Black full line:*** *median value of the variable under RCP8.5 scenario. Data source: NASA Earth Exchange - Global Daily Downscaled Climate Projections (NEX – GDDP) (Thrasher et al. 2012).*

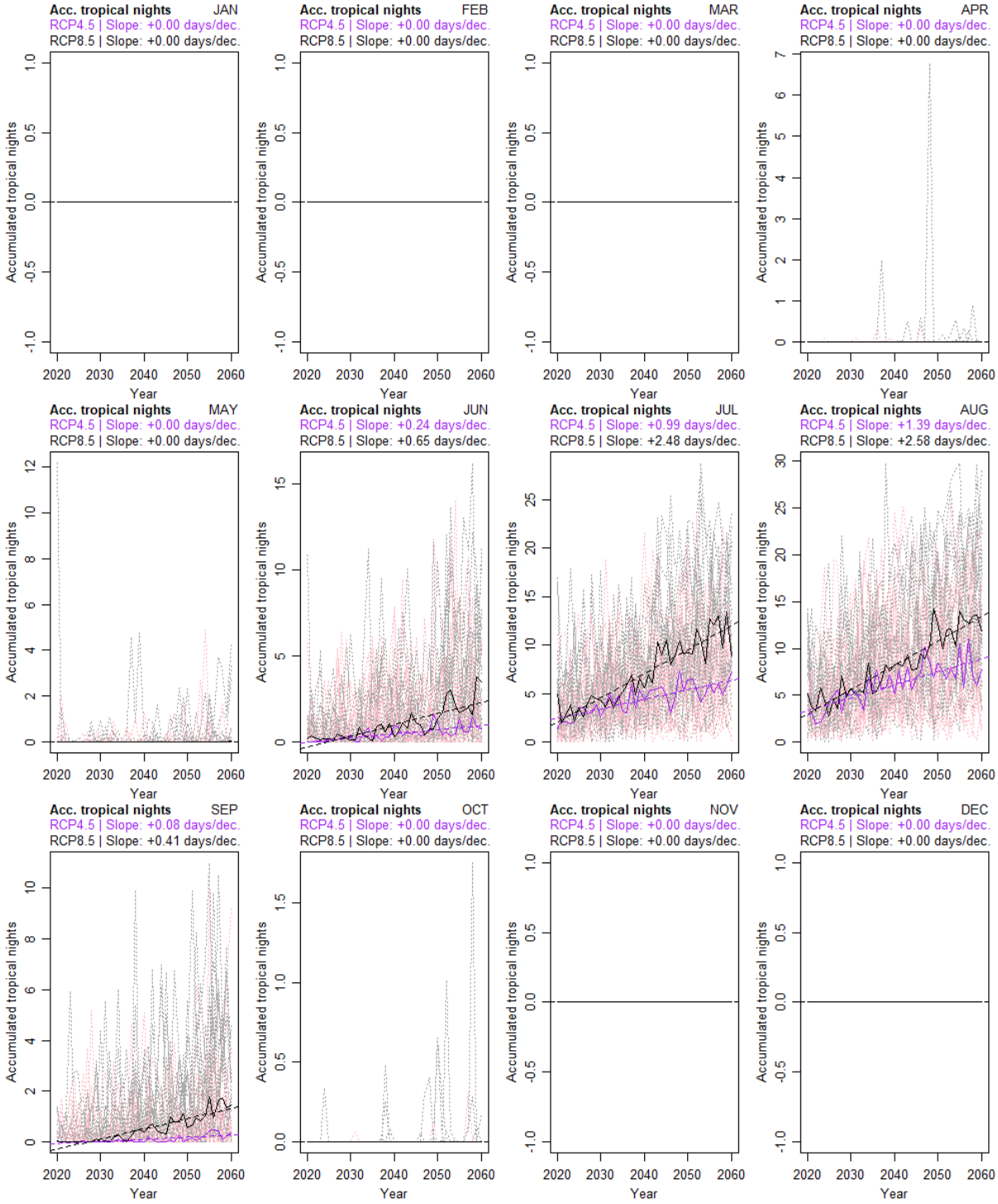

Table 34 – Characteristics of the trend from projected time series of monthly accumulated summer days and tropical nights days under the RCP4.5 scenario (linear models)

Data source: NASA Earth Exchange - Global Daily Downscaled Climate Projections (NEX – GDDP) (Thrasher et al. 2012).

RCP4.5						
Variable	**Month**	**Slope**	**p-value**	**R^2**	**Average value in 2040**	**Average value in 2060**
SD	January	+0.00 days/dec.	NA	NA	0.00 days	0.00 days
SD	February	+0.00 days/dec.	NA	NA	0.00 days	0.00 days
SD	March	+0.00 days/dec.	NA	NA	0.00 days	0.00 days
SD	April	+0.20 days/dec.	0.00	0.33	0.73 days	1.13 days
SD	May	+0.70 days/dec.	0.00	0.32	7.35 days	8.75 days
SD	June	+1.30 days/dec.	0.00	0.60	20.49 days	23.09 days
SD	July	+0.51 days/dec.	0.00	0.48	28.74 days	29.76 days
SD	August	+0.45 days/dec.	0.00	0.48	29.28 days	30.18 days
SD	September	+1.53 days/dec.	0.00	0.60	16.65 days	19.71 days
SD	October	+0.40 days/dec.	0.00	0.56	0.81 days	1.61 days
SD	November	+0.00 days/dec.	NA	NA	0.00 days	0.00 days
SD	December	+0.00 days/dec.	NA	NA	0.00 days	0.00 days
TrN	January	+0.00 days/dec.	NA	NA	0.00 days	0.00 days
TrN	February	+0.00 days/dec.	NA	NA	0.00 days	0.00 days
TrN	March	+0.00 days/dec.	NA	NA	0.00 days	0.00 days
TrN	April	+0.00 days/dec.	NA	NA	0.00 days	0.00 days
TrN	May	+0.00 days/dec.	NA	NA	0.00 days	0.00 days
TrN	June	+0.24 days/dec.	0.00	0.47	0.48 days	0.96 days
TrN	July	+0.99 days/dec.	0.00	0.61	4.42 days	6.41 days
TrN	August	+1.39 days/dec.	0.00	0.59	6.10 days	8.88 days
TrN	September	+0.08 days/dec.	0.00	0.45	0.09 days	0.26 days
TrN	October	+0.00 days/dec.	NA	NA	0.00 days	0.00 days
TrN	November	+0.00 days/dec.	NA	NA	0.00 days	0.00 days
TrN	December	+0.00 days/dec.	NA	NA	0.00 days	0.00 days

Table 35 – Characteristics of the trend from projected time series of monthly accumulated summer days and tropical nights days under the RCP8.5 scenario (linear models)

Data source: NASA Earth Exchange - Global Daily Downscaled Climate Projections (NEX – GDDP) (Thrasher et al. 2012).

RCP8.5						
Variable	**Month**	**Slope**	**p-value**	**R^2**	**Average value in 2040**	**Average value in 2060**
SD	January	+0.00 days/dec.	NA	NA	0.00 days	0.00 days
SD	February	+0.00 days/dec.	NA	NA	0.00 days	0.00 days
SD	March	+0.00 days/dec.	NA	NA	0.00 days	0.00 days
SD	April	+0.42 days/dec.	0.00	0.56	0.80 days	1.64 days
SD	May	+1.33 days/dec.	0.00	0.47	8.24 days	10.90 days
SD	June	+1.57 days/dec.	0.00	0.65	21.88 days	25.03 days
SD	July	+0.86 days/dec.	0.00	0.73	29.27 days	30.98 days
SD	August	+0.59 days/dec.	0.00	0.67	29.65 days	30.83 days
SD	September	+2.10 days/dec.	0.00	0.77	18.25 days	22.44 days
SD	October	+0.67 days/dec.	0.00	0.60	1.41 days	2.76 days
SD	November	+0.00 days/dec.	NA	NA	0.00 days	0.00 days
SD	December	+0.00 days/dec.	NA	NA	0.00 days	0.00 days
TrN	January	+0.00 days/dec.	NA	NA	0.00 days	0.00 days
TrN	February	+0.00 days/dec.	NA	NA	0.00 days	0.00 days
TrN	March	+0.00 days/dec.	NA	NA	0.00 days	0.00 days
TrN	April	+0.00 days/dec.	NA	NA	0.00 days	0.00 days
TrN	May	+0.00 days/dec.	0.06	0.06	0.00 days	0.01 days
TrN	June	+0.65 days/dec.	0.00	0.65	1.02 days	2.32 days
TrN	July	+2.48 days/dec.	0.00	0.82	7.04 days	12.00 days
TrN	August	+2.58 days/dec.	0.00	0.85	8.20 days	13.37 days
TrN	September	+0.41 days/dec.	0.00	0.81	0.53 days	1.34 days
TrN	October	+0.00 days/dec.	NA	NA	0.00 days	0.00 days
TrN	November	+0.00 days/dec.	NA	NA	0.00 days	0.00 days
TrN	December	+0.00 days/dec.	NA	NA	0.00 days	0.00 days

Degree days

The historical trends of monthly accumulated degree days are depicted in Figure 110 and Table 36. Overall, most of the months exhibit an increase in DD. The critical months with the largest increases in DD are June (+18.6°days/decade), August (+18.4°days/decade), and July (+16.0°days/decade).

The projected trends of monthly accumulated degree days can be observed in Figure 111 and Table 36. Again, most of the months show an increase in DD. Under the RCP4.5 scenario, the NEX median model indicates the largest increases in DD during the months of August (+12.8°days/decade), September (+12.3°days/decade), and July (+10.6°days/decade). In contrast, under the RCP8.5 scenario, the largest increase in DD can be observed for the months of August (+22.5°days/decade), July (+20.8°days/decade), and September (+19.4°days/decade).

Table 36 – Characteristics of the trends from the historical time series of the monthly accumulated degree days (linear models)
Data source: ERA5, ECMWF / Copernicus Climate Change Service (Muñoz Sabater 2019).

Variable	Month	Slope	p-value	Adjusted R^2	Average value in 1980	Average value in 2019
DD	January	+0.10°days/dec.	0.05	0.07	-0.05°days	0.35°days
DD	February	+0.44°days/dec.	0.21	0.02	0.49°days	2.21°days
DD	March	+2.18°days/dec.	0.19	0.02	12.65°days	21.14°days
DD	April	+10.25°days/dec.	0.03	0.09	55.11°days	95.10°days
DD	May	+2.70°days/dec.	0.65	-0.02	191.50°days	202.04°days
DD	June	+18.60°days/dec.	0.00	0.26	252.02°days	324.54°days
DD	July	+15.98°days/dec.	0.00	0.21	327.60°days	389.93°days
DD	August	+18.42°days/dec.	0.00	0.20	318.45°days	390.27°days
DD	September	+2.46°days/dec.	0.72	-0.02	201.52°days	211.09°days
DD	October	+1.83°days/dec.	0.64	-0.02	77.96°days	85.10°days
DD	November	+5.49°days/dec.	0.00	0.20	2.83°days	24.26°days
DD	December	+0.18°days/dec.	0.54	-0.02	0.72°days	1.43°days

Figure 110 – Historical monthly time series of accumulated degree days

Time series over 1980-2019 period. Data source: ERA5, ECMWF / Copernicus Climate Change Service (Muñoz Sabater 2019)

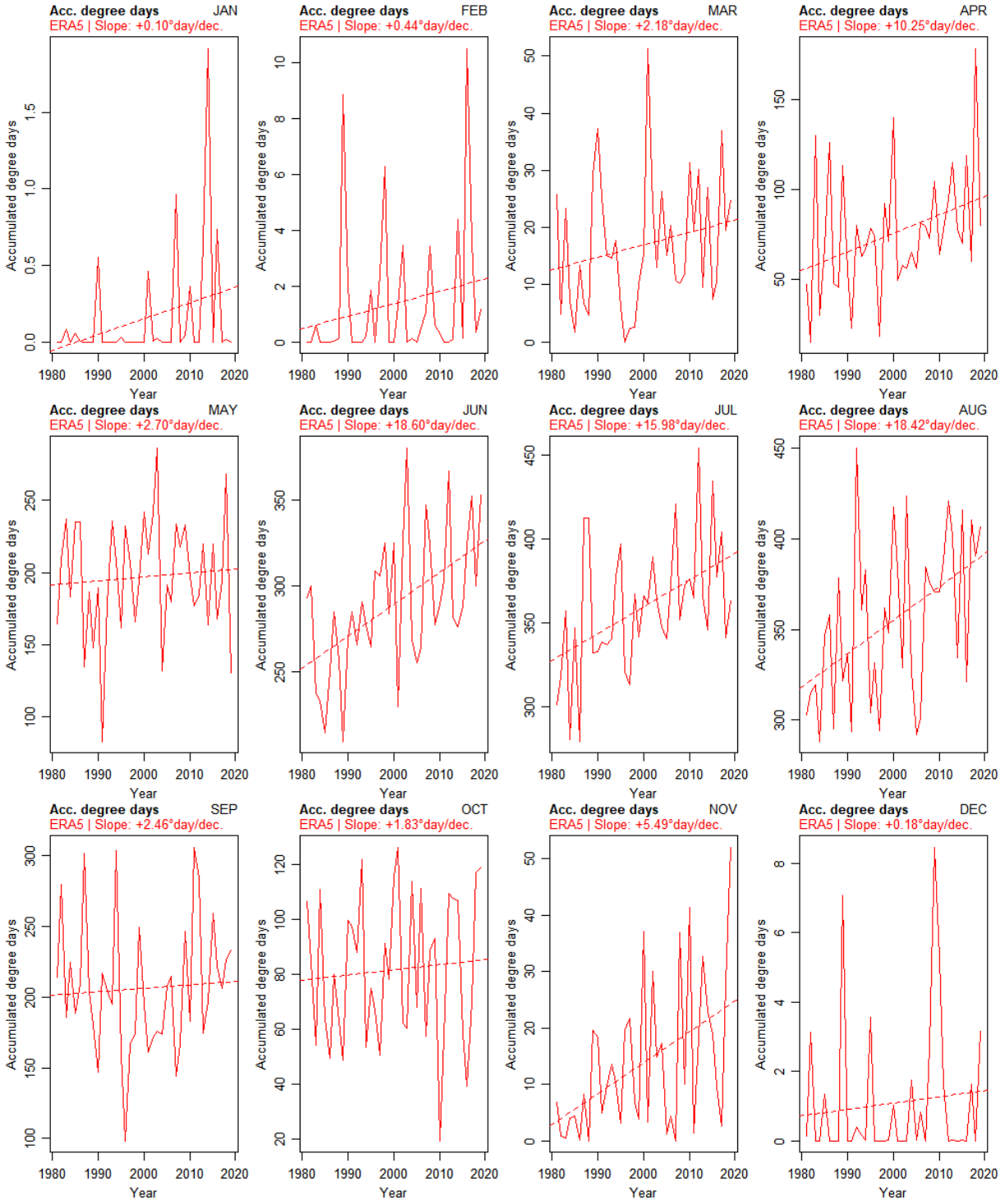

Figure 111 – Projected monthly time series of accumulated degree days

Time series over 2020-2060 period. ***Pink dotted line****: variable value for each model separately under the RCP4.5 scenario.* ***grey dotted line****: variable value for each model separately under the RCP8.5 scenario.* ***Purple full line:*** *median value of the variable under RCP4.5 scenario.* ***Black full line:*** *median value of the variable under RCP8.5 scenario. Data source: NASA Earth Exchange - Global Daily Downscaled Climate Projections (NEX – GDDP) (Thrasher et al. 2012).*

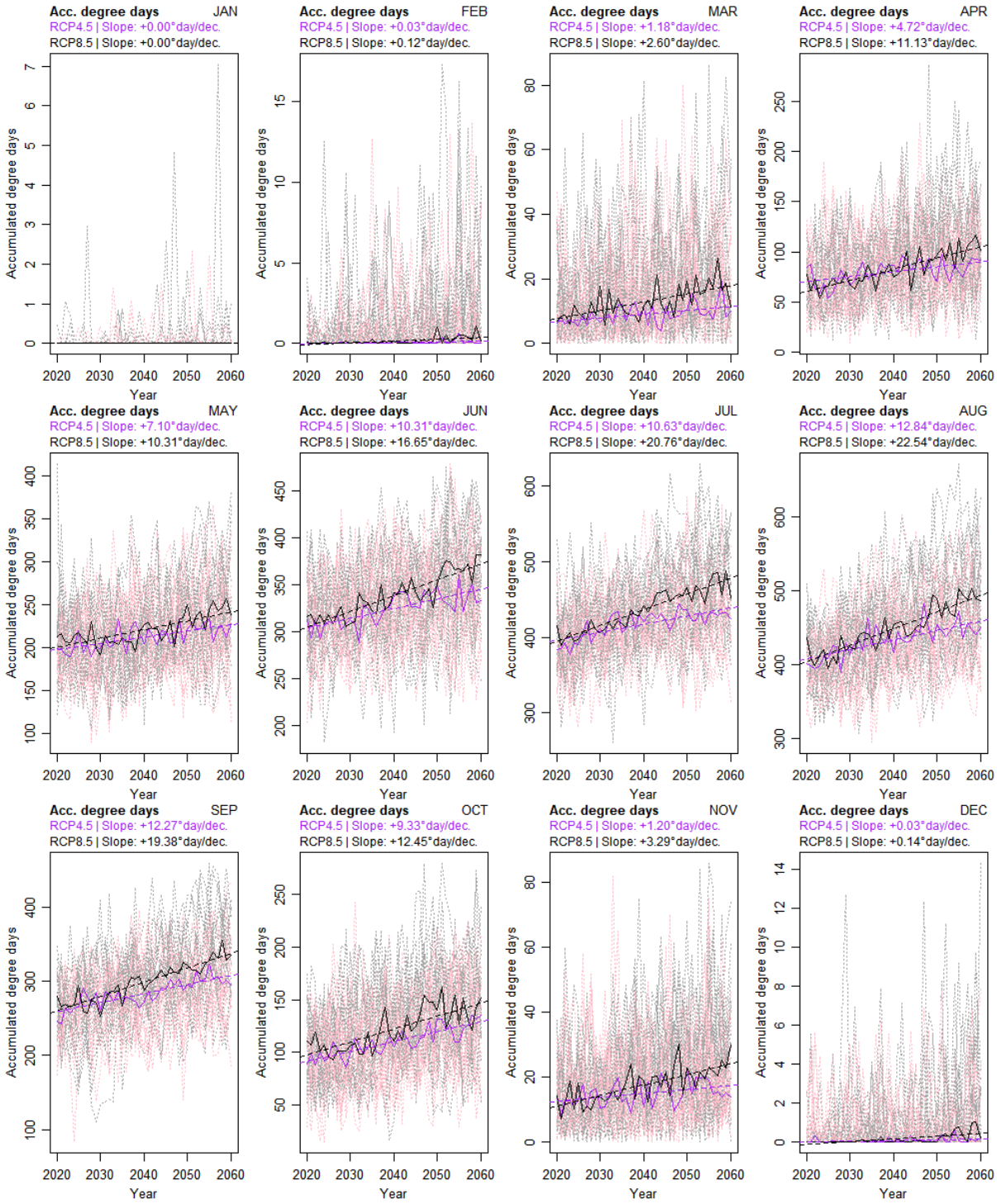

Table 37 – Characteristics of the trend from projected time series of monthly accumulated summer days and tropical nights days under both RCP4.5 and RCP8.5 scenario (linear models)

Data source: NASA Earth Exchange - Global Daily Downscaled Climate Projections (NEX – GDDP) (Thrasher et al. 2012).

RCP4.5						
Variable	**Month**	**Slope**	**p-value**	**R^2**	**Average value in 2040**	**Average value in 2060**
DD	January	+0.00°days/dec.	NA	NA	0.00°days	0.00°days
DD	February	+0.03°days/dec.	0.03	0.09	0.05°days	0.11°days
DD	March	+1.18°days/dec.	0.00	0.19	9.08°days	11.44°days
DD	April	+4.72°days/dec.	0.00	0.25	80.25°days	89.69°days
DD	May	+7.10°days/dec.	0.00	0.40	211.97°days	226.17°days
DD	June	+10.31°days/dec.	0.00	0.54	324.37°days	344.98°days
DD	July	+10.63°days/dec.	0.00	0.55	417.65°days	438.91°days
DD	August	+12.84°days/dec.	0.00	0.53	433.54°days	459.22°days
DD	September	+12.27°days/dec.	0.00	0.66	283.54°days	308.08°days
DD	October	+9.33°days/dec.	0.00	0.68	110.28°days	128.94°days
DD	November	+1.20°days/dec.	0.01	0.13	14.88°days	17.28°days
DD	December	+0.03°days/dec.	0.05	0.07	0.08°days	0.15°days
RCP8.5						
Variable	**Month**	**Slope**	**p-value**	**R^2**	**Average value in 2040**	**Average value in 2060**
DD	January	+0.00°days/dec.	NA	NA	0.00°days	0.00°days
DD	February	+0.12°days/dec.	0.00	0.32	0.16°days	0.40°days
DD	March	+2.60°days/dec.	0.00	0.39	12.71°days	17.91°days
DD	April	+11.13°days/dec.	0.00	0.65	82.96°days	105.23°days
DD	May	+10.31°days/dec.	0.00	0.53	220.98°days	241.60°days
DD	June	+16.65°days/dec.	0.00	0.76	338.74°days	372.05°days
DD	July	+20.76°days/dec.	0.00	0.84	435.88°days	477.39°days
DD	August	+22.54°days/dec.	0.00	0.81	448.91°days	493.98°days
DD	September	+19.38°days/dec.	0.00	0.82	299.09°days	337.84°days
DD	October	+12.45°days/dec.	0.00	0.58	122.08°days	146.99°days
DD	November	+3.29°days/dec.	0.00	0.52	17.57°days	24.16°days
DD	December	+0.14°days/dec.	0.00	0.36	0.15°days	0.43°days

Water deficit

Figure 112 and Table 38 provide a visual and numerical representation of the historical trends in monthly accumulated water deficit. The analysis of these trends indicates that most months have experienced an increase in water deficit over time, consistent with the annual analysis.

When looking at critical months, the data shows that September, August, and April have seen the largest decrease in water deficit, with an increase of 11.9 mm/decade, 8.2 mm/decade, and 8.3 mm/decade respectively. However, it's worth noting that May and July stand out as exceptions to this trend, with a decrease of 13.8 mm/decade and 5.4 mm/decade in water deficit respectively.

Table 38 – Characteristics of the trends from the historical time series of the monthly accumulated water deficit (linear models)

Data source: NASA LP DAAC - EBMOD16A2.006: Terra Net Evapotranspiration (Running, Mu, and Zhao 2021)

Variable	Month	Slope	p-value	Adjusted R^2	Average value in 1980	Average value in 2019
Wdef	January	-1.11 mm/dec.	0.29	0.01	7.26 mm	2.94 mm
Wdef	February	+2.06 mm/dec.	0.58	-0.04	6.96 mm	15.01 mm
Wdef	March	+3.01 mm/dec.	0.70	-0.05	41.46 mm	53.22 mm
Wdef	April	+8.33 mm/dec.	0.24	0.03	37.17 mm	69.65 mm
Wdef	May	-13.79 mm/dec.	0.04	0.18	124.26 mm	70.48 mm
Wdef	June	-2.76 mm/dec.	0.75	-0.05	107.15 mm	96.41 mm
Wdef	July	-5.36 mm/dec.	0.58	-0.04	135.69 mm	114.78 mm
Wdef	August	+8.36 mm/dec.	0.44	-0.02	89.23 mm	121.84 mm
Wdef	September	+11.86 mm/dec.	0.11	0.09	42.49 mm	88.75 mm
Wdef	October	+7.06 mm/dec.	0.22	0.03	15.27 mm	42.78 mm
Wdef	November	+3.39 mm/dec.	0.24	0.02	4.56 mm	17.79 mm
Wdef	December	+1.69 mm/dec.	0.06	0.14	-1.65 mm	4.95 mm

Figure 112 – Historical monthly time series of accumulated water deficit

Time series over 2001-2019 period. Data source: NASA LP DAAC - EBMOD16A2.006: Terra Net Evapotranspiration (Running, Mu, and Zhao 2021)

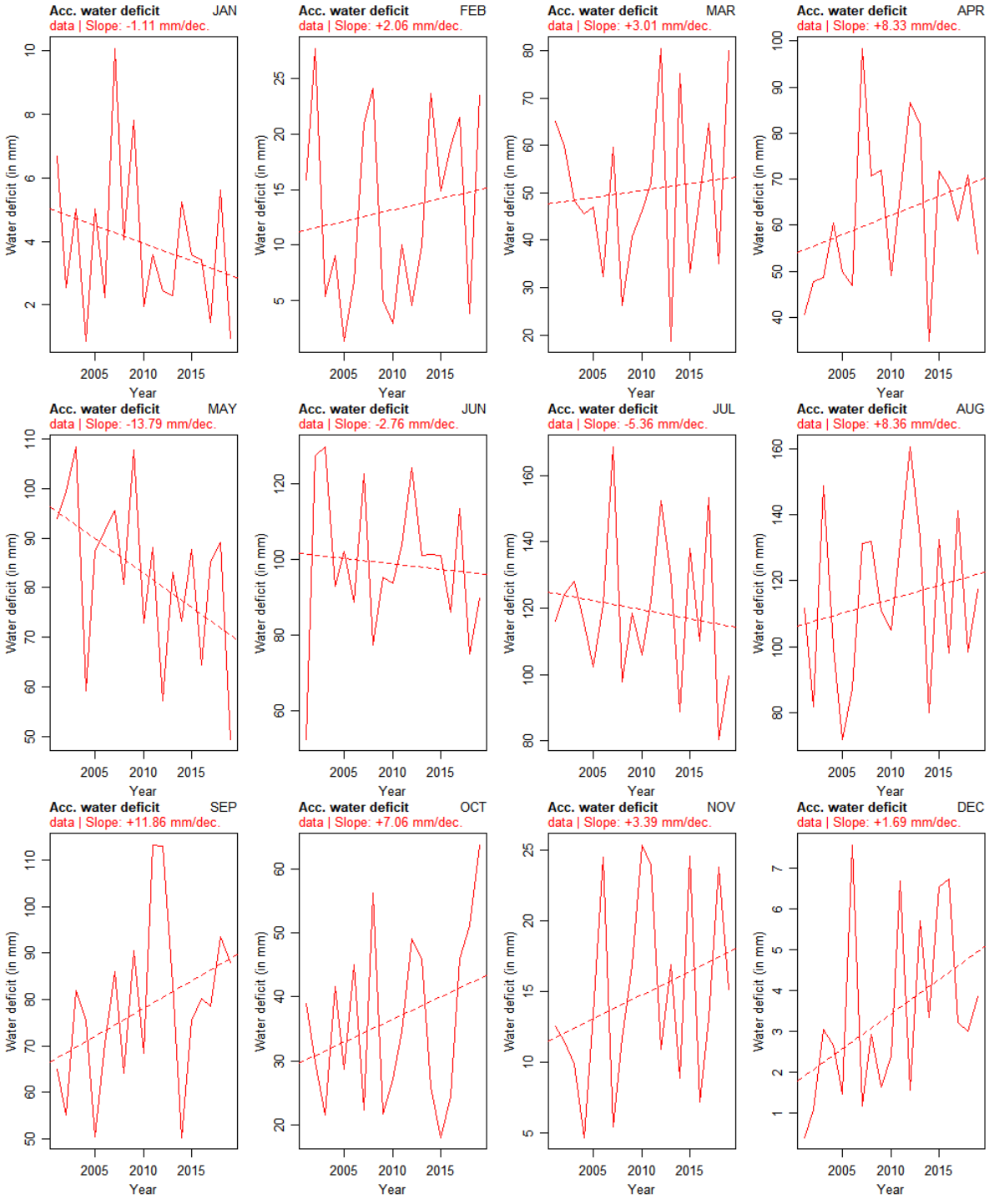

Snowfall and snow depth

Figure 113, Figure 114 and Table 39 provide an analysis of the historical monthly trends in snowfall and snow depth in the Republic of Serbia. The data reveals that most months have experienced a decrease in snowfall over time, with the largest decreases occurring in November, February, and December, at rates of -3.3 mm/decade, -2.6 mm/decade, and -0.9 mm/decade, respectively. However, there are two notable exceptions to this trend: January and March have seen an increase in snowfall, with rates of +2.2 mm/decade and +2.1 mm/decade, respectively.

Similarly, the analysis of historical trends in snow depth shows that most months have experienced a decrease over time, with the largest decreases occurring in February, March, and December, at rates of -19.5 mm/decade, -8 mm/decade, and -7.5 mm/decade, respectively. However, there is one exception to this trend: January has seen an increase in snow depth, with a rate of +2.5 mm/decade.

Table 39 – Characteristics of the trends from the historical time series of the monthly accumulated of frost days, ice days, and chill hours (linear models)
***In green**: Monthly accumulated frost days. **In blue:** monthly accumulated ice days. **In red:** monthly accumulated chill hours. Data source: ERA5, ECMWF / Copernicus Climate Change Service (Muñoz Sabater 2019).*

Variable	Month	Slope	p-value	Adjusted R^2	Average value in 1980	Average value in 2019
SnF	January	+2.22 mm/dec.	0.76	-0.05	25.59 mm	34.25 mm
SnF	February	-2.60 mm/dec.	0.77	-0.05	32.05 mm	21.89 mm
SnF	March	+2.07 mm/dec.	0.68	-0.05	5.95 mm	14.02 mm
SnF	April	-0.00 mm/dec.	1.00	-0.06	1.22 mm	1.22 mm
SnF	May	-0.02 mm/dec.	0.37	-0.01	0.07 mm	0.00 mm
SnF	June	-0.04 mm/dec.	0.43	-0.02	0.14 mm	-0.01 mm
SnF	July	+0.00 mm/dec.	NA	NA	0.00 mm	0.00 mm
SnF	August	-0.00 mm/dec.	0.56	-0.04	0.00 mm	0.00 mm
SnF	September	-0.00 mm/dec.	0.65	-0.04	0.01 mm	0.00 mm
SnF	October	-0.63 mm/dec.	0.33	0.00	2.72 mm	0.26 mm
SnF	November	-3.28 mm/dec.	0.25	0.02	16.70 mm	3.92 mm
SnF	December	-0.85 mm/dec.	0.88	-0.05	23.53 mm	20.20 mm
SnD	January	+2.53 mm/dec.	0.90	-0.05	82.13 mm	91.99 mm
SnD	February	-19.53 mm/dec.	0.70	-0.05	155.50 mm	79.31 mm
SnD	March	-7.97 mm/dec.	0.59	-0.04	55.12 mm	24.05 mm
SnD	April	-0.91 mm/dec.	0.11	0.09	4.26 mm	0.71 mm
SnD	May	-0.05 mm/dec.	0.01	0.27	0.23 mm	0.02 mm
SnD	June	-0.02 mm/dec.	0.30	0.01	0.10 mm	0.01 mm
SnD	July	+0.00 mm/dec.	0.42	-0.02	0.00 mm	0.01 mm
SnD	August	+0.00 mm/dec.	0.28	0.01	0.00 mm	0.01 mm
SnD	September	-0.01 mm/dec.	0.43	-0.02	0.05 mm	0.01 mm
SnD	October	-0.37 mm/dec.	0.33	0.00	1.70 mm	0.27 mm
SnD	November	-4.08 mm/dec.	0.18	0.05	18.77 mm	2.86 mm
SnD	December	-7.54 mm/dec.	0.58	-0.04	61.87 mm	32.46 mm

Figure 113 – Historical time series of the monthly average NDVI

Time series over 2001-2019 period. Data source: MODIS - NASA LP DAAC (Myneni, Knyazikhin, and Park 2015).

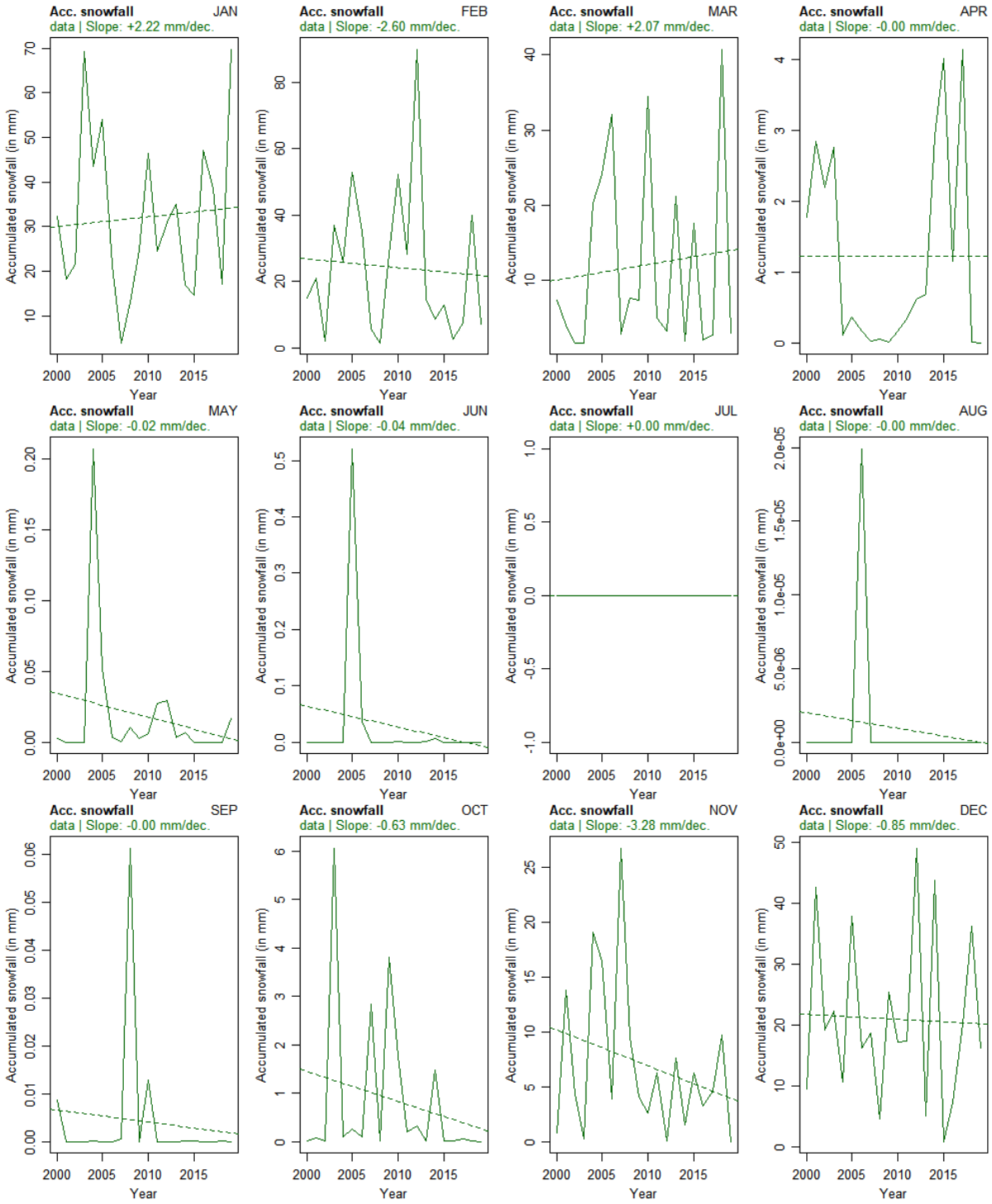

Figure 114 – Historical time series of the monthly average NDVI

Time series over 2001-2019 period. Data source: MODIS - NASA LP DAAC (Myneni, Knyazikhin, and Park 2015).

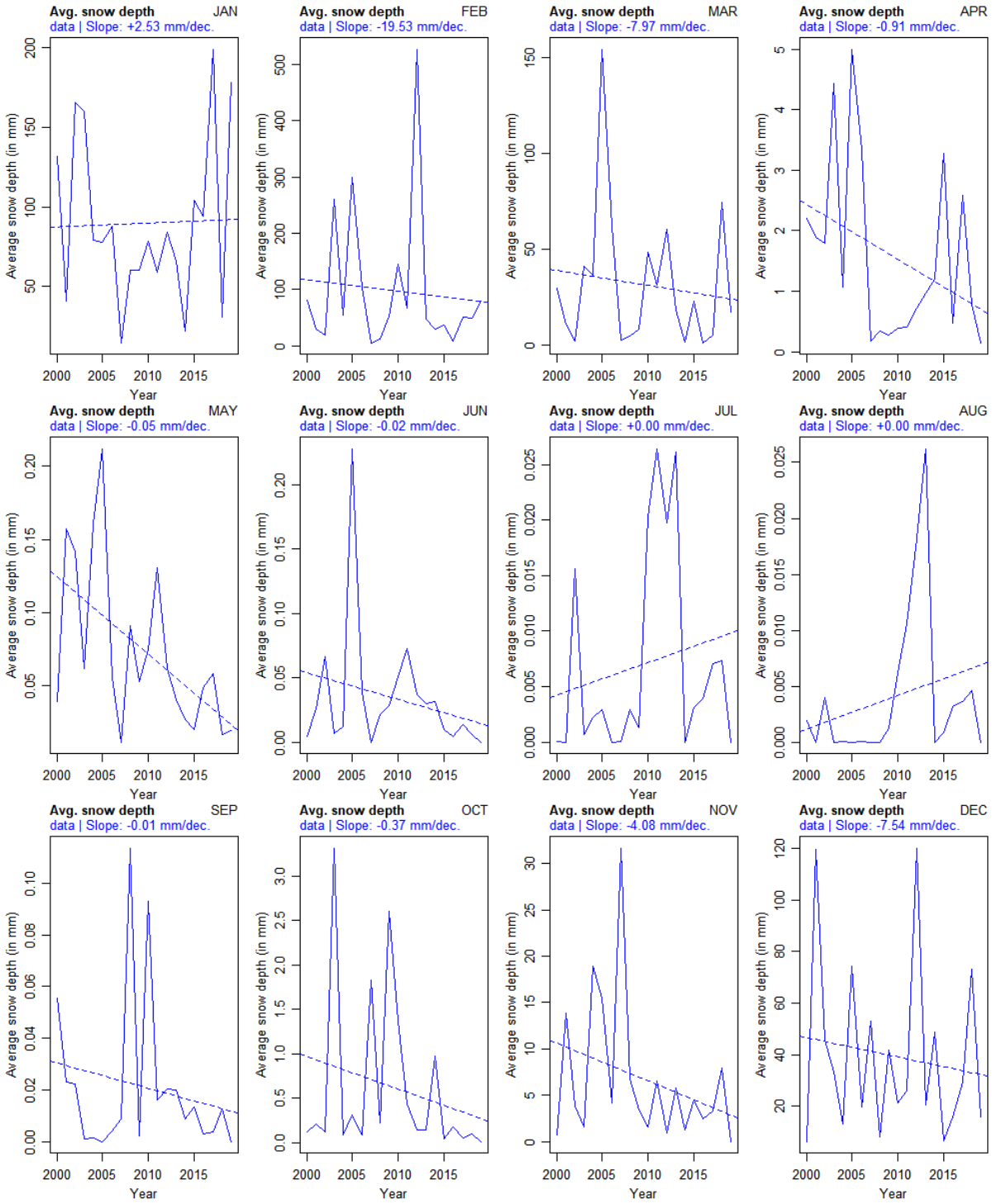

NDVI & LAI

in Figure 115, Figure 116 and Table 40 present the monthly trends of NDVI and LAI in the Republic of Serbia over time. The analysis reveals that NDVI shows a clear temporal dichotomy in its evolution. From November to July, NDVI tends to increase, with the largest increases occurring in December (+1049/decade), February (+446/decade), and January (+387/decade). However, from August to October, NDVI decreases, likely due to water stress at the end of the growth season.

On the other hand, LAI shows a more consistent increase over time. Most months have experienced an increase in LAI, with the largest increases occurring in April (+2.8/decade), June (+2.4/decade), and July (+2.0/decade).

Table 40 – Characteristics of the trends from the historical time series of the monthly accumulated of frost days, ice days, and chill hours (linear models)
***In green**: Monthly accumulated frost days. **In blue:** monthly accumulated ice days. **In red:** monthly accumulated chill hours. Data source: ERA5, ECMWF / Copernicus Climate Change Service (Muñoz Sabater 2019).*

Variable	Month	Slope	p-value	Adjusted R^2	Average value in 1980	Average value in 2019
NDVI	January	+387.06/dec.	0.35	0.00	1537.23	3046.76
NDVI	February	+446.29/dec.	0.33	0.00	1365.71	3106.23
NDVI	March	+295.53/dec.	0.27	0.02	3095.84	4248.39
NDVI	April	+329.11/dec.	0.10	0.10	4649.23	5932.74
NDVI	May	+146.53/dec.	0.00	0.36	6619.71	7191.18
NDVI	June	+285.93/dec.	0.00	0.53	6463.84	7578.98
NDVI	July	+133.85/dec.	0.36	-0.01	6876.48	7398.51
NDVI	August	-162.64/dec.	0.44	-0.02	7337.28	6702.98
NDVI	September	-223.04/dec.	0.23	0.03	6846.12	5976.26
NDVI	October	-199.82/dec.	0.28	0.01	5984.04	5204.74
NDVI	November	+56.54/dec.	0.74	-0.05	4321.91	4542.43
NDVI	December	+1049.08/dec.	0.00	0.37	148.03	4239.45
LAI	January	+0.26/dec.	0.31	0.01	1.48	2.50
LAI	February	+0.44/dec.	0.33	0.00	1.28	3.00
LAI	March	+0.59/dec.	0.32	0.00	3.91	6.20
LAI	April	+2.80/dec.	0.04	0.18	4.77	15.68
LAI	May	+0.90/dec.	0.33	0.00	22.35	25.87
LAI	June	+2.37/dec.	0.01	0.33	22.64	31.88
LAI	July	+2.06/dec.	0.02	0.24	23.92	31.95
LAI	August	+1.41/dec.	0.25	0.02	22.88	28.39
LAI	September	+0.29/dec.	0.77	-0.05	17.55	18.67
LAI	October	-0.33/dec.	0.57	-0.04	9.93	8.65
LAI	November	+0.24/dec.	0.28	0.01	3.92	4.87
LAI	December	+0.97/dec.	0.00	0.39	-0.15	3.64

Figure 115 – Historical time series of the monthly average NDVI

Time series over 2001-2019 period. Data source: MODIS - NASA LP DAAC (Myneni, Knyazikhin, and Park 2015).

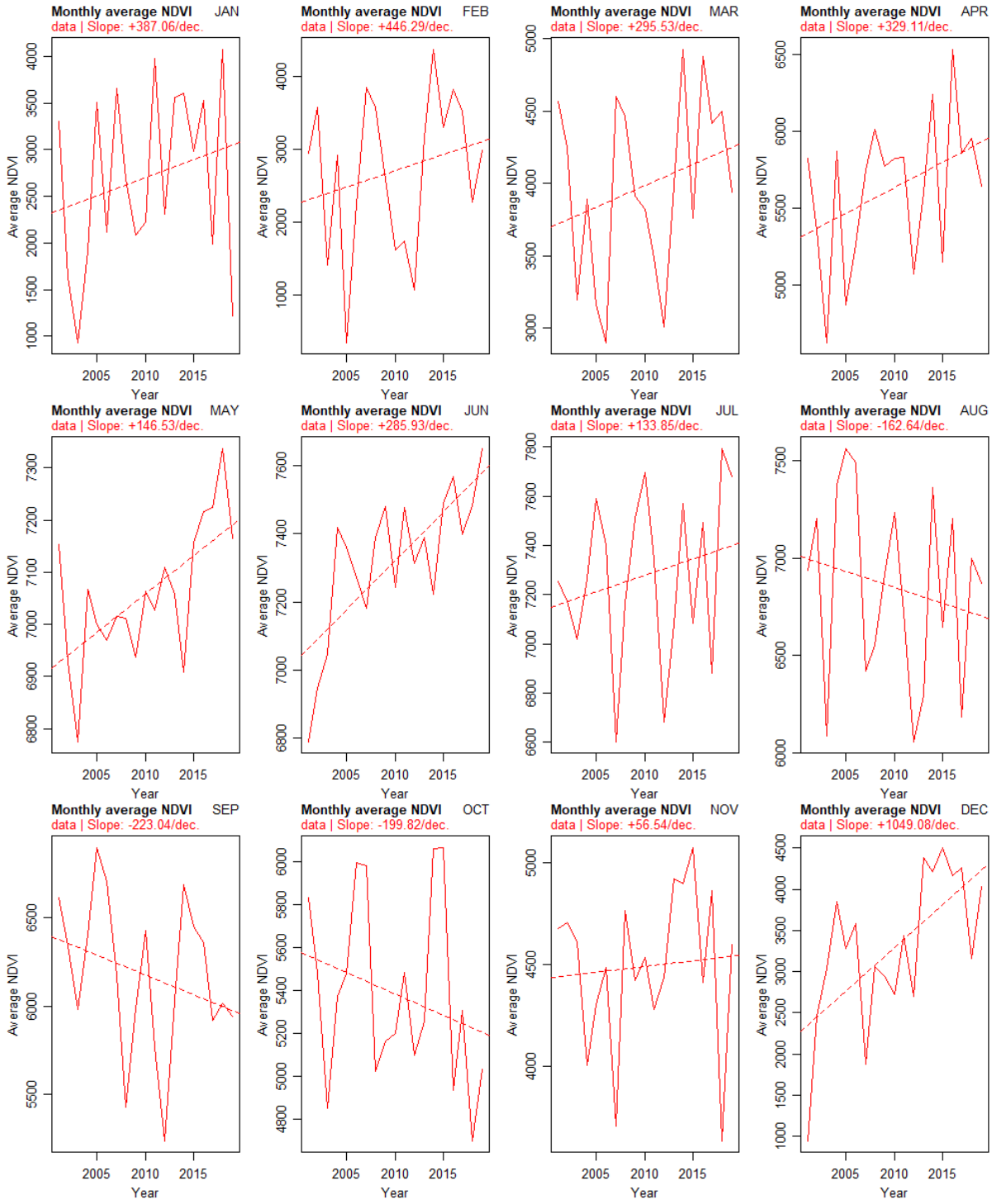

Figure 116 – Historical time series of the monthly average LAI

Time series over 2001-2019 period. Data source: MODIS - NASA LP DAAC (Didan 2015).

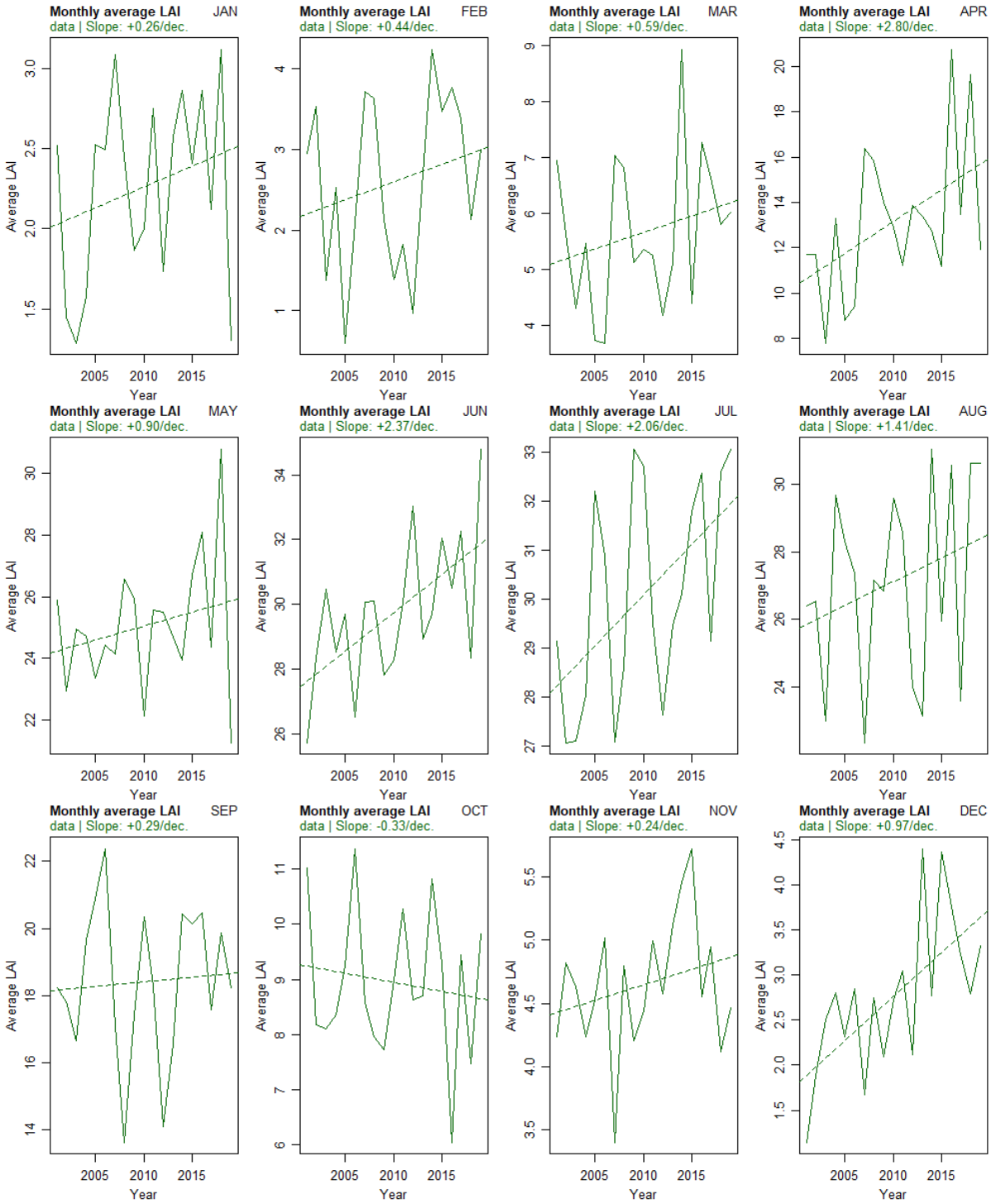

MODELLED DATA VALIDATION

Average temperature

Figure 117 – Validation of monthly modeled data against monthly historical data for average temperature *Overlap period: 2006-2019.* ***Green dots and line****: validation points for the median model of the NEX database under the RCP 4.5 scenario, and corresponding linear regression line.* ***Green dots and line****: validation points for the median model of the NEX database under the RCP 8.5 scenario, and corresponding linear regression line.* ***Green plume:*** *multi-model value range of the NEX database under the RCP 4.5 scenario.* ***Orange plume:*** *multi-model value range of the NEX database under the RCP 8.5 scenario.* ***Black dashed line:*** *1:1 line. Data source: Republic Hydrometeorological Service of Serbia, HidMet (Republic Hydrometeorological Service of Serbia 2020) and NASA Earth Exchange - Global Daily Downscaled Climate Projections (NEX – GDDP) (Thrasher et al. 2012).*

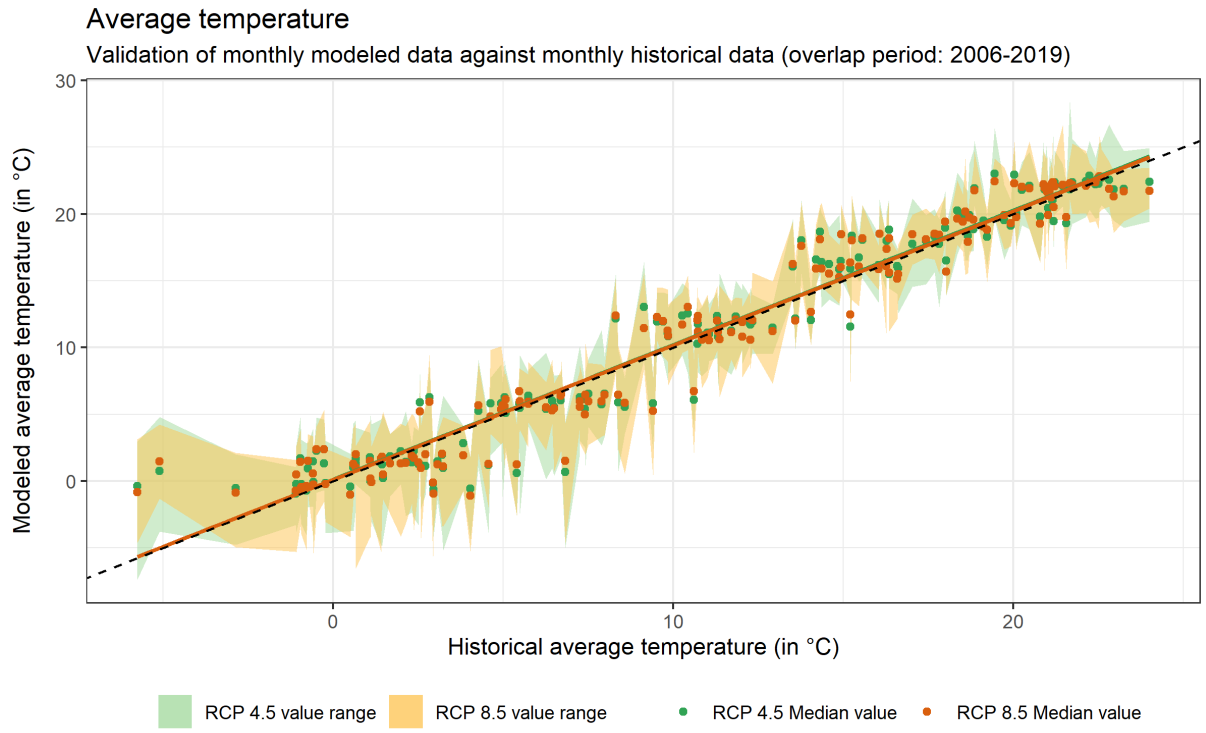

Table 41 – Validation metadata of the monthly modeled data against monthly historical data for average temperature

Data source: Republic Hydrometeorological Service of Serbia, HidMet (Republic Hydrometeorological Service of Serbia 2020) and NASA Earth Exchange - Global Daily Downscaled Climate Projections (NEX – GDDP) (Thrasher et al. 2012).

Scenario	RMSE	NRMSE	MAE	Adjusted R^2
RCP 4.5	1.87°C	0.24	1.38°C	0.95
RCP 8.5	1.83°C	0.24	1.40°C	0.95

The median models of the NEX ensemble are an excellent match for the observed HidMet average temperature data under both scenarios. The corresponding root mean square error (RMSE) and mean absolute error (MAE) values are notably low, and the normalized RMSE (NRMSE) is less than 0.25, which indicates that the RMSE is less than 25% of the standard deviation of the observed data. Therefore, we can conclude that the median models of the NEX ensemble are suitable for projecting average temperature in Serbia.

Maximum temperature

Figure 118 – Validation of monthly modeled data against monthly historical data for maximum temperature *Overlap period: 2006-2019.* ***Green dots and line****: validation points for the median model of the NEX database under the RCP 4.5 scenario, and corresponding linear regression line.* ***Green dots and line****: validation points for the median model of the NEX database under the RCP 8.5 scenario, and corresponding linear regression line.* ***Green plume:*** *multi-model value range of the NEX database under the RCP 4.5 scenario.* ***Orange plume:*** *multi-model value range of the NEX database under the RCP 8.5 scenario.* ***Black dashed line:*** *1:1 line. Data source: Republic Hydrometeorological Service of Serbia, HidMet (Republic Hydrometeorological Service of Serbia 2020) and NASA Earth Exchange - Global Daily Downscaled Climate Projections (NEX – GDDP) (Thrasher et al. 2012).*

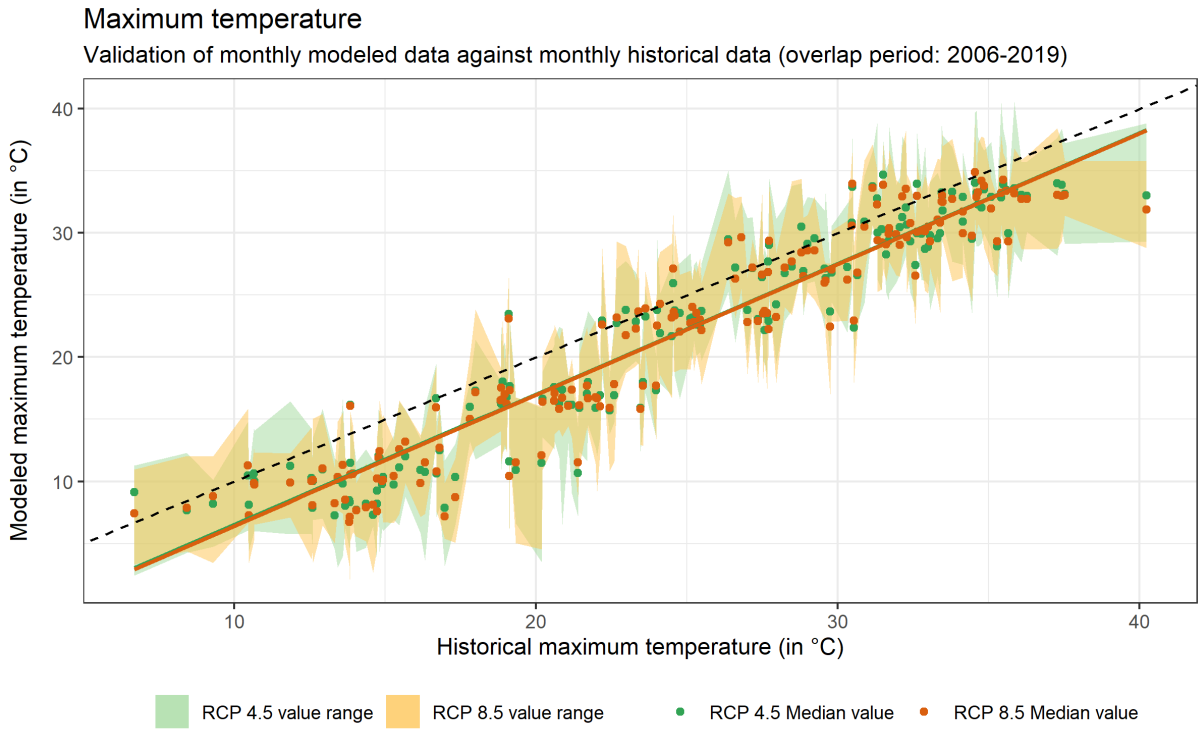

Table 42 – Validation metadata of the monthly modeled data against monthly historical data for maximum temperature

Data source: Republic Hydrometeorological Service of Serbia, HidMet (Republic Hydrometeorological Service of Serbia 2020) and NASA Earth Exchange - Global Daily Downscaled Climate Projections (NEX – GDDP) (Thrasher et al. 2012).

Scenario	RMSE	NRMSE	MAE	Adjusted R^2
RCP 4.5	3.84°C	0.49	3.16°C	0.91
RCP 8.5	3.88°C	0.49	3.19°C	0.91

The median models of the NEX ensemble are an excellent match for the observed HidMet maximum temperature data under both scenarios. The corresponding root mean square error and mean absolute error values are notably low, and the normalized RMSE (NRMSE) is less than 0.5, which indicates that the RMSE is less than 50% of the standard deviation of the observed data. Therefore, we can conclude that the median models of the NEX ensemble are suitable for projecting maximum temperature in Serbia.

Minimum temperature

Figure 119 – Validation of monthly modeled data against monthly historical data for minimum temperature *Overlap period: 2006-2019.* ***Green dots and line****: validation points for the median model of the NEX database under the RCP 4.5 scenario, and corresponding linear regression line.* ***Green dots and line****: validation points for the median model of the NEX database under the RCP 8.5 scenario, and corresponding linear regression line.* ***Green plume:*** *multi-model value range of the NEX database under the RCP 4.5 scenario.* ***Orange plume:*** *multi-model value range of the NEX database under the RCP 8.5 scenario.* ***Black dashed line:*** *1:1 line. Data source: Republic Hydrometeorological Service of Serbia, HidMet (Republic Hydrometeorological Service of Serbia 2020) and NASA Earth Exchange - Global Daily Downscaled Climate Projections (NEX – GDDP) (Thrasher et al. 2012).*

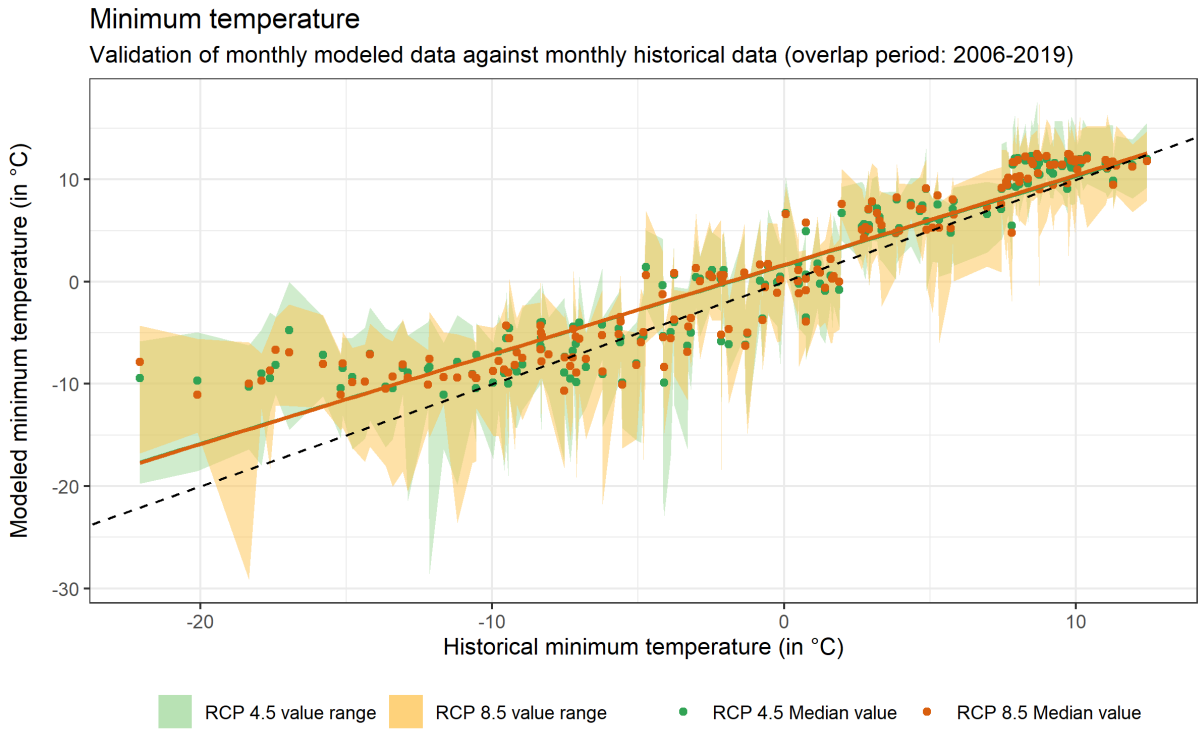

Table 43 – Validation metadata of the monthly modeled data against monthly historical data for minimum temperature

Data source: Republic Hydrometeorological Service of Serbia, HidMet (Republic Hydrometeorological Service of Serbia 2020) and NASA Earth Exchange - Global Daily Downscaled Climate Projections (NEX – GDDP) (Thrasher et al. 2012).

Scenario	RMSE	NRMSE	MAE	Adjusted R^2
RCP 4.5	3.45°C	0.41	2.63°C	0.87
RCP 8.5	3.43°C	0.41	2.61°C	0.87

The median models of the NEX ensemble are an excellent match for the observed HidMet minimum temperature data under both scenarios. The corresponding root mean square error and mean absolute error values are notably low, and the normalized RMSE (NRMSE) is close to 0.4, which indicates that the RMSE represents around 40% of the standard deviation of the observed data. Therefore, we can conclude that the median models of the NEX ensemble are suitable for projecting minimum temperature in Serbia.

Accumulated precipitation

Figure 120 – Validation of monthly modeled data against monthly historical data for accumulated precipitation *Overlap period: 2006-2019.* ***Green dots and line****: validation points for the median model of the NEX database under the RCP 4.5 scenario, and corresponding linear regression line.* ***Green dots and line****: validation points for the median model of the NEX database under the RCP 8.5 scenario, and corresponding linear regression line.* ***Green plume:*** *multi-model value range of the NEX database under the RCP 4.5 scenario.* ***Orange plume:*** *multi-model value range of the NEX database under the RCP 8.5 scenario.* ***Black dashed line:*** *1:1 line. Data source: Republic Hydrometeorological Service of Serbia, HidMet (Republic Hydrometeorological Service of Serbia 2020) and NASA Earth Exchange - Global Daily Downscaled Climate Projections (NEX – GDDP) (Thrasher et al. 2012).*

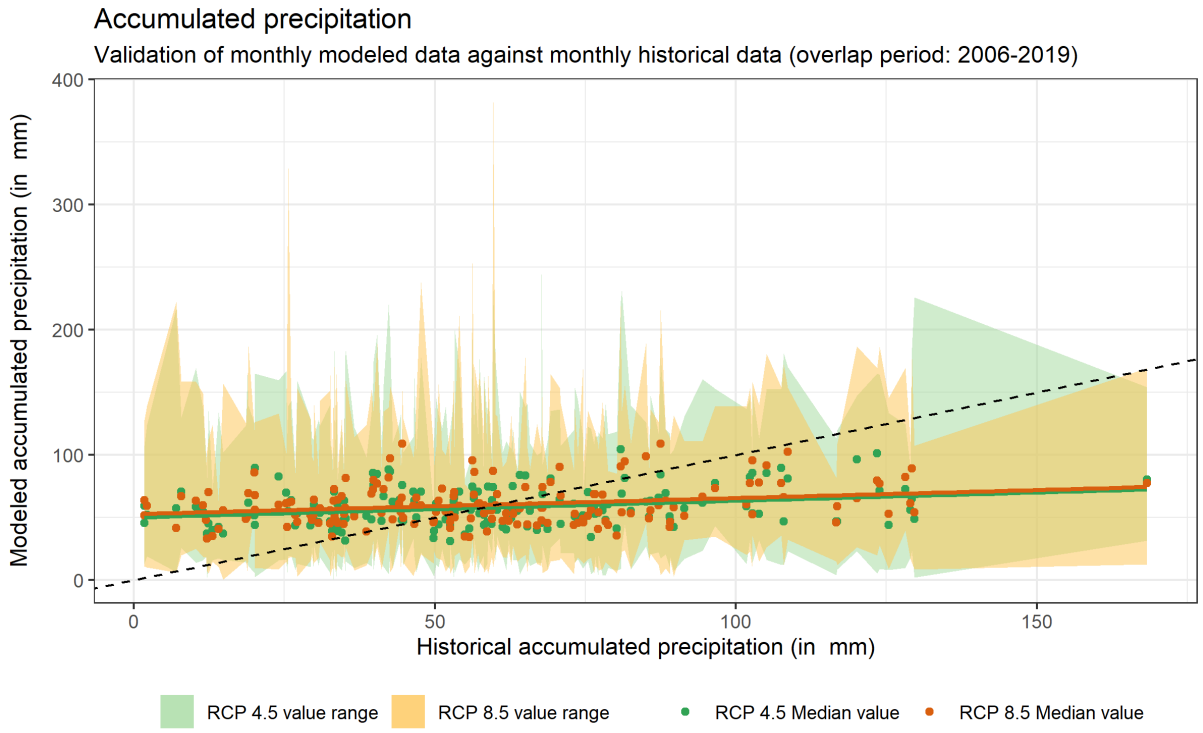

Table 44 – Validation metadata of the monthly modeled data against monthly historical data for accumulated precipitation

Data source: Republic Hydrometeorological Service of Serbia, HidMet (Republic Hydrometeorological Service of Serbia 2020) and NASA Earth Exchange - Global Daily Downscaled Climate Projections (NEX – GDDP) (Thrasher et al. 2012).

Scenario	RMSE	NRMSE	MAE	Adjusted R^2
RCP 4.5	30.56 mm	0.98	24.72 mm	0.07
RCP 8.5	31.01 mm	0.99	25.28 mm	0.06

The median models of the NEX ensemble do not provide a very good match for the observed HidMet accumulated precipitation data under both scenarios. The RMSE and MAE values are significantly high, and the normalized RMSE (NRMSE) is close to 1, which indicates that the RMSE is almost equal to the standard deviation of the observed data. Therefore, caution should be exercised when discussing the projected accumulated precipitation in Serbia.

Average precipitation intensity

Figure 121 – Validation of monthly modeled data against monthly historical data for accumulated precipitation *Overlap period: 2006-2019.* ***Green dots and line****: validation points for the median model of the NEX database under the RCP 4.5 scenario, and corresponding linear regression line.* ***Green dots and line****: validation points for the median model of the NEX database under the RCP 8.5 scenario, and corresponding linear regression line.* ***Green plume:*** *multi-model value range of the NEX database under the RCP 4.5 scenario.* ***Orange plume:*** *multi-model value range of the NEX database under the RCP 8.5 scenario.* ***Black dashed line:*** *1:1 line. Data source: Republic Hydrometeorological Service of Serbia, HidMet (Republic Hydrometeorological Service of Serbia 2020) and NASA Earth Exchange - Global Daily Downscaled Climate Projections (NEX – GDDP) (Thrasher et al. 2012).*

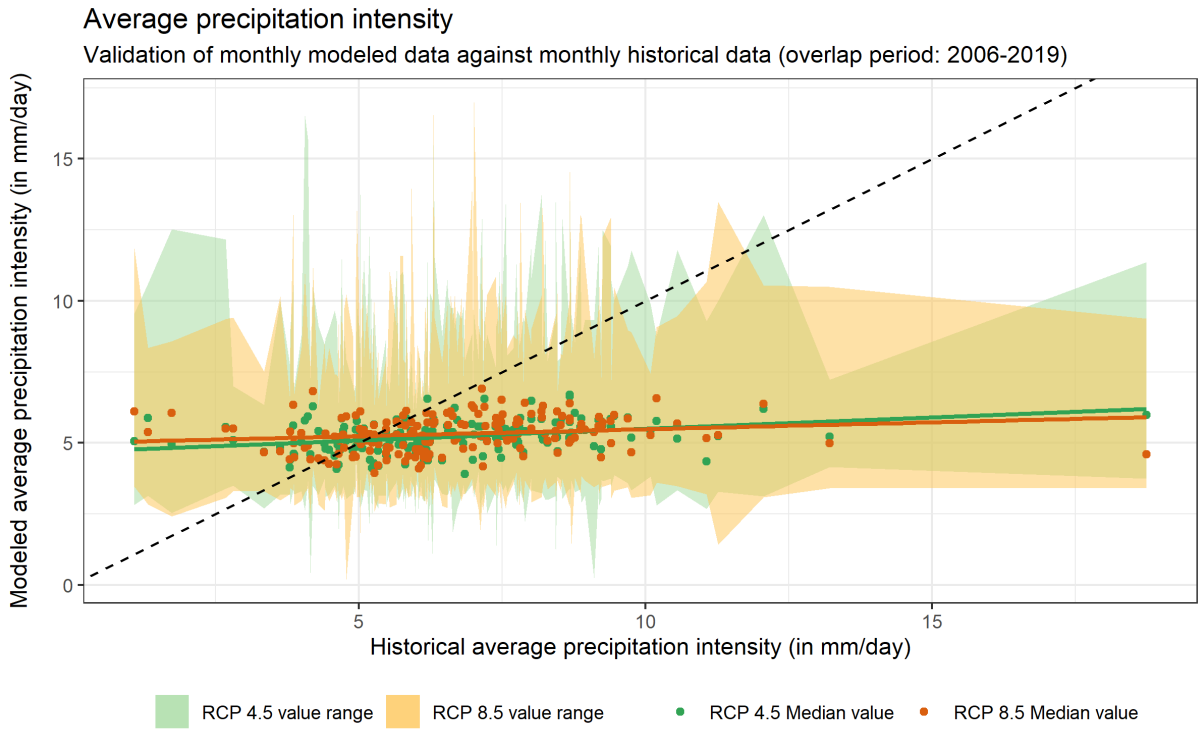

Table 45 – Validation metadata of the monthly modeled data against monthly historical data for accumulated precipitation

Data source: Republic Hydrometeorological Service of Serbia, HidMet (Republic Hydrometeorological Service of Serbia 2020) and NASA Earth Exchange - Global Daily Downscaled Climate Projections (NEX – GDDP) (Thrasher et al. 2012).

Scenario	RMSE	NRMSE	MAE	Adjusted R^2
RCP 4.5	2.51 mm/day	1.14	1.87 mm/day	0.1
RCP 8.5	2.53 mm/day	1.15	1.82 mm/day	0.02

The median models of the NEX ensemble do not provide a very good match for the observed HidMet average precipitation intensity data under both scenarios. The RMSE and MAE values are significantly high, and the normalized RMSE (NRMSE) is higher than 1, which indicates that the RMSE larger than the standard deviation of the observed data. Therefore, caution should be exercised when discussing the projected precipitation intensity in Serbia.

Accumulated frost days

Figure 122 – Validation of monthly modeled data against monthly historical data for accumulated frost days *Overlap period: 2006-2019.* ***Green dots and line****: validation points for the median model of the NEX database under the RCP 4.5 scenario, and corresponding linear regression line.* ***Green dots and line****: validation points for the median model of the NEX database under the RCP 8.5 scenario, and corresponding linear regression line.* ***Green plume:*** *multi-model value range of the NEX database under the RCP 4.5 scenario.* ***Orange plume:*** *multi-model value range of the NEX database under the RCP 8.5 scenario.* ***Black dashed line:*** *1:1 line. Data source: Republic Hydrometeorological Service of Serbia, HidMet (Republic Hydrometeorological Service of Serbia 2020) and NASA Earth Exchange - Global Daily Downscaled Climate Projections (NEX – GDDP) (Thrasher et al. 2012).*

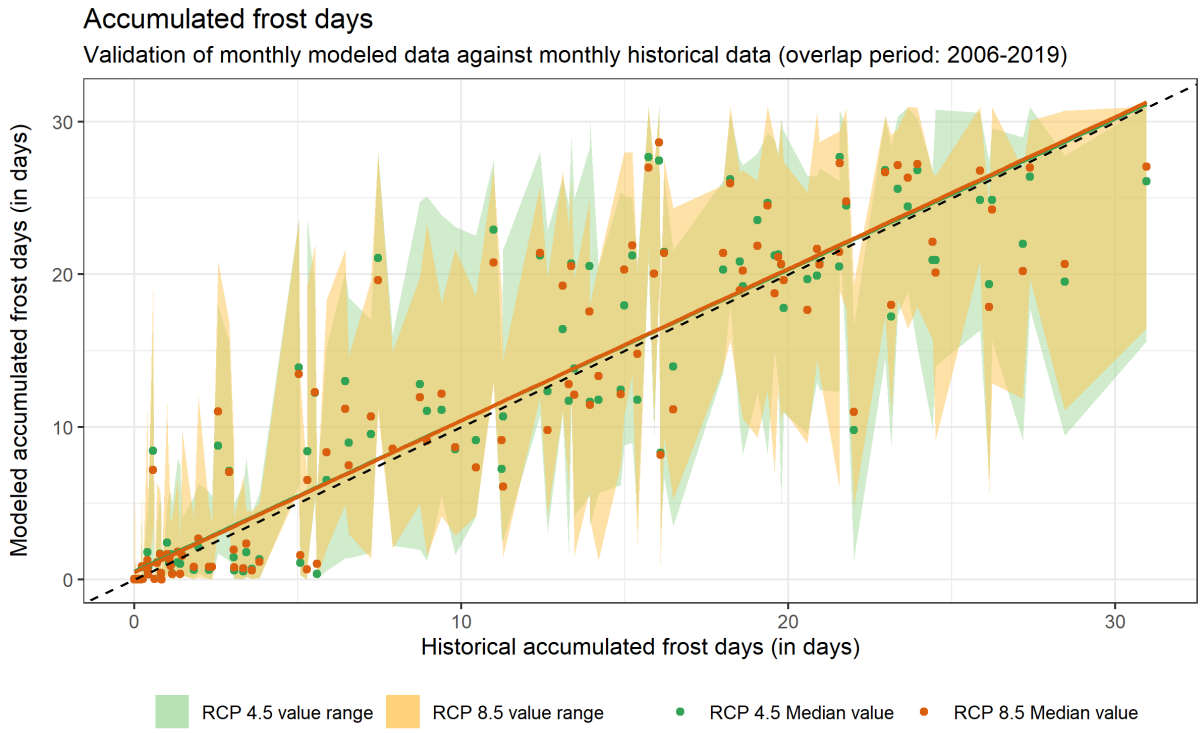

Table 46 – Validation metadata of the monthly modeled data against monthly historical data for accumulated frost days

Data source: Republic Hydrometeorological Service of Serbia, HidMet (Republic Hydrometeorological Service of Serbia 2020) and NASA Earth Exchange - Global Daily Downscaled Climate Projections (NEX – GDDP) (Thrasher et al. 2012).

Scenario	RMSE	NRMSE	MAE	Adjusted R^2
RCP 4.5	3.48 days	0.39	1.96 days	0.87
RCP 8.5	3.43 days	0.39	1.95 days	0.87

The median models of the NEX ensemble are an excellent match for the observed HidMet accumulated frost days data under both scenarios. The corresponding root mean square error and mean absolute error values are notably low, and the normalized RMSE (NRMSE) is lower than 0.4, which indicates that the RMSE represents less than 40% of the standard deviation of the observed data. Therefore, we can conclude that the median models of the NEX ensemble are suitable for projecting frost days in Serbia.

Accumulated ice days

Figure 123 – Validation of monthly modeled data against monthly historical data for accumulated ice days *Overlap period: 2006-2019.* ***Green dots and line****: validation points for the median model of the NEX database under the RCP 4.5 scenario, and corresponding linear regression line.* ***Green dots and line****: validation points for the median model of the NEX database under the RCP 8.5 scenario, and corresponding linear regression line.* ***Green plume:*** *multi-model value range of the NEX database under the RCP 4.5 scenario.* ***Orange plume:*** *multi-model value range of the NEX database under the RCP 8.5 scenario.* ***Black dashed line:*** *1:1 line. Data source: Republic Hydrometeorological Service of Serbia, HidMet (Republic Hydrometeorological Service of Serbia 2020) and NASA Earth Exchange - Global Daily Downscaled Climate Projections (NEX – GDDP) (Thrasher et al. 2012).*

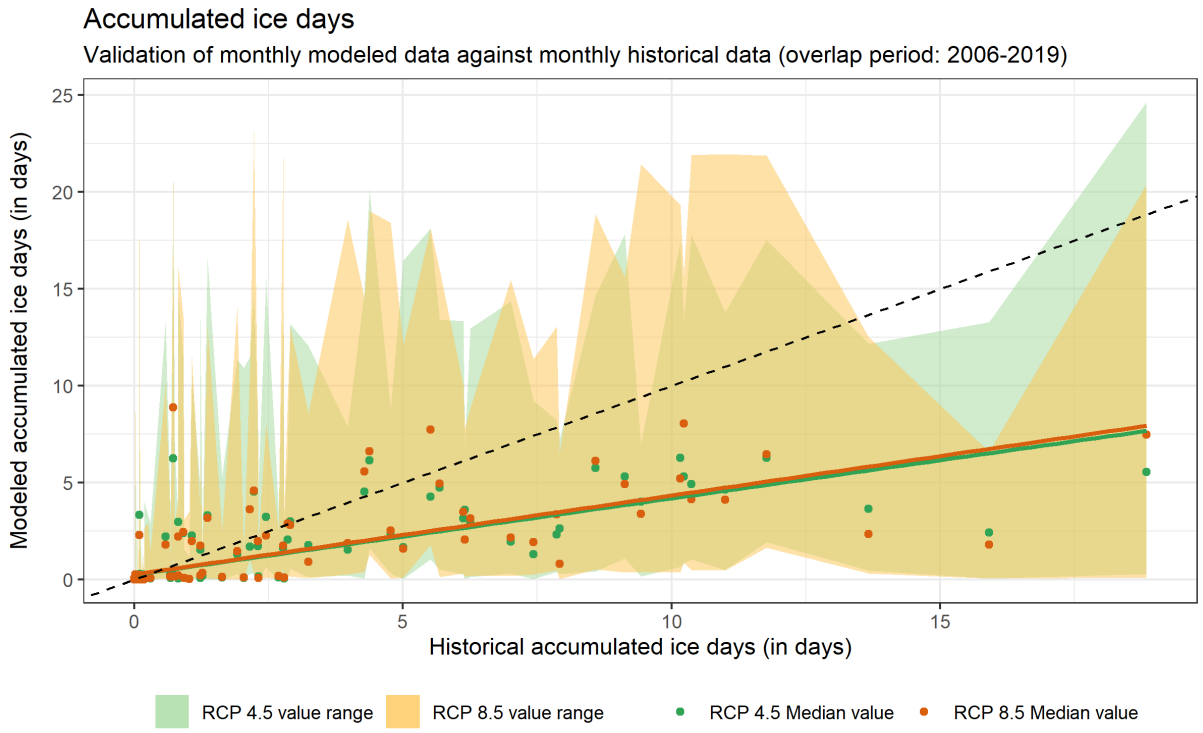

Table 47 – Validation metadata of the monthly modeled data against monthly historical data for accumulated ice days

Data source: Republic Hydrometeorological Service of Serbia, HidMet (Republic Hydrometeorological Service of Serbia 2020) and NASA Earth Exchange - Global Daily Downscaled Climate Projections (NEX – GDDP) (Thrasher et al. 2012).

Scenario	RMSE	NRMSE	MAE	Adjusted R^2
RCP 4.5	2.35 days	0.71	0.97 days	0.61
RCP 8.5	2.41 days	0.73	0.99 days	0.53

The median models of the NEX ensemble do not provide a very good match for the observed HidMet accumulated ice days data under both scenarios. The RMSE and MAE values are significantly high, and the normalized RMSE (NRMSE) is higher than 0.7, which indicates that the RMSE represents more than 70% the standard deviation of the observed data. Therefore, caution should be exercised when discussing the projected accumulated ice days in Serbia.

Accumulated chill hours

Figure 124 – Validation of monthly modeled data against monthly historical data for accumulated chill hours *Overlap period: 2006-2019.* ***Green dots and line****: validation points for the median model of the NEX database under the RCP 4.5 scenario, and corresponding linear regression line.* ***Green dots and line****: validation points for the median model of the NEX database under the RCP 8.5 scenario, and corresponding linear regression line.* ***Green plume:*** *multi-model value range of the NEX database under the RCP 4.5 scenario.* ***Orange plume:*** *multi-model value range of the NEX database under the RCP 8.5 scenario.* ***Black dashed line:*** *1:1 line. Data source: Republic Hydrometeorological Service of Serbia, HidMet (Republic Hydrometeorological Service of Serbia 2020) and NASA Earth Exchange - Global Daily Downscaled Climate Projections (NEX – GDDP) (Thrasher et al. 2012).*

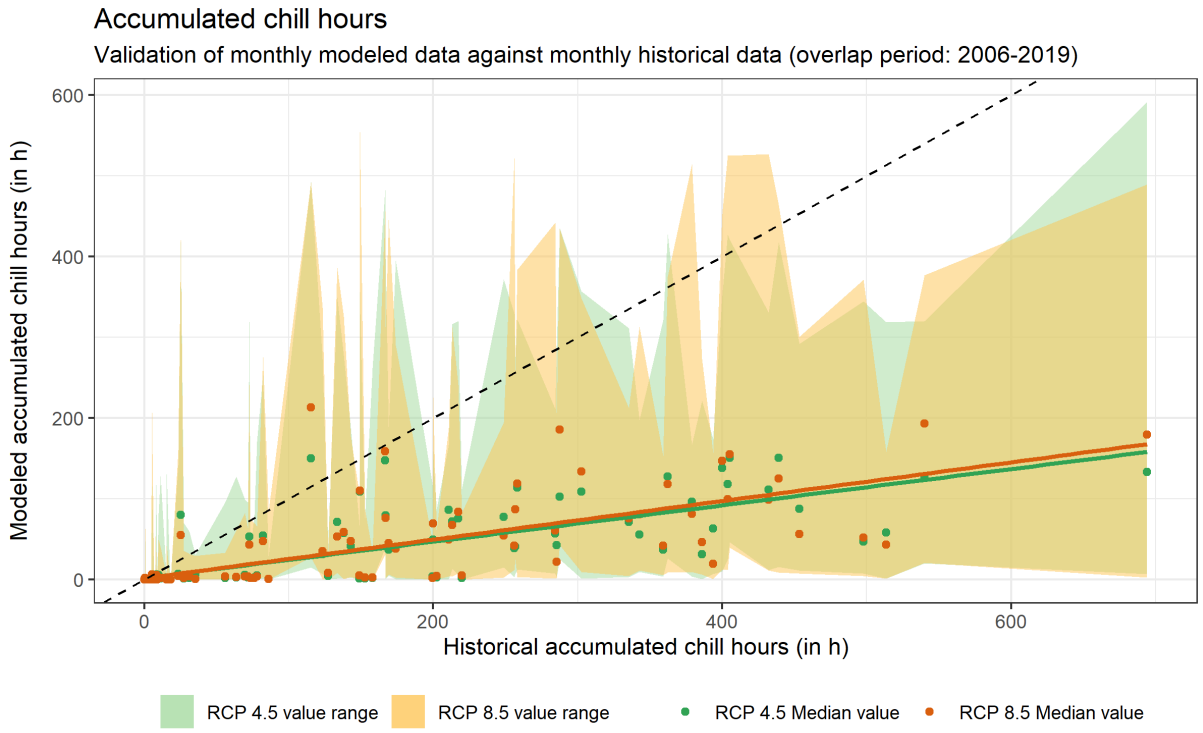

Table 48 – Validation metadata of the monthly modeled data against monthly historical data for accumulated chill hours

Data source: Republic Hydrometeorological Service of Serbia, HidMet (Republic Hydrometeorological Service of Serbia 2020) and NASA Earth Exchange - Global Daily Downscaled Climate Projections (NEX – GDDP) (Thrasher et al. 2012).

Scenario	RMSE	NRMSE	MAE	Adjusted R^2
RCP 4.5	128.96 h	0.91	64.10 h	0.65
RCP 8.5	127.73 h	0.9	63.67 h	0.59

The median models of the NEX ensemble do not provide a very good match for the observed HidMet accumulated chill hours data under both scenarios. The RMSE and MAE values are significantly high, and the normalized RMSE (NRMSE) is higher than 0.9, which indicates that the RMSE represents more than 90% the standard deviation of the observed data. Therefore, caution should be exercised when discussing the projected accumulated chill hours in Serbia.

Accumulated summer days

Figure 125 – Validation of monthly modeled data against monthly historical data for accumulated summer days

Overlap period: 2006-2019. ***Green dots and line****: validation points for the median model of the NEX database under the RCP 4.5 scenario, and corresponding linear regression line.* ***Green dots and line****: validation points for the median model of the NEX database under the RCP 8.5 scenario, and corresponding linear regression line.* ***Green plume:*** *multi-model value range of the NEX database under the RCP 4.5 scenario.* ***Orange plume:*** *multi-model value range of the NEX database under the RCP 8.5 scenario.* ***Black dashed line:*** *1:1 line. Data source: Republic Hydrometeorological Service of Serbia, HidMet (Republic Hydrometeorological Service of Serbia 2020) and NASA Earth Exchange - Global Daily Downscaled Climate Projections (NEX – GDDP) (Thrasher et al. 2012).*

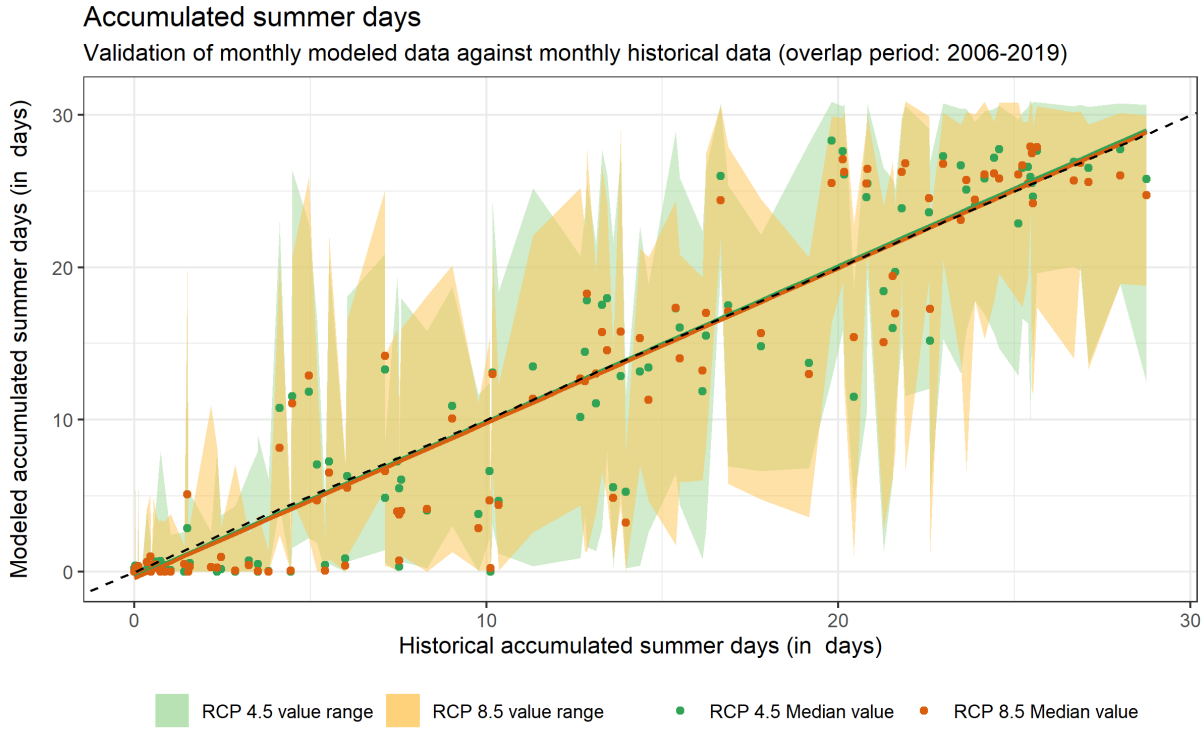

Table 49 – Validation metadata of the monthly modeled data against monthly historical data for accumulated summer days

Data source: Republic Hydrometeorological Service of Serbia, HidMet (Republic Hydrometeorological Service of Serbia 2020) and NASA Earth Exchange - Global Daily Downscaled Climate Projections (NEX – GDDP) (Thrasher et al. 2012).

Scenario	RMSE	NRMSE	MAE	Adjusted R^2
RCP 4.5	2.95 days	0.32	1.71 days	0.91
RCP 8.5	2.92 days	0.31	1.70 days	0.91

The median models of the NEX ensemble are an excellent match for the observed HidMet accumulated summer days data under both scenarios. The corresponding root mean square error and mean absolute error values are notably low, and the normalized RMSE (NRMSE) is close to 0.3, which indicates that the RMSE represents close to 30% of the standard deviation of the observed data. Therefore, we can conclude that the median models of the NEX ensemble are suitable for projecting accumulated summer days in Serbia.

Accumulated tropical nights

Figure 126 – Validation of monthly modeled data against monthly historical data for accumulated tropical nights

Overlap period: 2006-2019. ***Green dots and line****: validation points for the median model of the NEX database under the RCP 4.5 scenario, and corresponding linear regression line.* ***Green dots and line****: validation points for the median model of the NEX database under the RCP 8.5 scenario, and corresponding linear regression line.* ***Green plume:*** *multi-model value range of the NEX database under the RCP 4.5 scenario.* ***Orange plume:*** *multi-model value range of the NEX database under the RCP 8.5 scenario.* ***Black dashed line:*** *1:1 line. Data source: Republic Hydrometeorological Service of Serbia, HidMet (Republic Hydrometeorological Service of Serbia 2020) and NASA Earth Exchange - Global Daily Downscaled Climate Projections (NEX – GDDP) (Thrasher et al. 2012).*

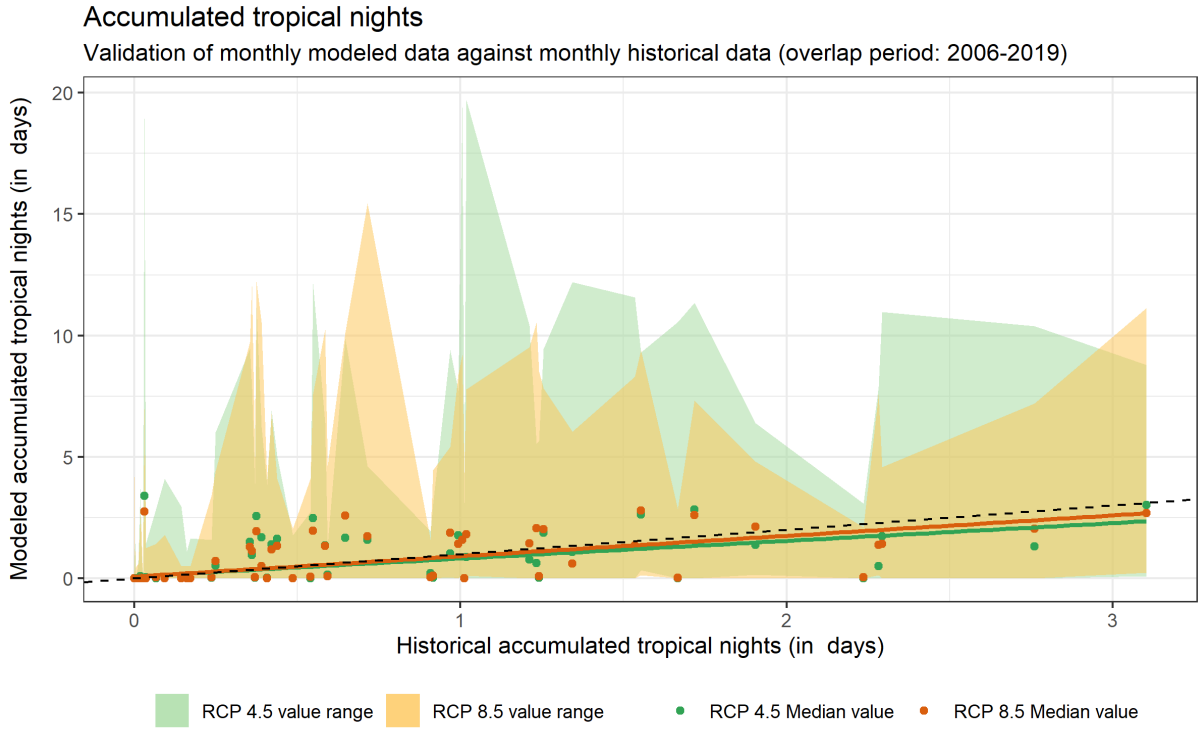

Table 50 – Validation metadata of the monthly modeled data against monthly historical data for accumulated tropical nights

Data source: Republic Hydrometeorological Service of Serbia, HidMet (Republic Hydrometeorological Service of Serbia 2020) and NASA Earth Exchange - Global Daily Downscaled Climate Projections (NEX – GDDP) (Thrasher et al. 2012).

Scenario	RMSE	NRMSE	MAE	Adjusted R^2
RCP 4.5	0.55 days	0.96	0.22 days	0.38
RCP 8.5	0.50 days	0.87	0.21 days	0.49

The median models of the NEX ensemble do not provide a very good match for the observed HidMet accumulated tropical nights data under both scenarios. The RMSE and MAE values are significantly high, and the normalized RMSE (NRMSE) is higher than 0.8, which indicates that the RMSE represents more than 80% the standard deviation of the observed data. Therefore, caution should be exercised when discussing the projected accumulated tropical nights in Serbia.

Accumulated degree days

Figure 127 – Validation of monthly modeled data against monthly historical data for accumulated degree days *Overlap period: 2006-2019.* ***Green dots and line****: validation points for the median model of the NEX database under the RCP 4.5 scenario, and corresponding linear regression line.* ***Green dots and line****: validation points for the median model of the NEX database under the RCP 8.5 scenario, and corresponding linear regression line.* ***Green plume:*** *multi-model value range of the NEX database under the RCP 4.5 scenario.* ***Orange plume:*** *multi-model value range of the NEX database under the RCP 8.5 scenario.* ***Black dashed line:*** *1:1 line. Data source: Republic Hydrometeorological Service of Serbia, HidMet (Republic Hydrometeorological Service of Serbia 2020) and NASA Earth Exchange - Global Daily Downscaled Climate Projections (NEX – GDDP) (Thrasher et al. 2012).*

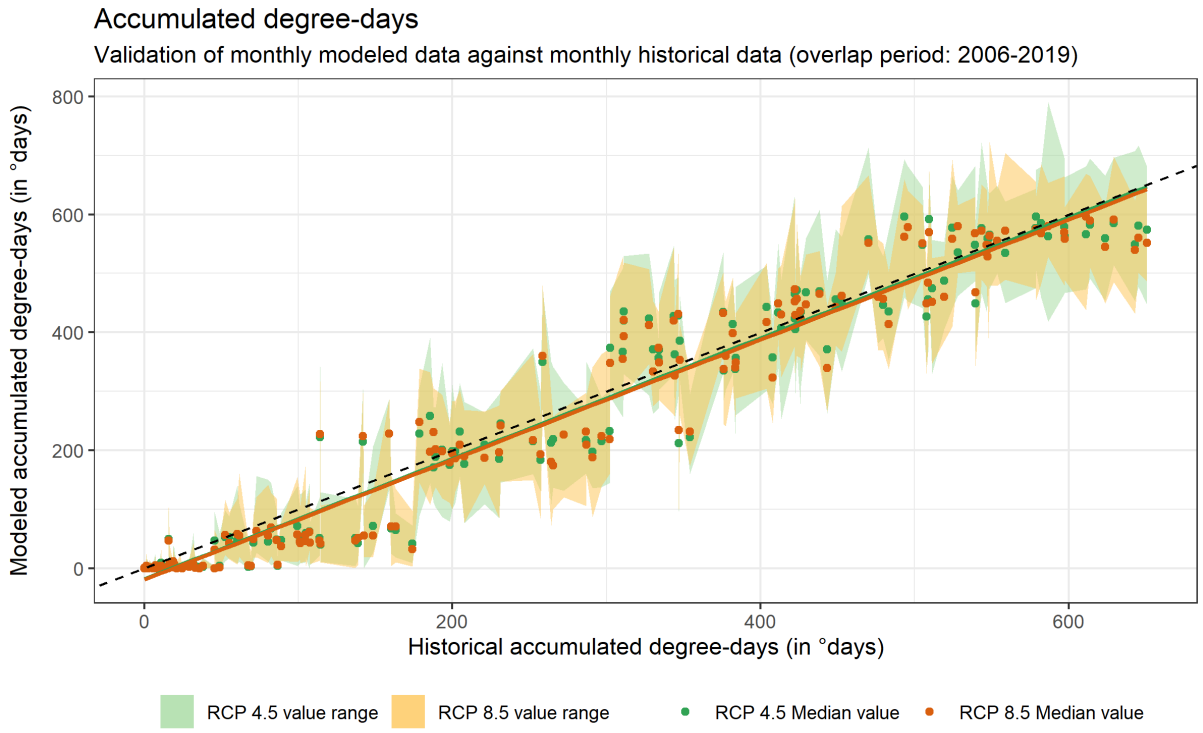

Table 51 – Validation metadata of the monthly modeled data against monthly historical data for accumulated degree days

Data source: Republic Hydrometeorological Service of Serbia, HidMet (Republic Hydrometeorological Service of Serbia 2020) and NASA Earth Exchange - Global Daily Downscaled Climate Projections (NEX – GDDP) (Thrasher et al. 2012).

Scenario	RMSE	NRMSE	MAE	Adjusted R^2
RCP 4.5	50.74°days	0.25	38.98°days	0.95
RCP 8.5	50.65°days	0.25	38.65°days	0.95

The median models of the NEX ensemble are an excellent match for the observed HidMet accumulated degree days data under both scenarios. The corresponding root mean square error (RMSE) and mean absolute error (MAE) values are notably low, and the normalized RMSE (NRMSE) is close to 0.25, which indicates that the RMSE represent close to 25% of the standard deviation of the observed data. Therefore, we can conclude that the median models of the NEX ensemble are suitable for projecting accumulated degree days in Serbia.

Accumulated wet days

Figure 128 – Validation of monthly modeled data against monthly historical data for accumulated wet days *Overlap period: 2006-2019.* ***Green dots and line****: validation points for the median model of the NEX database under the RCP 4.5 scenario, and corresponding linear regression line.* ***Green dots and line****: validation points for the median model of the NEX database under the RCP 8.5 scenario, and corresponding linear regression line.* ***Green plume:*** *multi-model value range of the NEX database under the RCP 4.5 scenario.* ***Orange plume:*** *multi-model value range of the NEX database under the RCP 8.5 scenario.* ***Black dashed line:*** *1:1 line. Data source: Republic Hydrometeorological Service of Serbia, HidMet (Republic Hydrometeorological Service of Serbia 2020) and NASA Earth Exchange - Global Daily Downscaled Climate Projections (NEX – GDDP) (Thrasher et al. 2012).*

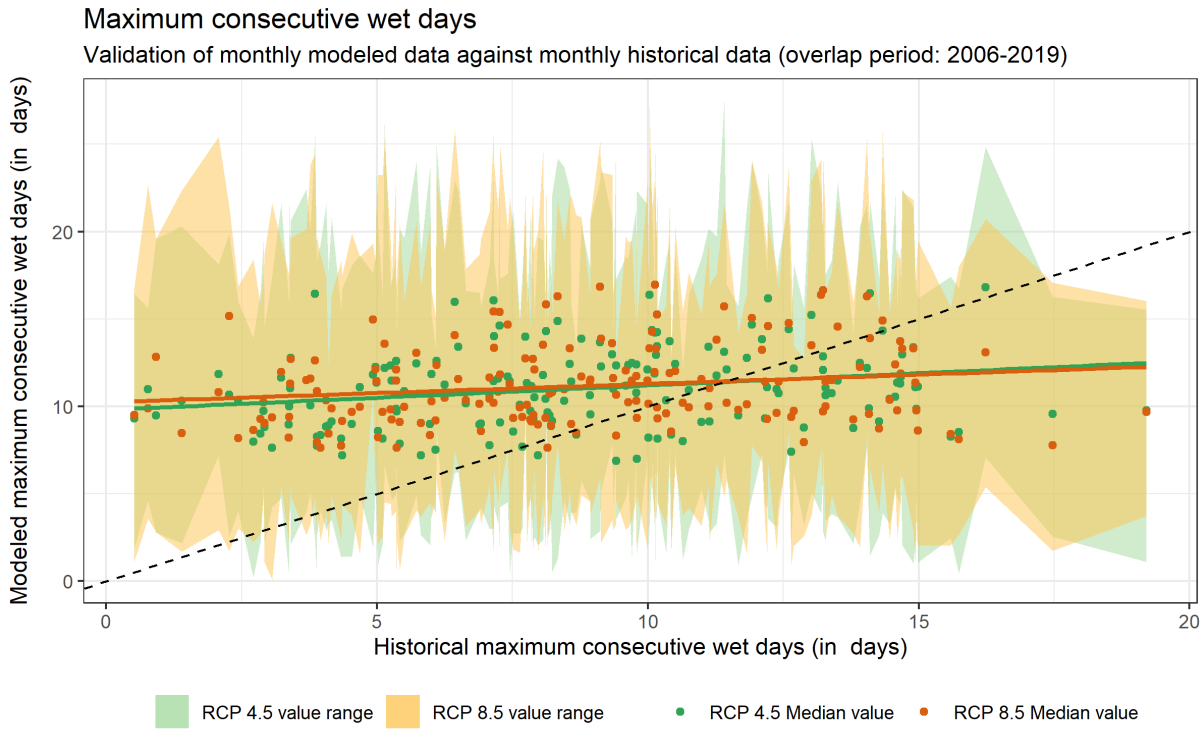

Table 52 – Validation metadata of the monthly modeled data against monthly historical data for accumulated wet days

Data source: Republic Hydrometeorological Service of Serbia, HidMet (Republic Hydrometeorological Service of Serbia 2020) and NASA Earth Exchange - Global Daily Downscaled Climate Projections (NEX – GDDP) (Thrasher et al. 2012).

Scenario	RMSE	NRMSE	MAE	Adjusted R^2
RCP 4.5	4.63 days	1.18	3.88 days	0.05
RCP 8.5	4.80 days	1.18	3.98 days	0.03

The median models of the NEX ensemble do not provide a very good match for the observed HidMet accumulated wet days data under both scenarios. The RMSE and MAE values are significantly high, and the normalized RMSE (NRMSE) is higher than 1, which indicates that the RMSE larger than the standard deviation of the observed data. Therefore, caution should be exercised when discussing the projected accumulated wet days in Serbia.

Accumulated very wet days

Figure 129 – Validation of monthly modeled data against monthly historical data for accumulated very wet days

Overlap period: 2006-2019. ***Green dots and line****: validation points for the median model of the NEX database under the RCP 4.5 scenario, and corresponding linear regression line.* ***Green dots and line****: validation points for the median model of the NEX database under the RCP 8.5 scenario, and corresponding linear regression line.* ***Green plume:*** *multi-model value range of the NEX database under the RCP 4.5 scenario.* ***Orange plume:*** *multi-model value range of the NEX database under the RCP 8.5 scenario.* ***Black dashed line:*** *1:1 line. Data source: Republic Hydrometeorological Service of Serbia, HidMet (Republic Hydrometeorological Service of Serbia 2020) and NASA Earth Exchange - Global Daily Downscaled Climate Projections (NEX – GDDP) (Thrasher et al. 2012).*

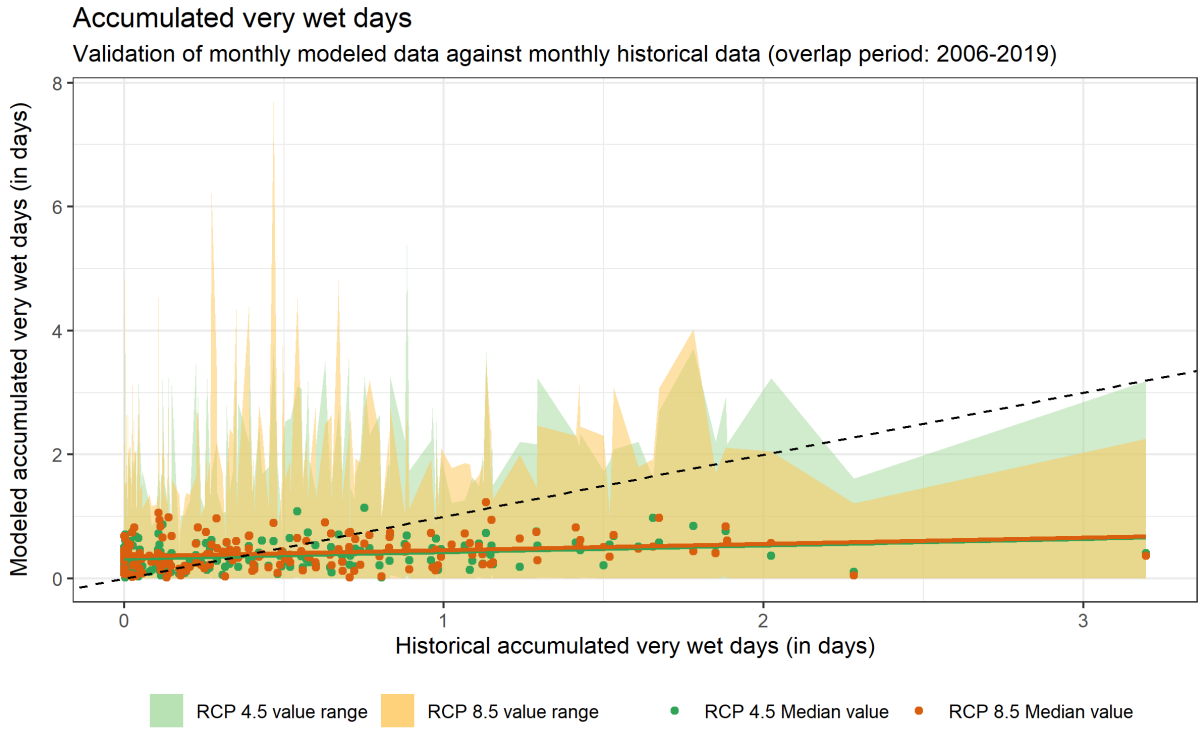

Table 53 – Validation metadata of the monthly modeled data against monthly historical data for accumulated very wet days

Data source: Republic Hydrometeorological Service of Serbia, HidMet (Republic Hydrometeorological Service of Serbia 2020) and NASA Earth Exchange - Global Daily Downscaled Climate Projections (NEX – GDDP) (Thrasher et al. 2012).

Scenario	RMSE	NRMSE	MAE	Adjusted R^2
RCP 4.5	0.56 days	1.01	0.40 days	0.07
RCP 8.5	0.57 days	1.03	0.41 days	0.04

The median models of the NEX ensemble do not provide a very good match for the observed HidMet accumulated very wet days data under both scenarios. The RMSE and MAE values are significantly high, and the normalized RMSE (NRMSE) is higher than 1, which indicates that the RMSE larger than the standard deviation of the observed data. Therefore, caution should be exercised when discussing the projected accumulated very wet days in Serbia.

Average duration of the longest dry spell

Figure 130 – Validation of monthly modeled data against monthly historical data for average duration of the longest dry spell

Overlap period: 2006-2019. ***Green dots and line****: validation points for the median model of the NEX database under the RCP 4.5 scenario, and corresponding linear regression line.* ***Green dots and line****: validation points for the median model of the NEX database under the RCP 8.5 scenario, and corresponding linear regression line.* ***Green plume:*** *multi-model value range of the NEX database under the RCP 4.5 scenario.* ***Orange plume:*** *multi-model value range of the NEX database under the RCP 8.5 scenario.* ***Black dashed line:*** *1:1 line. Data source: Republic Hydrometeorological Service of Serbia, HidMet (Republic Hydrometeorological Service of Serbia 2020) and NASA Earth Exchange - Global Daily Downscaled Climate Projections (NEX – GDDP) (Thrasher et al. 2012).*

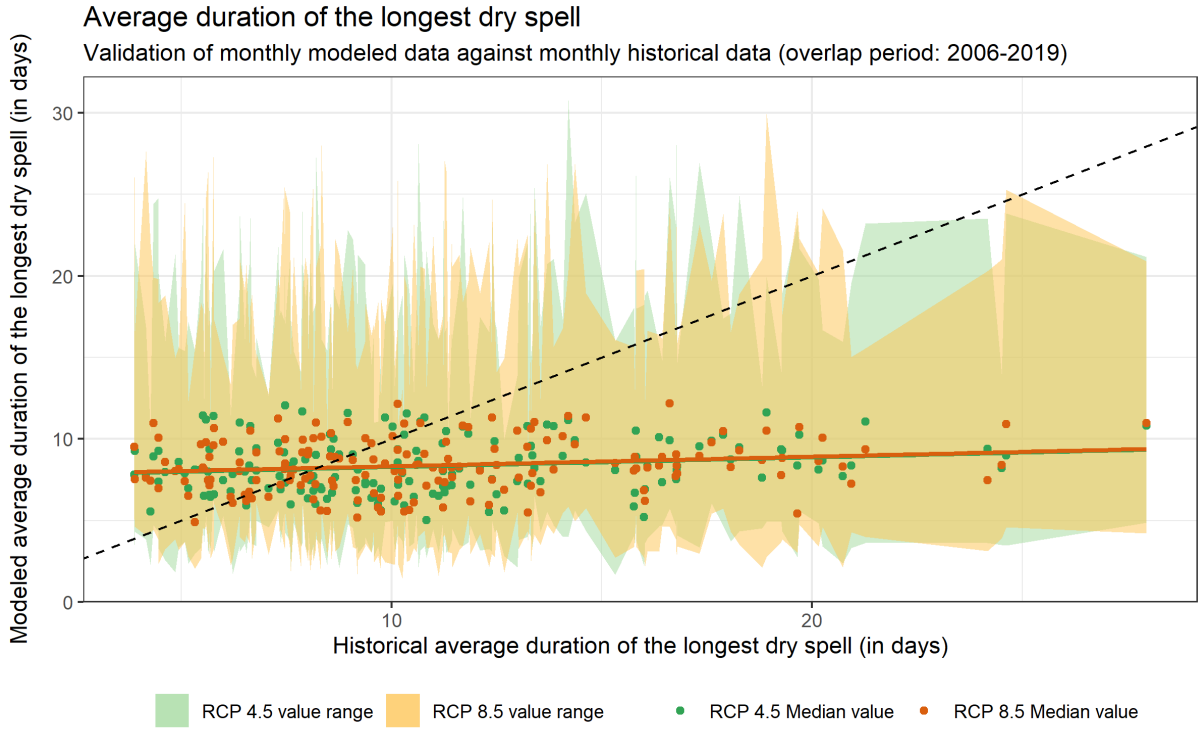

Table 54 – Validation metadata of the monthly modeled data against monthly historical data for average duration of the longest dry spell

Data source: Republic Hydrometeorological Service of Serbia, HidMet (Republic Hydrometeorological Service of Serbia 2020) and NASA Earth Exchange - Global Daily Downscaled Climate Projections (NEX – GDDP) (Thrasher et al. 2012).

Scenario	RMSE	NRMSE	MAE	Adjusted R^2
RCP 4.5	5.50 days	1.14	4.20 days	0.02
RCP 8.5	5.47 days	1.13	4.09 days	0.03

The median models of the NEX ensemble do not provide a very good match for the observed HidMet average duration of the longest dry spell data under both scenarios. The RMSE and MAE values are significantly high, and the normalized RMSE (NRMSE) is higher than 1, which indicates that the RMSE larger than the standard deviation of the observed data. Therefore, caution should be exercised when discussing the projected average duration of the longest dry spell in Serbia.

BIBLIOGRAPHY

Buchhorn, Marcel, Bruno Smets, Luc Bertels, Myroslava Lesiv, Nandin-Erdene Tsendbazar, D. Masiliunas, L. Linlin, Martin Herold, and S. Fritz. 2020. 'Copernicus Global Land Service: Land Cover 100m: Collection 3: Epoch 2015: Globe (Version V3.0.1)'. *Zenodo*, 1–14.

Center for International Earth Science Information Network - CIESIN - Columbia University. 2018. 'Gridded Population of the World, Version 4 (GPWv4): Population Density Adjusted to Match 2015 Revision UN WPP Country Totals, Revision 11'. Palisades, NY: NASA Socioeconomic Data and Applications Center (SEDAC).

Didan, K. 2015. 'MOD13A1 MODIS/Terra Vegetation Indices 16-Day L3 Global 500m SIN Grid V006'. Distributed by NASA EOSDIS Land Processes DAAC. 2015. https://doi.org/10.5067/MODIS/MOD13A1.006. Accessed 2021-06-24.

Ellenberg, H. 1988. 'Vegetation Ecology of Central Europe. Fourth Edition'. *Vegetation Ecology of Central Europe. Fourth Edition*.

European Commission Joint Research Centre. n.d. 'European Soil Data Centre (ESDAC)'. Accessed 21 March 2021. esdac.jrc.ec.europa.eu.

European Environmnet Agency (EEA). 2020. 'Copernicus Land Monitoring Service 2020'. 2020. https://land.copernicus.eu/global/.

Farr, Tom G., Paul A. Rosen, Edward Caro, Robert Crippen, Riley Duren, Scott Hensley, Michael Kobrick, et al. 2007. 'The Shuttle Radar Topography Mission'. *Reviews of Geophysics* 45 (2). https://doi.org/10.1029/2005RG000183.

Führer, Erno, László Horváth, Anikó Jagodics, Attila Machon, and Ildikó Szabados. 2011. 'Application of a New Aridity Index in Hungarian Forestry Practice'. *Idojaras* 115 (3): 205–16.

Hansen, M C, P. V. Potapov, R. Moore, M. Hancher, S. A. Turubanova, A. Tyukavina, D. Thau, et al. 2013. 'High-Resolution Global Maps of 21st-Century Forest Cover Change'. *Science* 342 (6160): 850–53. https://doi.org/10.1126/science.1244693.

Hengl, Tomislav. 2018. 'Sand Content in % (Kg / Kg) at 6 Standard Depths (0, 10, 30, 60, 100 and 200 Cm) at 250 m Resolution', December. https://doi.org/10.5281/ZENODO.2525662.

Hengl, Tomislav, and Surya Gupta. 2019. 'Soil Water Content (Volumetric %) for 33kPa and 1500kPa Suctions Predicted at 6 Standard Depths (0, 10, 30, 60, 100 and 200 Cm) at 250 m Resolution', April. https://doi.org/10.5281/ZENODO.2784001.

Miletić, Boban, Saša Orlović, Branislava Lalić, Vladimir Đurđević, Mirjam Vujadinović Mandić, Ana Vuković, Marko Gutalj, Stefan Stjepanović, Bratislav Matović, and Dejan B. Stojanović. 2021. 'The Potential Impact of Climate Change on the Distribution of Key Tree Species in Serbia under RCP4.5 and RCP 8.5 Scenarios'. *Austrian Journal of Forest Science* 138 (4): 183–208.

Muñoz Sabater, J. 2019. 'ERA5-Land Hourly Data from 1981 to Present'. Copernicus Climate Change Service (C3S) Climate Data Store (CDS). 2019. https://doi.org/10.24381/cds.e2161bac.

Myneni, R., Y. Knyazikhin, and T. Park. 2015. 'MCD15A2H MODIS/Terra+Aqua Leaf Area Index/FPAR 8-Day L4 Global 500m SIN Grid V006. 2015'. Distributed by NASA EOSDIS Land Processes DAAC. 2015. https://doi.org/10.5067/MODIS/MCD15A2H.006.

Nachtergaele, Freddy, Harrij Van Velthuizen, Luc Verelst, Niels Batjes, Koos Dijkshoorn, Vincent Van Engelen, Guenther Fischer, et al. 2010. 'The Harmonized World Soil Database', no. August: 34–37.

OpenStreetMap Contributors. 2020. 'OpenStreetMap (OSM)'. OpenStreetMap Foundation. 2020.

Panagos, Panos, Marc Van Liedekerke, Arwyn Jones, and Luca Montanarella. 2012. 'European Soil Data Centre: Response to European Policy Support and Public Data Requirements'. *Land Use Policy* 29 (2): 329–38. https://doi.org/10.1016/j.landusepol.2011.07.003.

Pekel, Jean-François, Andrew Cottam, Noel Gorelick, and Alan S. Belward. 2016. 'High-Resolution Mapping of Global Surface Water and Its Long-Term Changes'. *Nature* 540 (7633): 418–22. https://doi.org/10.1038/nature20584.

Rajkovic, B, M Vujadinovic, and A Vukovic. 2013. 'Report on Revisited Climate Change Scenarios Including Review on Applied Statistical Method for Removing of Systematic Model Errors, with Maps of Temperature, Precipitation and Required Climate Indices Changes'. MERZ, Belgrade, Serbia.

Republic Hydrometeorological Service of Serbia. 2020. 'Meteorological Yearbooks'. Meteorological Yearbooks. 2020. http://www.hidmet.gov.rs/ciril/meteorologija/klimatologija_godisnjaci.php%0A.

Rodell, Matthew, P. R. Houser, U. Jambor, J. Gottschalck, K. Mitchell, C. J. Meng, K. Arsenault, et al. 2004. 'The Global Land Data Assimilation System'. *Bulletin of the American Meteorological Society* 85 (3): 381–94. https://doi.org/10.1175/BAMS-85-3-381.

Running, S., Q. Mu, and M. Zhao. 2021. 'MODIS/Terra Net Evapotranspiration 8-Day L4 Global 500m SIN Grid V061 [Data Set].' NASA EOSDIS Land Processes DAAC. 2021. https://doi.org/10.5067/MODIS/MOD16A2.061%0A.

Srbijavode. 2020. 'Srbijavode GIS Portal'. 2020. https://geoportal.srbijavode.rs/visios/Portal.

Statistical Office of the Republic of Serbia. 2020. 'Statistical Office of the Republic of Serbia'. 2020. https://www.stat.gov.rs/.

Thrasher, B., E. P. Maurer, C. McKellar, and P. B. Duffy. 2012. 'Technical Note: Bias Correcting Climate Model Simulated Daily Temperature Extremes with Quantile Mapping'. *Hydrology and Earth System Sciences* 16 (9): 3309–14. https://doi.org/10.5194/hess-16-3309-2012.

United Nations Development Programme (UNDP), and Serbian Ministry of Agriculture Forestry and Water Management. n.d. 'Serbia NAP - Advancing Medium And Long-Term Adaptation Planning In The Republic Of Serbia'. Accessed 1 January 2022. https://cca.neopix.dev/eng/.

World Bank. 2020. 'World Bank Data: Population'. World Bank Data Website. 2020.